Nuclear Safety
NEA/CSNI/R(2014)14
February 2015
www.oecd-nea.org

Post-BEMUSE Reflood Model Input Uncertainty Methods (PREMIUM) Benchmark Phase II: Identification of Influential Parameters

OECD
BETTER POLICIES FOR BETTER LIVES

NEA
NUCLEAR ENERGY AGENCY

Unclassified **NEA/CSNI/R(2014)14**

Organisation de Coopération et de Développement Économiques
Organisation for Economic Co-operation and Development **23-Feb-2015**

English text only

NUCLEAR ENERGY AGENCY
COMMITTEE ON THE SAFETY OF NUCLEAR INSTALLATIONS

Post-BEMUSE Reflood Model Input Uncertainty Methods (PREMIUM) Benchmark Phase II: Identification of Influential Parameters

JT03370933

Complete document available on OLIS in its original format

NEA/CSNI/R(2014)14
Unclassified

English text only

ORGANISATION FOR ECONOMIC CO-OPERATION AND DEVELOPMENT

The OECD is a unique forum where the governments of 34 democracies work together to address the economic, social and environmental challenges of globalisation. The OECD is also at the forefront of efforts to understand and to help governments respond to new developments and concerns, such as corporate governance, the information economy and the challenges of an ageing population. The Organisation provides a setting where governments can compare policy experiences, seek answers to common problems, identify good practice and work to co-ordinate domestic and international policies.

The OECD member countries are: Australia, Austria, Belgium, Canada, Chile, the Czech Republic, Denmark, Estonia, Finland, France, Germany, Greece, Hungary, Iceland, Ireland, Israel, Italy, Japan, Luxembourg, Mexico, the Netherlands, New Zealand, Norway, Poland, Portugal, the Republic of Korea, the Slovak Republic, Slovenia, Spain, Sweden, Switzerland, Turkey, the United Kingdom and the United States. The European Commission takes part in the work of the OECD.

OECD Publishing disseminates widely the results of the Organisation's statistics gathering and research on economic, social and environmental issues, as well as the conventions, guidelines and standards agreed by its members.

NUCLEAR ENERGY AGENCY

The OECD Nuclear Energy Agency (NEA) was established on 1 February 1958. Current NEA membership consists of 31 countries: Australia, Austria, Belgium, Canada, the Czech Republic, Denmark, Finland, France, Germany, Greece, Hungary, Iceland, Ireland, Italy, Japan, Luxembourg, Mexico, the Netherlands, Norway, Poland, Portugal, the Republic of Korea, the Russian Federation, the Slovak Republic, Slovenia, Spain, Sweden, Switzerland, Turkey, the United Kingdom and the United States. The European Commission also takes part in the work of the Agency.

The mission of the NEA is:

- to assist its member countries in maintaining and further developing, through international co-operation, the scientific, technological and legal bases required for a safe, environmentally friendly and economical use of nuclear energy for peaceful purposes, as well as
- to provide authoritative assessments and to forge common understandings on key issues, as input to government decisions on nuclear energy policy and to broader OECD policy analyses in areas such as energy and sustainable development.

Specific areas of competence of the NEA include the safety and regulation of nuclear activities, radioactive waste management, radiological protection, nuclear science, economic and technical analyses of the nuclear fuel cycle, nuclear law and liability, and public information.

The NEA Data Bank provides nuclear data and computer program services for participating countries. In these and related tasks, the NEA works in close collaboration with the International Atomic Energy Agency in Vienna, with which it has a Co-operation Agreement, as well as with other international organisations in the nuclear field.

COMMITTEE ON THE SAFETY OF NUCLEAR INSTALLATIONS

Within the OECD framework, the NEA Committee on the Safety of Nuclear Installations (CSNI) is an international committee made of senior scientists and engineers, with broad responsibilities for safety technology and research programmes, as well as representatives from regulatory authorities. It was set up in 1973 to develop and co-ordinate the activities of the NEA concerning the technical aspects of the design, construction and operation of nuclear installations insofar as they affect the safety of such installations.

The committee's purpose is to foster international co-operation in nuclear safety amongst the NEA member countries. The CSNI's main tasks are to exchange technical information and to promote collaboration between research, development, engineering and regulatory organisations; to review operating experience and the state of knowledge on selected topics of nuclear safety technology and safety assessment; to initiate and conduct programmes to overcome discrepancies, develop improvements and research consensus on technical issues; and to promote the co-ordination of work that serves to maintain competence in nuclear safety matters, including the establishment of joint undertakings.

The clear priority of the committee is on the safety of nuclear installations and the design and construction of new reactors and installations. For advanced reactor designs the committee provides a forum for improving safety related knowledge and a vehicle for joint research.

In implementing its programme, the CSNI establishes co-operative mechanisms with the NEA's Committee on Nuclear Regulatory Activities (CNRA) which is responsible for the programme of the Agency concerning the regulation, licensing and inspection of nuclear installations with regard to safety. It also co-operates with the other NEA's Standing Committees as well as with key international organizations (e.g., the IAEA) on matters of common interest.

Post-BEMUSE Reflood Model Input Uncertainty Methods (PREMIUM) Benchmark Phase II: Identification of Influential Parameters

A. Kovtonyuk, A. Petruzzi, F. D'Auria (GRNSPG/UNIPI, Italy)

in collaboration with

Bel V (Belgium), Tractebel (Belgium), NRI (Czech Republic), VTT (Finland), CEA (France), IRSN (France), GRS (Germany), KIT (Germany), KAERI (Rep. of Korea), KINS (Rep. of Korea), OKBM (Russian Federation) and UPC & CSN (Spain).

LIST OF REVISIONS

Revision	Date	Scope of revision	Pages	File ID
Rev. 0	27 November 2012	draft issued for comments	43	PREMIUM_Report_Phase-II_rev0
Rev. 0.1	28 November 2012	draft issued for comments	220	PREMIUM_Report_Phase-II_rev0.1
Rev. 0.2	14 December 2012	working version	220	PREMIUM_Report_Phase-II_rev0.2
Rev. 1.0	20 December 2012	revised draft issued for comments	233	PREMIUM_Report_Phase-II_rev1.0
Rev. 1.1	09 July 2013	revised final issued for comments	233	PREMIUM_Report_Phase-II_rev1.1
Rev. 1.2	21 October 2013	revised final	233	PREMIUM_Report_Phase-II_rev1.2
final	Oct.-Nov. 2014	Corrections, reformatting	214	CSNI-R-2014-14_FINAL

LIST OF ABBREVIATIONS

BAF	Bottom of Active Fuel (in FEBA - bottom of electrically heated fuel rod simulator)
BE	Best Estimate
BEMUSE	Best-Estimate Methods Uncertainty and Sensitivity Evaluation
BIC	Boundary and Initial Conditions
BWR	Boiling Water Reactor
CC	Coordination Commettee
CCFL	Counter Current Flow Limiting
CEA	Commissariat à l'Energie Atomique
CHF	Critical Heat Flux
CSN	Consejo de Seguridad Nuclear
CSNI	Committee on the Safety of Nuclear Installations
DIMNP	Dipartimento di Ingegneria Meccanica Nucleare e della Produzione
DNB	Departure from Nucleate Boling
DP	Pressure Drop
ECC	Emergency Core Cooling
ECCS	Emergency Core Cooling System
GRNSPG	Gruppo di Ricerca Nucleare San Piero a Grado
GRS	Gesellschaft für Anlangen - und Reaktorsicherheit
HPIS	High Pressure Injection System
HT	Heat Transfer
HTC	Heat Transfer Coefficient
IAEA	International Atomic Energy Agency
IBP	Input Basic Parameter
ICP	Input Coefficient Parameter
ID	Identification
IGP	Input Global Parameter
INEL	Idaho National Engineering Laboratory
IP	Input Parameter
IRSN	L'Institut de Radioprotection et de Sûreté Nucléaire
ITF	Integral Test Facility
LB LOCA	Large-Break Loss-Of-Coolant Accident
LOCA	Loss-Of-Coolant Accident
LP	Lower Plenum
LPIS	Low Pressure Injection System

LWR	Light-Water Reactor
NA	Not Available
NEA	Nuclear Energy Agency (of the OECD)
NPP	Nuclear Power Plant
OECD	Organisation for Economic Co-operation and Development
PCT	Peak Cladding Temperature
PDF	Probability Distribution Function
PREMUIM	Post-BEMUSE Reflood Model Input Uncertainty Methods
PWR	Pressurized-Water Reactor
QF	Quench Front
R	Response
R5	RELAP5
RTA	Relevant Thermal-hydraulic Aspect
SETF	Separate-Effect Test Facility
SB LOCA	Small-Break Loss-Of-Coolant Accident
TAF	Top of Active Fuel (in FEBA - top of electrically heated fuel rod simulator)
TH	Thermal Hydraulic
TH-SYS	Thermal-Hydraulic SYStem (referred to code)
UNIPI	Università di Pisa
UP	Upper Plenum
UPC	Universitat Politècnica de Catalunya
WGAMA	CSNI Working Group on Analysis and Management of Accidents

TABLE OF CONTENTS

LIST OF FIGURES

LIST OF TABLES

EXECUTIVE SUMMARY

The objective of the Post-BEMUSE Reflood Model Input Uncertainty Methods (PREMIUM) benchmark is to progress on the issue of the quantification of the uncertainty of the physical models in system thermal-hydraulic codes by considering a concrete case: the physical models involved in the prediction of core reflooding. The PREMIUM benchmark consists of five phases:

- Phase I: mainly, definition of the different uncertainty methods;
- Phase II: determination of the physical models influential in reflooding using the test 216 of the FEBA programme;
- Phase III: quantification of the uncertainties of the parameters associated with the physical models identified as influential within Phase II, using FEBA/SEFLEX experimental results;
- Phase IV: validation of the found uncertainties within Phase III by propagating them in the 2-D PERICLES reflood experiment; this phase will be performed blindly except for the coordinators;
- Phase V: synthesis report.

This report presents the results of Phase II. Phase II is dedicated to the identification of the uncertain code parameters associated with physical models used in the simulation of reflooding conditions. This identification is made on the basis of the Test 216 of the FEBA/SEFLEX programme according to the following steps:

- identification of influential phenomena;
- identification of the associated physical models and parameters, depending on the used code;
- quantification of the variation range of identified input parameters through a series of sensitivity calculations.

A procedure for the identification of potentially influential code input parameters has been set up in the Specifications of Phase II of PREMIUM benchmark. A set of quantitative criteria has been as well proposed for the identification of influential IP and their respective variation range.

Thirteen participating organisations, using 8 different codes (7 system thermal-hydraulic codes and 1 sub-channel module of a system thermal-hydraulic code) submitted Phase II results. The base case calculations show spread in predicted cladding temperatures and quench front propagation that has been characterized. All the participants, except one, predict a too fast quench front progression. Besides, the cladding temperature time trends obtained by almost all the participants show oscillatory behaviour which may have numeric origins.

Adopted criteria for identification of influential input parameters differ between the participants: some organisations used the set of criteria proposed in Specifications “as is”, some modified the quantitative thresholds proposed in Specifications, and others used their own methodologies. This fact was a partial reason for the different ranges of input parameter variation identified by participants, in addition to differences of the physical models adopted by the different codes. Therefore, such different variation ranges of IP and, correspondingly, such different variation ranges of cladding temperature and time of rewet, make rather difficult the task of meaningful and easy-comprehendible comparison of Phase II results.

Out of a total of 72 input parameters, initially considered by all participants, only 6 were identified as influential by more than 4 participants that are:

- bundle power;
- wall heat transfer coefficient;
- interphase friction coefficient;
- interphase heat transfer coefficient;
- heat transfer (enhancement) at the quench front;
- droplet diameter.

It should be noted that actual parameters considered in parameter “Heat transfer (enhancement) at the quench front” are code-specific and may have different influence on calculation results.

Several participants discarded some identified influential parameters (e.g., droplet diameter) due to existing relation between this kind of parameters so-called “Input Coefficient Parameters” and more global parameters (e.g. interfacial friction coefficient and interphase heat transfer coefficient which use the droplet diameter) so-called “Input Global Parameters”. Some participants also discarded identified influential so-called “Input Basic Coefficients” (e.g. bundle power) since their uncertainty has not to be determined in the Phase III but will be provided by the coordinator from experimental data.

The behaviour of the variation of the responses at the extremes of IP range of variation greatly depends on the type of input parameter and on the code used. Mainly, the following two different behaviours can be characterized:

- For some parameters, like power, wall heat transfer and interphase heat transfer coefficients, a qualitative (but not quantitative) agreement between different codes is observed.
- For other parameters, like interphase friction coefficient and droplet diameter, a contrary behaviour (i.e. in correspondence of one of the extreme of the IP range, the direction of change of the responses is different) between different codes and even between different selected models within the same code can be observed. This suggests that the effect of such parameters on the cladding temperatures is quite complex, probably because it involves a lot of physical models (e.g., via interphase friction and interphase heat transfer coefficients for the droplet diameter).

It shall be noted that the analysis of differences between the reflood models of different codes is out of scope of the PREMIUM benchmark. Nevertheless, it is recommended to take into account the physical models/ input parameters found as influential by the other participants in order to select the influential input parameters for which uncertainties are to be quantified within the Phase III of PREMIUM. In particular, input parameters identified as influential by other participants using the same code should be considered.

1. INTRODUCTORY REMARKS

The objective of Post-BEMUSE Reflood Model Input Uncertainty Methods (PREMIUM) benchmark is to progress on the issue of the quantification of the uncertainty of the physical models in system thermal-hydraulic codes, by considering a concrete case: the physical models involved in the prediction of core reflooding.

Within the frame of PREMIUM the quantification of the uncertainties will be performed for the influential physical models in the reflooding. More precisely, the participants will:

- determine the parameters of their code associated with these physical models;
- quantify the uncertainties of these parameters using FEBA/SEFLEX experimental result;
- validate the found uncertainties by propagating them in the 2-D reflood PERICLES experiment.

The benchmark will be concluded by a synthesis report with recommendations. If it will appear of interest from the point of view of safety significance, it might be followed by the writing of a Best Practice Guidelines report.

At the Phase II of the PREMIUM benchmark, the participants are asked to identify which physical models of their codes can be considered as influential in the reflooding scenario using data from the FEBA/SEFLEX experiment, to select the related uncertain input parameters and to propose the quantification of variation range of associated parameters through a series of sensitivity calculations.

As a result, the participants report the following information:

1. identification of influential phenomena;
2. identification of the associated physical models and parameters depending on the used code;
3. quantification of the range of variation of identified input uncertainties through a series of sensitivity calculations.

2. OUTLINE OF SPECIFICATIONS FOR PHASE II

2.1 Definitions

Here below the definitions attributing to the "selection of influential input parameters (IP)" concept are introduced. An example of classification of input parameters according to introduced definitions is provided on Figure 2.1.

- **Response (R):** a physical quantity that can be measured or deduced (calculated) from measurements (e.g. cladding temperatures, time when rewet starts, etc.).
- **Input Global Parameter (IGP):** an IP associated with a physical model (e.g., HTC).
- **Input Basic Parameter (IBP):** an IP that can be
    - BIC parameter: e.g., mass flow rate, power, etc.
    - geometrical parameter: e.g., hydraulic diameter
    - material property parameter: e.g., conductivity of Zircaloy, UO_2, etc.
    - discretization parameter: e.g., length of nodes, size of meshes, etc.
- **Input Coefficient Parameter (ICP):** a single coefficient inside a correlation which can be distinguished as follows
    - a parameter accessible from input deck for a code: e.g., K_{loss} coefficients in RELAP
    - a numerical constant value not accessible from input deck
    - a derived quantity parameter: e.g., quality, Re, etc.

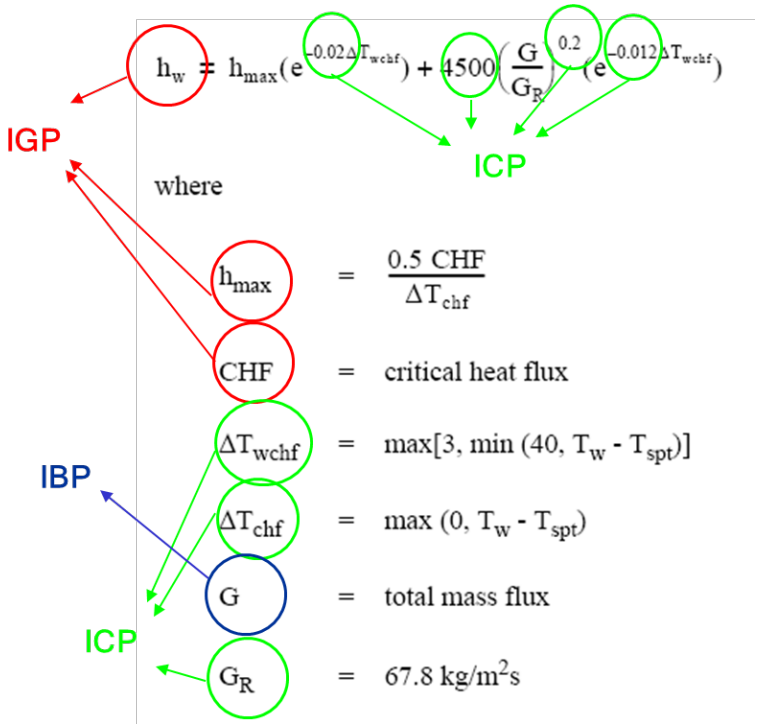

Figure 2.1: Example of Classification of Input Parameters

2.2 Procedure for identification of influential input parameters

The following procedure is proposed to the participant for identification of input parameters and selection if influential ones:

- **Step #1:** Set up an initial list of IP. In order to develop a preliminary list of input parameters, the participant should use their knowledge of the related phenomena physics, corresponding correlations implemented in the code intended for use. A sample list of all types (Input Global Parameter, Input Basic Parameter and Input Coefficient Parameter) is provided in "Full List of Considered Input Parameters" in Appendix A. At this stage an engineering judgment may be applied to sort out immediately non-influential parameters.
- **Step #2:** The BE values of all the IP from the preliminary list shall be selected and documented. A code reference calculation to be performed and main responses to be documented.
- **Step #3:** Set up and document criteria for selection of influential input parameters. A set of criteria is proposed.
- **Step #4:** Perform a number of required sensitivity code runs corresponding to the methodology (criteria) set up at the Step #3. If criteria proposed are adopted then one code calculation should be performed for a single variation of a single IP from the preliminary list. Otherwise, in case another methodology for IP selection is set, and alternative procedure for sensitivity study, based on Monte Carlo or Latin Hypercube sampling, may be adopted. Main responses for each sensitivity run to be documented.
- **Step #5:** Apply the criteria for selection of influential Input Parameters. At this stage, the use of engineering judgment shall be minimized. If a participant decides to keep the parameter that does not meet the criteria, a reasonable justification shall be provided.

- **Step #6:** Document the list of influential Input Parameters and supposed range of variation and/or PDF (if available).

2.3 Proposed criteria for selection of influential input parameters

A set of criteria for selection of influential Input Parameters has been proposed in Specifications for Phase II /1/. After an initial list of input parameters has been set up by an analyst and the required sensitivity studies have been performed, a selection of influential" IP is performed using the following methodology.

An influential IP has to be such that its extreme value in the range of variation causes the following change in the two main reflood responses:

- **Criterion #1:** The absolute value of variation in rod surface temperature T_{clad} is $\mathbf{\Delta T_{ref} = 50K}$;
- **Criterion #2:** The variation in rewet time t_{rew} is $\mathbf{\Delta t_{rew} = 10\%}$.

Additionally, a confirmation criterion may be applied with respect to the quench front propagation:

- **Criterion #3:** The variation in elevation of the quench front versus time $\mathbf{\Delta QF_{elev} = 10\%}$.

Once the potential influential IP have been selected, the following criteria must be applied in order to ensure the "realism" of the uncertainty of these Input Parameters:

- **Criterion #4:** Limited qualitative impact on the responses' time trends. Notably, the variation of an IP should not cause the drastic changes in rod surface temperature time trends (sudden deviations, oscillations) which may be caused by phenomenology different from that of reflood or by physical or numerical instabilities.
- **Criterion #5:** The range of variation (to make the parameter "influential") shall be consistent with the level of knowledge on the correspondent IP, e.g. the change in NiCr density cannot be larger than the real known physical limits.
- **Criterion #6** (if applicable): In case a preliminary uncertainty evaluation is available, the range of variation of the single IP should not be responsible of the overall uncertainty of the responses.

3. EXPERIMENTAL FACILITY AND TEST DESCRIPTION

3.1 FEBA facility description

For the evaluation step of the PREMIUM benchmark the tests from the FEBA/SEFLEX programme have been chosen.

The FEBA/SEFLEX programme was performed at KfK Karlsruhe, Germany. The test facility was designed for the reflooding tests with possibility of maintaining constant flooding rates and constant back pressure. The test section consists of a full-length 5 x 5 rod bundle of PWR fuel rod dimensions utilizing electrically heated rods with a cosine power profile approximated by 7 steps of different power density in axial direction. The rod bundle is placed in housing made of stainless steel and insulated with Triton Kao Wool to reduce heat losses to environment. The cross-section of the FEBA rod bundle is shown in the Figure 3.1.

The outer diameter of the heater rod is 10.75 mm. The pitch of the rod grid is 14.3 mm. The dimensions of the quadratic housing are: inner side length 78.5 mm and wall thickness 6.5 mm. The inner size of the housing is chosen in such a way that the hydraulic diameter of the bundle array for all rods is the same and equal 13.47 mm. The heated length is 3900 mm. The spacers decrease the flow cross section about 20%. The applied spacers were original PWR spacers as used by KWU. The location of the spacers can be found in the Figure 3.2. More detailed information may be found in /2/.

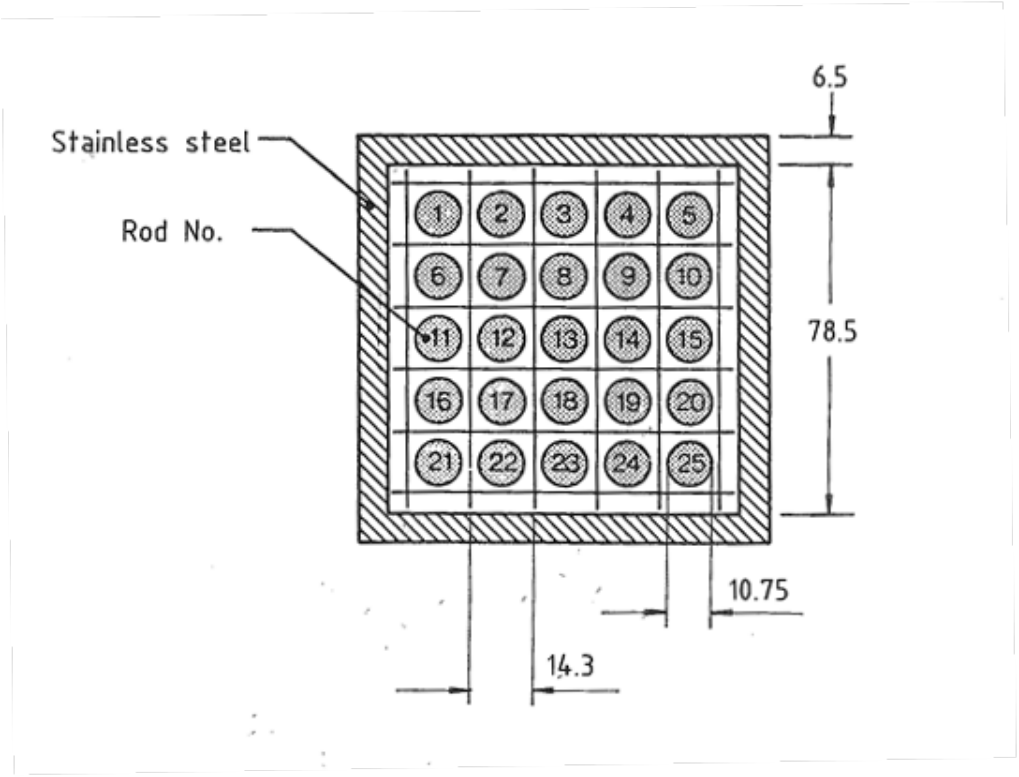

Figure 3.1: FEBA rod bundle – cross-section view

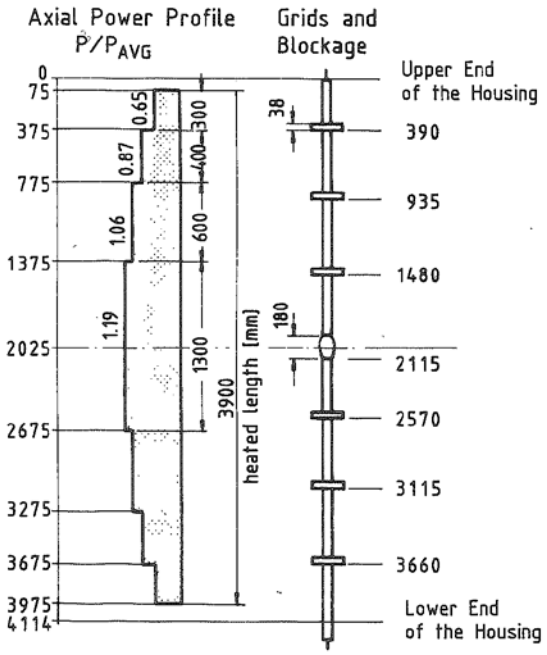

Figure 3.2: Axial view of the FEBA heater rod and axial power profile distribution

3.2 Test 216 description

The identification of influential input parameters within the frame of Phase II has been performed based on test 216 of FEBA/SEFLEX experimental programme.

Prior to the test run the fuel rod simulators were heated in stagnant steam to desired initial cladding temperature, using a low rod power. In the meantime the test bundle housing was being heated up passively to the requested initial temperature by radiation from the rods. The aim of choosing the thick wall ("active wall") was to prevent premature quenching of the wall relative to the bundle quench front progression.

During the heat up period the inlet plenum was cooled by circulating water to maintain the desired temperature. The steam filled ducts were heated up to a temperature slightly above the saturation temperature.

By starting of the test run the bundle power was increased to the required level simulating decay heat according to 120% ANS-Standard about 40 s after reactor shut down. Simultaneously the water supply was activated.

The initial and boundary conditions of test 216 are presented in Table 3.1and Figure 3.3. The measured cladding temperatures are presented in Figure 3.4. More detailed information on test conduction and measured data can be found in /2/.

Table 3.1: Test 216 conditions

Test No.	Inlet velocity (cold), cm/s	System pressure, Bar	FW temperature, °C		Bundle power, kW	
			0-30 s	end	0 s	end
216	3.8	4.1	48	37	200	120% ANS

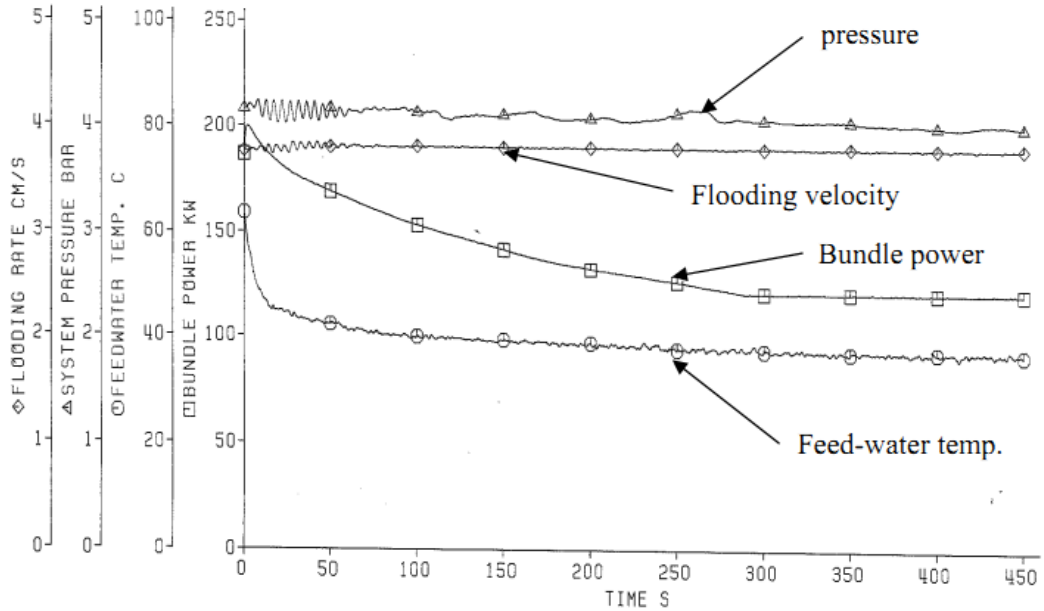

Figure 3.3: Test 216 boundary conditions

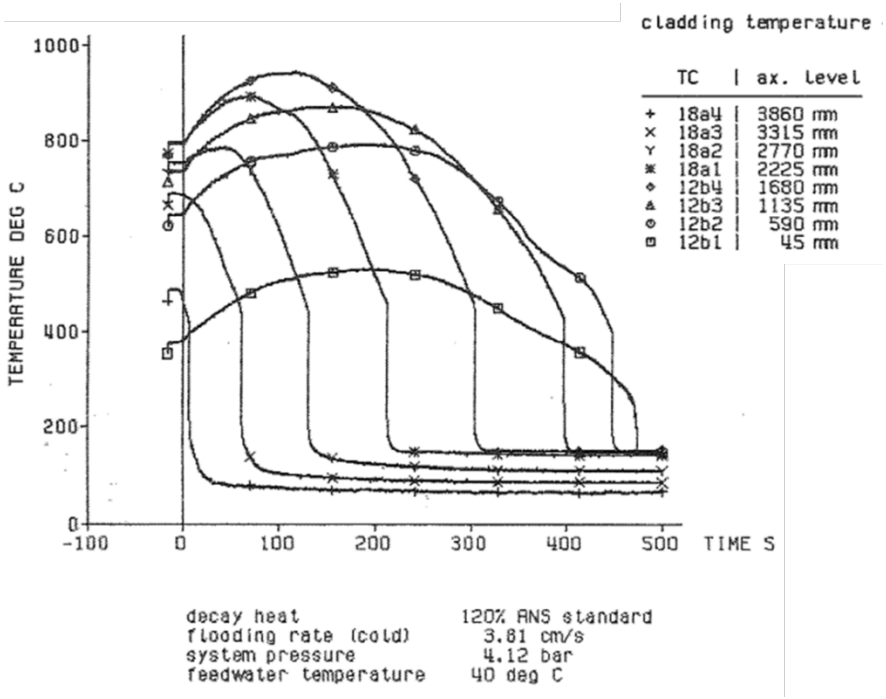

Figure 3.4: Test 216 measured cladding temperatures

4. RESULTS OF PHASE II

4.1 Participants and codes

In total, 13 participating organisations submitted their results for Phase II. The list of the participants and the codes applied are provided in Table 4.1.

All applied codes are 1-D system thermal-hydraulic codes, except COBRA-TF module applied by KAERI which is a sub-channel code.

Table 4.1: List of participating organisations

Participant	Country	Code
Bel V	Belgium	CATHARE 2 V2.5_2 mod8.1
TRACTEBEL	Belgium	RELAP5/MOD3.3
NRI	Czech Republic	ATHLET 2.1A
VTT	Finland	APROS 5.11.02
CEA	France	CATHARE 2 V2.5_2 mod8.1
IRSN	France	CATHARE 2 V2.5_2 mod8.1
GRS	Germany	ATHLET 2.2B
KIT	Germany	TRACE Version 5 patch3
UNIPI	Italy	RELAP5/MOD3.3 patch3
KAERI	Republic of Korea	COBRA-TF Module of MARS-KS Code
KINS	Republic of Korea	MARS-KS-003
OKBM	Russian Federation	RELAP/SCDAPSIM/MOD3.4
UPC & CSN	Spain	RELAP5/MOD3.3 patch4

4.2 Summary of Adopted Nodalizations

Most of participants adopted a nodalization representing the test section of FEBA with single vertical channel and single heater rod/heat structure. A specific CHAN component of TRACE code has been used by KIT, which actually simulates 5x5 bundle. KAERI, in its turn, modelled 1/8 of the bundle with a sub-channel COBRA-TF module of MARS-KS code. All participants included the model of the test section housing.

Different approaches were adopted by participants for modelling the spacer grids: some organisations actually reduced the flow area at the location of the grids and activated special models for heat transfer enhancement; others took into account the grids only by applying form loss coefficients at the corresponding elevations.

The number of axial nodes, representing the test section, in the participants' nodalizations ranges from 20 to 78 (Table 4.2 and Figure 4.1) and depends on the type of the numerical scheme adopted by each code and by the nodalization techniques adopted in different organisations. It should be mentioned, that the

provided number of axial nodes does not take into account the possible refinement, as it can be the case in the vicinity of the quench front to calculate the axial conduction (whenever performed by a code).

Table 4.2: characteristics of adopted nodalizations

Participant	Code	Number of axial nodes	Max linear heat rate, W/cm
GRS	ATHLET 2.2B	23	N/A
NRI	ATHLET 2.1A	66	24.4
Bel V	CATHARE 2 V2.5_2 mod8.1	46	24.4
CEA	CATHARE 2 V2.5_2 mod8.1	40	24.4
IRSN	CATHARE 2 V2.5_2 mod8.1	39	N/A
KAERI	MARS-KS1.3(COBRA-TF Module)	26	24.4
KINS	MARS-KS-003	39	23.8
OKBM	RELAP/SCDAPSIM Mod3.4	39	24.4
Tractebel	RELAP5 Mod3.3	51	N/A
UNIPI	RELAP5 Mod3.3 patch3	20	24.4
UPC	RELAP5 Mod3.3 patch4	25	24.3
KIT	TRACE Version 5 patch 3	43	N/A
VTT	APROS 5.11.02	78	24.4

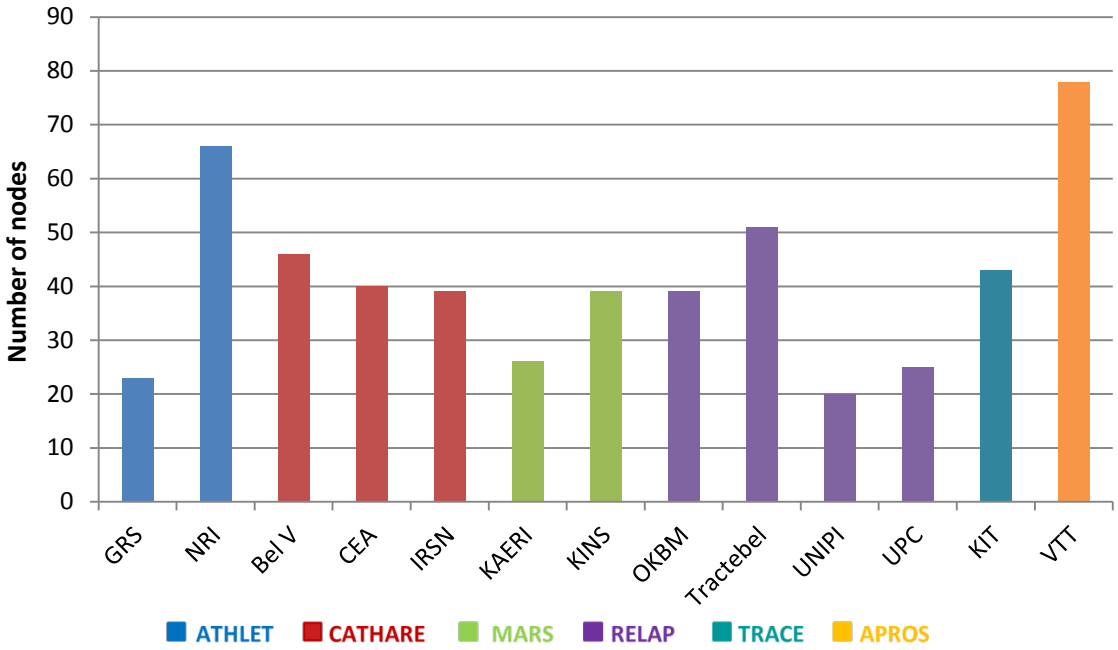

Figure 4.1: fidelity of adopted nodalizations.

4.3 Base Case Results

First, the base case calculations have been performed by participants. Obtained cladding temperatures at bottom (3860 mm from top of housing), 2/3 height (1680 mm, corresponding to the highest value of the experimentally measured cladding temperatures, equal to 940°C) and top (590 mm) of the active part are presented on Figure 4.2, Figure 4.3 and Figure 4.4 respectively. Quench front propagation is presented on Figure 4.5. The Table 4.3, Figure 4.6 and Figure 4.7 summarize the overall models' performance.

The calculated time trends of cladding temperature at different elevations show rather big spread, in terms of maximum temperature and time of rewet, with respect to experimentally measured data. Almost all codes, except RELAP/SCDAPSIM Mod3.4 applied by OKBM, predict faster quench front propagation. The possible reason of difference is that RELAP/SCDAPSIM Mod3.4 code does not have a specific model for reflood conditions but applies generic heat transfer correlations.

Paying more attention to the prediction of the cladding temperatures, one can note that:

- Bottom of the bundle (Figure 4.2): There is a quite large spread of the temperatures after the quenching, reaching 60-70°C. This may be due to the differently modelled initial conditions (some participants actually modelled the heat-up phase while others initialized their models at conditions corresponding to the beginning of transient) and the fact that reported temperature trends could be taken at slightly different elevations, because of different meshing adopted in participants' nodalizations.
- Other elevations (Figure 4.3 and Figure 4.4): Results of almost all the participants show somewhat oscillatory behaviour which may have the numeric origins and not observed in the experimental trends.

Regarding the overall bundle behaviour prediction, i.e. peak cladding temperature and bundle rewet time, most of the participants obtained rather satisfactory results with PCT ranging +42/-82 °C, respectively for KIT and VTT (Figure 4.6). It may be noted that RELAP group and APROS code generally under predicted the PCT while TRACE code (applied only by one participant) resulted in maximum over

prediction. The predicted bundle quench time (Figure 4.7) shows significant spread of ±30% with respect to measured value. The reported over predicting values (later quench time) are somewhat contradictory to the time of rewet predicted at the TAF (Figure 4.4) where almost all participants predicted earlier rewet. Indeed, in the Figure 4.5 at the "tail" of the quench front propagation (above the compared cladding temperature at 590 mm position) it can be seen that some codes show rather linear increase behaviour instead of more rapid quenching in experiment thus resulting in late times of total bundle rewet.

Nevertheless, the obtained base case results reproduce qualitatively the experimental trends and therefore the models can be further subjected to sensitivity studies in order to determine the most influential input parameters.

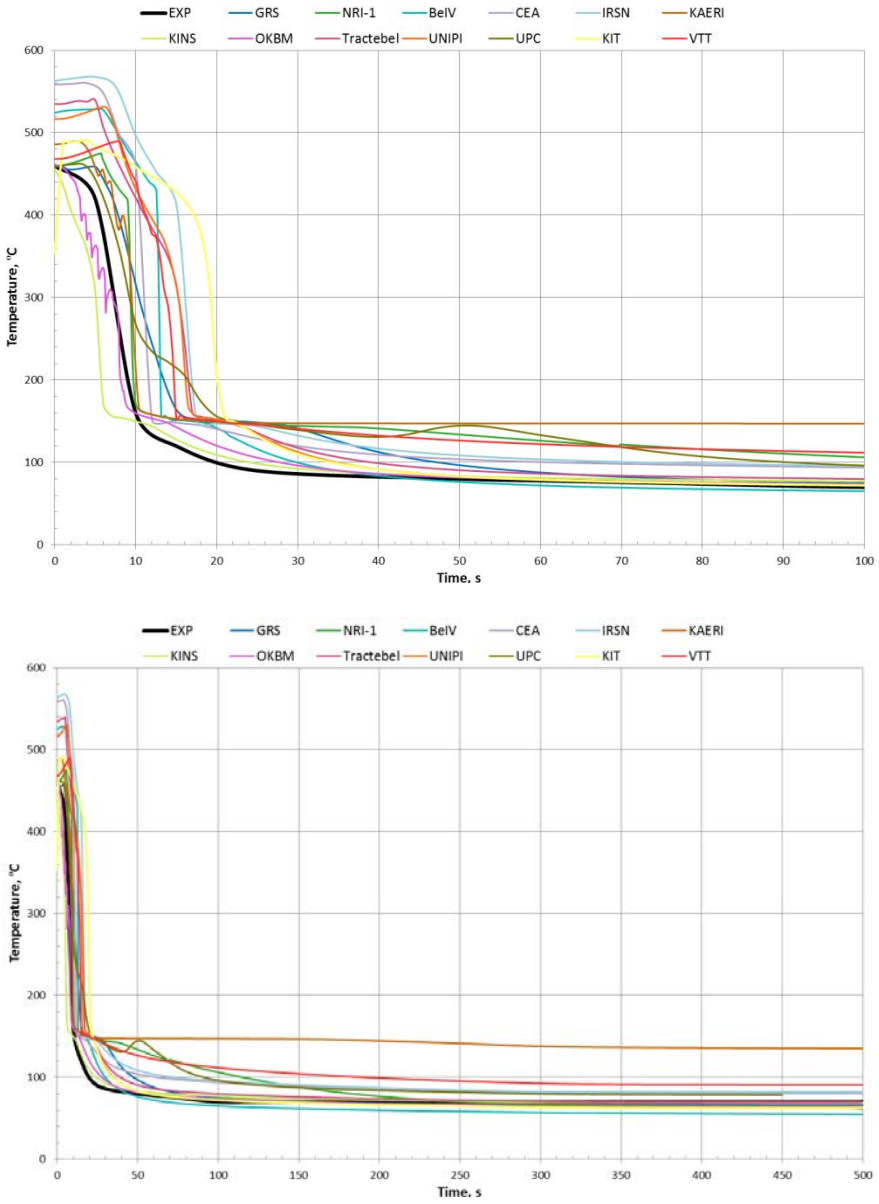

Figure 4.2: cladding temperature at BAF in Base Case (top – first 100 s, bottom – full transient)

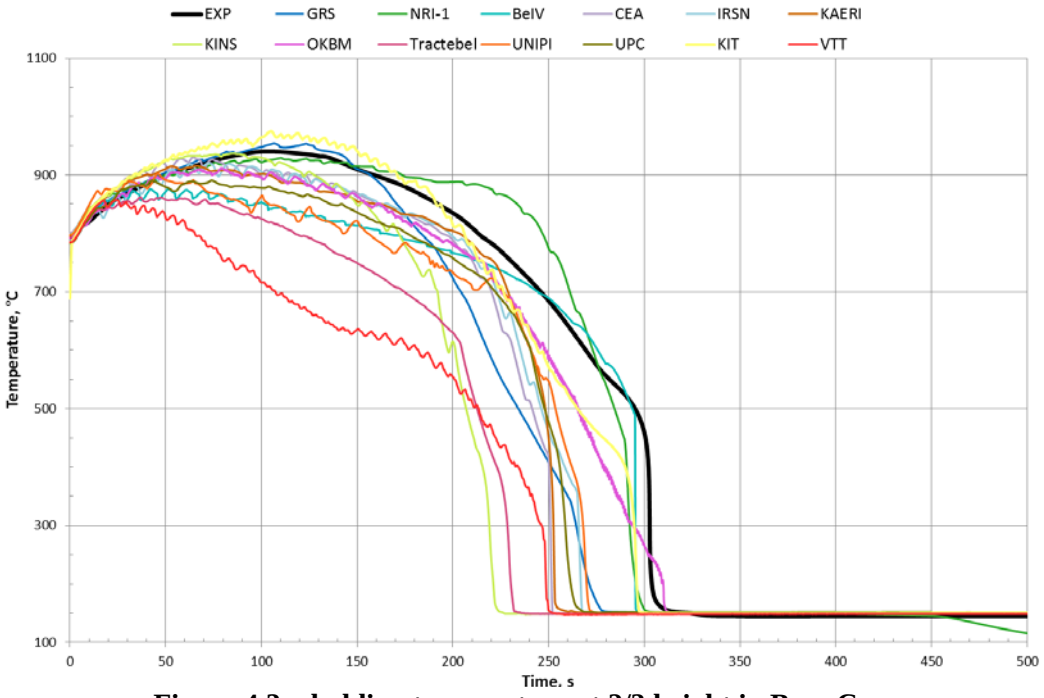

Figure 4.3: cladding temperature at 2/3 height in Base Case

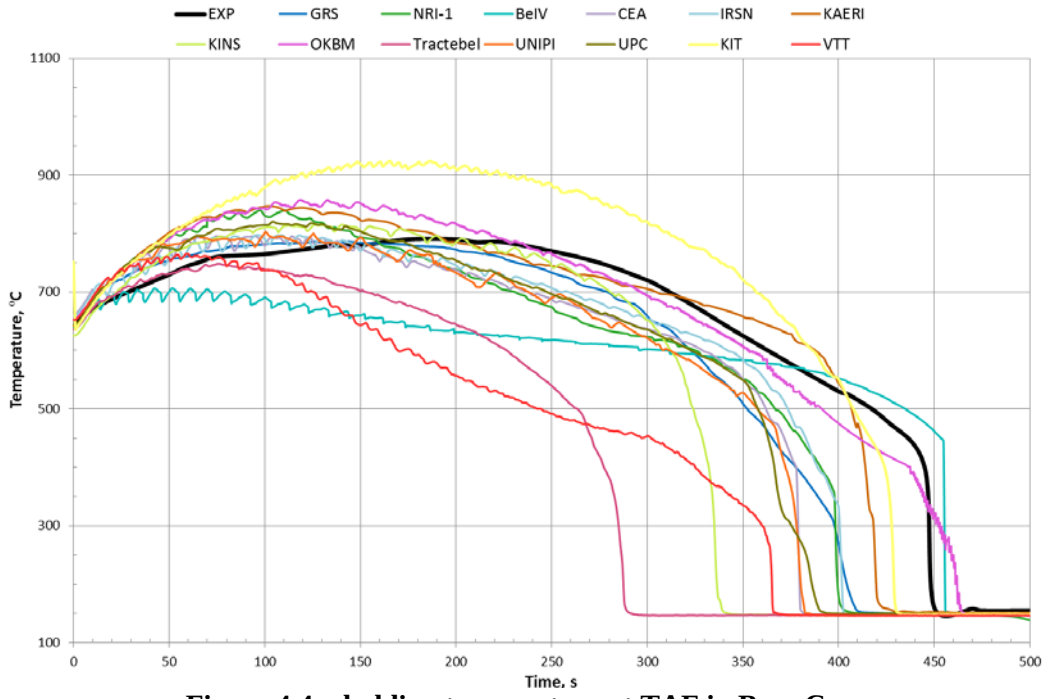

Figure 4.4: cladding temperature at TAF in Base Case

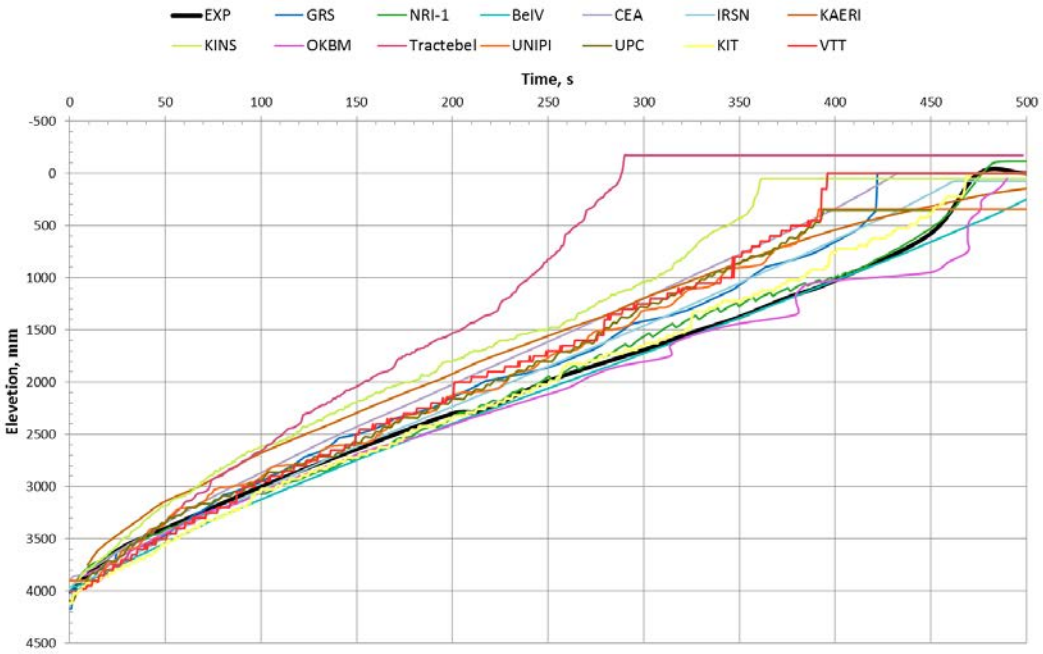

Figure 4.5: quench front propagation in Base Case

Table 4.3: summary of Base Case calculations

Participant	Code	PCT, °C	Bundle quenched, s
Experiment		940	~450
GRS	ATHLET 2.2B	958	422
NRI	ATHLET 2.1A	933	477
Bel V	CATHARE 2 V2.5_2 mod8.1	877	516
CEA	CATHARE 2 V2.5_2 mod8.1	931	429
IRSN	CATHARE 2 V2.5_2 mod8.1	925	462
KAERI	MARS-KS1.3(COBRA-TF Module)	921	587
KINS	MARS-KS-003	946	350
OKBM	RELAP/SCDAPSIM Mod3.4	915	489
Tractebel	RELAP5 Mod3.3	870	290
UNIPI	RELAP5 Mod3.3 patch3	908	378
UPC	RELAP5 Mod3.3 patch4	890	392
KIT	TRACE Version 5 patch 3	978	430
VTT	APROS 5.11.02	858	396

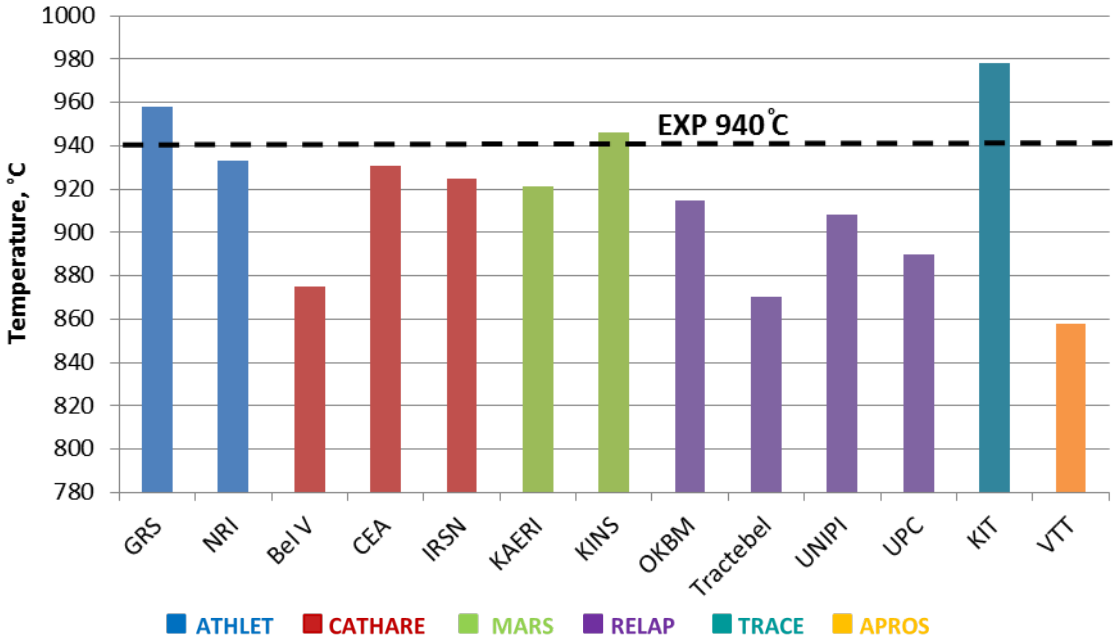

Figure 4.6: PCT comparison in Base Case

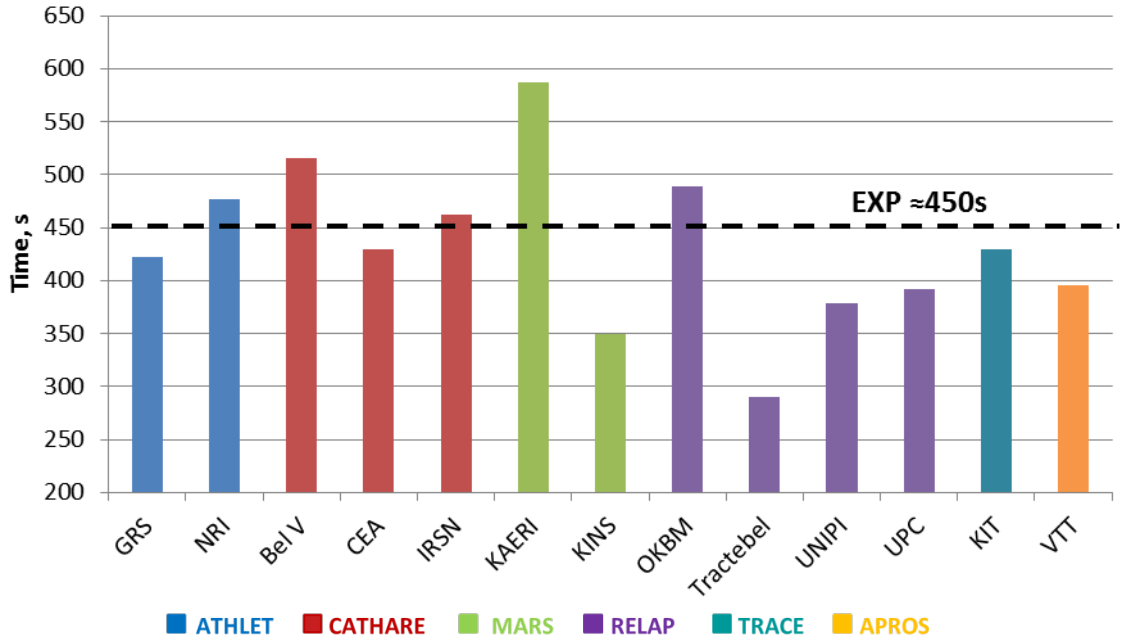

Figure 4.7: Bundle quench time comparison in Base Case

4.4 Initial Consideration of Influential IP

Following the base case calculation, each participant compiled an initial list of considered influential input parameters (IP). An example list of input parameters potentially influent for reflood has been provided to participants in the Specifications for Phase II /1/. Each participant considered about 20 parameters, except VTT and KIT who initially considered 40 and 56 parameters respectively.

In total, 72 various input parameters where considered by all participants. The list of all parameters is available in Tab A.1.1 of 1.1.1.1.Appendix A. These parameters were categorized into Input Basic Parameters (IBP), Input Global Parameters (IGP) and Input Coefficient Parameters (ICP) according to the definitions in section 0. This resulted in 26 IBPs, 14 IGPs and 33 ICPs. To each parameter an Identification Number (ID) has been assigned for further convenient reference.

Due to the variety of considered parameters and to the fact that IGP and ICP are code dependent, this list was not easy to establish. Therefore, some actual code-specific parameters considered by participants, are represented in Appendix A and further Figures by single parameters, such as “forced convection with vapour” or “film-boiling heat transfer” are represented by the single “wall heat transfer” parameter (parameter ID 27). A precise description of the actual IP considered by each participant is given for the most influential of them, further on in this report, in Table 4.7 and Table 4.12, and in the individual reports of participants in Appendix B.

On Figure 4.8 the statistics shows which parameters where chosen by the majority of the participants. The list of input parameters, considered by at least 5 participants, is provided in Table 4.4.

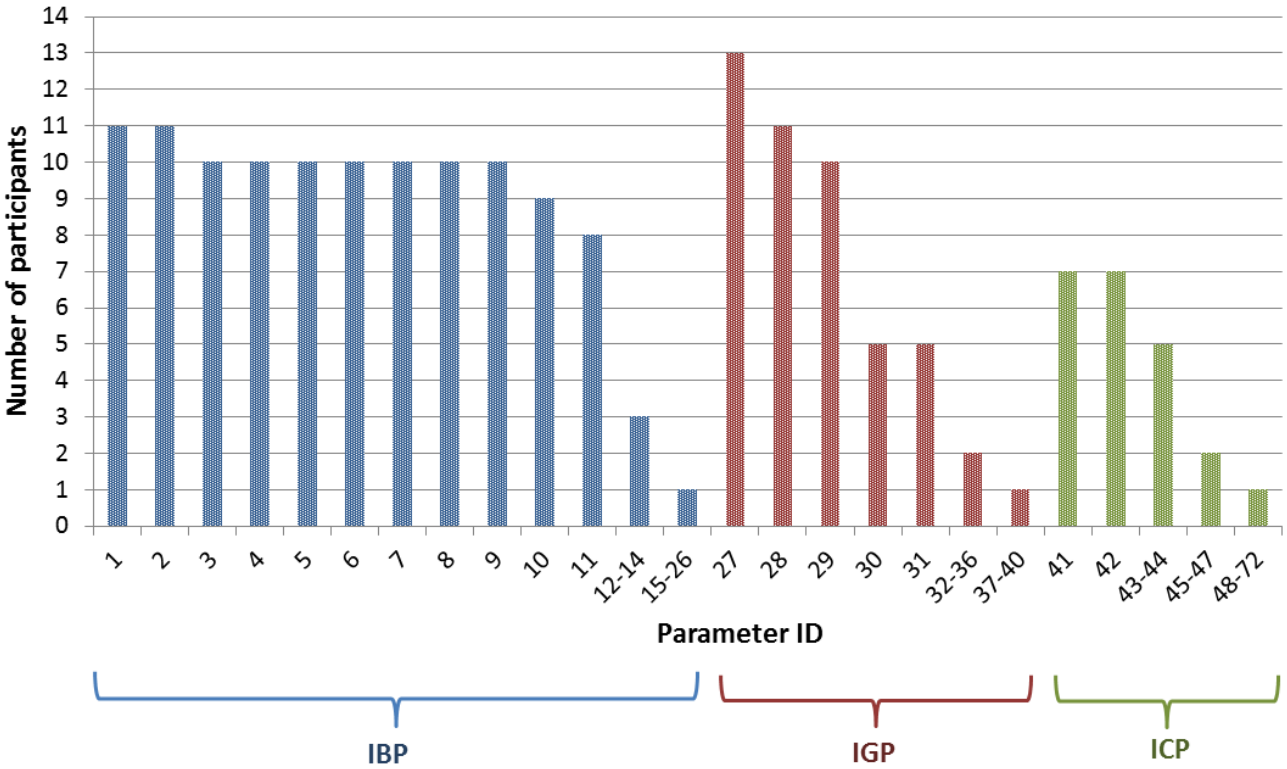

Figure 4.8: Initially considered input parameters

Table 4.4: Input parameters initially considered by majority

ID	Parameter
Input Basic Parameters	
1	Inlet liquid temperature
2	Power/power density
3	Pressure
4	Inlet liquid mass flow/flux/velocity
5	Thermal conductivity of heater
6	Heat capacity of heater
7	Thermal conductivity of insulation
8	Heat capacity of insulation
9	Spacer Form loss coefficients
10	Initial wall temperatures
11	Hydraulic diameter
12-26	...
Input Global Parameters	
27	Wall heat transfer
28	Interfacial friction
29	Interphase heat transfer
30	Wall friction
31	Heat transfer (enhancement) at the quench front
32-40	...
Input Coefficient Parameters	
41	Droplet diameter
42	Droplet critical Weber number
43-72	…

4.5 Identified Influential IP

As the following step, participants performed the sensitivity studies and selected the most influential parameters. The criteria used for selection differ from one participant to another. Some organisations applied the set of criteria proposed in Specifications for Phase II (recited in section 0), some participants used the proposed criteria as a base but modified the quantitative thresholds (e.g., ΔT_{ref} = 30K instead of 50K), others applied their own methodology. In the latter case, not all participants provided precise quantitative criteria adopted by them for selection of influential IP. Table 4.5 provides information regarding approaches adopted by participants.

Applying the adopted set of criteria, participants identified the input parameters, influential for their reflood models. Figure 4.9 shows the number of parameters identified as influential. The statistics on influential input parameters identified by number of participants in shown on Figure 4.10 (to compare with Figure 4.8). The parameters, considered as influential by at least 5 participants are shown in bold and coloured in Table 4.6.

For each of 6 input parameters (except “heat transfer (enhancement) at the quench front”) identified by at least 5 participants as influential a Table and 3 Figures are provided with indicated range of variation of input parameter and variation of maximum cladding temperature at selected elevation (2225 mm or 1680 mm) and time of rewet at this elevation which correspond to extremes of the aforementioned range. When more than one code-specific parameter has been identified by a participant for the same parameter ID, the variations of responses were considered separately for each code-specific parameter and the results reported on the following Figures using the markers of the same colour but different shape (only one marker per participant is indicated on the Figures’ legends). The parameter “number of droplets in evaporation model” (ID 60), used by GRS in ATHLET code calculations, has been added for comparison in the Table 4.10 and Figure 4.20 through Figure 4.22 which summarize the results for “Interphase HTC” parameter (ID 29) provided by other participants. This is due to the proportional relation between the “number of droplets in evaporation model” and the interphase heat transfer in ATHLET code.

For parameter ID 31 “Heat transfer (enhancement) at the quench front” only a Table with indicated ranges of variation of input parameter and variation of maximum cladding temperature and time of rewet is provided. Since the actual parameters, corresponding to the parameter ID 31, are code specific (CATHARE, APROS and ATHLET), the comparative analysis is not performed within the frame of this report. The relative information may be found in each user report in Appendix B.

Table 4.5: Adopted criteria for selection of influential IP

Participant	Code	Criteria
GRS	ATHLET 2.2B	own
NRI	ATHLET 2.1A	own
Bel V	CATHARE 2 V2.5_2 mod8.1	as in Spec
CEA	CATHARE 2 V2.5_2 mod8.1	modified Spec
IRSN	CATHARE 2 V2.5_2 mod8.1	as in Spec
KAERI	MARS-KS1.3(COBRA-TF Module)	modified Spec
KINS	MARS-KS-003	modified Spec
OKBM	RELAP/SCDAPSIM Mod3.4	modified Spec
Tractebel	RELAP5 Mod3.3	own
UNIPI	RELAP5 Mod3.3 patch3	as in Spec
UPC	RELAP5 Mod3.3 patch4	as in Spec
KIT	TRACE Version 5 patch 3	own
VTT	APROS 5.11.02	as in Spec

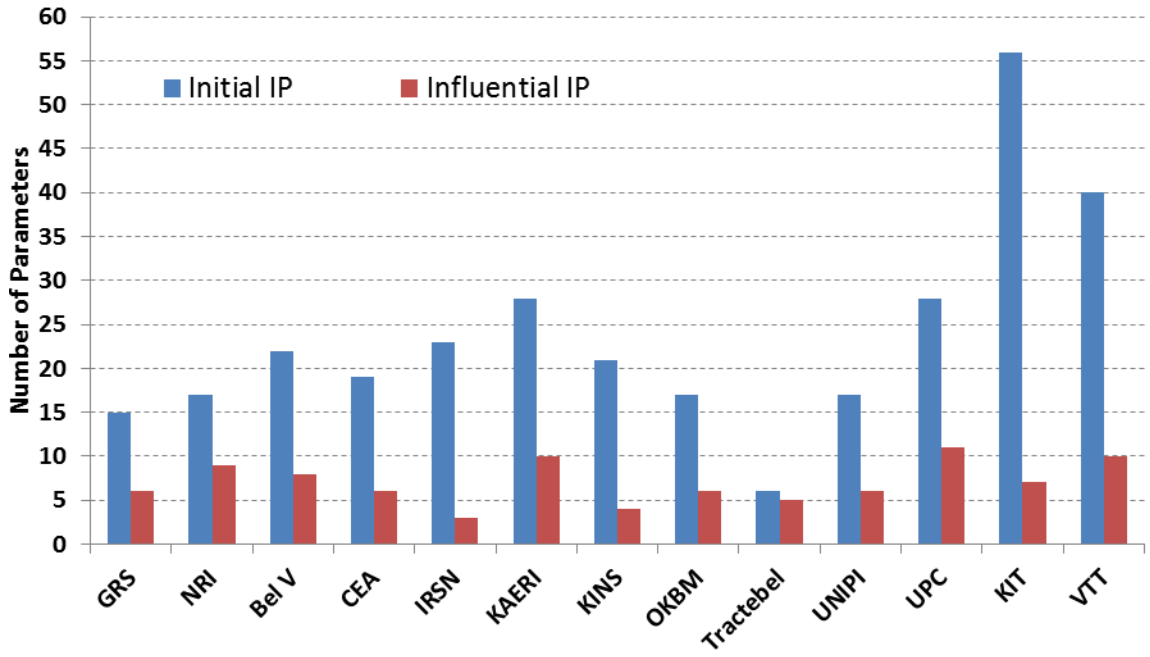

Figure 4.9: Selection of influential IP by participants

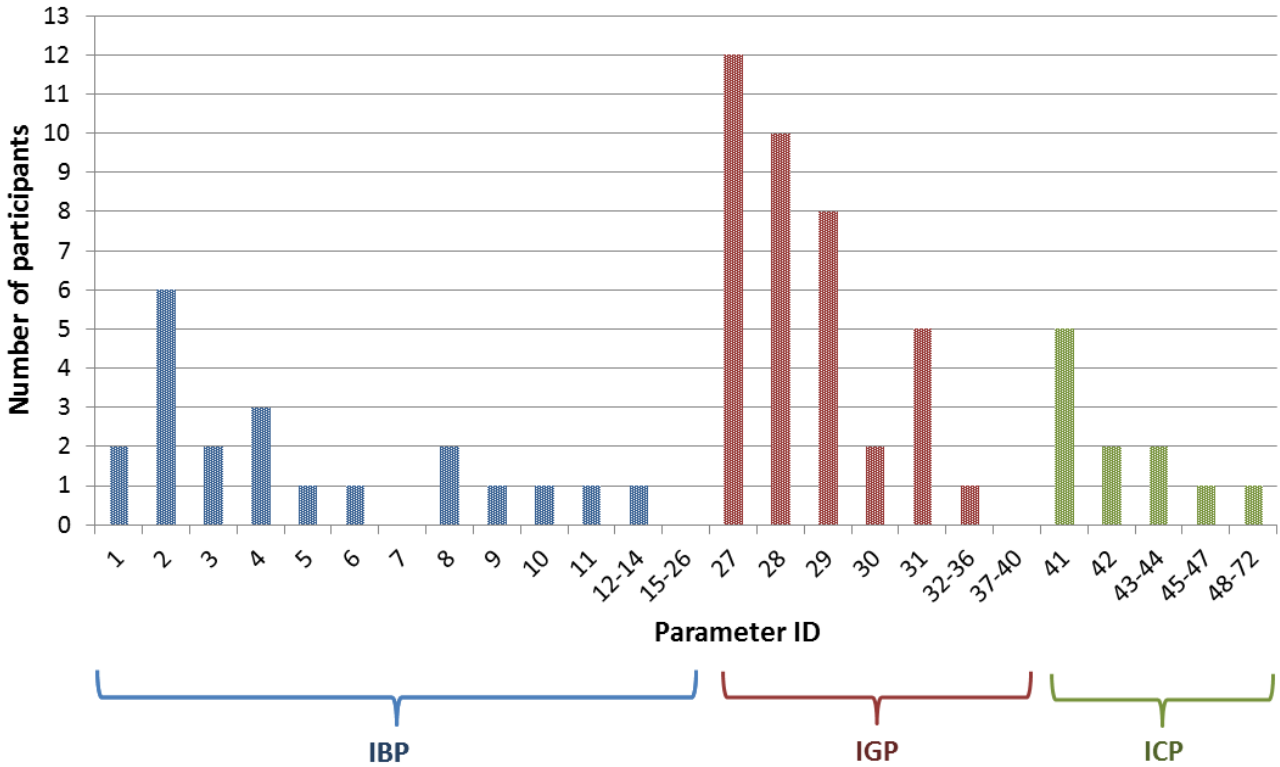

Figure 4.10: Selected influential input parameters

Table 4.6: Parameters identified as influential by majority

ID	Parameter
Input Basic Parameters	
1	Inlet liquid temperature
2	**Power/power density**
3	Pressure
4	Inlet liquid mass flow/flux/velocity
5	Thermal conductivity of heater
6	Heat capacity of heater
7	Thermal conductivity of insulation
8	Heat capacity of insulation
9	Spacer Form loss coefficients
10	Initial wall temperatures
11	Hydraulic diameter
12-26	...
Input Global Parameters	
27	**Wall heat transfer**
28	**Interfacial friction**
29	**Interphase heat transfer**
30	Wall friction
31	**Heat transfer (enhancement) at the quench front**
30-40	...
Input Coefficient Parameters	
41	**Droplet diameter**
42	Droplet critical Weber number
43-73	…

Table 4.7: Power variation range and responses variations

Participant	Code	Parameter	Multiplier MIN	Multiplier MAX	T_{clad} variation [°C]	t_{rew} variation [s]
NRI	ATHLET 2.1A	Power	0.80	1.20	-78.5/+102.1	-44.6/-21.3
Bel V	CATHARE 2 V2.5_2 mod8.1	Average Rod Heat Flux	0.90	1.10	-5/+30	-21/+21
KAERI	MARS-KS1.3 (COBRA-TF Module)	Heater Power	0.98	1.02	-12.0/+7.9	-5.0/5.3
OKBM	RELAP/SCDAPSIM Mod3.4	Power density – bundle power	0.95	1.05	-24.5/+31.5	-18.5/+19.2
UPC	RELAP5 Mod3.3 patch4	Power density	0.90	1.10	-22 / +29	-22 / +20
KIT	TRACE Version 5 patch 3	Assembly power	0.90	1.10	-37.6/+34.4	-23.1/+18.1

Table 4.8: Wall HTC variation range and responses variations

Participant	Code	Parameter	Multiplier MIN	Multiplier MAX	T_{clad} variation [°C]	t_{rew} variation [s]
GRS	ATHLET 2.2B	Forced convection to steam – multiplier	0.85	1.25	+33/-55	+8/-11
		Film boiling – multiplier	0.65	1.30	+19/-38	+6/-8
Bel V	CATHARE 2 V2.5_2 mod8.1	Wall-fluid global heat transfer	0.80	1.20	+60/-30	+30/-20
CEA	CATHARE 2 V2.5_2 mod8.1	Wall-fluid global heat transfer	0.50	2.00	+95/-108	+57.1/-45.1
IRSN	CATHARE 2 V2.5_2 mod8.1	Wall-fluid global Heat Transfer downstream quench front	0.50	3.00	+144 / −97	+66 / −81
KINS	MARS-KS-003	Convection to superheated vapour (linear interpolation between Reynold number 3000 and 10000)	0.50	1.50	+68.7/-37.2	-
OKBM	RELAP/SCDAPSIM Mod3.4	Wall heat transfer coefficient (all modes)	0.90	1.10	+41.6/-37.9	+23.1/-19.2
Tractebel	RELAP5 Mod3.3	Heat transfer wall to liquid	0.80	1.20	1.8/0.9	6.0/-6.0
		Heat transfer wall to vapour	0.80	1.20	5.7/-3.0	-41.0/11.0
UNIPI	RELAP5 Mod3.3 patch3	Film boiling wall-to-liquid HTC	0.50	3.00	+13 / -34	+58 / -62
		Film boiling wall-to-vapour HTC	0.65	4.00	+59 / -44	0 / -30
UPC	RELAP5 Mod3.3 patch4	Film boiling wall-to-fluid HTC	0.40	2.00	+50 / -23	+60 / -34
		Film boiling wall-to-vapour HTC	0.40	2.00	+25 / -33	-48 / -8
KIT	TRACE Version 5 patch 3	HTC vapour	0.80	1.24	+1.4/-12.7	-1.1/-8.2
		HTC DFFB	0.68	1.48	+6.4/-20.6	-1.0/-1.0
VTT	APROS 5.11.02	Heat transfer to dry wall / Forced convection to gas	0.50	1.50	+102 / -70	+13 / -10

Table 4.9: Interphase friction coefficient variation range and responses variations

Participant	Code	Parameter	Multiplier MIN	Multiplier MAX	T_{clad} variation [°C]	t_{rew} variation [s]
Bel V	CATHARE 2 V2.5_2 mod8.1	Interfacial friction	0.90	5.00	0/0	-5/+100
CEA	CATHARE 2 V2.5_2 mod8.1	Interfacial friction	0.10	10.00	+12/-54	-25.8/+54.4
IRSN	CATHARE 2 V2.5_2 mod8.1	Interfacial friction downstream quench front	0.25	4.00	+20 / −32	-21 / +23
KAERI	MARS-KS1.3(COBRA-TF Module)	Droplet friction factor	0.50	2.00	+22.3/-27.6	+6.0/-8.0
OKBM	RELAP/SCDAPSIM Mod3.4	Interface friction coefficient	0.80	1.20	-52.3/+55.3	-31.3/+34.6
Tractebel	RELAP5 Mod3.3	Junction interphase friction	2.00	10.00	+15.7/+68	+65/+238
		Interphase friction	2.00	10.00	+13/+63	+66/+261
UNIPI	RELAP5 Mod3.3 patch3	Resulting interphase friction at junctions	0.50	1.50	-12 / +11	-55 / +45
		Junction interphase drag for bubbles and droplets	0.50	1.50	-15/+15	-46/+40
UPC	RELAP5 Mod3.3 patch4	Interfacial friction coefficient: global	0.50	1.50	0 / +12	-49 / +40
		Interfacial friction coefficient: dispersed vapour	0.50	1.50	+9/-18	-15/+20
		Interfacial friction coefficient: bubbles and droplets	0.50	1.50	-7/+13	-45/+45
KIT	TRACE Version 5 patch 3	Interfacial drag coefficient	0.85	1.15	-16.2/+7.5	-12.0/+6.1
VTT	APROS 5.11.02	Interfacial friction	0.10	10.00	-155 / -46	-33.5 / +85

Table 4.10: Interphase HTC variation range and responses variations

Participant	Code	Parameter	Multiplier MIN	Multiplier MAX	T_{clad} variation [°C]	t_{rew} variation [s]
CEA	CATHARE 2 V2.5_2 mod8.1	Interface-vapour heat transfer	0.50	2.00	+20/-20	+3.2/-2.5
KAERI	MARS-KS1.3 (COBRA-TF Module)	Interfacial HT model of Droplet	0.50	2.00	+36.5/-34.5	+36.5/-34.5
KINS	MARS-KS-003	Interfacial heat transfer of drop-steam (TRACE blowing factor)	0.50	2.00	+29.4/-44.78	-
Tractebel	RELAP5 Mod3.3	Dry wall Dispersed heat transfer	0.80	1.20	6.8/-5.5	1.0/-5.0
		Heat Partitioning (either on dry or wet wall)	0.80	1.20	6.9/-6.7	7.0/-4.0
UNIPI	RELAP5 Mod3.3 patch3	Interphase heat transfer in dispersed flow for dry wall	0.20	5.00	+79 / -56	+31 / -85
UPC	RELAP5 Mod3.3 patch4	Interphase heat transfer coefficient: dry wall	0.10	10.00	+57 / -15	+9 / -77
KIT	TRACE Version 5 patch 3	HTC interface	0.75	1.25	+18.9/-16.7	+2.0/-3.0
VTT	APROS 5.11.02	Heat transfer between gas and interface	0.05	2.00	+163 / -48	+33 / -2
GRS	ATHLET 2.2B	Number of droplets (equivalent with interfacial area for high void fraction) in evaporation model	1.0	10.0	0.0/-62	0.0/-19

Table 4.11: Droplet diameter variation range and responses variations

Participant	Code	Parameter	Multiplier MIN	Multiplier MAX	T_{clad} variation [°C]	t_{rew} variation [s]
CEA	CATHARE 2 V2.5_2 mod8.1	Global droplet diameter	0.50	2.00	-25/+25	+7.8/-5.7
Tractebel	RELAP5 Mod3.3	Droplet Min/Max diameter	0.80	1.20	-6.9/3.9	11.0/-9.0
UNIPI	RELAP5 Mod3.3 patch3	Minimum droplet diameter	0.70	2.50	0 / 0	+55 / -48
UPC	RELAP5 Mod3.3 patch4	Minimum droplet diameter: volumes	0.33	2.00	-22 / +36	-59 / +22
		Minimum droplet diameter: junctions	0.33	2.00	+76/-8.0	+22/-45
VTT	APROS 5.11.02	Max droplet diameter above quench front	0.5	3.2	-74 / +90	+39 / +7.5

Table 4.12: Heat transfer at quench front variation range and responses variations

Participant	Code	Parameter	Multiplier MIN	Multiplier MAX	T_{clad} variation [°C]	t_{rew} variation [s]
GRS	ATHLET 2.2B	Heat transfer at quench front	1.00	10.00	0.0/-11	0.0/-68
Bel V	CATHARE 2 V2.5_2 mod8.1	Specific parameter to very local QF progression (K2)	0.50	1.50	0.0/-20	+100/-70
CEA	CATHARE 2 V2.5_2 mod8.1	Very local QF progression (K2)	0.50	2.00	+6/-40	+46.7/-57.3
IRSN	CATHARE 2 V2.5_2 mod8.1	K2 reflood parameter	0.50	2.00	+1/-18	+37/-59
VTT	APROS 5.11.02	Additional heat flux near quench front	0.50	7.50	-59/-278	+26/-53.5

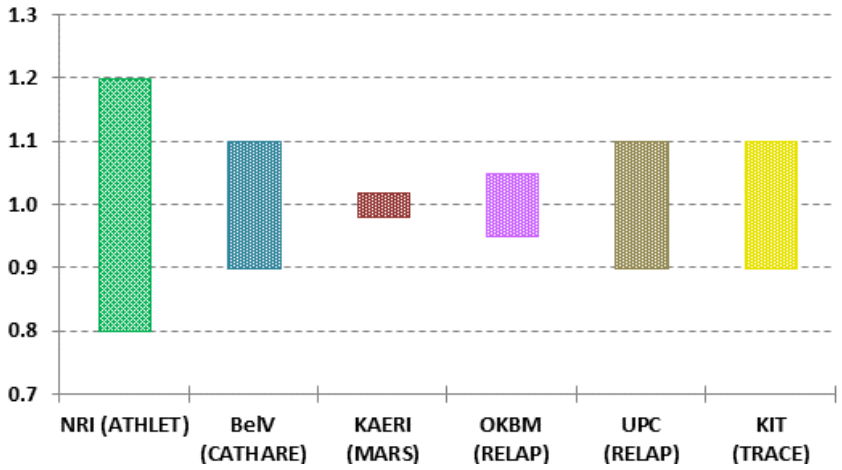

Figure 4.11: Power variation range (multiplier)

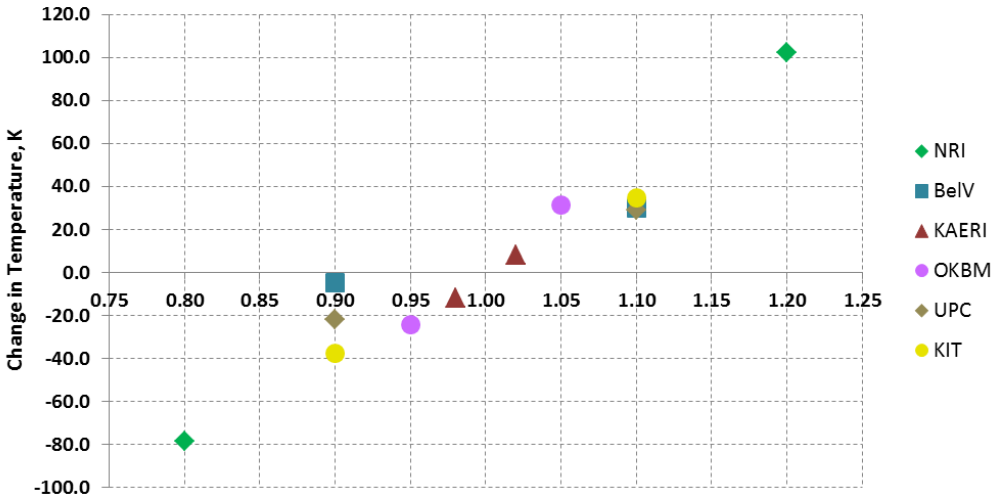

Figure 4.12: Cladding temperature vs power (multiplier)

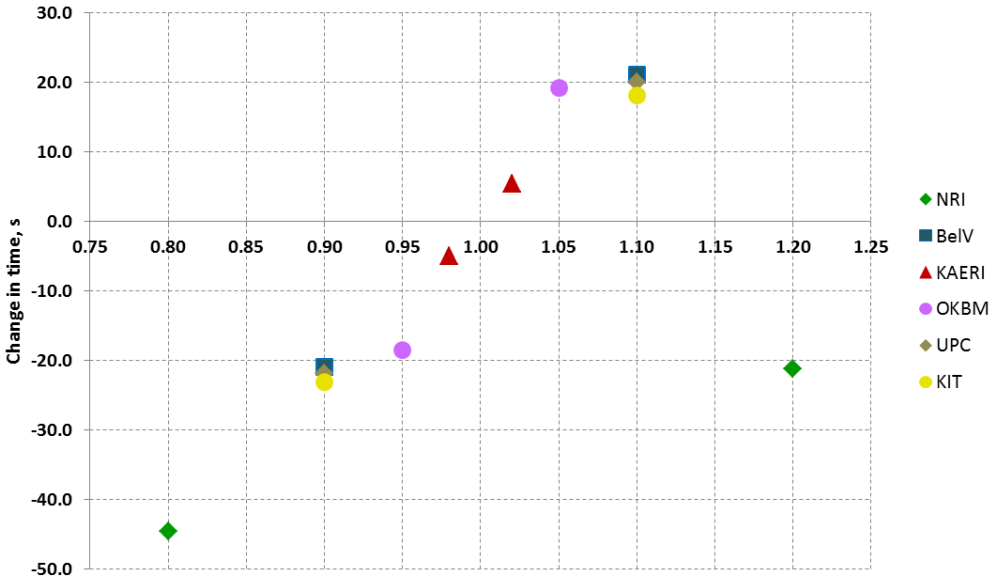

Figure 4.13: Time of rewet vs power (multiplier)

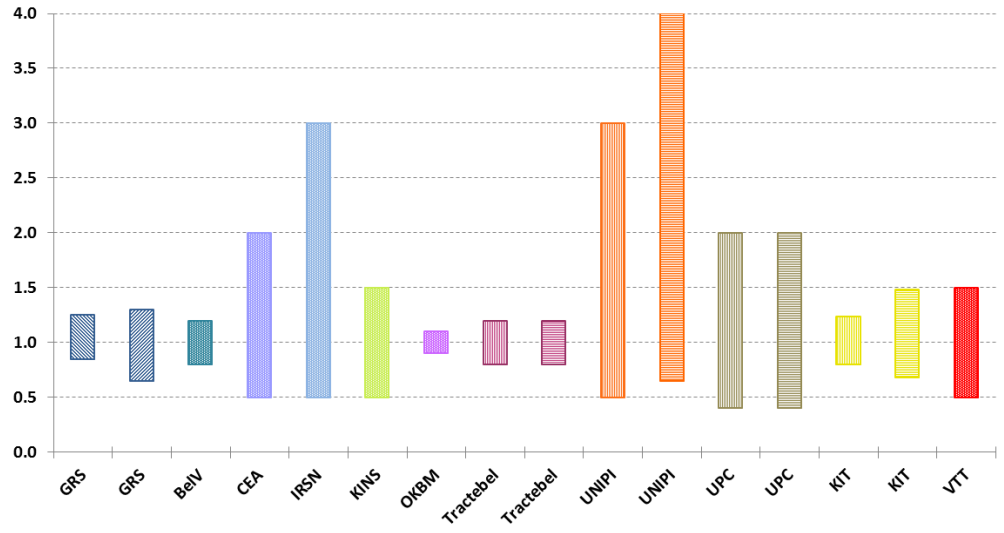

Figure 4.14: Wall HTC variation range (multiplier)

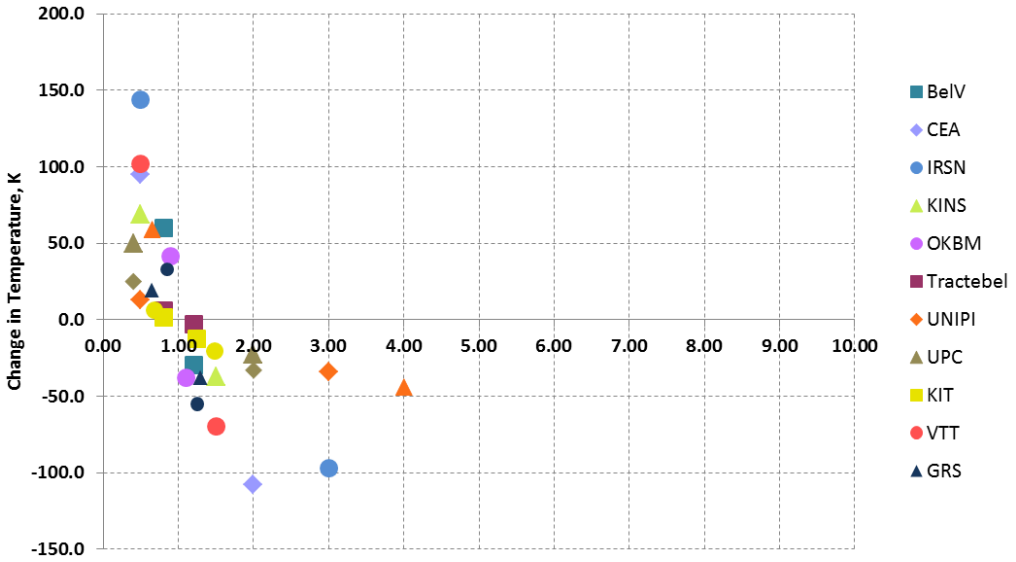

Figure 4.15: Cladding temperature vs wall HTC (multiplier)

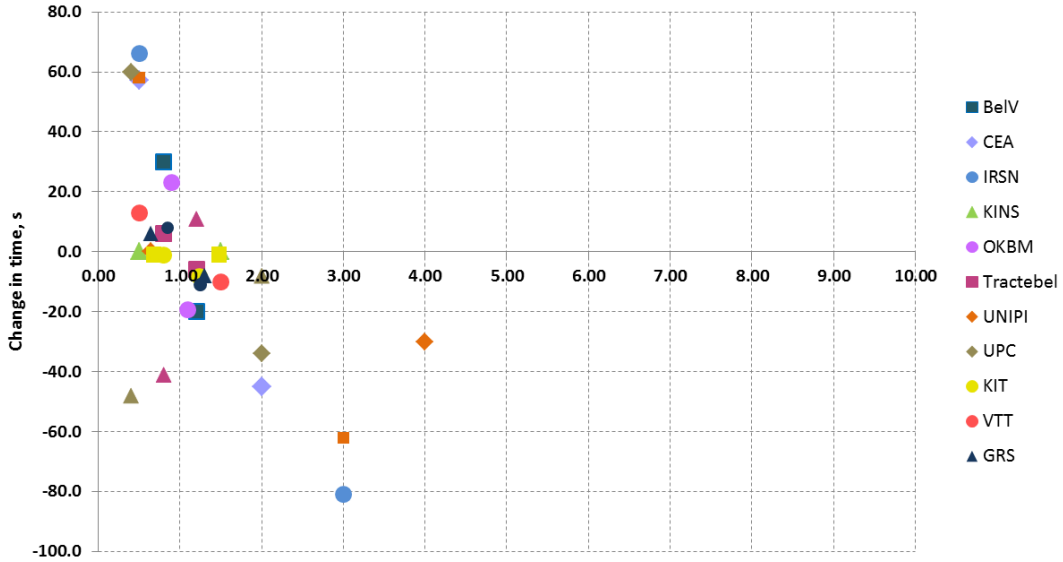

Figure 4.16: Time of rewet vs wall HTC (multiplier)

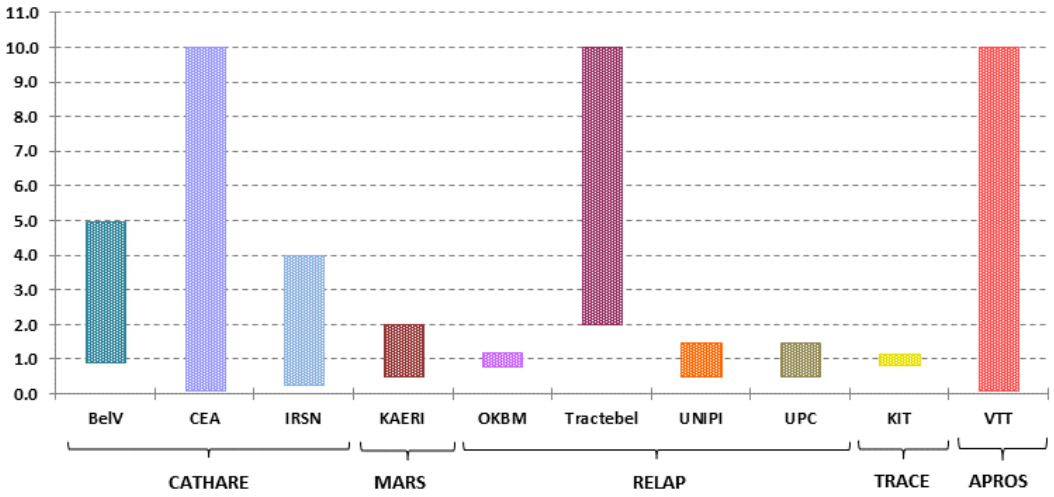

Figure 4.17: Interphase friction coefficient variation range (multiplier)

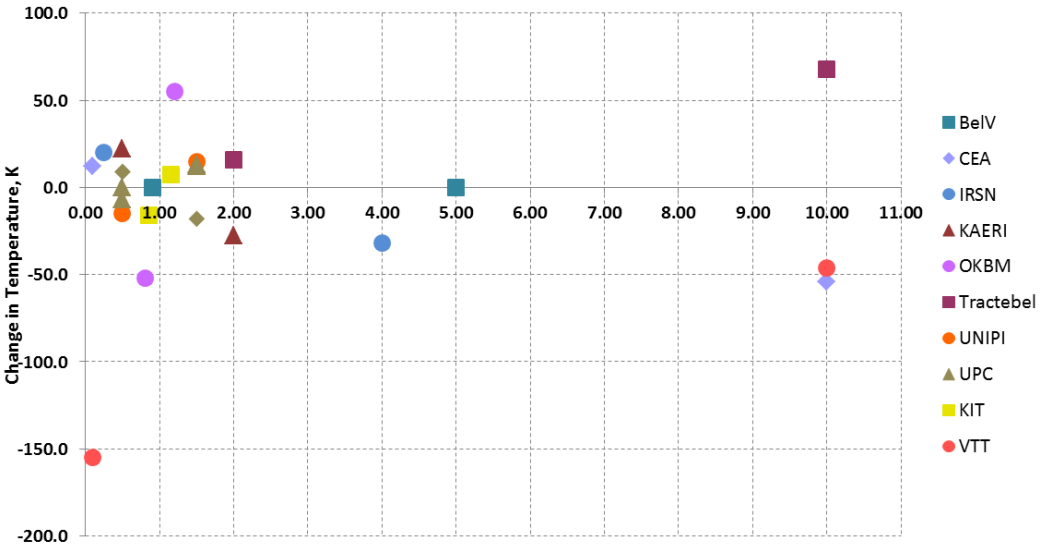

Figure 4.18: Cladding temperature vs interphase friction coefficient (multiplier)

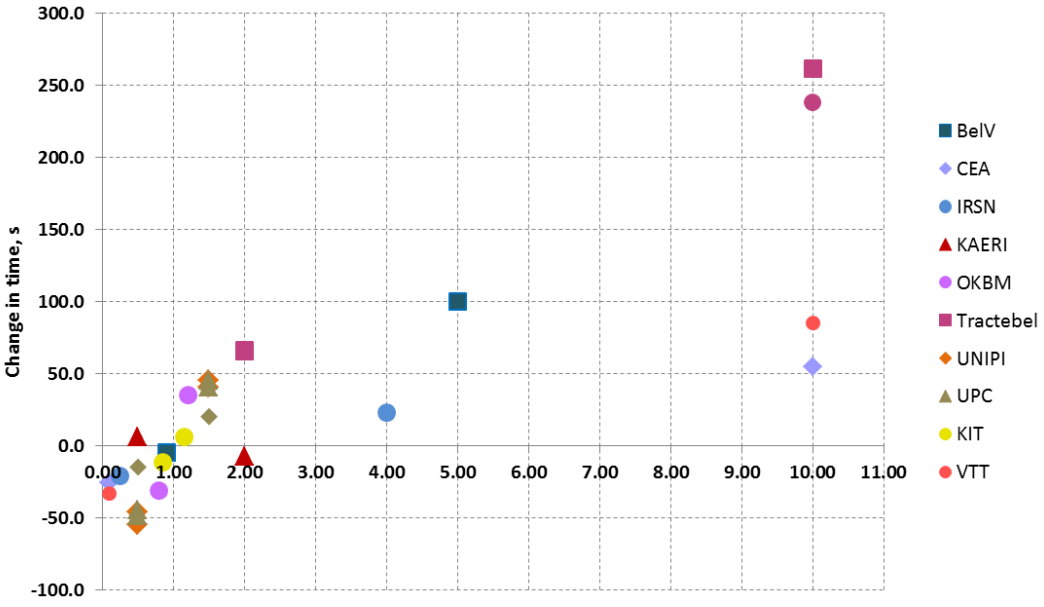

Figure 4.19: Time of rewet vs interphase friction coefficient (multiplier)

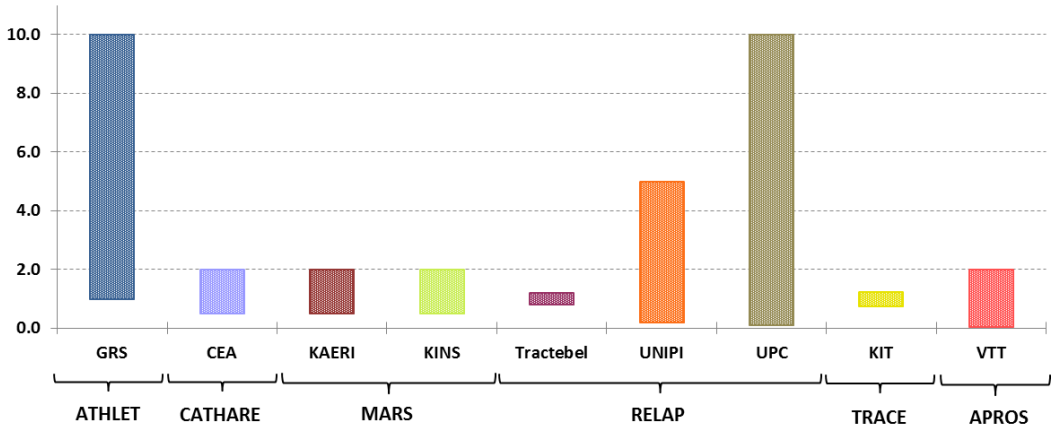

Figure 4.20: Interphase HTC variation range (multiplier)

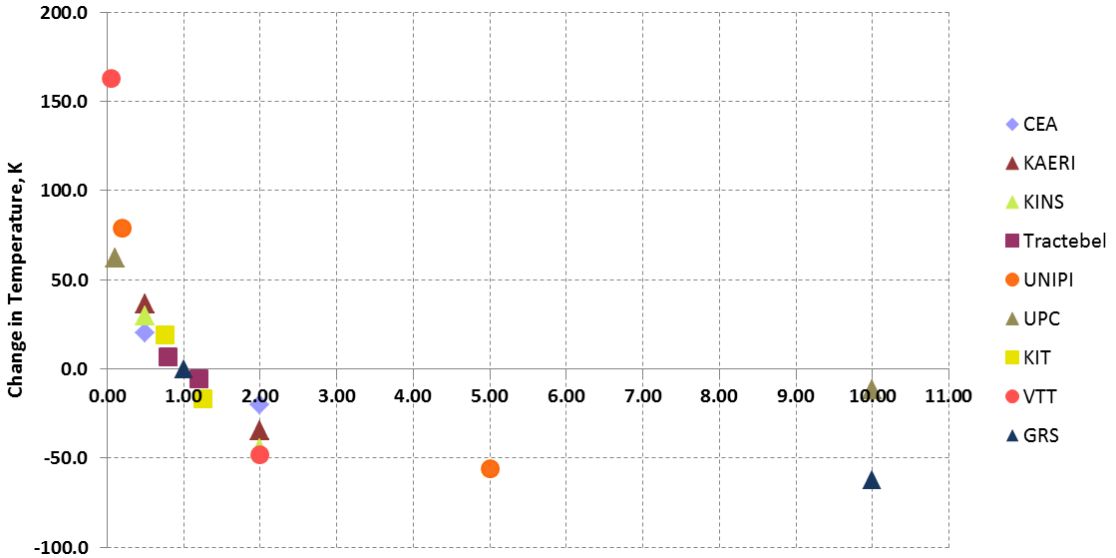

Figure 4.21: Cladding temperature vs interphase HTC (multiplier)

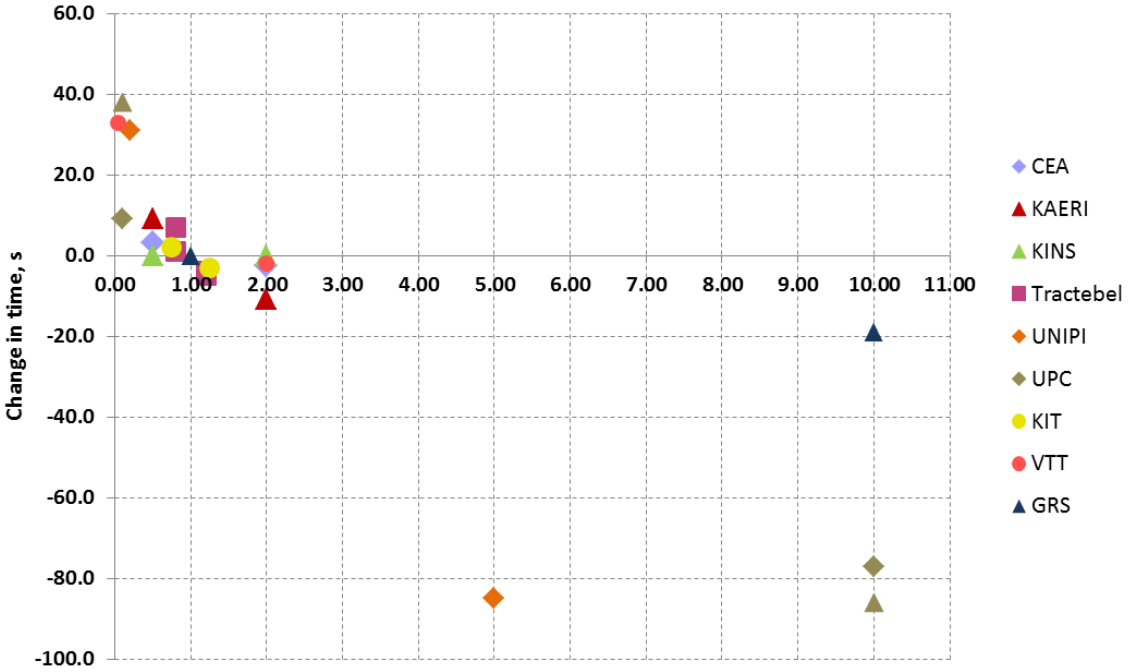

Figure 4.22: Time of rewet vs interphase HTC (multiplier)

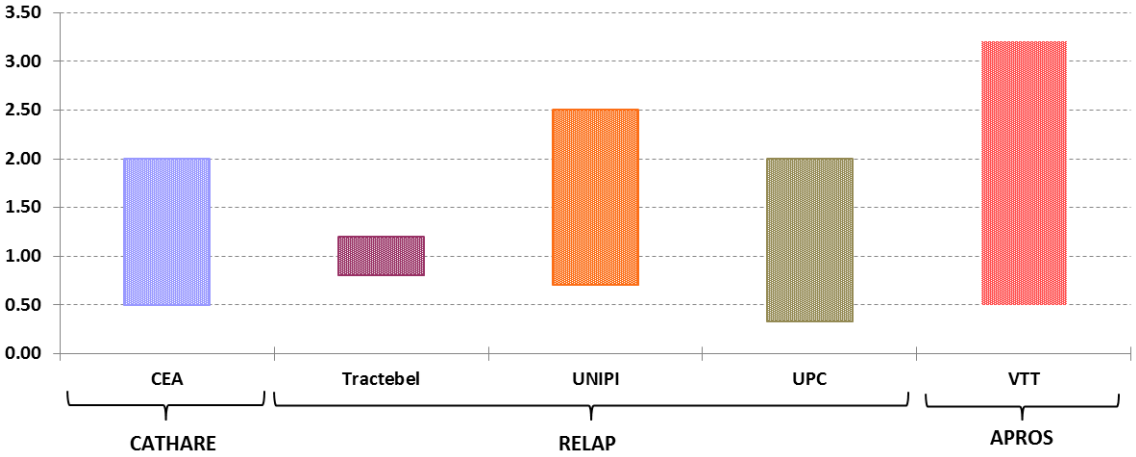

Figure 4.23: Droplet diameter variation range (multiplier)

Figure 4.24: Cladding temperature vs droplet diameter (multiplier)

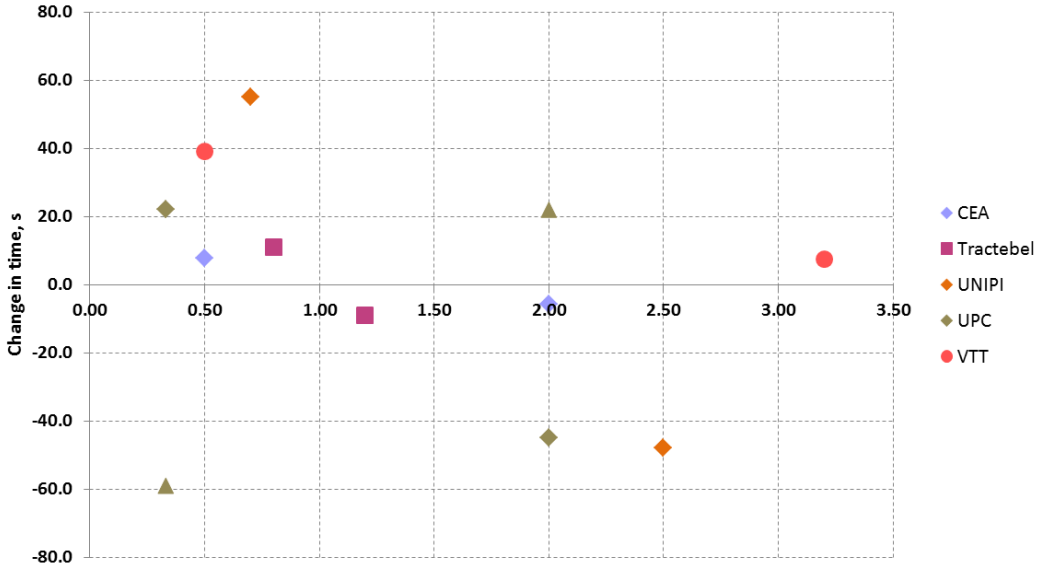

Figure 4.25: Time of rewet vs droplet diameter (multiplier)

Six participating organisations identified bundle power (density) as an influential input parameter. Five participants reported rather large variation of power range (from 5%, to even 20%). Only one participant who varied bundle power (KAERI) used the realistic power variation range (Figure 4.11). The variations in both responses (cladding temperature (Figure 4.12) and time of rewet (Figure 4.13)) are linear and consistent between different participants and codes with respect to change in power. Only in NRI results (who applied the largest variation range 20%) the earlier rewet time is observed on both extreme of power variation range. It should be noted, that the bundle power has been identified by participants as influential through a significant variation (10% to 20% variation for 4 out of 6 participants). Besides, its uncertainty has to be considered as known a priori. The bundle power uncertainty quantification is not a subject of the benchmark and it should be obtained on the basis of experiment descriptions. For both experiments FEBA (Phase III) and PERICLES (Phase IV) the bundle power uncertainty will be provided by the Phase coordinator.

Eleven participating organisations identified heat transfer coefficient at the wall as an influential input parameter (Figure 4.14). The comparison between identified ranges of variation and corresponding responses of heat transfer coefficient at the wall is complicated by the fact that some participants considered separate wall-to-liquid and wall-to-vapour HTC while others considered only one global HTC (GRS considered 3 parameters related to wall heat transfer). Hence, the different IP variation ranges were obtained. The variations in cladding temperature show non-linear behaviour (Figure 4.15); however this behaviour is monotonic, and would be more linear by using a logarithmic scale for the value of the multiplier. The observed behaviour is also different between the different codes but more similar for the same code (e.g., RELAP5 or CATHARE “groups”). On the contrary, the variations in time of rewet show significant spread between the different participants and codes (Figure 4.16). TRACE and MARS show very low sensitivity of time of rewet with respect to variation in wall HTC comparing to other codes.

Ten participating organisations identified interphase friction coefficient as an influential input parameter (Figure 4.17). The variation ranges chosen by the participants are very different. They range from rather large variations for CATHARE code chosen by CEA and for APROS by VTT to quite small variations ranges chosen for RELAP by OKBM and for TRACE by KIT. Tractebel performs only one side variation (2.0-10.0). It claims taking into account the bias, inherent to the original model of interphase friction in RELAP5 code. Contrary (positive and negative) changes of cladding temperature with interphase friction variation by participants can be observed. The analysis of Table 4.9 allows speculation on the reasons. Such differences may be caused by variation of different correlations by different participants: for interphase friction for dispersed droplet flow (described also as interphase friction downstream from the quench front) and global interphase friction. Application of multiplier to global interfacial friction leads to positive dependency (larger multiplier causes larger cladding temperature). Application of multiplier to interfacial friction factor for dispersed droplet flow results in negative dependency. It can be seen very well in the results of UPC with RELAP code. UPC considers both correlations separately. The results for interfacial friction for bubbles and droplets/global correlation (triangles in the Figure 4.18) show positive dependency and the results for dispersed droplet flow (rhomb in the Figure 4.18) show negative dependency. It may be noted that the smaller variation of interfacial friction performed for RELAP by OKBM leads to the larger variation of cladding temperature observed among all RELAP users (which suggests the nodalization-dependency). Reduction of cladding temperature for both increasing and decreasing interphase friction coefficient in APROS code should be noted also. The variations in time of rewet are qualitatively similar for all codes, except KAERI calculations with COBRA-TF (Figure 4.19).

Eight participating organisations identified interphase heat transfer coefficients as an influential input parameter (Figure 4.20). Obtained variation ranges are different due to different adopted set of criteria for selection of influential input parameters and differences in code models. Nevertheless, the variations in cladding temperature are qualitatively similar between different codes (Figure 4.21), although rather different values of this temperature were achieved by decreasing interphase HTC. Like for the wall heat transfer, the variation of the cladding temperature with respect to the interphase heat transfer coefficients is monotonic, and shows more linear behaviour by using a logarithmic scale for the value of the multiplier. A similar behaviour is observed in variation of time of rewet (Figure 4.22).

Five participating organisations identified droplet diameter as an influential input parameter (Figure 4.23). Similar variation ranges of the input parameter were identified for the different codes (except Tractebel who used own criteria for IP selection). Here, UPC considered separate variation of droplet diameter in the

calculation of friction for volumes (triangles on the Figure) and for junctions (rhombs on the Figure) while UNIPI and Tractebel considered simultaneous variation of this parameter both for volumes and junctions. It is remarkable, that UNIPI and Tractebel (RELAP5) predicted almost no variation in cladding temperature on the contrary to UPC who used the same code but treated volumes and junctions separately. The similarity of CATHARE results to those obtained by RELAP for volumes may be noted. The variations in time of rewet show significant spread (Figure 4.25) depending on the code and selected model.

Five participating organisations identified the enhancement in heat transfer at the quench front as an influential input parameter (Table 4.12). Since the actual parameters identified are code specific, therefore the comparative analysis between those parameters was not performed in the frame of the benchmark. Nevertheless, it may be noted that the variation ranges of K2 parameter of CATHARE code are similar between the code users, but the corresponding variation of responses is rather different. It might be concluded that in CATHARE code the influence of K2 reflood parameter is input-data-deck dependent.

5. SELECTED INPUT PARAMETERS FOR PHASE III

Finally, from the parameters, identified as influential, the participants selected those to be used at the Phase III (Figure 5.1). Here, some organisations reduced the number of input parameters due to following reasons:

- some influential IP will be fixed at the following calculations, as it can be the case for the IBP, since their uncertainty is usually given from experimental data (will be provided by Phase III coordinator);
- some ICP being a part of the correlation for already considered IGP, as it is the case for the droplet diameter, being constitutive to the interphase friction and the interphase heat transfer coefficients.

The statistics on input parameters to be used in Phase III by number of participants is shown on Figure 5.2 (to compare with Figure 4.8 and Figure 4.10).

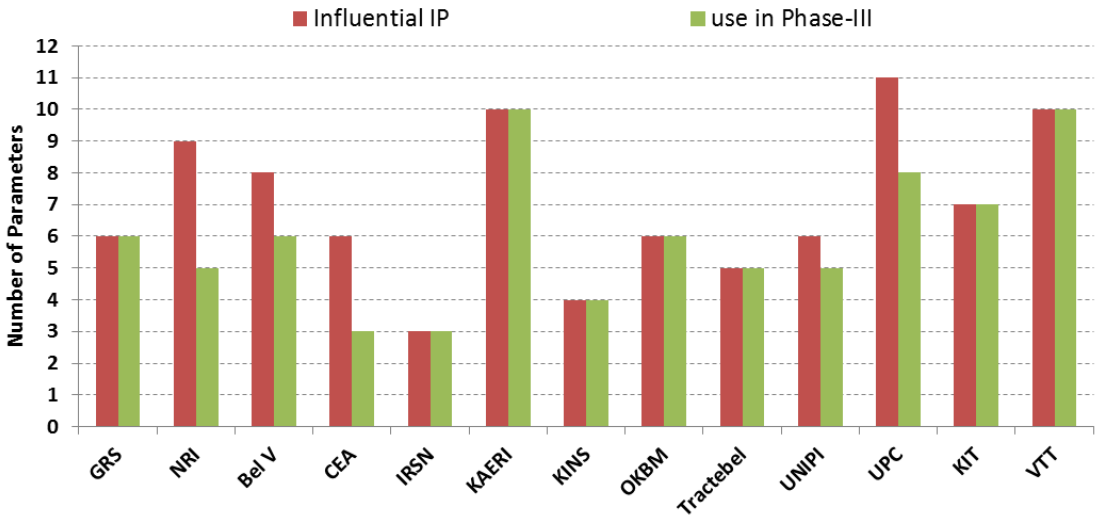

Figure 5.1: IP to be used in Phase III by participants

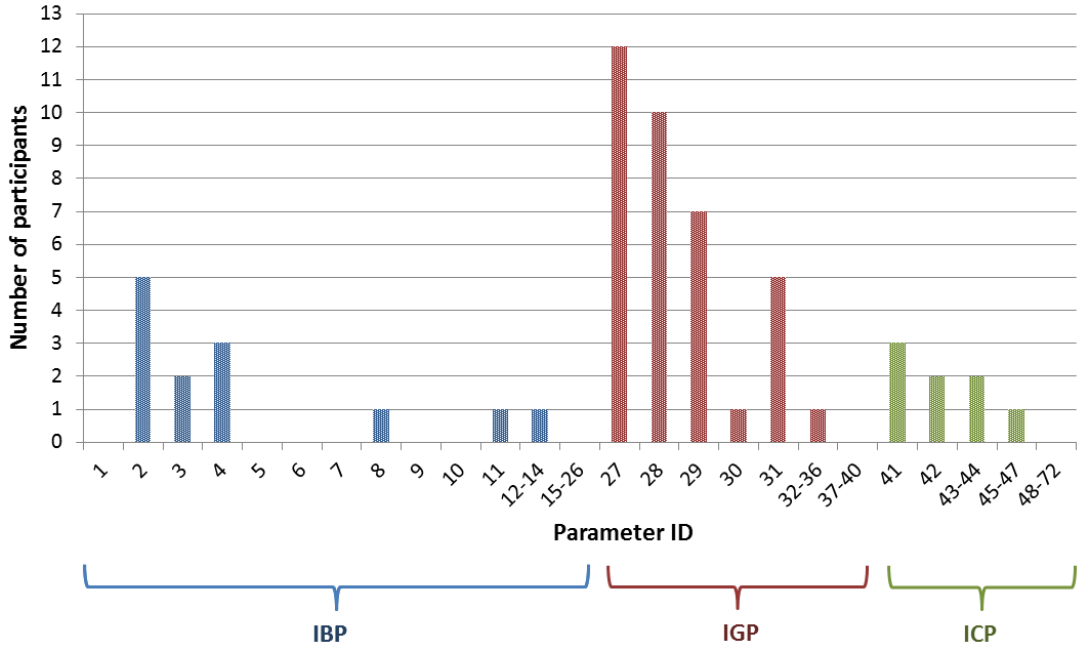

Figure 5.2: Input parameters to be used in Phase III

6. CONCLUSIONS

A procedure for the identification of influential code input parameters has been set up in Specification of Phase II of OECD/NEA PREMIUM benchmark. A set of quantitative criteria has been proposed for identification of influential IP and their respective variation range. A sample list of parameters, potentially influential on reflood phenomena, was provided in Specifications.

The influential IP identification has been performed based on the experimental test 216 of FEBA facility. Geometrical properties, boundary conditions and measured data were provided to benchmark participants.

Thirteen participating organisations, using 8 different codes (7 system thermal-hydraulic codes and 1 sub-channel module of a system thermal-hydraulic code) submitted Phase II results. The base case calculations show spread in predicted cladding temperatures and quench front propagation that has been characterized. All the participants, except one, predict a too fast quench front progression. Besides, the cladding temperature time trends obtained by almost all the participants show oscillatory behaviour which may have the numeric origins.

Adopted criteria for identification of influential input parameters differ between the participants: some organisations used the set of criteria proposed in Specifications “as is”, some modified the quantitative thresholds proposed in Specifications, and others used their own methodologies (no detailed quantitative information on adopted criteria was provided in these cases). This fact was a partial reason for the different ranges of input parameter variation identified by participants, besides differences to the physical models adopted by the different codes. Therefore, such different ranges of IP variation and, correspondingly, in different variations of cladding temperature and time of rewet, render rather difficult the task of meaningful and easy-comprehendible comparison of Phase II results.

Out of total 72 input parameters, initially considered by all participants, only 6 were identified as influential by more than 4 participants:

- bundle power;
- wall heat transfer coefficient;
- interphase friction coefficient;
- interphase heat transfer coefficient;
- heat transfer (enhancement) at the quench front;
- droplet diameter.

It should be noted that actual parameters considered in parameter “Heat transfer (enhancement) at the quench front” are code-specific and may have different influence on calculation results.

Several participants discarded some identified influential parameters (e.g., droplet diameter) due to existing relation between “coefficient” parameter and “global” parameter. Some participants also discarded identified influential Input Basic Coefficients (e.g., bundle power) since their uncertainty is not to be determined in the Phase III but will be provided by the coordinator from experimental data.

The behaviour of the variation of the responses at the extremes of IP range of variation greatly depends on the type of input parameter and on the code used. Mainly, the following two different behaviours can be characterized:

- For some parameters, like power, wall HTC and interphase HTC a qualitative agreement between different codes is observed (but not quantitative).
- For other parameters, like interphase friction coefficient and droplet diameter, a contrary behaviour (i.e., in correspondence of one of the extreme of the IP range, the direction of change of the responses is different) between different codes and even between different selected models within the same code can be observed. It shows that the effect of such parameters on the cladding temperatures is quite complex, probably because it involves a lot of physical models (e.g.: via interphase friction and interphase heat transfer coefficients for the droplet diameter).

It shall be noted that, the analysis of differences between the reflood models of different codes is out of scope of the PREMIUM benchmark. It is recommended to take into account those results obtained with the same code as the ones to be applied in the Phase III of PREMIUM Benchmark.

REFERENCES

/1/ A. Petruzzi, A. Kovtonyuk, F. D'Auria, ***Specifications for Phase-II of the PREMIUM benchmark,*** PREMIUM-1/01(11) Rev.1, Pisa, Italy, March 2012.

/2/ T. Skorek, ***Description of FEBA Test Facility and FEBA/SEFLEX Experimental Program,*** OECD/NEA PREMIUM benchmark, GRS, Germany, October 2012.

/3/ J.C. Chen, ***Correlation for boiling Heat transfer to Saturated Fluids in convective Flow,*** 1-EC Process Design and Development, Vol. 5, No 3, July 1966.

/4/ K.J. Liesch, G. Raemhild, K. Hofmann, ***Zur Bestimmung des Wärmeübergangs und der kritischen Heizflächenbelastung in Hinblick auf besondere Verhältnisse in den Kühlkanälen eines DWR die schweren Kühlmittelverluststörfällen,*** *MRR 150, 19765*.

/5/ D.C. Groeneveld, ***An investigation of Heat Transfer in the Liquid deficient Regime,*** AECL-3281, December 1968.

/6/ I. Voitek, ***uswertung der 25-Stabbündel-Versuche mit dem Rechenprogramm BRUDI-VA,*** GRS-A-208, September 1978.

/7/ H. Austregesilo et al., ***ATHLET Mod2.2 Cycle A Models and Methods,*** GRS-P-1, Vol.4, GRS, July 2009.

/8/ ***TRACE V5.0 Theory manual – Field equations, solution methods and physical models,*** U.S. Nuclear Regulatory Commission, 2008

/9/ M.I. Drucker, V. K. Dhir, and R. B. Duffey, ***Two-Phase Heat Transfer for Flow in Tubes and Over Rod Bundles with Blockages,*** *J. Heat Transfer, 106, 856-864, 1984*

A. APPENDIX: FULL LIST OF CONSIDERED INPUT PARAMETERS

Tab A.1.1 List of all considered input parameters

ID	Parameter
Input Basic Parameters	
1	Inlet liquid temperature
2	Power/power density
3	Pressure
4	Inlet liquid mass flow/flux/velocity
5	Thermal conductivity of heater
6	Heat capacity of heater
7	Thermal conductivity of insulation
8	Heat capacity of insulation
9	Spacer Form loss coefficients
10	Initial wall temperatures
11	Hydraulic diameter
12	Flow area
13	Spacer blockage ratio
14	Wall roughness
15	Thermal loss
16	Power Peaking factor
17	Housing thickness
18	Liquid density
19	Liquid specific heat
20	Liquid thermal conductivity
21	Liquid dynamic viscosity
22	Vapour density
23	Vapour specific heat
24	Vapour thermal conductivity
25	Vapour dynamic viscosity
26	Wall emissivity
Input Global Parameters	
27	Wall heat transfer
28	Interfacial friction
29	Interphase heat transfer
30	Wall friction
31	Heat transfer (enhancement) at the quench front: - 2-D wall conduction: k2 (CATHARE specific) - Additional heat flux near quench front (APROS specific) - Heat transfer at quench front (ATHLET specific)
32	CHF correlation/table

33	Turbulent HT correlation
34	Laminar HT correlation
35	Chen nuclear boiling correlation
36	Modified Bromley correlation
37	Vapour FLETCH SEASET correlation
38	Pool boiling CHF(Zuber)
39	Spacer enhancement HTC
40	Quench front height
Input Coefficient Parameters	
41	Droplet diameter
42	Droplet critical Weber number
43	Rate of entrainment
44	Quench front threshold distance for HTC transitions
45	Droplet two phase enhancement
46	Interfacial area
47	Minimum temperature of stable film boiling
48	Droplet entrainment Interfacial friction
49	Droplet entrainment Interface to Fluid
50	Drop evaporation efficiency of transition boiling heat transfer
51	Droplet breakup efficiency
52	T_CHF (depends on Q_NB&Q_CHF) of Biasi, Zuber CHF correlation
53	Tmin (Boerrenson coefficient correlation)
54	Grid heat transfer enhancement
55	Hot wall flow regime criteria
56	Relative velocity in bundle
57	HTC MgO – Cladding interface
58	HTC housing – isolation interface
59	Two phase flow multiplier - pressure
60	No of droplets in evaporation model
61	Forslund-Rohsenow equation
62	Effect of spacer grids on CHF and transition boiling heat transfer coefficient
63	Variable property effect
64	Entrance length effect
65	Vapour film thickness
66	Non-dimensional film thickness
67	Bundle correction factor
68	Emissivity (liquid)
69	Nusselt interface (liquid)
70	Terminal velocity
71	Nusselt droplet I
72	Nusselt droplet II

B. APPENDIX: FULL REPORTS OF PARTICIPANTS' RESULTS

B.1 Bel V (Belgium) results

Model description

Information about the code version and the software platform (Windows, Unix, Linux etc.) that has been used for the calculations.

Tab B.1.1 Bel V code and software platform

Institution name	Code version	Software platform
Bel V	CATHARE CAT2V2.5_2 mod8.1	Windows

Nodalization and basic geometrical properties

The test run 216 of FEBA experiment has been selected. The test section (heated part), rods and housing have been modelled.

On the 25 identical rods included in the test section, one single hydraulic channel (*GRAPP*) has been modelled with one heater rod (*CRAYONS*), the housing (*HOUSING*) and two boundary conditions (*ENTREE* and *OUTPUT*).

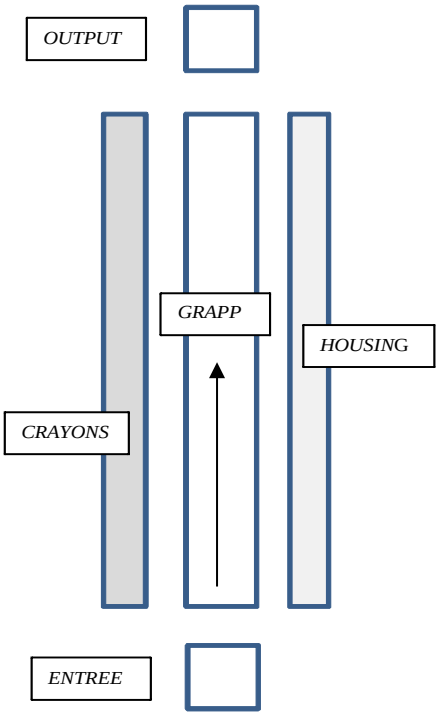

Fig B.1.1 FEBA nodalization

The main geometrical parameters:

Tab B.1.2 Model main geometrical parameters

FEBA 216 Facility component	CATHARE model	Total height (m)	Flow area (for one single hydraulic channel) (m^2)	Hydraulic diameter (for one single hydraulic channel) (m)	Heating perimeter (for one single rod) (m)	Pressure loss coeff. corr. to spacer grids (total value for 1 single hydraulic channel)	Total heat transfer area of the 25 heater rods (m^2)	Maximum linear heat rate (W/m)
Inlet	Inlet boundary condition (imposed injection velocity) (*ENTREE*, BC3B)	NA	NA	NA	NA	NA	NA	NA
Test section	One single hydraulic vertical channel 46 axial nodes (*GRAPP*, AXIAL)	3.9	155.73D-6	1.3444E-02	NA	1.68	NA	NA
Heater rod	One single heating structure 46 axial nodes (*CRAYONS*, WALL)	3.9	NA	NA	3.3772D-2	NA	24.05 = 9.6180E-01* 25	2.4410E+03
Housing	Non heating structure 46 axial nodes (*HOUSING*, WALL)	3.9	NA	NA	1.256D-2	NA	NA	NA
Outlet	Outlet boundary condition (imposed constant pressure) (*OUTPUT*, BC5A)	NA	NA	NA	NA	NA	NA	NA

Boundary and initial conditions

The boundary conditions applied to the model:

- Pressure = 4.12 10^5 Pa imposed constant at the outlet of the test section
- Flooding temperature follows the experimental time trend given in Figure 7 of the paper describing the FEBA facility [1].
- Flooding velocity = 3.8 10^{-2} m/s imposed constant at the inlet of the test section, after a delay of 7 s to take into account the delayed quenching observed in the time evolution of the clad temperatures at 3.860m during the experiment.
- Rod power follows the experimental time trend given in Figure 7 of the paper describing the FEBA facility [1].

- No heat losses modelled.

Adopted models (flags)

The radiation model between the housing and the heater rod was activated during the initialization step to raise the housing temperature. Afterwards, this radiation model was deactivated until the end of the calculation.

Assumptions and steady-state achievement

The conditions corresponding to the Start of Transient have been reached in 3 steps:

1. filling of the test section with stagnant vapour at saturation temperature;
2. rising of the temperature of the housing until it reaches 635°C at 1.625m elevation; during this step, a radiation model between housing and heater rod is activated;
3. rising of the temperature of the heater rod until its maximum value reaches the desired value (794°C)

During step 1, a steady-state calculation is performed with the heating power set to zero. During steps 2 and 3, transient calculations are performed with heating power set according to the 120% ANS-Standard law about 40 s after reactor shut down.

Then, the transient calculation is launched with the injection of a constant liquid mass flow rate at the bottom of the test section with a delay of 7 s to take into account the delayed quenching observed on the experimental values of cladding temperatures at elevation 3.860 m. The heating power heating power is set according to the 120% ANS-Standard law about 40 s after reactor shutdown.

Figure with comparison of measured and calculated axial temperature distribution of the following parameters at the instant immediately prior to Start of Transient is provided below.

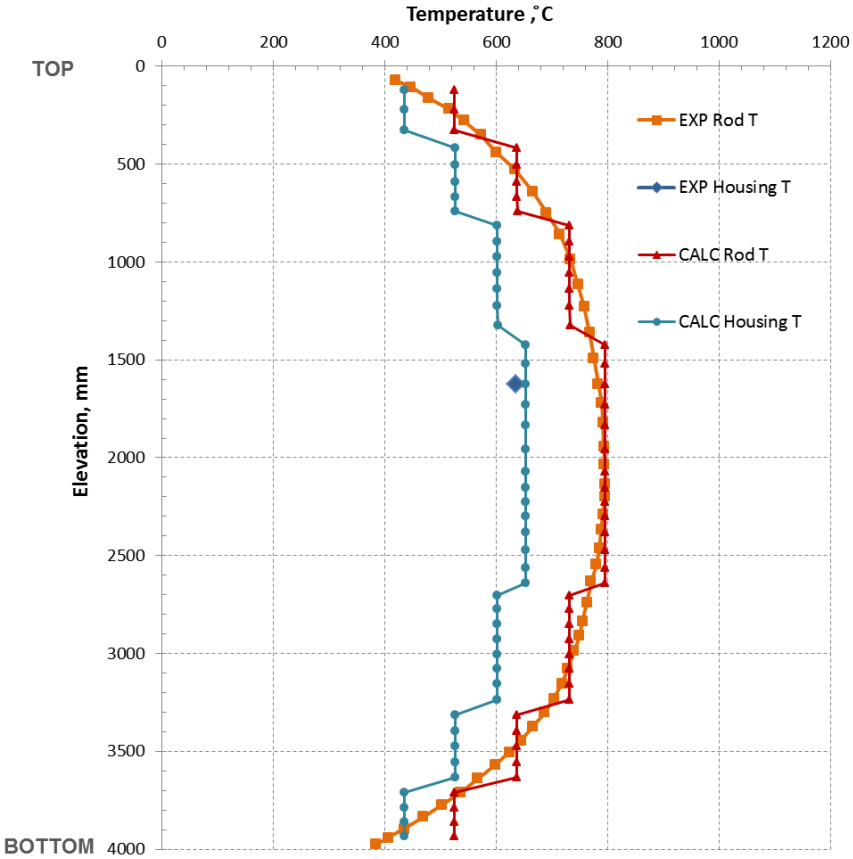

Fig B.1.2 Steady-state temperature profile

Base case results: *Figures of all (exp-calc) responses*

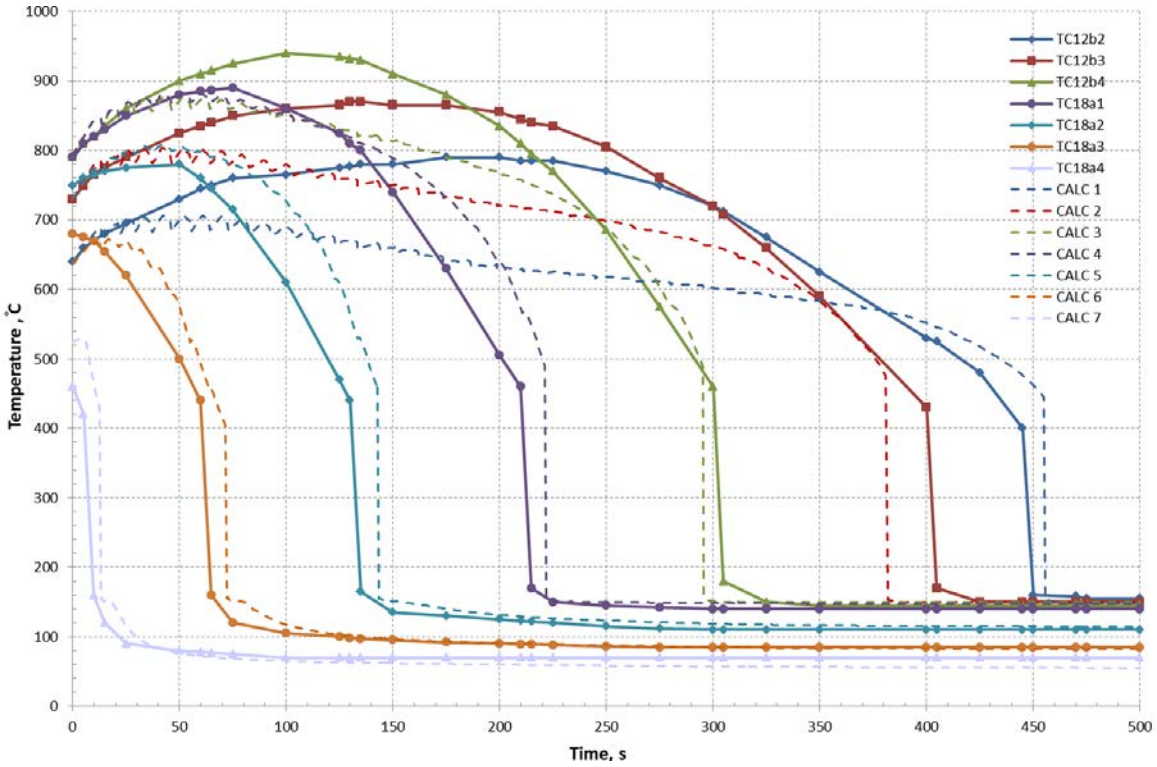

Fig B.1.3 Base case cladding temperatures

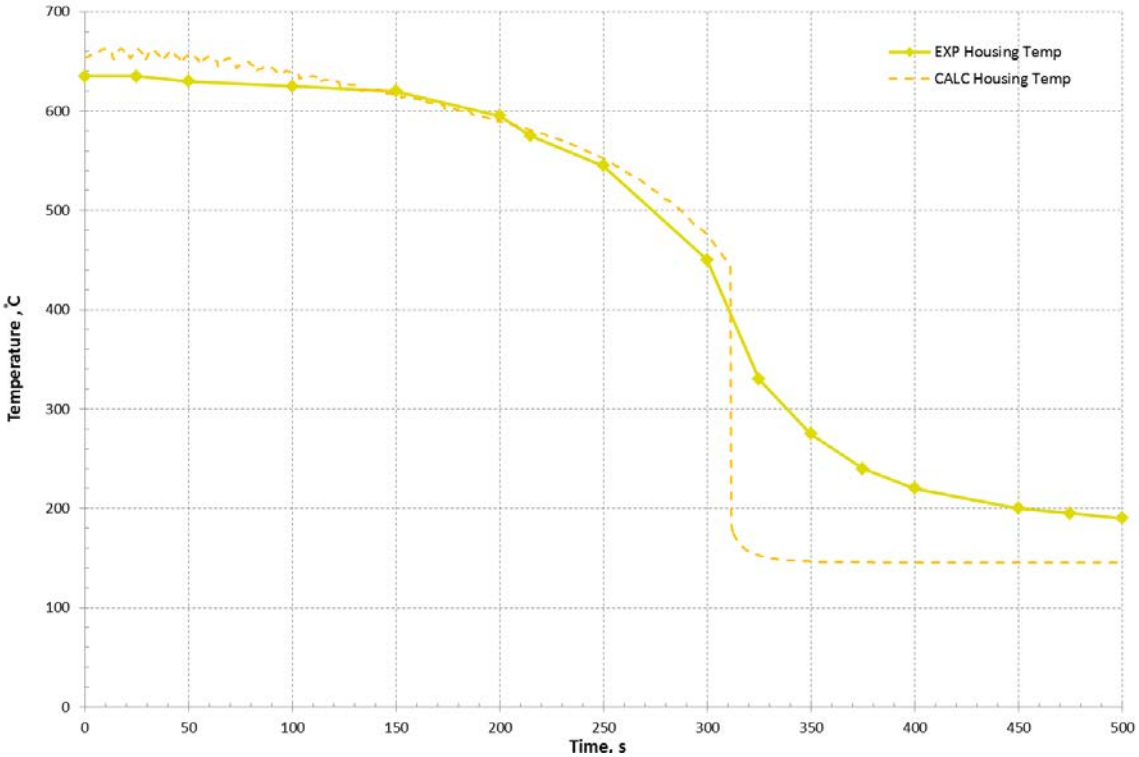

Fig B.1.4 Base case housing temperature

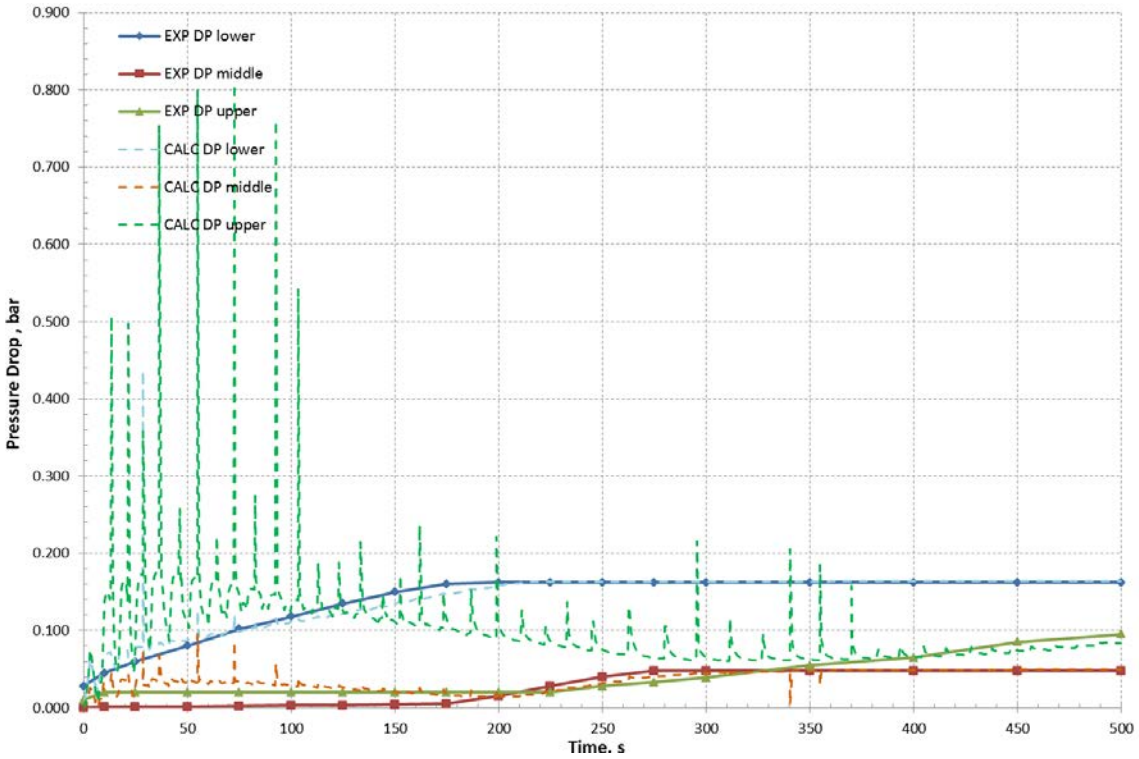

Fig B.1.5 Base case pressure drops

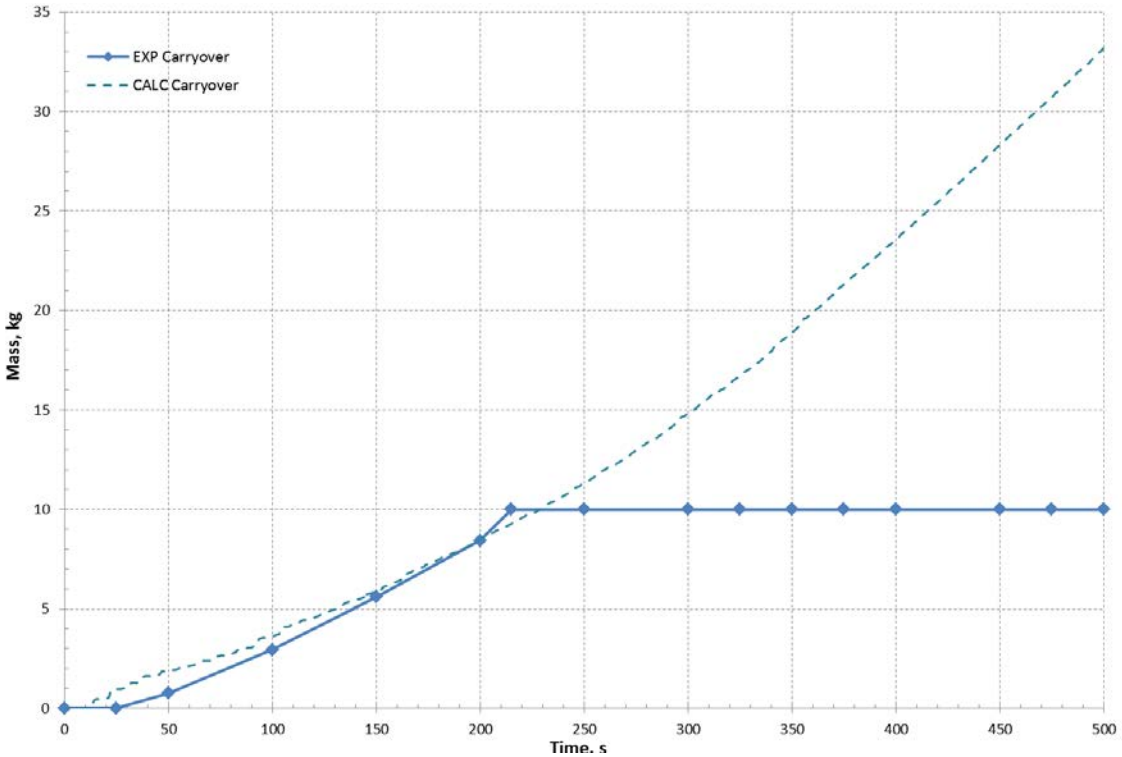

Fig B.1.6 Base case liquid carryover

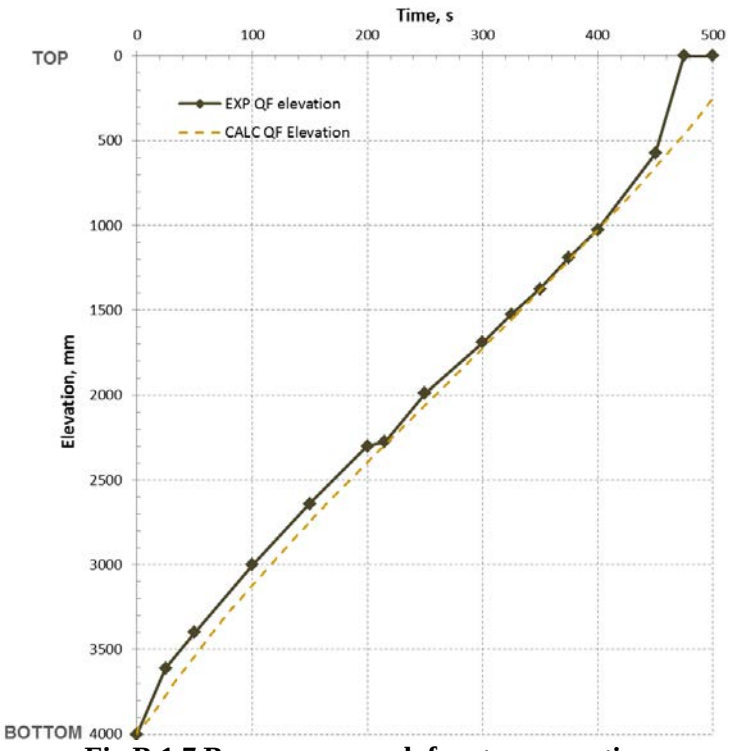

Fig B.1.7 Base case quench front propagation

PCT and bundle quench time

Tab B.1.3 Base case PCT and bundle quench

Institution name	PCT (°C)	Position (mm)	Bundle quench (s)
Bel V	877	2152.5	516

Criteria for selection of influential input parameters

The criteria used for the selection of influential input parameters are the criteria included in the Specifications of the Phase II /1/.

Selection of the Influential Input Parameters

Criterion #1: The absolute value of variation in rod surface temperature T_{clad} is $\mathbf{\Delta T_{ref} = 50K}$;

Criterion #2: The variation in rewet time t_{rew} is $\mathbf{\Delta t_{rew} = 10\%}$

And in complement the

Criterion #3: The variation in elevation of the quench front versus time $\mathbf{\Delta QF_{elev} = 10\%}$

Values found for the application of the criteria #1 and #2 are given in the Final list of Influential Parameters (see §4.2 of the present note).

The criteria #4 and #5 have been also applied to ensure the realism of these Input Parameters.

Criterion #4: limited qualitative impact on the responses' time trends. Notably, the variation of an IP should not cause the drastic changes in rod surface temperature time trends (sudden deviations, oscillations) which may be caused by phenomenology different from that of reflood or by physical or numerical instabilities.

Criterion #5: the range of variation (to make the parameter "influential") shall be consistent with the level of knowledge on the correspondent IP, e.g. the change in Zr density cannot be larger than the real known physical limits.

Selection of parameters
Initial list of parameters

The initial list in a format of a table (prior to analysis performed) of input parameters considered as potentially influential for reflood-related phenomena is provided hereafter The Sample List provided in Appendix A of Specifications for the Phase II is used as a basis. The considered input parameters are classified according to the Definitions provided in Specifications for Phase II.

Tab B.1.4 Initial list of input parameters

Input Basic Parameter	
1	Pressure
2	Flooding velocity
3	Injection fluid Temperature
4	Initial wall Temperature
5	Average Rod Heat Flux
6	Clad (Ni Cr 80 20) Thermal conductivity
7	Clad (Ni Cr 80 20) Heat capacity
8	MgO Thermal conductivity
9	MgO Heat capacity
10	Hydraulic diameter
11	Form loss coefficient (for the whole test section)
Input Global Parameter	
1	Interphase heat transfer
2	Interfacial friction
3	Wall heat transfer
4	A parameter specific to the very local quench front progression, depending on the system code: K2 reflood parameter
Input Coefficient Parameter	
1	Quench front threshold distance for HTC transitions
2	Droplet Weber(critical) nb Interfacial friction (DStream QF)
3	Droplet Weber(critical) nb Interfacial friction (UStream QF)
4	Droplet entrainment Interfacial friction (DStream QF)
5	Droplet entrainment Interfacial friction (UStream QF)
6	Droplet entrainment Interface to Fluid HF (DStream QF)
7	Droplet entrainment Interface to Fluid HF (UStream QF)

where HF: Heat Flux QF: Quench Front

Final list of Influential Parameters

Tab B.1.5 Final list of influential input parameters

Parameter	Sub-routine	Fortran variable / Key word	Multiplier REF / REF value	Multiplier MIN	Multiplier MAX	T_{clad} variation [°C]	Position [mm]	t_{rew} variation [s]	Position [mm]
Pressure	Input deck	NA	4.12 D5 Pa	0.97	1.05	-20/-20	1680	-60/-80	1135
Flooding velocity	Input deck	NA	3.8 D-2 m/s	0.90	1.10	+20/-10	1680	+20/-20	1135
Average Rod Heat Flux	Input deck	NA	Fig 7 [1]	0.90	1.10	-5/+30	1680	-21/+21	590
Interfacial friction	Input deck	SP1TOI	1	0.90	5.00	0/0	1680	-5/+100	1135
Wall heat transfer	Input deck	PQPT	1	0.80	1.20	+60/-30	1680	+30/-20	1135
Specific parameter to very local QF progression, code dep.	Input deck	P1K2FDT	1	0.50	1.50	0/-20	1680	+100/-70	1135
QF threshold distance for HTC transitions	Input deck	SP1DZ0	0.60 m	0.05 m	0.70 m	+ 30/0	1680	+50/+10	1135
Droplet entrainment Interfacial friction (DStream QF)	Input deck	SP1ETOD	1	0.70	100	0/+30	590	0/+30	590

Wall-to-fluid heat transfer model

The text of this chapter 5 has been written by the CEA and has been included in the Bel V contribution with the kind authorization of CEA.

Independently of reflood, all the different modes of heat transfers with walls are taken into account by CATHARE. The classical 3 zones of the boiling curve are considered:

Zone A: transfers with a wetted wall. The physicals models of CATHARE are:

- natural and forced convection with liquid in both laminar and turbulent regimes;
- subcooled and saturated nucleate boiling with criteria for onset of nucleate boiling and net vapour generation;
- film condensation (with or without non-condensable gases).

Zone C: post dry-out heat transfers. The physical models of CATHARE are:

- natural and forced convection with gas (or vapour) in both laminar and turbulent regimes;
- radiation to vapour and liquid;
- film boiling for inverted annular, inverted-slug and dispersed flows.

The interface-vapour heat transfer (qve) is also involved in the post dry-out heat transfer. Indeed, the wall temperature is determined as much by the wall-vapour heat transfer via (T_w-T_v) as by qve via (T_v-T_{sat}(P)).

Zone B: Transition boiling.

Three "dry-out" criteria are used to reach the dry-out of the wall (zones B and C):

- the flow is in pure gas conditions;
- the wall temperature is higher than the minimum stable film temperature;
- the total wall-liquid heat flux is higher than the critical heat flux.

It is important to note that each physical model is unique. No choice among several correlations is proposed to the user, in order to reduce the user effect.

PQPT is defined as the multiplier of the sum of these different heat fluxes with walls.

As already explained in §1.3, some of these physical models are modified in case of reflood. They are:

- gas (or vapour) convection, natural and forced (PPHCFR);
- nucleate boiling;
- film boiling (PPHBOR);
- the transition boiling is suppressed.

Two heat exchange modes are added for reflood:

- a 2-D conduction wall to fluid heat transfer, performed with a very fine meshing moving with the quench front, denoted as k2 for CATHARE (P1K2FDT); it replaces the transition boiling and the minimum stable film temperature;
- an evaporation flux added to the interface-wall heat transfer, which takes into account the violent boiling and the liquid sputtering just downstream from the quench front; this flux is considered on a given distance, which is SP1DZ0 (reference value: 60 cm).

Downstream from the quench front, all these different fluxes are added in a global wall heat flux the multiplier of which is PQFDT.

Two types of reflood are modelled in CATHARE: bottom up and top down. For the FEBA modelling, only the bottom up reflood is used.

Conclusions

A Final list of Influential Input Parameters (IIP) has been set-up according to the specifications of Phase II.

These IPP are of three different types:

- Input Basic Parameters (IBP): Geometry, BIC conditions, etc.;
- Input Global Parameters (IGP): Associated with a physical model;
- Input Coefficient Parameter (ICP): Coefficient inside a physical correlation.

The list of Input Parameters (IP) which will be used by Bel V for the Phase III of the PREMIUM project will also take into account the insights given by CEA during the second PREMIUM meeting (UNIPI, 4-5/06/2012).

For Phase III of PREMIUM, Bel V will use the method CIRCE developed by CEA.

The application of the CIRCE method is limited to a few number of IP, typically 2 to 4. Nevertheless, in this respect, IBP should be considered separately from the IGP and ICP, as the uncertainties of IBP are known a priori, so their number is not limited in the CIRCE method.

As pointed out by CEA, the influence of ICP is taken into account via the IGP which are associated to the physical model, as ICP are associated to the coefficients used in the physical correlations used to describe the physical models. This is a second reason why, for Phase III, IGP will be used and ICP will not be used.

B.2 Tractebel (Belgium) results

Model description

Tab B.2.1 Tractebel code and software platform

Institution name	Code version	Software platform
Tractebel Engineering	Relap5/Mod3.3 e.g	Linux RedHat Enterprise v.4. Kernel 2.4.21.

Nodalization and basic geometrical properties

The FEBA test section for experiment 216 of Series I has been modelled with the following (main) hydraulic components (bottom-up), whose layout is portrayed in Figure below:

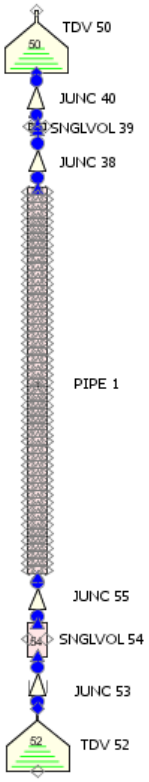

Fig B.2.1 FEBA nodalization

- Time Dependent Volume (TDV) #52: modelling the hydraulic fill, containing the boundary conditions (BC) of the reflood inventory (i.e., Pressure, Temperature, and Velocity of the injected inventory).
- Single Volume (SNGLVOL) # 54: represents the unheated bundle height (0.139 m) below the bottom of active fuel (BOAF).
- PIPE # 1: modelling the bundle height between the top of active fuel and the BOAF, plus the unheated bundle length (3.975 m).
- SNGLVOL # 39: modelling the orifice plate on the top of the bundle.
- TDVOL #50: modelling the hydraulic sink.

Bundle Model – PIPE #1

The apportioning of the bottom of bundle unheated length (0.139 m) into a separate volume (SNGVOL 54) is inconsequential to the model performance. The nodalization of the FEBA test section has been selected in order to get a compromise between the location of the spacers and a uniform hydraulic node length. To that regard, Table B.2.2 provides the hydraulic cell length for PIPE #1.

As to the rest of the component's geometrical parameters, suffices to say that the spacers (bottom) have been located exactly at the corresponding cell-to-cell interface. The spacers volume, (inferred from a reduction of the bundle free area of 20%, and spacers length given in KfK 3657 report) were calculated and deducted from the immediately above hydraulic cell volume, therefore calculating the equivalent cell cross section as cell-volume/cell-height.

The cell-to-cell junctions hydraulic diameter at spacers locations (given that there is not enough information in the available documentation) were calculated as [nominal cross section]*[0.8/1.2], that is, assuming a 20% reduction in the effective cross section and a 20% increase in the wetted perimeter.

For the bundle locations with spacer, the form loss coefficient is calculated on the basis of abrupt area change (KFAC=1). The rod bundle interphase friction model was enabled.

For the friction terms, the wall roughness was set to 1.E-5 and the cells hydraulic (volume-) hydraulic diameter was calculated on the basis of the effective volume-averaged cell cross section.

The rest of the parameters of interest are included within Table below.

The associated heat structures (HS) with the bundle are:

- HS 10, corresponding to the rods.
- HS 11, corresponding to the test section housing.

Tab B.2.2 PIPE #1 rod bundle model: parameters of interest

Cell #	**Cell height (m)**	**Cell #**	**Cell X-section (m^2)**
1 to 4 and 47 to 50	0.07875	Remaining ones	0.00389319
5 to 18 and 33 to 46	0.07785714	5, 12, 26, 33, 40, 47	0.0038636
19 to 25	0.07528571	**Cell Junctions Hydraulic Diameter (m)**	
26 to 32	0.08042857	Nominal	0.01344445
51	0.075	With Spacer	0.00896296
Cell-to-cell with spacer interface		**Cell Junctions X-Section (m^2)**	
(4,5) (11, 12) (25, 26) (32, 33) (39, 40) (46, 47)		Nominal	0.00389319
Form Loss Coefficient		With Spacer	0.00311455
Junctions with spacer	Full Abrupt Area Change		
Junctions without spacer	0.0	**Cell Volume-averaged Hydraulic Diameter (m)**	
Interphase Friction Model		Nominal	0.01344445
Rod Bundle		With Spacer	0.01334228
Options		**Wall roughness (m)**	0.00001
Thermal tracking ON, Non-Equilibrium ON, Choke OFF			

HS – 10 (Rods)

HS-10 is populated with 57 axial cells; the difference between the PIPE #1 and HS-10 number of cells is motivated by some of the axial power profile steps locations not corresponding to hydraulic cells locations. Therefore, there are some hydraulic cells which are associated to two different heat structure axial cells. The wall thickness, corresponding with the rods geometry is 5.375e-3 m (i.e., the rod radius).

Table B.2.3 displays the location of the radial nodes, being radial node 8 the one selected for the measurement of the clad temperature.

Tab B.2.3 HS-10 location of the radial nodes

Interval Index	Mess Thickness (m)	End Position (m)	Material	Source
1	3.839286e-4	3.839286e-4	4	0
2	3.839286e-4	7.678571e-4		
3	6.735715e-4	1.441429e-3		
4	6.735714e-4	2.115e-3		
5	1.35e-4	2.25e-3	3	1
6	8.21429e-4	3.071429e-3	4	0
7	1.253571e-3	4.325e-3		
8	8.75e-4	5.2e-3	3	
9	1.75e-4	5.375e-3		

As to the characteristics of this HS type, the rods themselves were modelled using symmetry boundary conditions with 9 Word Format, while the fluid side corresponds to a vertical bundle without cross flow with 12 Word Format. The heat transfer hydraulic diameter, the heated length forward and the spacer length forward have been entered; the last two parameters according to the axial cell mid-point. The natural circulation length (though doesn't affect the results), was entered equal to the bundle height. The only parameter that deserves other attention is the Fouling Factor; the Fouling factor has been calculated for the axial cells above spacers at their mid-point, and based upon a correlation extracted from ORNL THTF tests data regression.

Tab B.2.4 Axial power profile

Axial Level	Power Multiplier
1 to 3	0.013108195
4	0.010611396
5	3.34E-03
6 to 9	0.017345894
10	0.016391074
11	1.16E-03
12 to 18	0.021134077
19	0.013766233
20	8.27E-03
21 to 28	0.023725992
29 to 35	0.024509603
36	0.023725992
37	8.27E-03
38	0.013766233
39 to 45	0.021134077
46	1.16E-03
47	0.016391073
48 to 51	0.017345894
52	3.34E-03
53	0.010611395
54 to 56	0.013108195
57	0
Note: 1 corresponds to the bottom.	

The total heat transfer area from this heat structure is 3.47346448 m^2 (extracted from the output file), while the calculated according to 25 rods * ((10.75/1000) * PI * 4.365) = 3.47346265 m^2.

This HS had enabled the Reflood option, with a Maximum Number of Intervals equal to 128.

HS – 11 (Housing)

HS-11 is populated with 57 axial cells, corresponding to the same locations as the HS-10. The wall thickness, corresponding with the rods geometry is 6.5e-3 m. Table B.2.3 displays the location of the radial nodes, being radial node 8 the one selected for the measurement of the clad temperature.

Tab B.2.5 HS-11 (Housing) geometry

Interval Index	Mess Thickness (m)	End Position (m)	Material	Source
1	1.625e-3	0.040875	5	0
2	1.625e-3	0.0425		
3	1.625e-3	0.044125		
4	1.625e-3	0.04575		

As to the characteristics of this HS type, the wall is modelled using symmetry boundary conditions with 9 Word Format, while the fluid side corresponds to the default option with 9 Word Format. The heat transfer hydraulic diameter is the only parameter that was entered.

The housing is thermally insulated with a HTC=0.0 in its external side.

The total heat transfer area from this heat structure is 1.37061 m^2.

This HS had enabled the Reflood option, with a Maximum Number of Intervals equal to 128.

Orifice Plate Model

A single volume (SNGLVOL 39) models the plate, with a height of 0.024 m and a cross-section of 2.8273e-3 m^2.

The interphase friction model enabled is the corresponding to a pipe, the HD equal to 0.0360005 m, and the wall roughness 3.5 e-5 m.

The junction (JUNC 38) which connects the TOAF (unheated zone) with the hydraulic sink (TDV 50) has a cross section of 2.8273e-3 m^2, a HD of 3.60005e-3 m. The choke option is disabled, and the form loss factor is 1 (Abrupt area change).

The CCFL model is enabled, Wallis scaling with a slope of 1.0 and an intercept for the vapour phase of 0.725.

Model of Junctions

The junctions' cross section corresponds to the same one as from the elements above/below, no form losses, choking disabled.

Boundary and initial conditions

The following boundary conditions have been applied to the model:

- inlet coolant Pressure and Temperature: Table B.2.6; this BC will define the flooding inventory density;
- outlet Pressure: 4.12 bar with a quality equal to 1.0;
- flooding velocity: 0.0381 m/s;
- power: Table B.2.4 (axial power profile) * HS properties * Power (Table B.2.7);
- heat losses: none.

Tab B.2.6 Reflood Boundary Conditions at the TDV #52

Time	Pressure (Pa)	Temperature (K)
0	4.12E+05	336
12.5	4.12E+05	320
25	4.12E+05	317
50	4.12E+05	315
100	4.12E+05	313
150	4.12E+05	312
250	4.12E+05	311
350	4.12E+05	310
500	4.12E+05	310

Tab B.2.7 Decay heat curve

Time	Power (Watt)
0	2.00E+04
0	1.88E+05
2.5	2.00E+05
5	1.93E+05
10	1.90E+05
20	1.80E+05
30	1.75E+05
50	1.68E+05
75	1.60E+05
100	1.53E+05
150	1.41E+05
200	1.33E+05
250	1.26E+05
300	1.21E+05
400	1.21E+05
500	1.21E+05

Adopted models (flags)

The following specific models and flags activated both for hydrodynamic and heat transfer processes:

- Bundle interphase friction model has been activated in the hydraulic nodes of the bundle.
- “Vertical bundle without cross flow” heat transfer mode has been set at the boundary of the heat structure representing the heater rods (HS-10).
- Choked flag disabled everywhere.
- At all volumes the following flags were enabled: thermal tracking, Non-equilibrium, interphase friction.

- Rod (Right - 1) to housing (Left - 2) radiation considered, with a total of 57 radiation enclosures (one-to-one), both with a emissivity of 0.7. The radiation from the housing to the housing itself was neglected (corners effect disregarded, i.e. S21=1; S22=0 for all enclosures). The minimum threshold for activation is set to the default (900 K, and void fraction equal to 0.5).

Assumptions and steady-state achievement

No developmental options have been enabled rather than the "0" (list options) and the number "50" (activate R-T critical flow model, which is inconsequential at all effects), though the former one is meaningless as all choked junctions flags have been disabled.

For the pre-transient, no steady state calculation was performed but a set-up of the clad and housing temperatures. The housing temperatures were offset about 150 K from the cladding, except at the top; this comes motivated that after a long conditioning period and given that the steam at the top of the bundle will be likely superheated to a certain degree, the radiation drives the housing to almost the same temperature as the clad.

As to the initial conditions, all junction flow was set to stagnation (0.0 m/s), while the steam was set to saturation all along the volumes; we deem not critical to set the steam at the right temperatures given that it will be dumped at the transient onset. Comparisons of the temperatures to the specified ones are shown in Figures below.

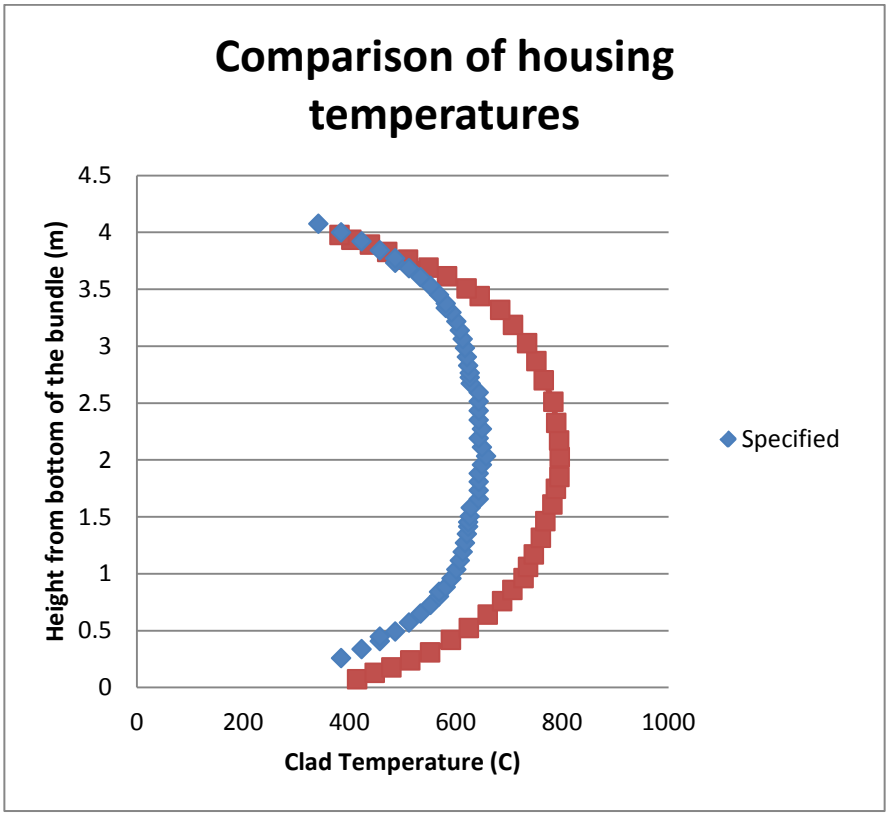

Fig B.2.2 Steady-state housing temperature profile

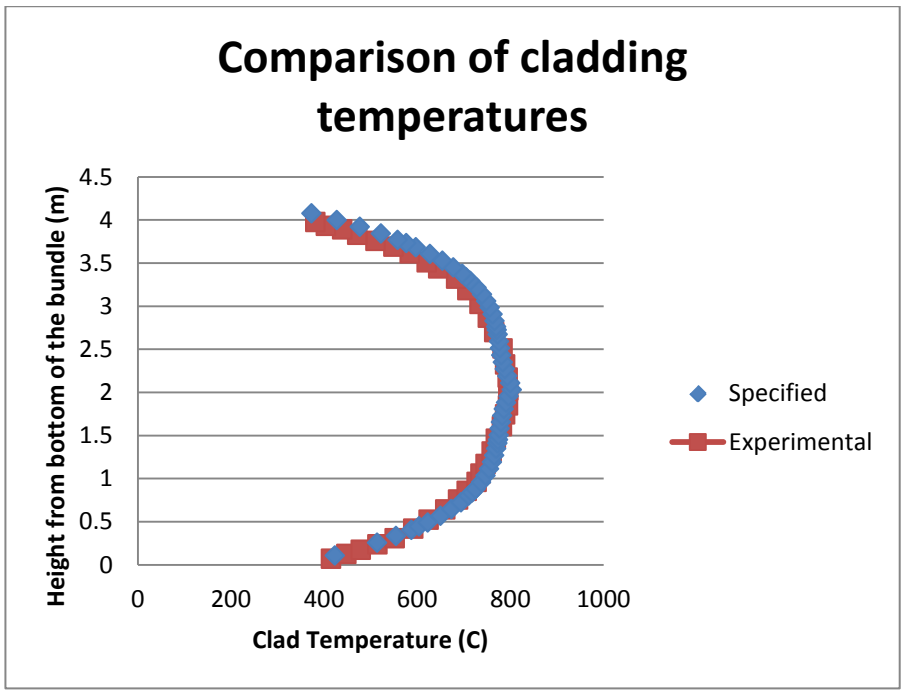

Fig B.2.3 Steady-state cladding temperature profile

Base case results

Reference case stands for the standard, all-to-nominal, Relap5/Mod 3.3 calculation.

Figures of all (exp-calc) responses

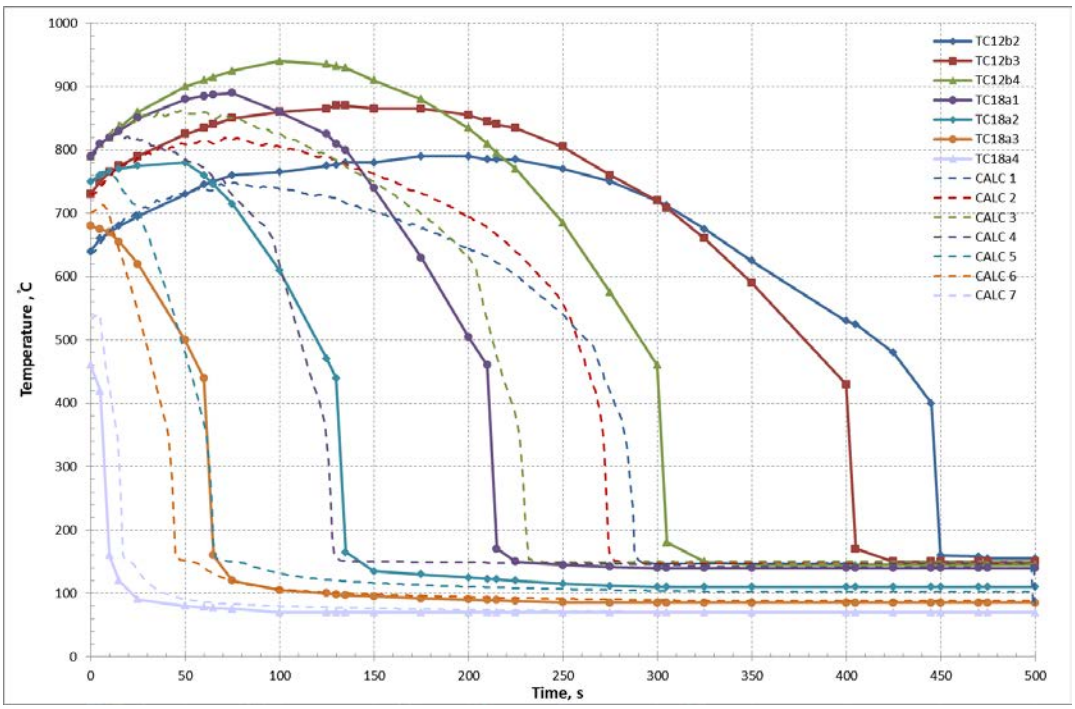

Fig B.2.4 Base case cladding temperatures

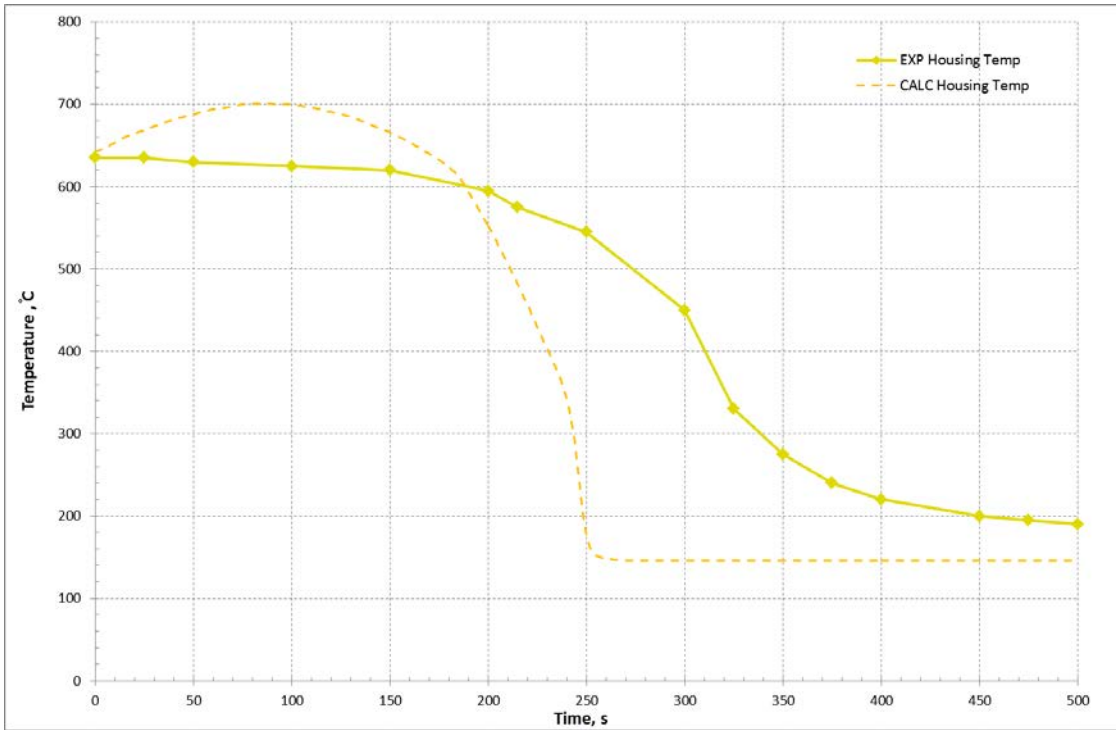

Fig B.2.5 Base case housing temperature

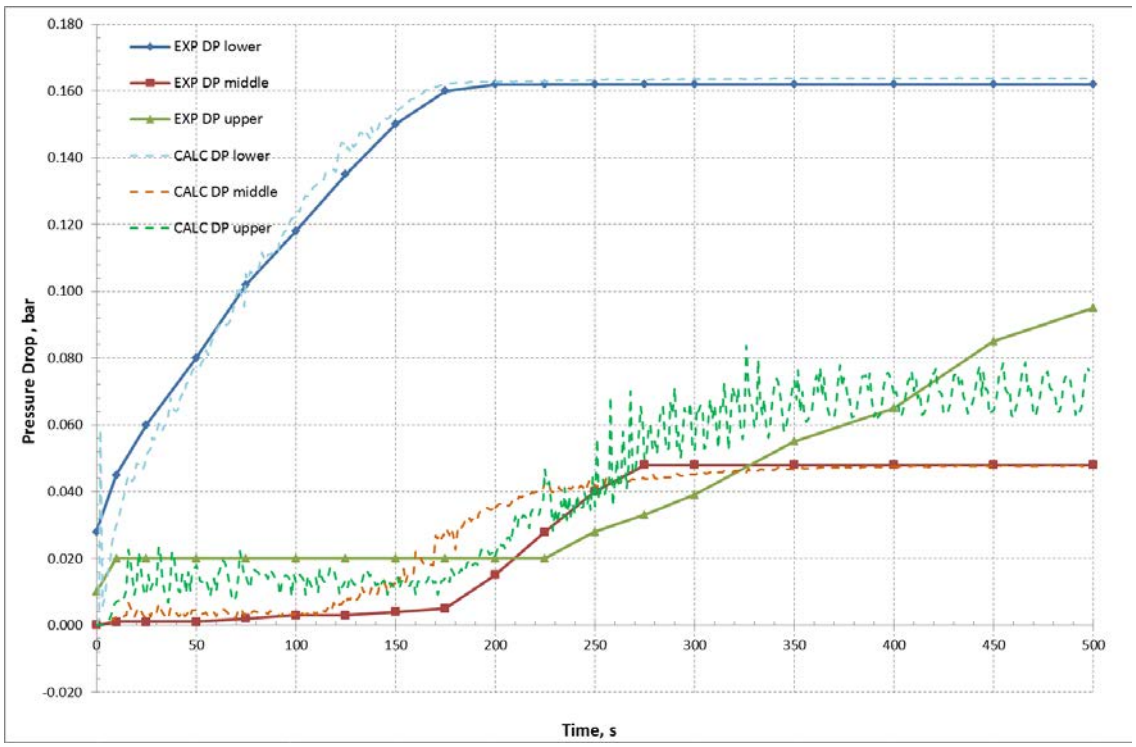

Fig B.2.6 Base case pressure drops

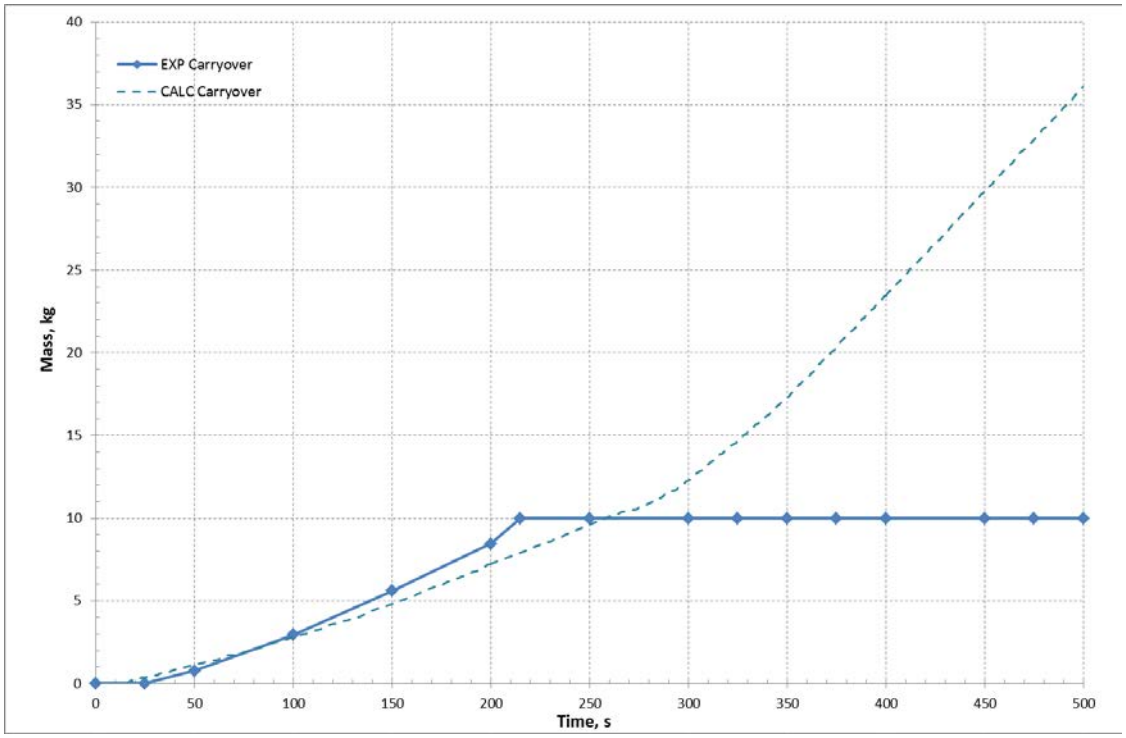

Fig B.2.7 Base case liquid carryover

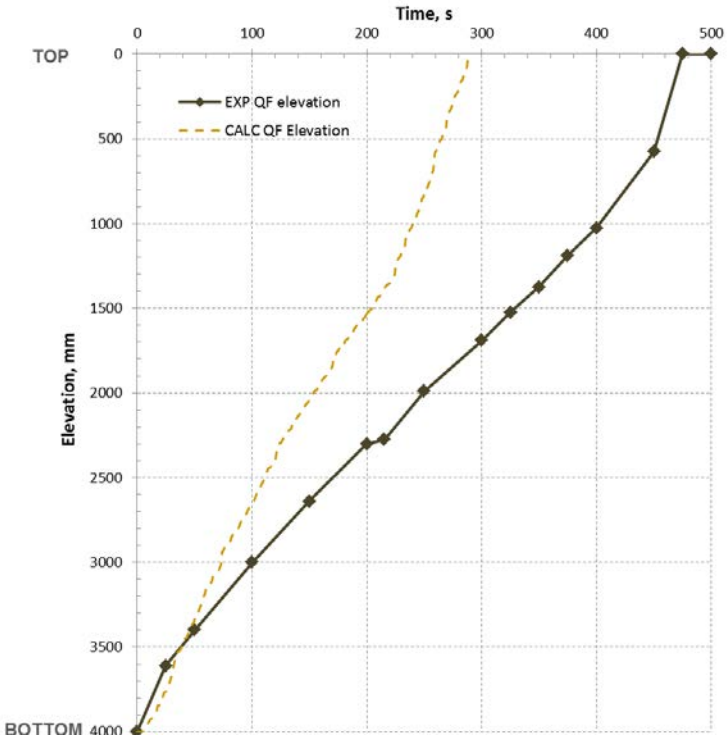

Fig B.2.8 Base case quench front propagation

PCT and bundle quench time

Tab B.2.8 Base case PCT and bundle quench

Institution name	PCT (˚C)	Position (mm)	Rewet time (s)	Bundle quench (s)
Tractebel	869.8	2593.92 from the bundle bottom	191 s	290

Criteria for selection of influential input parameters

The parameters which affect the figures of merit proposed at the PREMIUM benchmark (PCT, quenching) were selected according to expert judgment, based on:

- Literature review (i.e., SECY-8357, NUREG-630, NUREG-1230, NUREG/CR-5249 and 6744, etc.).
- Understanding of the LOCA reflood behaviour (from analyses of FLECHT, NEPTUN etc.).
- Experience in LOCA methodology and analyses.

Selection of parameters

Initial list of parameters

The following table is the initial list in of input parameters considered as potentially influential for reflood-related phenomena:

Tab B.2.9 Initial list of input parameters

Input Basic Parameter	
1	Bundle Power
2	Flooding velocity
3	Pressure
4	Material properties
5	Geometry (hot conditions)
6	Radiation parameters and view factors
Input Global Parameter	
1	(subcooled and saturated) Film boiling heat transfer coefficient
2	Transition boiling heat transfer coefficient
3	Heat partitioning
4	Interphase friction
Input Coefficient Parameter	
1	Droplet Weber (critical) number
2	Quench front threshold distance for HTC transitions
3	Droplet diameter
Notes	Red: Assessed parameters. Blue: Un-assessed parameters.

Final list of Influential Parameters

The following table provides the final list of influential parameters, their localization in the Relap5/Mod3.3 code, their preliminary ranging, and the single-parametric sensitivity study results.

The following parameters are considered as important:

- Bundle Power.
- Interphase friction (Junction or Total).
- Transition and Film Boiling packages.
- Heat partitioning.
- Dispersed phase characteristics (droplet max. and min. diameters).

A sensitivity study based on Monte-Carlo sampling has also been performed using the DAKOTA tool. The results confirm the importance of the above identified parameters.

Tab B.2.10 Final list of influential input parameters

Parameter	Subroutine	Fortran keyword	Multiplier REF / REF value	Multiplier MIN	Multiplier MAX	T_{clad} variation [°C]	Position [mm]	t_{rew} variation [s]
Bundle power	By a control variable in the Relap input deck	N/A	1.0	0.95	1.05	-9.2/9.3	2593.92 (*)	-7.0/8.0
Volume interphase friction	FIDIS2	fic		0.8	1.2	1.2/-0.5		1.0/0.0
Junction interphase friction	FIDISJ			2.0	10.0	15.7/68		65.0/238.0
Interphase friction	PHANTJ	fij				13./63.1		66.0/261.0
Wet wall Dispersed heat transfer	DISPWETHIF	hifc		0.8	1.2	-0.3/0.2		-1.0/-1.0
		higc				-2./0.6		1.0/0.0
		hgfc				-0.3/0.2		-1.0/-1.0
Dry wall Dispersed heat transfer	DISPDRYHIF	hifc				-0.2/-0.5		0.0/-1.0
		higc				6.8/-5.5		1.0/-5.0
		hgfc1				0.0/0.0		0.0/0.0
Heat Partitioning (either on dry or wet wall)	PHANTV	hif				-0.3/-0.1		0.0/-1.0
		hig				6.9/-6.7		7.0/-4.0
		hgf				0.0/0.0		0.0/0.0
Transition and Film Boiling packages	PSTDNB	hfb				1.8/0.9		6.0/-6.0
		hv				5.7/-3.0		-41.0/11.0
Droplet Min/Max diameter	FIDSV and FIDIS2	dcon(2), dcon(3)				-6.9/3.9		11.0/-9.0
		dcon(1)				0.0/0.0		0.0/0.0
Notes	(*) From bottom of bundle Red: considering as important							

Wall-to-fluid heat transfer model

The reflood model adopted for both the bundle and the housing was the <Nearly Empty Reflood> with 128 intervals.

Conclusions

A "best possible" simulation of the FEBA test 216 has been performed using Relap5/Mod3.3, with the standard user guidelines and best practices. The known code deficiency (or bias) in the RELAP5/Mod3.3 interphase friction model was not corrected (i.e., the junction hydraulic diameter was set to the default value).

The Relap5/Mod3.3 code models, closure laws, and correlations involved in a reflood scenario have been screened. The following list of influential parameters is considered as important:

- Bundle Power.
- Interphase friction (FIDISJ or PHANTJ).
- Transition and film boiling heat transfer package (PSTDNB).
- Heat partitioning (DISPDRYHIF, PHANTV).
- Maximum and minimum droplet diameters (FIDSV and FIDIS2).

In order to be as much practical as possible for subsequent applications of the developed code with uncertain attributes, and to be consistent with the current LOCA analysis methodology, the following parameters were identified as somewhat influential but not assessed:

- Material properties.
- Reflood mass flow rate.
- Quench front location.
- Weber critical number.
- Geometry.

It is confirmed from the single-parametric sensitivity studies based on the Relap5/Mod3.3 simulation of the FEBA test 216 that:

- The PCT is mainly controlled by the bundle power and interphase friction model uncertainty;
- The rewet time is mainly controlled by the interphase friction and the transition and film boiling model uncertainty.

Tab B.2.11 Min and Max PCT and rewet time

Minimum PCT (C)	860.6	Bundle Power	Fortran keyword	N/A	Multiplier value	0.95
Maximum PCT (C)	937.8	FIDISJ		fic		10.0
Minimum rewet time	150 s	PSTDNB		hv		0.8
Maximum rewet time	452 s	PHANTJ		fij		10.0

In addition, a sensitivity study based on Monte-Carlo sampling confirms the importance of the above identified parameters.

In conclusion, the uncertainties of the following models of Relap5/Mod3.3 will be quantified in phase III:

- Interphase friction (FIDISJ or PHANTJ).
- Transition and film boiling heat transfer package (PSTDNB).
- Heat partitioning (DISPDRYHIF or PHANTV).

It should be noted that the uncertainty on Relap5/Mod3.3 interphase friction (junctions) model includes a well-known bias, which would be treated carefully.

B.3 NRI (Czech Republic) results

Model description

Tab B.3.1 NRI code and software platform

Institution name	Code version	Software platform
UJV REZ, a.s.	ATHLET Mod 2.1 Cycle A	Windows

Nodalization and basic geometrical properties

The calculated model consists of totally 6 thermo-fluid objects and 2 heat conduction objects (rods and insulation of the housing). The FEBA experiment facility is modelled by three branches (lower plenum, upper plenum and time depending volume) and three pipes (housing, connecting pipe and feed water line as single junction pipe). The housing and core (25 heated rods) are internally divided into 66 sub volumes.

Provide the main geometrical parameters:

- Total height of the heated part 3.9 m, unheated parts 0.075 m at the top and 0.139 m at the bottom of the core;
- Heated part flow area 0.00389 m^2, hydraulic diameter 0.01344 m, wall roughness 4.0E-06 m;
- Flow area 0.00311 m^2, hydraulic diameter 0.0096 m;
- Total heat transfer area of the heater rods 3.293 m^2;
- Maximum linear heat rate 24.41 W/cm.

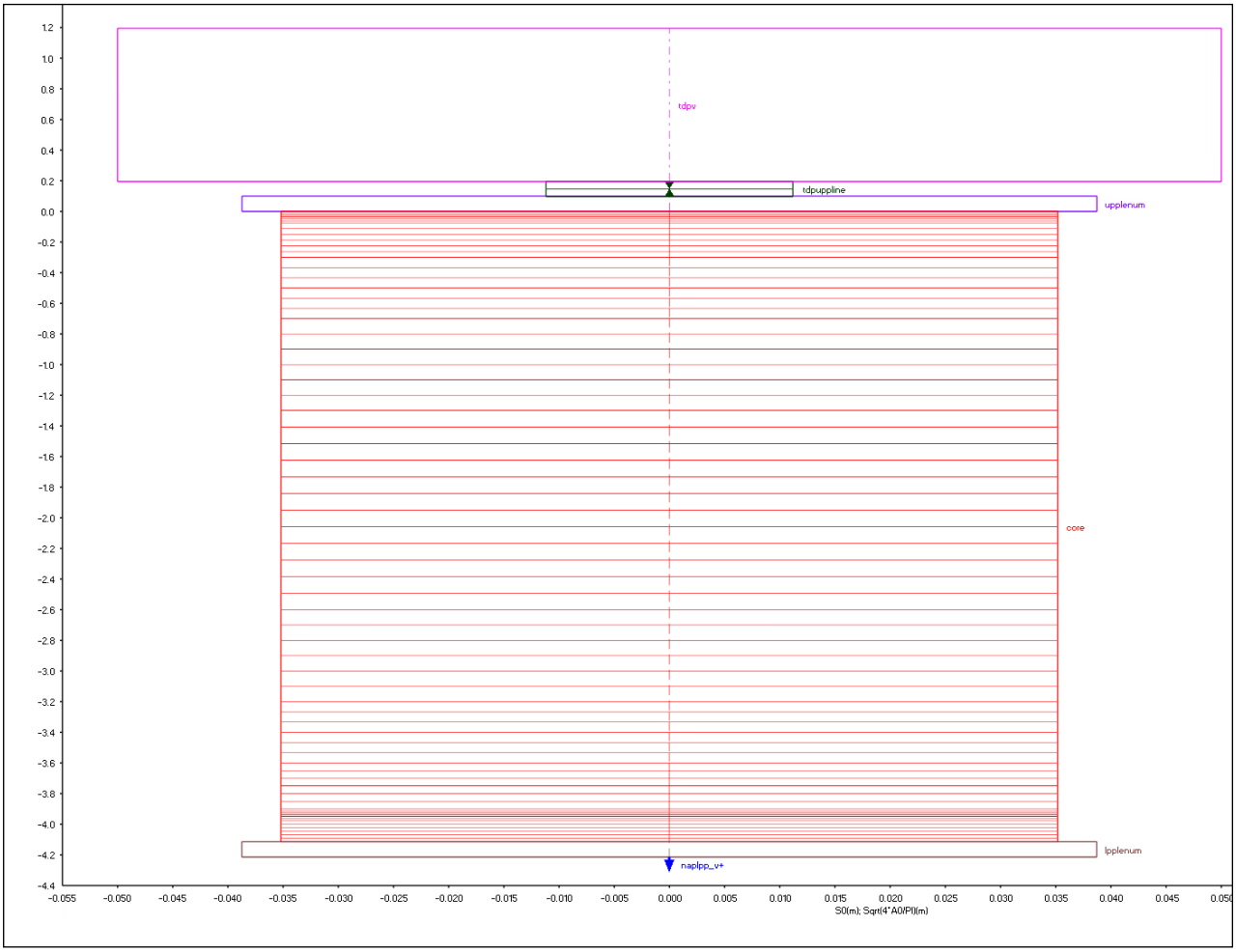

Fig B.3.1 FEBA nodalization

Boundary and initial conditions

Describe the boundary conditions applied to the model:

- Pressure 0.41 MPa
- Flooding temperature – Table B.3.2
- Flooding mass flow rate 0.0 kg/s
- Power – Table B.3.3
- Heat losses 17 W

Tab B.3.2 Flooding temperature

Time [s]	Temperature [°C]
0.0	63.0
12.5	47.0
25.0	44.0
50.0	42.0
100.0	40.0
150.0	39.0
500.0	39.0

Tab B.3.3 Core power

Time [s]	Power [kW]
< 0	10.0
0.0	187.5
2.5	200.0
5.0	192.5
10.0	190.0
20.0	180.0
30.0	175.0
50.0	167.5
75.0	160.0
100.0	152.5
150.0	141.25
200.0	132.5
250.0	126.25
300.0	121.25
400.0	121.25

Adopted models (flags)

List and describe the specific models and flags activated both for hydrodynamic and heat transfer processes:

- Quench front model for the selection of the suitable heat transfer correlation and simulation of the rewetting process. The activation of the model is defined by a GCSM signal.
- Rewetting model for calculation of rewetting temperature and selection of correlations for calculation of the critical heat flux
- Time dependent volume model simulating constant pressure and temperature of the atmosphere.

The radiation model hasn't been taken into account in the calculations.

Assumptions and steady-state achievement

The steady state calculation has been performed for 10000 s. The initial conditions (pressure and temperature profile) were reached.

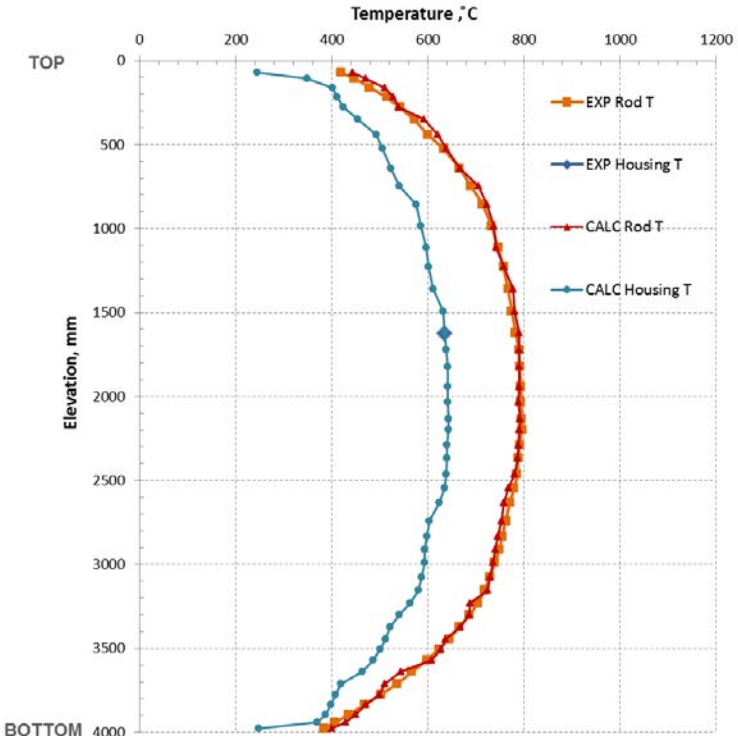

Fig B.3.2 Steady-state temperature profile

Base case results

Figures of all (exp-calc) responses

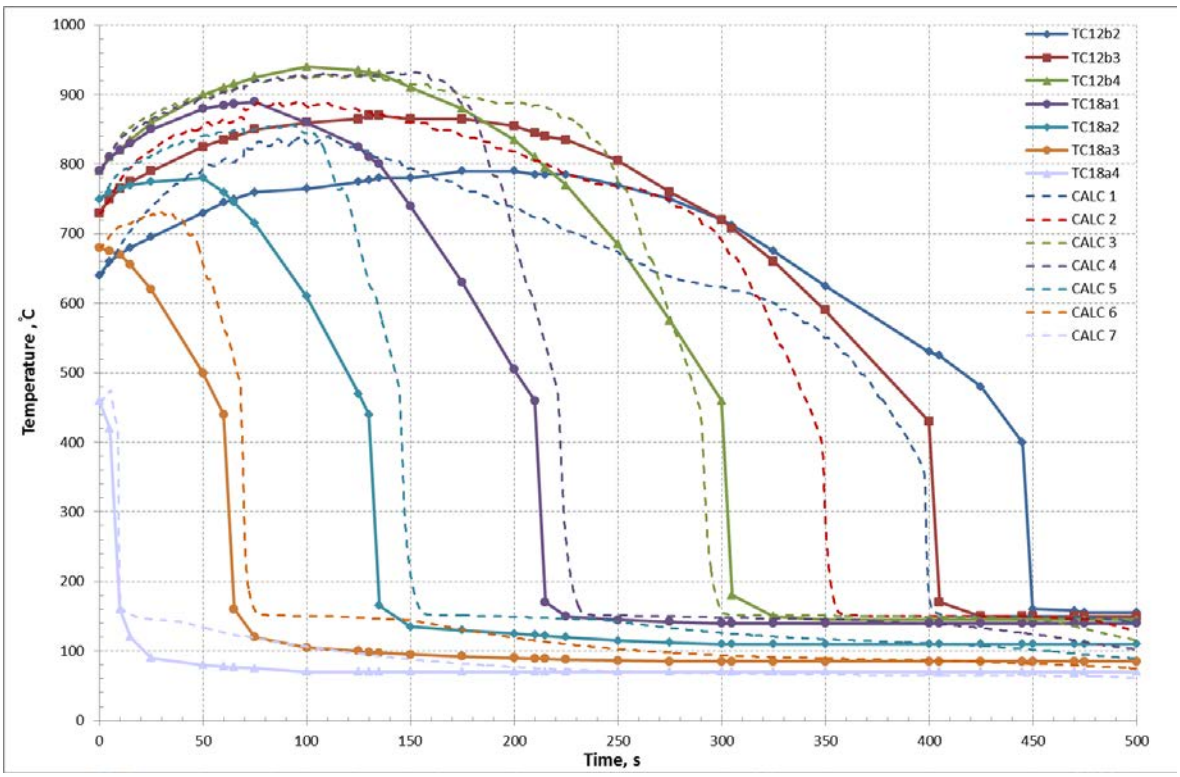

Fig B.3.3 Base case cladding temperatures

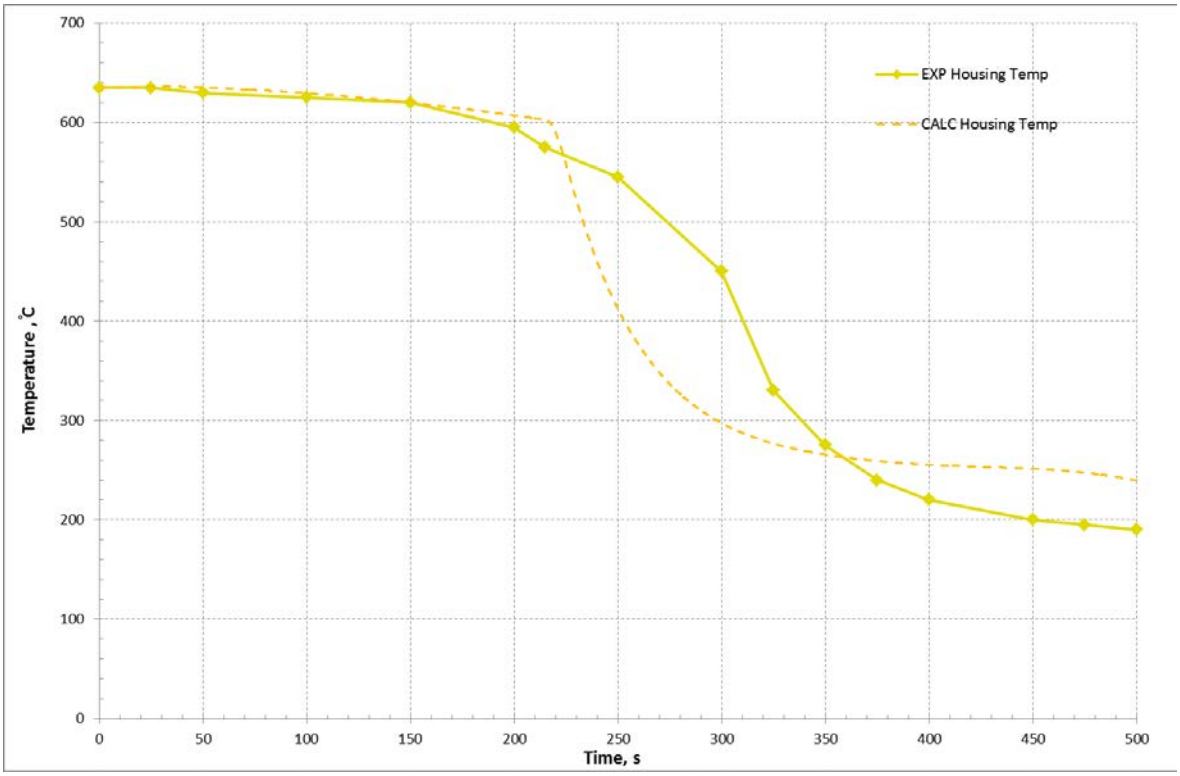

Fig B.3.4 Base case housing temperature

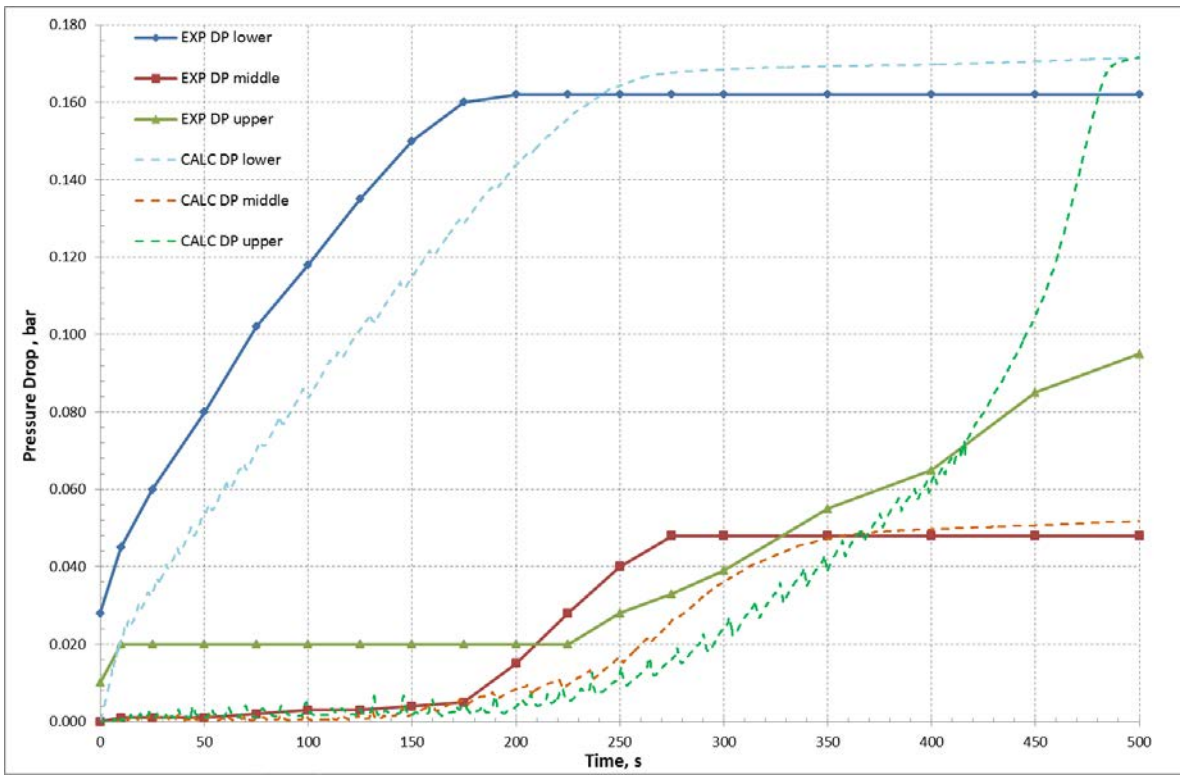

Fig B.3.5 Base case pressure drops

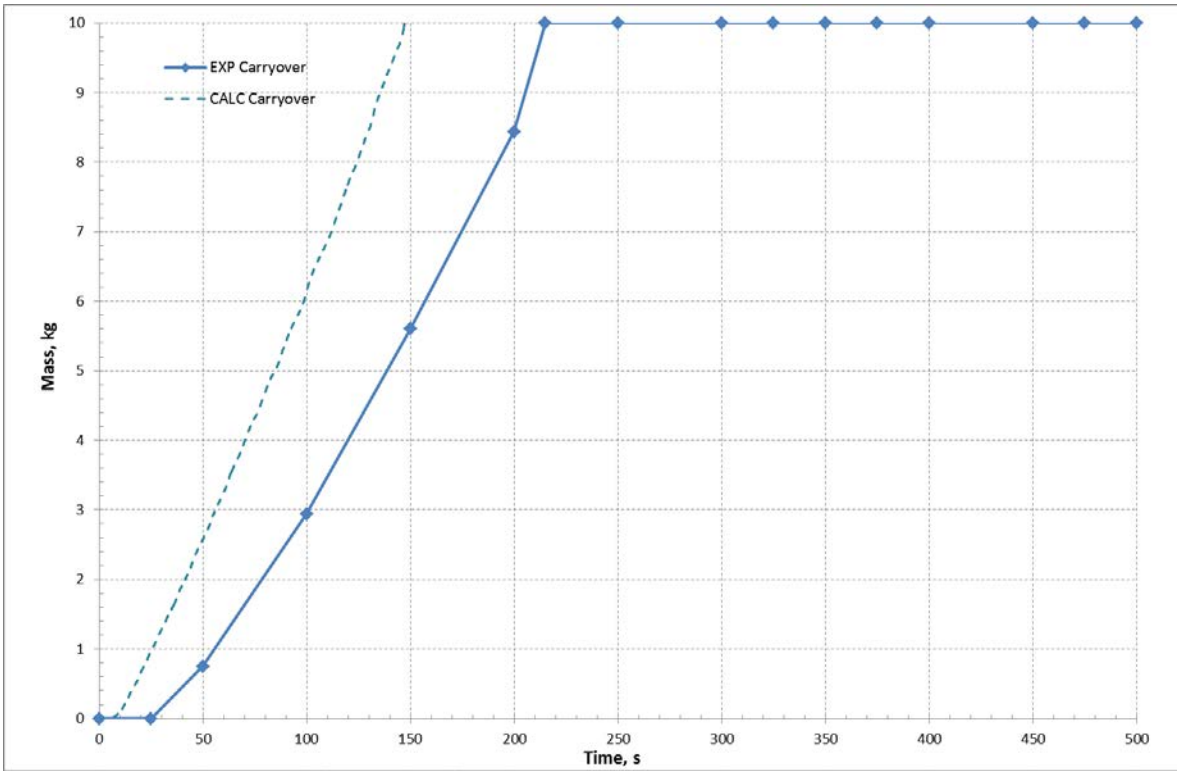

Fig B.3.6 Base case liquid carryover

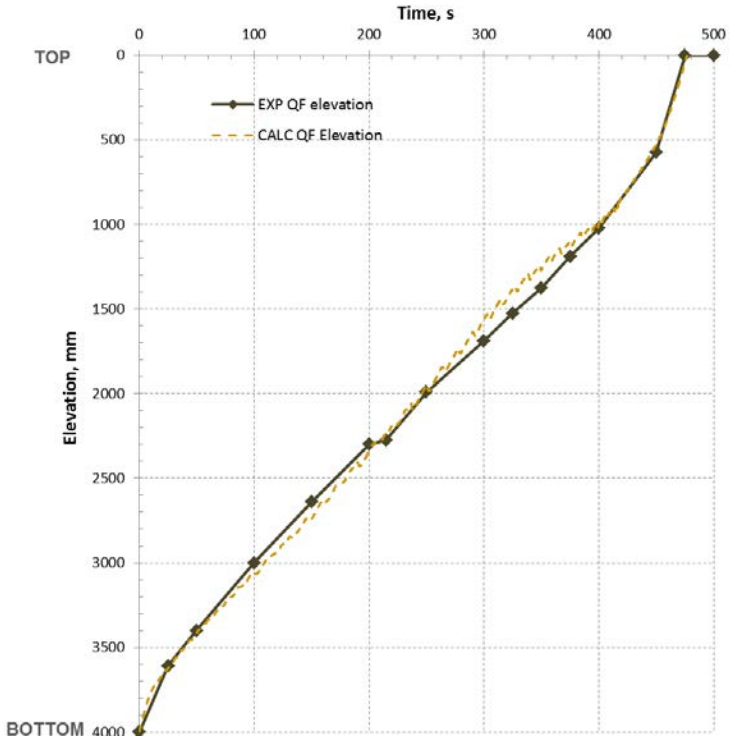

Fig B.3.7 Base case quench front propagation

PCT and bundle quench time

Tab B.3.4 Base case PCT and bundle quench

Institution name	PCT (°C)	Position (mm)	Bundle quench (s)
UJV REZ, a.s.	933.3	2225	476.9

Criteria for selection of influential input parameters

The most important input parameters are initial rod surface temperatures, power, feed water mass flow and its temperature, wall heat transfer, thermal conductivity and heat capacity of cladding, heater and insulator.

Selection of parameters
Initial list of parameters

Tab B.3.5 Initial list of input parameters

Input Basic Parameter	
1	Power
2	Feed water mass flow
3	Feed water temperature
4	Initial rod surface temperatures
5	Pressure
6	Flow area
7	Hydraulic diameter
8	Thermal conductivity of heater and insulation
9	Heat capacity of heater and insulation
10	Form loss coefficients
11	Thermal loss
Input Global Parameter	
1	Selection of heat transfer correlations for film boiling heat transfer coefficient
2	Selection of correlation for calculation of QF velocity
3	Selection of HTC for vapour condensation
Input Coefficient Parameter	
1	Various coefficients used in correlations
2	Local loss coefficients
3	Wall roughness

Final list of Influential Parameters

Tab B.3.6 Final list of influential input parameters

Parameter	Subroutine	Fortran variable / Keyword	Multiplier REF / REF value	Multiplier MIN	Multiplier MAX	T_{clad} variation [°C]	Position [mm]	t_{rew} variation [s]	Position [mm]
Power	input deck		1.0	0.8	1.2	-78.5/+102.1	1680/2225	-44.6/-21.3	1680/2225
Feed water mass flow	input deck		1.0	0.9	1.1	+24.7/-20.2	1680/2225	+99.4/-12.3	1680/2225
Feed water temperature	input deck		Ref. table	-5°C	5°C	+0.37/-1.9	2225/2225	-2/+3.3	2225/2225
Pressure	input deck		0.41	0.3	0.5	+33/-6.6	2225/1680	+25.2/+58.9	2225/1680
Flow area	input deck		1.0	0.9	1.1	+23.1/+20	2225/2225	+5.6/-2.7	2225/2225
Hydraulic diameter	input deck		1.0	0.9	1.1	-10.2/+3.7	2225/2225	+3.7/-1.4	2225/2225
Thermal conductivity of heater	input deck		1.0	0.8	1.2	-0.65/-2.0	2225/2225	+2.3/+0.3	2225/2225
Heat capacity of heater	input deck		1.0	0.9	1.1	+1.7/-5.2	2225/2225	-3.3/+5.4	2225/2225
Wall roughness	input deck		4.0E-06	1.0E-05	1.0E-07	-1.4/+0.2	2225/2225	+0.3/0.0	2225/2225

Wall-to-fluid heat transfer model

Special reflood model was used for the calculation of the experiment.

Conclusions

The calculation of the reflood experiment on FEBA test facility was provided with help of system thermal-hydraulic code ATHLET. The calculated initial conditions were in relatively good agreement with experiment values. Small differences are in course of cladding temperatures. Quench front propagation is in very good agreement, but on the other hand the carryover mass is a little bit faster.

Totally 9 parameters were chosen for sensitivity calculations. The most influential parameter is total power of the core and subsequent are pressure, feed water mass flow, flow area and hydraulic diameter. The rest of parameters hasn’t so significant influence.

B.4 VTT (Finland) results

Model description

Tab B.4.1 VTT code and software platform

Institution name	Code version	Software platform
VTT Technical Research Centre of Finland	APROS 5.11.02 (dev)	Windows

Nodalization and basic geometrical properties

The APROS model of the FEBA facility consists of the lower plenum, heated test section with spacer grids, upper grid plate with upper plenum and the housing. Inlet boundary condition is modelled with a branch with constant velocity and varying temperature (according to provided data), while the outlet is modelled as a constant pressure point. Figure 1 shows the nodalization and axial geometry of the model.

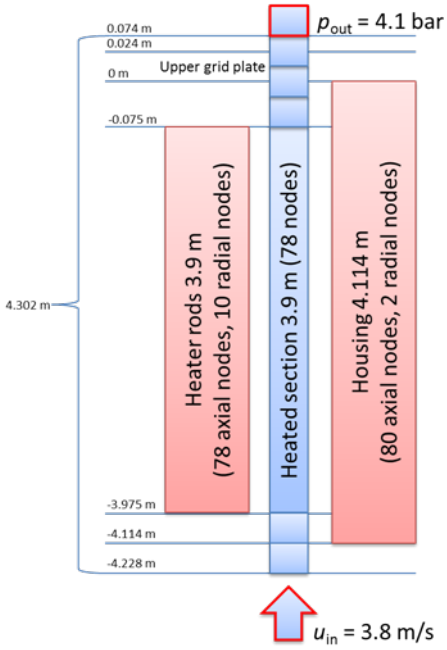

Fig B.4.1 FEBA nodalization

The heater rods are modelled with a single powered heat structure with 10 radial and 78 axial nodes. The flow channel is divided into 78 nodes for the heated part with additional nodes above and below for heat transfer with housing and lower and upper plenum modelling.

The main geometrical parameters for the model are:

- Total height/length (including the heated and the unheated parts): 4.302 m
- Heated part flow area, hydraulic diameter, relative wall roughness: $3.89 \cdot 10^{-3}$ m^2, $1.34 \cdot 10^{-2}$ m, $1 \cdot 10^{-5}$
- Flow area, hydraulic diameter and pressure loss coefficients at the position of the spacer grids: 80 % heated part area or $3.11 \cdot 10^{-3}$ m^2, $6.45 \cdot 10^{-3}$ m, 1.5
- Total heat transfer area of the heater rods: $1.32 \cdot 10^{-1}$ m^2
- Maximum linear heat rate: 60.9 kW/m
- Upper grid plate area, hydraulic diameter and pressure loss coefficient: $2.83 \cdot 10^{-3}$ m^2, 0.01 m, 1.5
- Housing is modelled as a slab with the same volume and inner area as in the experiment making it a bit thicker due to corners being removed; housing height, breadth and thickness: 4.114 m, 0.314 m, $7.04 \cdot 10^{-3}$ m

Boundary and initial conditions

The boundary conditions applied to the model are:

- Pressure: 4.1 bar
- Flooding temperature: as in FEBA-desc-ap5.docx
- Flooding velocity: 3.8 cm/s
- Power: as in FEBA-desc5.pdf
- Heat losses: not accounted for

Adopted models (flags)

Specific models activated for hydrodynamic and heat transfer processes are:

- Bundle interfacial friction correlation has been activated (PI12_CCFL_CORRELATION = 3)
- Droplet breaking factor is used (PI12_DROP_BREAK_FACTOR = 1)

Radiation heat transfer from heater rods to the housing has not been taken into account in the calculations.

Assumptions and steady-state achievement

The transient is started from a fully-specified state of the model, i.e. no steady-state or conditioning phase calculation is performed. The given axial heater rod temperature profile is imposed on the heater rod heat structure, with constant temperature in the radial direction. The housing axial temperature distribution is assumed to be 0.815 times that of the heater rods thus reaching a maximum temperature of 641 °C and difference to maximum cladding temperature of 146 °C. The hydraulic nodes are initially filled with steam at 400 °C.

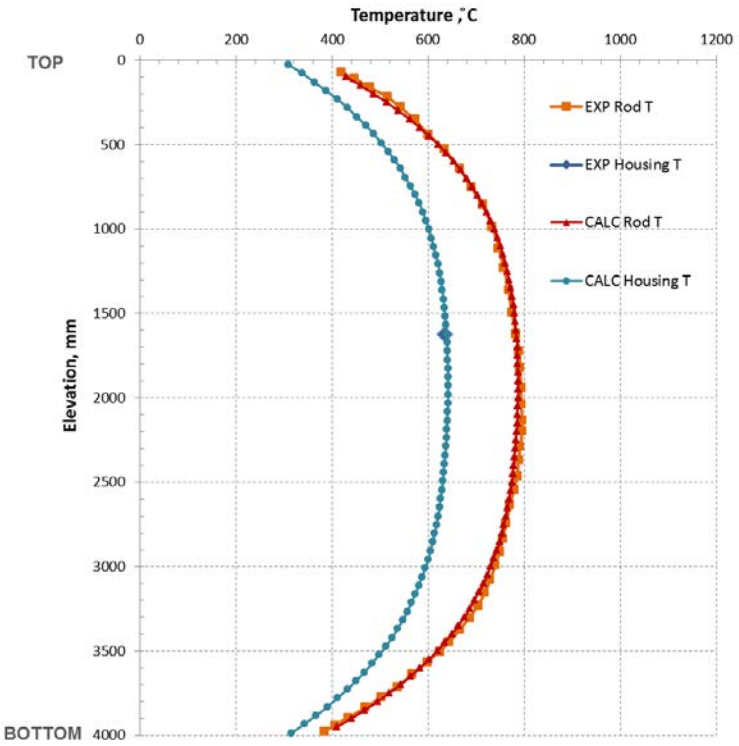

Fig B.4.2 Steady-state temperature profile

Base case results

Figures of all (exp-calc) responses

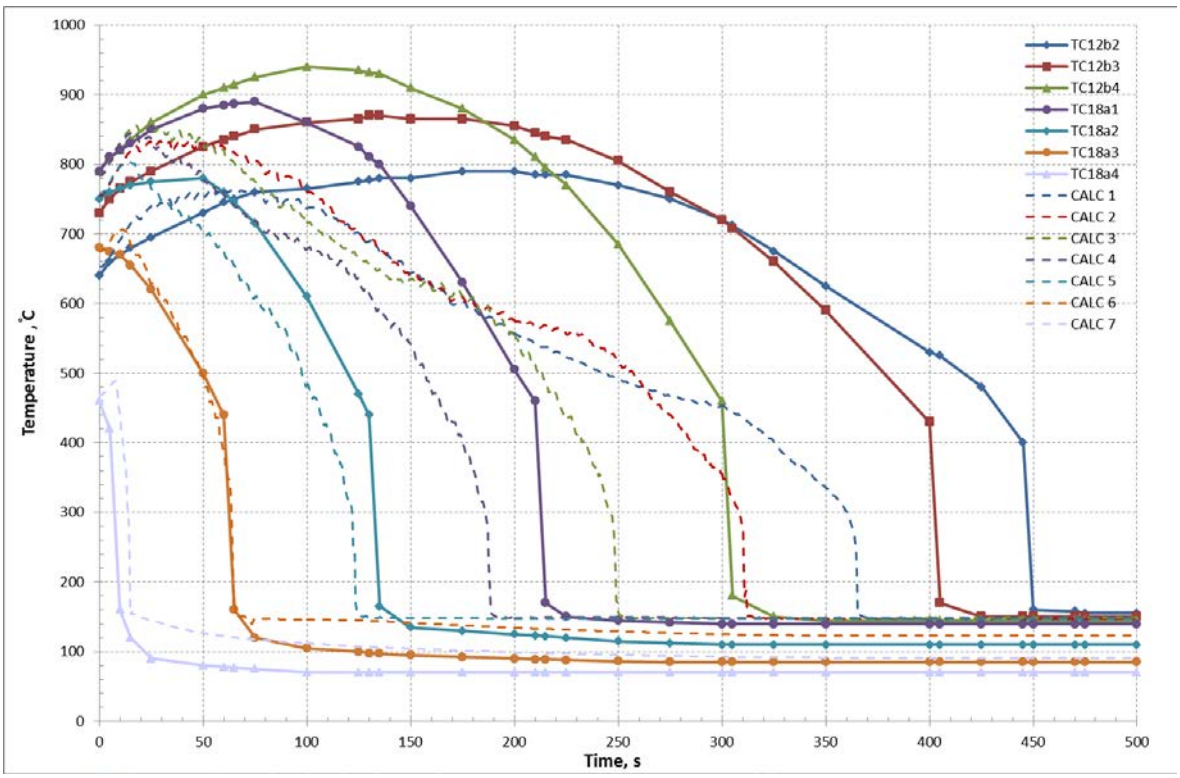

Fig B.4.3 Base case cladding temperatures

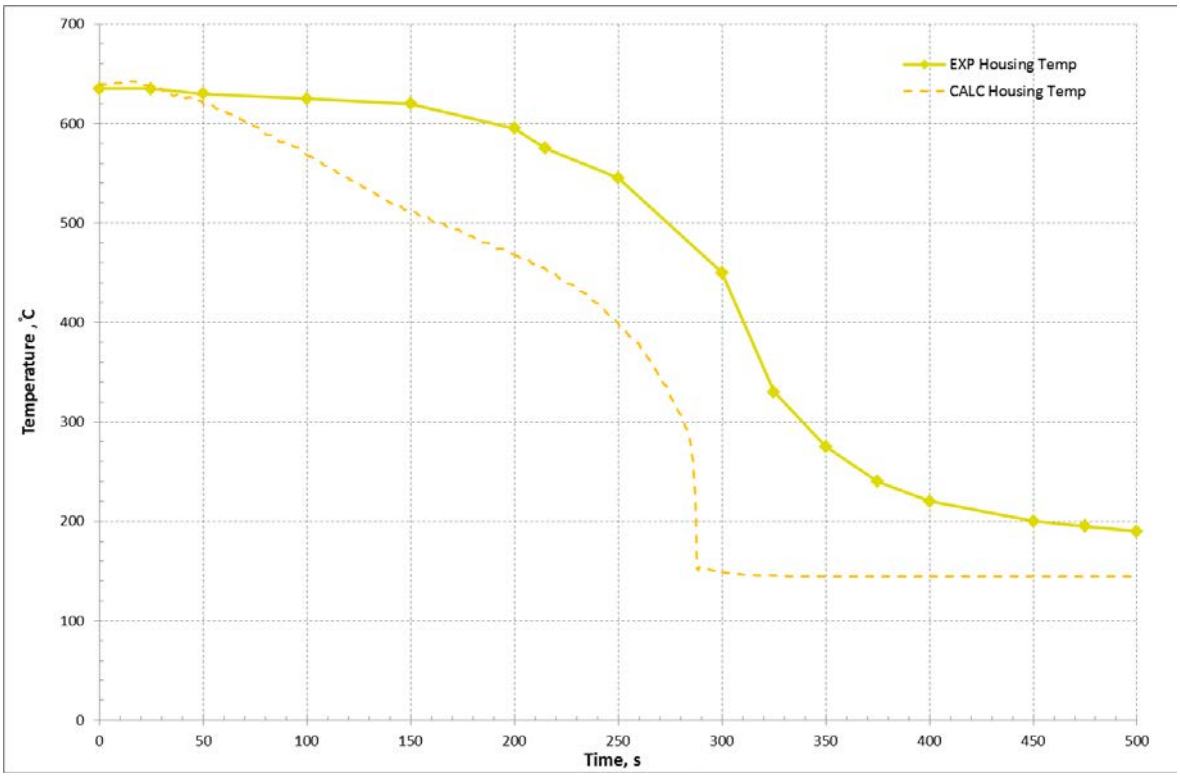

Fig B.4.4 Base case housing temperature

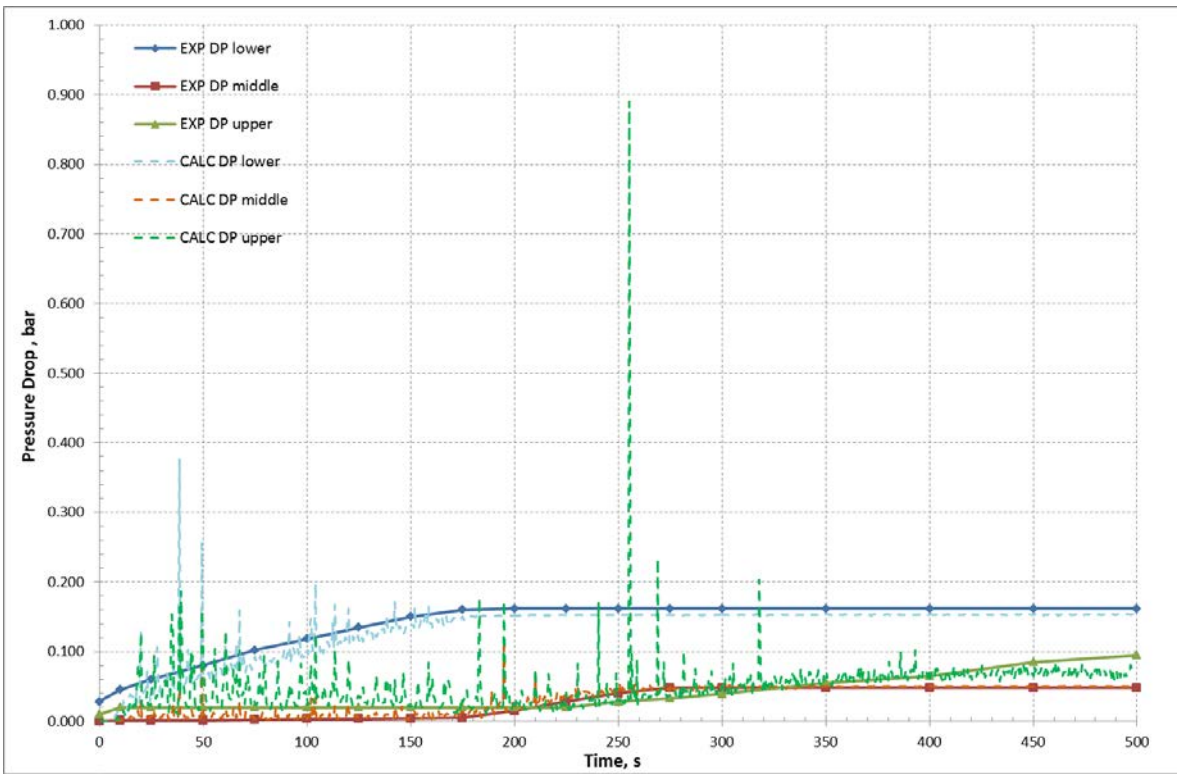

Fig B.4.5 Base case pressure drops

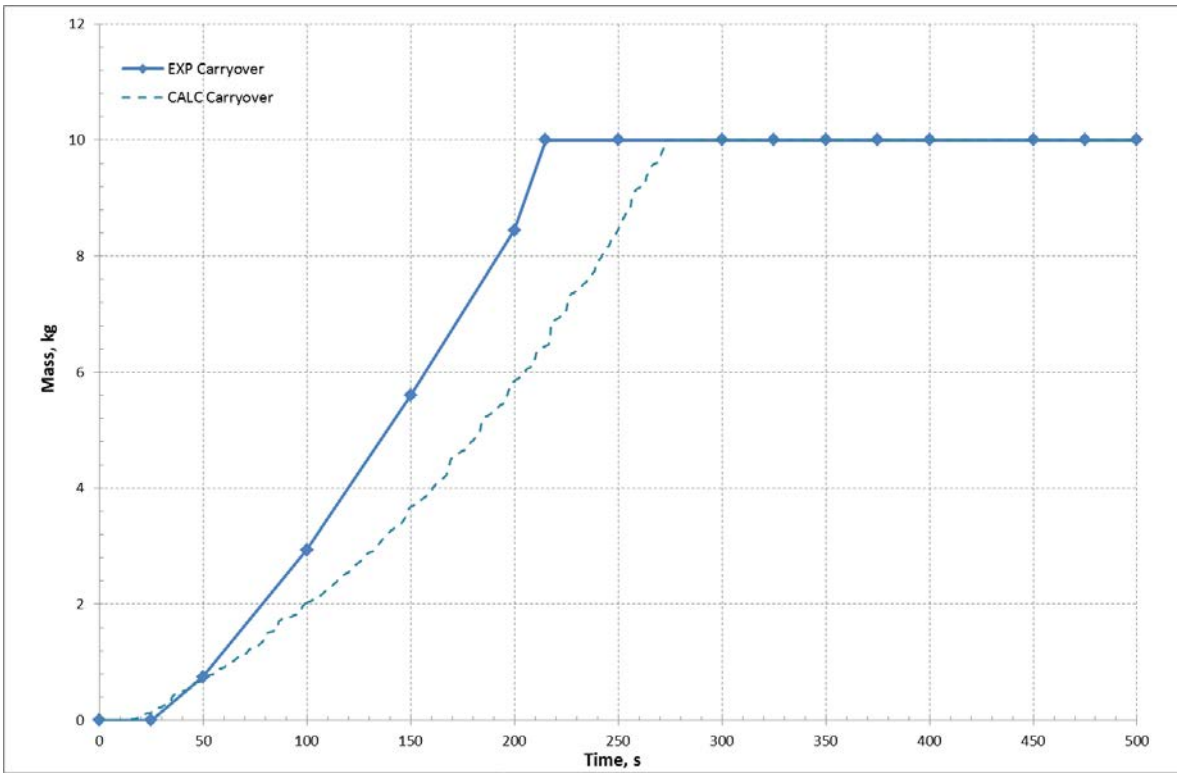

Fig B.4.6 Base case liquid carryover

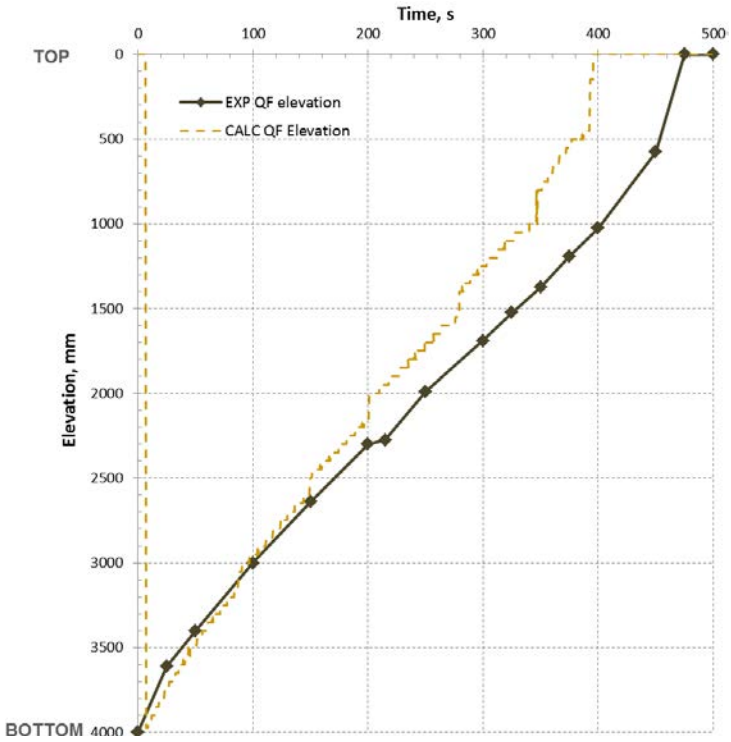

Fig B.4.7 Base case quench front propagation

PCT and bundle quench time

Tab B.4.2 Base case PCT and bundle quench

Institution name	PCT (˚C)	Position (mm)	Bundle quench (s)
VTT Technical Research Centre of Finland	858.3512	1600	396

Criteria for selection of influential input parameters

The criteria for choosing the influential input parameters is basically as suggested in the Phase II specification:

- Selection of the initial ranges of variation for each parameter is based on engineering judgment (experience from the code development, validation and behaviour in different scenarios). The initial ranges should preferably be somewhat overestimated rather than underestimated, they should taking into account the limits of physical reality, but also they should not provoke qualitative change is in the result time trends
- Influential parameters are those that in the extremes of their ranges of variation cause a substantial change (≥ 50 °C) in the wall temperature with respect to the reference case

The initial parameter list comprised of practically all the available parameters that could potentially be influential to the main responses, which include heater rod cladding temperatures, rewetting time instant, quench front elevation, pressure differences within the housing and water carry over from the top of the housing. For the large part, only input basic parameters and global parameters were considered. The exception to this are some correlations specific for reflooding, where coefficient parameters were considered as well.

Selection of parameters

Initial list of parameters

The initial list in a format of a table (prior to analysis performed) of input parameters considered as potentially influential for reflood-related phenomena is provided (see below). The considered input parameters are classified according to the definitions provided in Specifications for Phase II.

Tab B.4.3 Initial list of input parameters

Input Basic Parameter	
1	Channel free flow area
2	Channel hydraulic diameter
3	Housing thickness
4	Inlet water velocity
5	System pressure
6	Inlet water temperature
7	Rod power
8	Channel form loss coefficient
9	Grid spacer form loss
10	Grid spacer area
11	Grid spacer hydraulic diameter
12	Fuel rod filler heat capacity density
13	Fuel rod filler thermal conductivity
14	Fuel rod heater/cladding heat capacity density
15	Fuel rod heater/cladding thermal conductivity
16	Housing heat capacity density
17	Housing thermal conductivity
18	Rod initial temperatures
19	Housing initial temperatures
Input Global Parameter	
1	Wall friction coefficient / Liquid
2	Wall friction coefficient / Gas
3	Minimum film boiling temperature
4	Heat transfer to wetted wall / Forced convection to liquid
5	Heat transfer to wetted wall / Nucleate boiling
6	Heat transfer to dry wall / Film boiling
7	Heat transfer to dry wall / Forced convection to gas
8	Heat transfer to dry wall / Natural convection to gas
9	Heat transfer between liquid and interface
10	Heat transfer between gas and interface
11	Critical heat flux
12	Interfacial friction
13	Quench front height
Input Coefficient Parameter	
1	Rate of entrainment
2	Rate of entrainment / Lower void limit

3	Rate of entrainment / Upper void limit
4	Additional heat flux near quench front (AHFNQF)
5	AHFNQF / Temperature gradient coefficient
6	Max droplet diameter
7	Max droplet diameter above quench front
8	Critical Weber number for droplets

Final list of Influential Parameters

The final list of parameters has been comprised using of the criteria described above. All parameters that were dropped had significantly lover impact on the calculation results than the parameters that are included in the list. Some parameters failed to fulfil the criteria but are still included due to relatively large impact compared to the parameters that were dropped and small difference to the criteria.

Tab B.4.4 Final list of influential input parameters (variations at 1600mm)

Parameter	Subroutine	Fortran variable / Key word	Multiplier REF / REF value	Multiplier MIN	Multiplier MAX	T_{clad} variation [°C]	Position [mm]	t_{rew} variation [s]	Position [mm]
Rate of entrainment	input deck	t6unco	1.0	0.7	1.3	+46 / -39	1600	+4 / 0	1600
Wall friction coefficient / Liquid	input deck	t6unco	1.0	0.5	2.0	+54 / -33	1600	+10.5 / -10.5	1600
Minimum film boiling temperature	input deck	t6unco	1.0	0.65	1.5	+48 / +43	1600	+56.5 / -14	1600
Heat transfer to dry wall / Forced convection to gas	input deck	t6unco	1.0	0.5	1.5	+102 / -70	1600	+13 / -10	1600
Additional heat flux near quench front	input deck	t6unco	1.0	0.5	7.5	+36 / -306	1600	+42.5 / -75.5	1600
Max droplet diameter above quench front	input deck	t6unco	0.54	0.27	1.73	-74 / +90	1600	+39 / +7.5	1600
Heat transfer between gas and interface	input deck	t6unco	1.0	0.05	2.0	+163 / -48	1600	+33 / -2	1600
Critical heat flux	input deck	t6unco	1.0	0.5	1.5	+49 / +24	1600	+13.5 / -2.5	1600
Interfacial friction	input deck	t6unco	1.0	0.1	10.0	-155 / -46	1600	-33.5 / +85	1600
Quench front height	input deck	t6unco	0.745	0.495	0.995	+32 / -31	1600	+12.5 / +6.5	1600

In the case where the elevation in question is 1600 mm below reference level the maximum cladding temperature variation is considered during a time interval of 0-180s to remove the effects of differences in rewetting time. However for 2 parameters (“Additional heat flux near quench front” and “Interfacial friction”) this timeframe still includes rewetting on one of the limits. Both of these parameters have excessive ranges of variation, which also causes qualitative differences in the cladding temperature time trends.

Tab B.4.5 Final list of influential input parameters (variations at 2200mm)

Parameter	Subroutine	Fortran variable / Key word	Multiplier REF / REF value	Multiplier MIN	Multiplier MAX	T_{clad} variation [°C]	Position [mm]	t_{rew} variation [s]	Position [mm]
Rate of entrainment	input deck	t6unco	1.0	0.7	1.3	+29 / -25	2200	+2 / -0.5	2200
Wall friction coefficient / Liquid	input deck	t6unco	1.0	0.5	2.0	+63 / -36	2200	+8.5 / -5	2200
Minimum film boiling temperature	input deck	t6unco	1.0	0.65	1.5	+58 / +38	2200	+28.5 / -6.5	2200
Heat transfer to dry wall / Forced convection to gas	input deck	t6unco	1.0	0.5	1.5	+100 / -63	2200	+6 / -3.5	2200
Additional heat flux near quench front	input deck	t6unco	1.0	0.5	7.5	-59 / -278	2200	+26 / -53.5	2200
Max droplet diameter above quench front	input deck	t6unco	0.54	0.27	1.73	-48 / +87	2200	+21 / +3.5	2200
Heat transfer between gas and interface	input deck	t6unco	1.0	0.05	2.0	+126 / -31	2200	+19 / -2	2200
Critical heat flux	input deck	t6unco	1.0	0.5	1.5	+42 / -25	2200	+7.5 / -1.5	2200
Interfacial friction	input deck	t6unco	1.0	0.1	10.0	-139 / +80	2200	-29.5 / +59	2200
Quench front height	input deck	t6unco	0.745	0.495	0.995	+47 / -29	2200	+8 / +7.5	2200

In the case where the elevation in question is 2200 mm below reference level the maximum cladding temperature variation is considered during a time interval of 0-130s to remove the effects of differences in rewetting time. However for 2 parameters (“Additional heat flux near quench front” and “Interfacial friction”) this timeframe still includes rewetting on one of the limits. Both of these parameters have excessive ranges of variation, which also causes qualitative differences in the cladding temperature time trends.

Wall-to-fluid heat transfer model

In APROS, the wall-to-fluid heat is calculated as follows:

- First the heat transfer zone is deduced using void fraction, wall temperature, minimum film boiling temperature, wall heat flux and the critical heat flux. The considered heat transfer zones are wetted wall zone, dry wall zone and the transition zone
- In the wetted wall zone, the heat flux is calculated using a forced convection correlation or a nucleate boiling correlation
- In the dry wall conditions, the wall heat flux is calculated using a film boiling correlation, a forced convection correlation, or a natural convection correlation. The correlation that gives the highest heat flux is always chosen.
- In the transition zone, the heat flux is interpolated between the critical heat flux and the heat flux calculated for the dry zone

In the case of reflooding, the following changes are made to the above:

- The quench front is tracked by finding the lowest node that is not in the wetted wall zone. Above the quench front, a zone of increased heat flux is established. In this zone, a parameter called "rate of reflooding" is calculated as $(z - z_{qf}) / \Delta z$, where z_{qf} is the quench front height, and Δz is the height of the zone of increased heat flux.
- Above the quench front, an additional heat flux, dependent on the axial wall temperature gradient, is added to the wall heat flux multiplied with the rate of reflooding
- Also above the quench front, the correlations used to deduce the droplet size and the ratio of entrainment are altered. These affect the calculation of interfacial phenomena.

Conclusions

The performed analyses show that APROS underestimates the reflooding time and the peak cladding temperature in the case of the FEBA experiment. The main reasons for the observed behaviour are believed to be i) inadequate modelling of the interfacial heat transfer for the gas phase, and ii) inadequate modelling of the additional heat flux above the quench front.

The interfacial heat transfer coefficient of gas above the quench front seems to be over predicted to the extent that no substantial overheating of the gas phase can occur. This then reflects directly to the behaviour of the wall temperatures above the quench front, and finally also to the reflooding time. The additional heat flux above the quench front calculated by APROS is based on tube data at pressure of 1 bar. It is expected that this heat flux should probably be a few times larger for a bundle geometry. Also the pressure-dependence of this term increases the uncertainty of the predictions.

The results shown here have been obtained without taking into account any known code biases. Also the code used to run the calculations is not a frozen and validated version of APROS, due to the necessity of having to add the uncertainty coefficients into the code.

The final list of parameters that is to be used in the Phase III is presented above. The fact that the reference calculation results deviate so clearly from the experimental data may pose problems in the Phase III: it is anticipated that if no biases are taken into account in the process, the resulting uncertainty intervals will be remarkably wide.

In any case, the observed inadequacies in the physical modelling should addressed in the future development of APROS.

B.5 CEA (France) results

Model description

Tab B.5.1 CEA code and software platform

Institution name	Code version	Software platform
CEA (France)	V25_2 mod8.1	unix

Nodalization and basic geometrical properties

THE CEA uses a 1-D modelling of the FEBA experiment. Only the heated part of the test section is modelled . Three elements are considered in the modelling:

- The test section denoted as GRAPP and modelled with a 1-D axial component, with 40 axial meshes. Its section is that of the experiment, i.e. corresponding to a square of 78.5 mm side.
- The fuel rod simulators, denoted as CRAYONS, which are internal walls.
- The housing, denoted as BOITIER. It is an external wall.
  In addition, two boundary conditions are modelled: the inlet one, denoted as ENTREE, where the water is injected and the outlet, denoted as OUTPUT, where the pressure is imposed.

The general scheme of the modelling is shown on the Figure below.

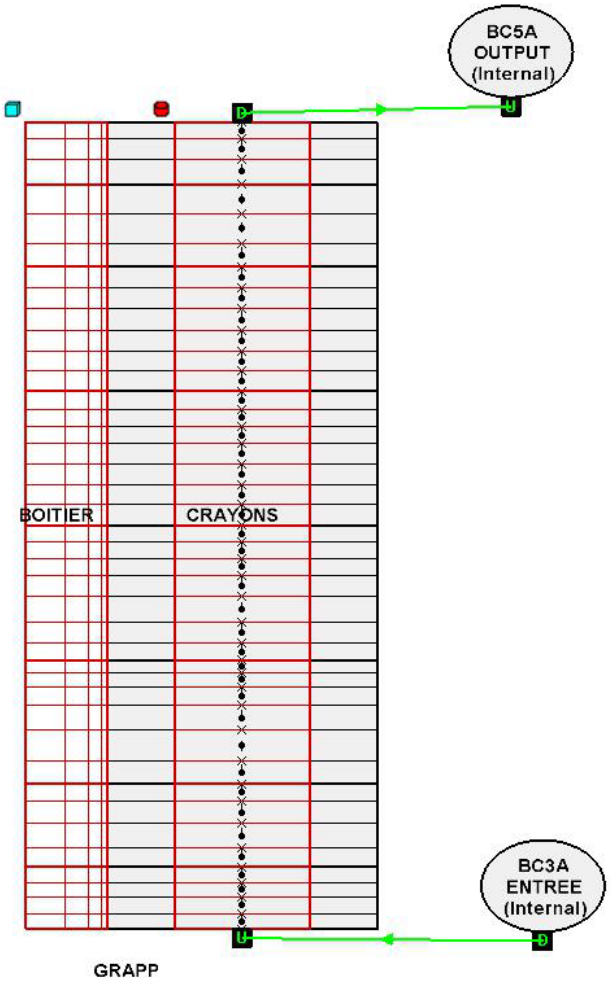

Fig B.5.1 FEBA nodalization

The main features of this modelling are listed below:

- Total height: 3900 mm;
- Heated part flow area A: It is calculated as the difference between the square of 78.5 mm side and the section of the 25 fuel rod simulators:

$$A = (78.5 * 10^{-3})^2 - 25 * [\pi * (5.375 * 10^{-3})^2] = (3893.2 * 10^{-6}) \text{ m}^2;$$

- Friction perimeter P_f. It is the perimeter of the housing plus that of the 25 fuel rod simulators:

$$P_f = (4 * 78.5 * 10^{-3}) + 25 * (\pi * 10.75 * 10^{-3}) = (1158.3 * 10^{-3}) \text{ m};$$

- Hydraulic diameter D_h: it is not an input of the data deck. CATHARE automatically calculates it by supposing the following relationship, where A is the flow area and P_f the friction perimeter:

$$D_h = \frac{4A}{P_f}$$

  Consequently, the hydraulic diameter equals 0.0134 m.
- The spacer grids are only taken into account via a form loss coefficient, equal to 1.38 for each grid;
- Total heat transfer area of the heater rods S: only a heating perimeter P_h is given in the CATHARE input data deck, calculated by considering the external perimeter of the 25-fuel-rod simulators, equal to:

$$P_h = 25 * (\pi * 10.75 * 10^{-3}) = (844.3 * 10^{-3}) \text{ m}$$

The total heat transfer area is consequently equal to $P_h * 3.9 = 3.2928$ m^2.

- Maximum linear heat rate. Only the volumetric heat rate is needed in the CATHARE input deck. Its maximum value denoted as W_{max} is $1.3186*10^{+9}$ W/m^3. It corresponds with a maximum linear power equal to 8000*1.19/3.9 = 2441 W/m (the power of the 25 fuel rods is 200 kW, i.e. 8 kW per fuel rod, their length is 3.9 m and the ratio for the maximum power is 1.19).
- 40 axial meshes are considered. All of them have roughly the same length, around 10 cm, with the following conditions:
  - The elevation of the thermocouples 12b1, 12b2, 12b3, 18a1, 18a2, 18a3 and 18a4 corresponds exactly to scalar nodes of the meshing.
  - In the same way, the limits between two levels of power (3660, 3115, 2570 mm, etc.) correspond also exactly to scalar nodes.
  - No constraint is imposed for the elevation of the spacer grids.

Boundary and initial conditions

The boundary and initial conditions are described below. The time t = 0 s corresponds with the beginning of the reflood, i.e. after the phase of heating of the fuel rod simulators and the housing.

- Pressure: 4.1E5 Pa, imposed at the outlet (OUTPUT).
- Flooding temperature: The experimental decreasing time trend is imposed with a slight delay. Indeed, as written above, only the heated section is modelled, whereas the measurement of the temperature of the water entering the section is performed under this heated part. Consequently the entering temperature is imposed with a delay of 6s, according to the Table B.5.2.

Tab B.5.2 time trend of the temperature of the inlet water considered in the CATHARE input deck

Time	0.	6.	15.	31.	105.	256.	457.	1.D+6
Inlet temperature	$T_{saturation}$	59.8	48.4	44.1	40.	38.	36.9	36.9

- Flooding velocity or mass flow rate: 3.8 cm/s.
- Power: As soon as cold water is injected, the full power is imposed, i.e., 8 kW per fuel rod. The decrease of the power vs. time (more precisely the dimensionless multiplier of the power) is given in the Table B.5.3, which follows the experimental data:
- Flooding velocity or mass flow rate: 3.8 cm/s.
- Power: As soon as cold water is injected, the full power is imposed, i.e., 8 kW per fuel rod. The decrease of the power vs. time (more precisely the dimensionless multiplier of the power) is given in the Table B.5.3, which follows the experimental data:

-

Tab B.5.3 time trend of the power considered in the CATHARE input deck

time	0.	13.	30.	50.	76.	110.	166.	214.	287.	497.
Multiplier of the power	1.	0.932	0.88	0.839	0.798	0.749	0.688	0.65	0.603	0.603

Before the beginning of the reflood, a low level of power is imposed to reproduce the operational procedure. The experimental level of power being not given, its value is tuned so that to have correct initial values of the temperature of the housing (≈635°C at 1625 mm) and of the cladding temperature (≈800°C at 1680 mm). The value of the power obtained by this way of doing is equal to 6.25% of the nominal power.

- Heat losses: Due to the thickness of the housing, the test section can be considered as well isolated and consequently no heat losses are modelled .
- Form losses: A value equal to 1.38 is imposed for each spacer grid, at the vector node the closest one to the position of the spacer grid.
- Material properties: They are deduced from the FEBA properties given with the specifications, for NiCr, MgO and the V2A steel used for the housing. Regressions have been performed for the conductivity and the volumetric heat capacity (ρCp), including the variation of the density vs. temperature.
- Initial conditions, before heating of the fuel rods and the housing: The test section is filled with superheated stagnant vapour at 4.1E5 Pa. The temperature of the vapour is arbitrary taken equal to 200°C. In fact the housing is heated by radiation from the heater rods, and the radiation model of CATHARE is activated only for a wall temperature 25°C higher than the saturation temperature.

Adopted models (flags)

The main specific model activated for the description of the transient is the reflood model. It is activated after the heating phase at low power, at the end of which the housing temperature at 1625 mm equals ≈635°C and the cladding temperature at 1680 mm equals ≈800°C. The reflood model has two main features. The first one is the consideration of additional wall to fluid heat transfers: A 2-D conduction calculation of the fluid to wall heat flux is performed via a very fine 2-D meshing moving at the speed of the quench front. And an evaporation flux between wall and interface is introduced just downstream from the quench front to take into account the violent boiling and the liquid sputtering. The second feature is that, downstream from the quench front, some physical models (interfacial heat transfers, wall to fluid heat transfers, interfacial friction) are modified with respect to the case without reflood.

For the housing, two different options were possible for the description of the fluid to wall heat transfers: considering the standard correlations without reflood or the correlations modified for reflood. The housing being quite thick, its inertia is rather important and using standard correlations could be justified. Nevertheless, a behaviour similar to reflood, with a kind of softened quench front, is observed on the experimental time trend of the housing temperature at 1625 mm. Consequently the reflood correlations are used for the housing to fluid heat transfers.

The radiation between the fluid and the walls is taken into account. It is activated from the start since the considered initial vapour temperature is high enough (200°C). Nevertheless the specific wall to wall radiation model of CATHARE is not used.

Assumptions and steady-state achievement

The procedure used to reach the “initial” conditions corresponding to the start of the reflood (t = 0 s) is as close as possible to the experimental one. Experimentally and in the CATHARE input data deck, the fuel rod simulators are heated in stagnant steam using a low rod power. But the experimental value of this power is not provided. Consequently, in the CATHARE input data deck, it is tuned in order to reach roughly at the same time the experimental initial housing temperature at 1625 mm and the experimental initial cladding temperature at 1680 mm (respectively 635°C and 800°C). For that, a power equal to 6.25% of the nominal power is considered. The heating of the housing is obtained by radiation, from the fuel rod simulator to the

fluid, and from the fluid to the housing. In CATHARE, this radiation is active as long as the wall temperature is 25°C higher than the saturation temperature. That is the reason why the initial value of the vapour temperature, before the activation of radiation, is taken equal to 200°C.

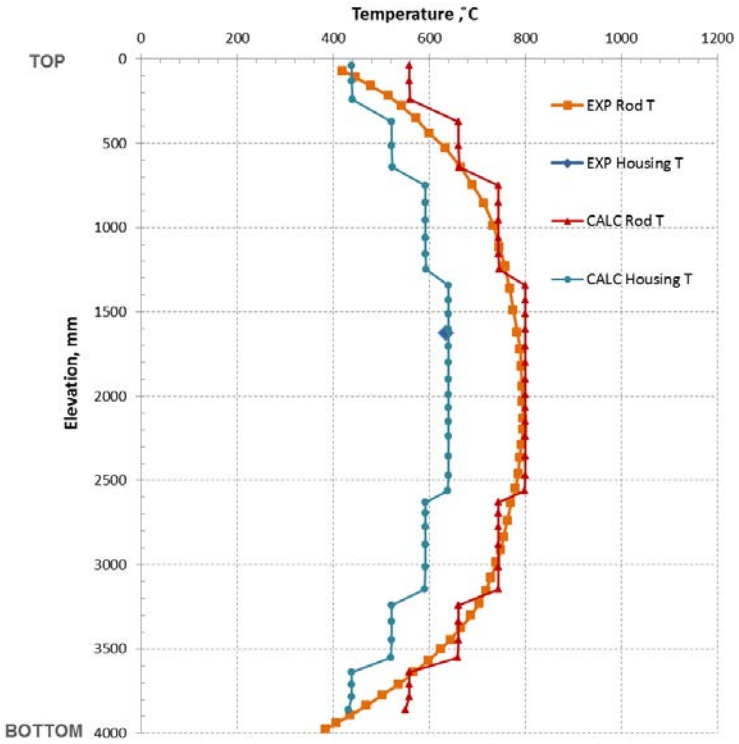

Fig 5.2 Steady-state temperature profile

Base case results

The main features of the calculation are the followings:

- The initial maximum cladding and housing temperatures are well predicted. The calculated profile for the cladding temperature is less smooth than the experimental one, with a high influence of the axial power steps.
- The quench front progression is a little bit too quick.
- The cladding temperatures are well predicted, at least in the first part of the transient. When the quench front becomes close, the cladding temperatures are underestimated due to the too early prediction of the quench front progression.
- The prediction of the liquid carryover and the pressure drops are satisfactory.
- Oscillations are present for the cladding temperatures vs. time and the pressure drops, especially in the lower part. Consequently, the liquid carryover is not very regular.

Figures of all (exp-calc) responses

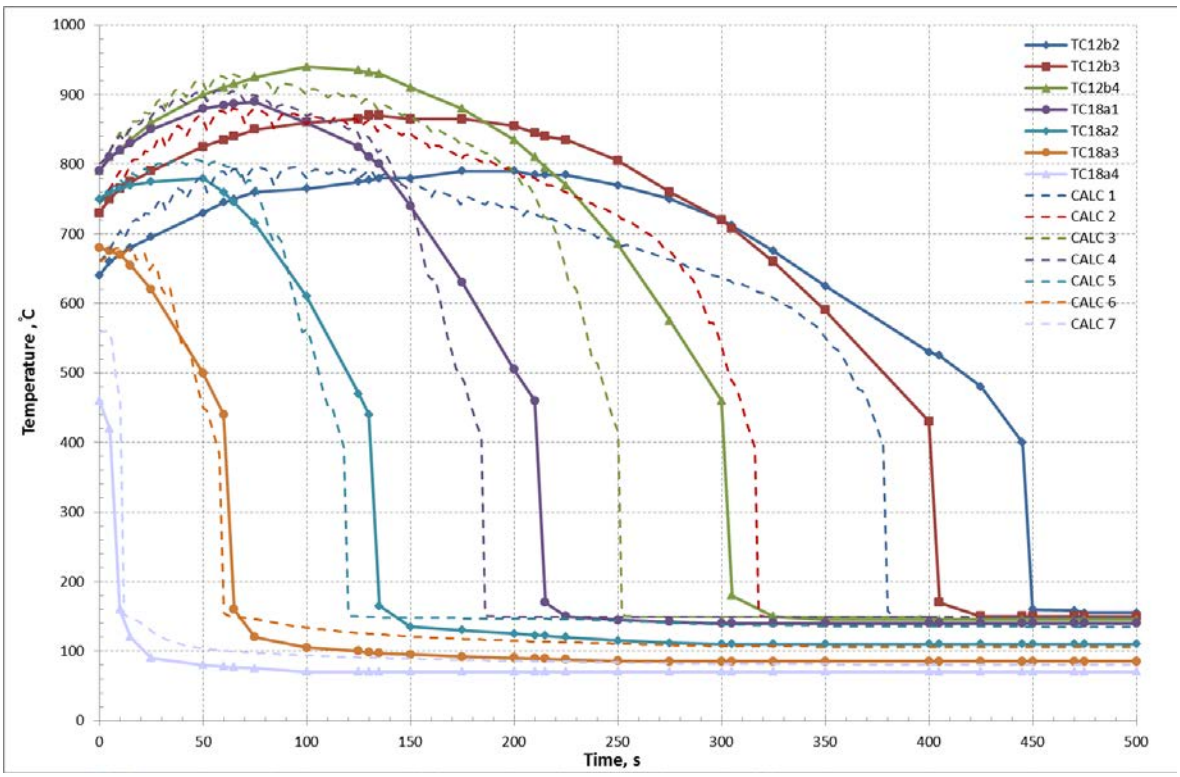

Fig B.5.3 Base case cladding temperatures

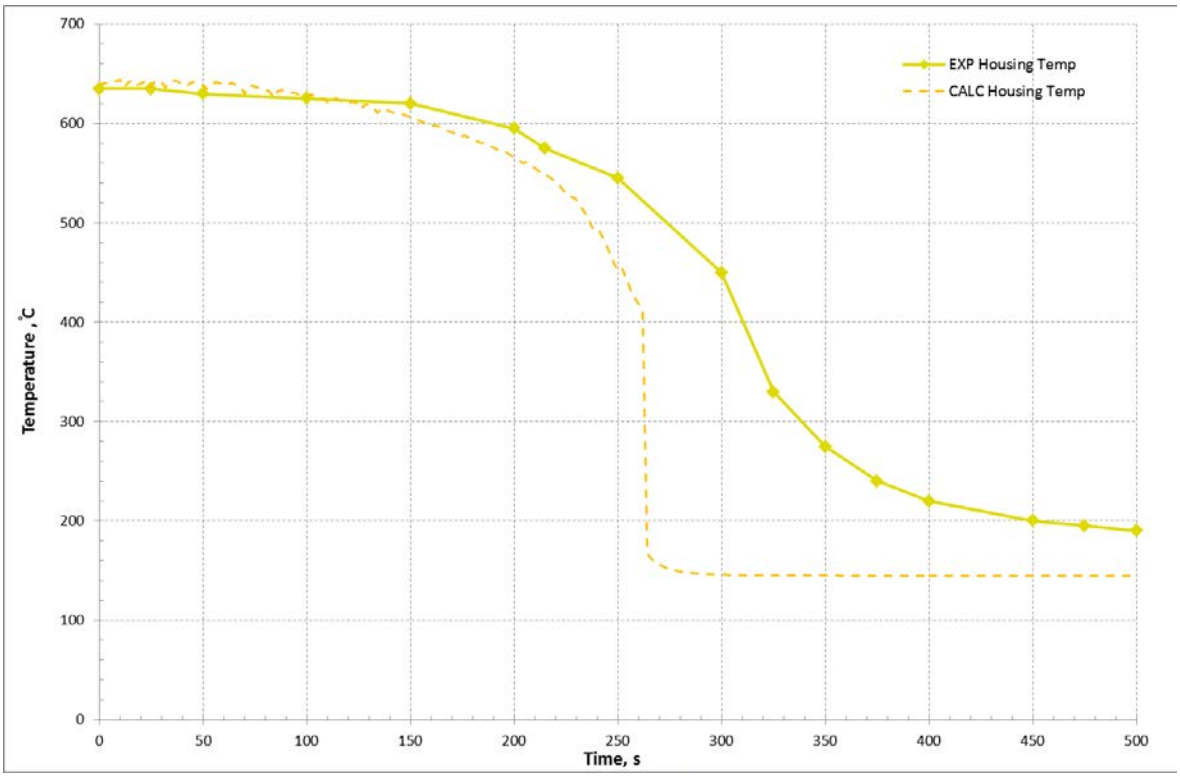

Fig B.5.4 Base case housing temperature

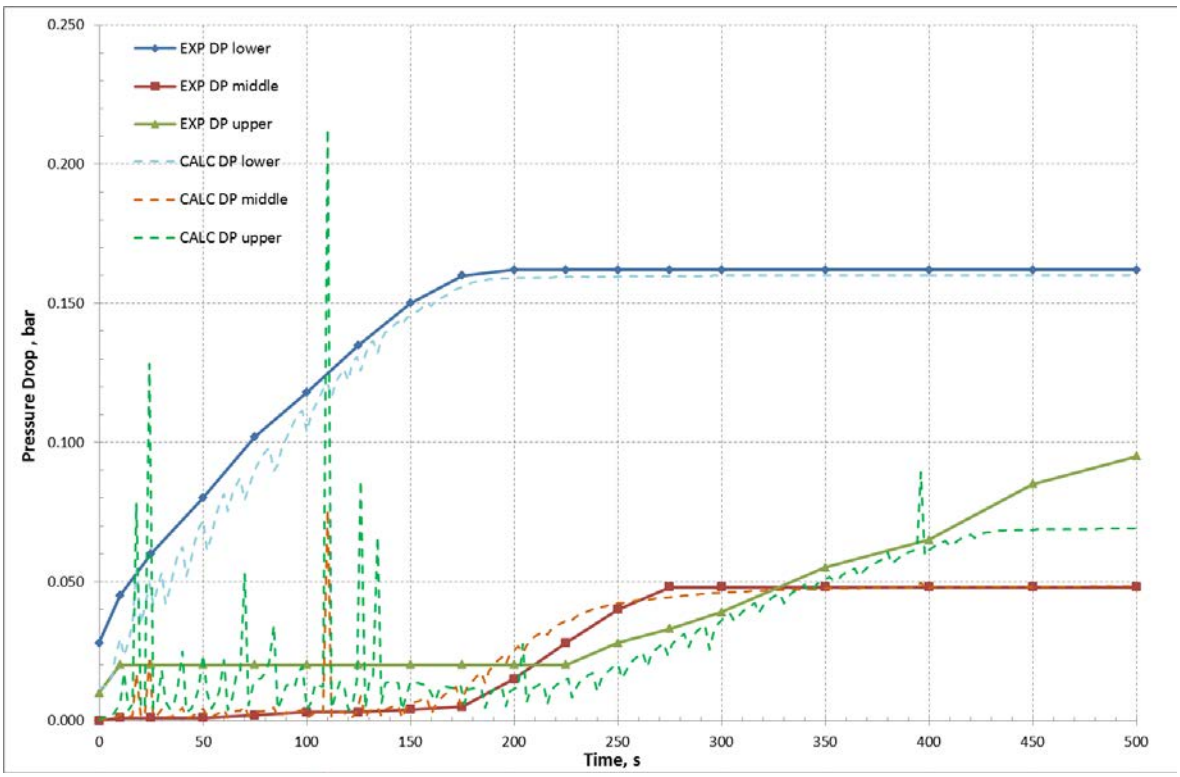

Fig B.5.5 Base case pressure drops

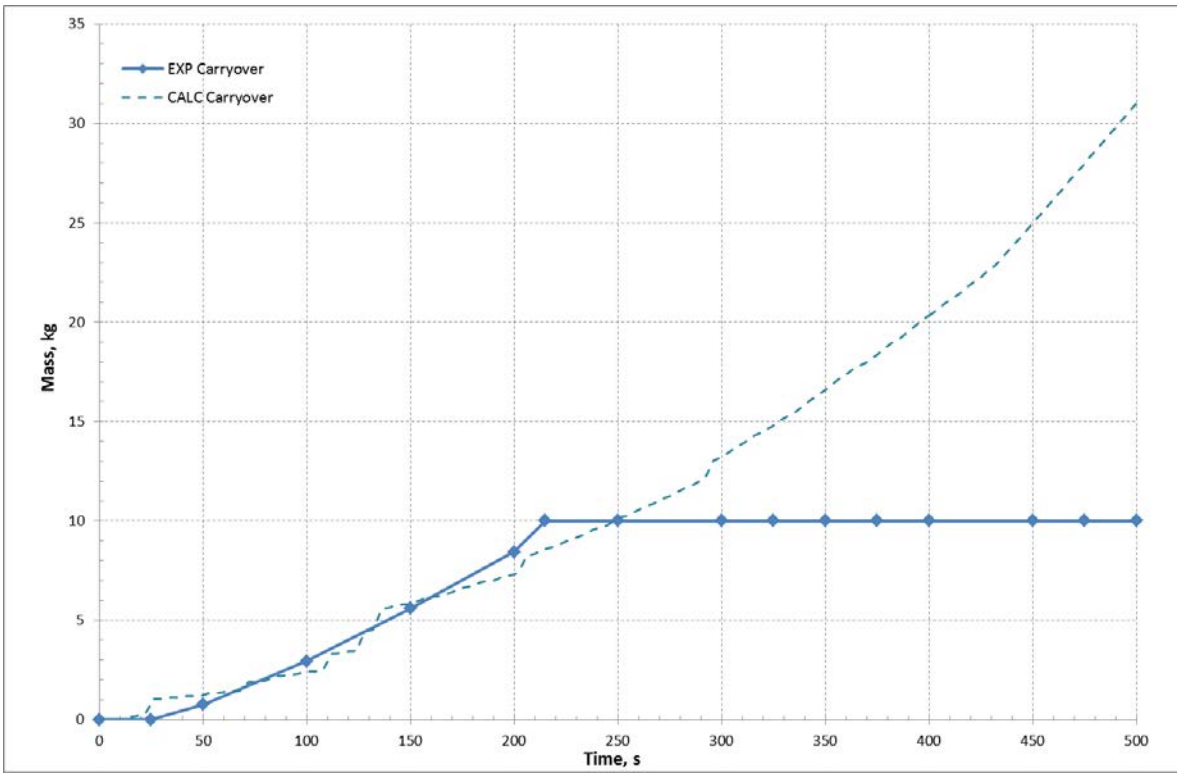

Fig B.5.6 Base case liquid carryover

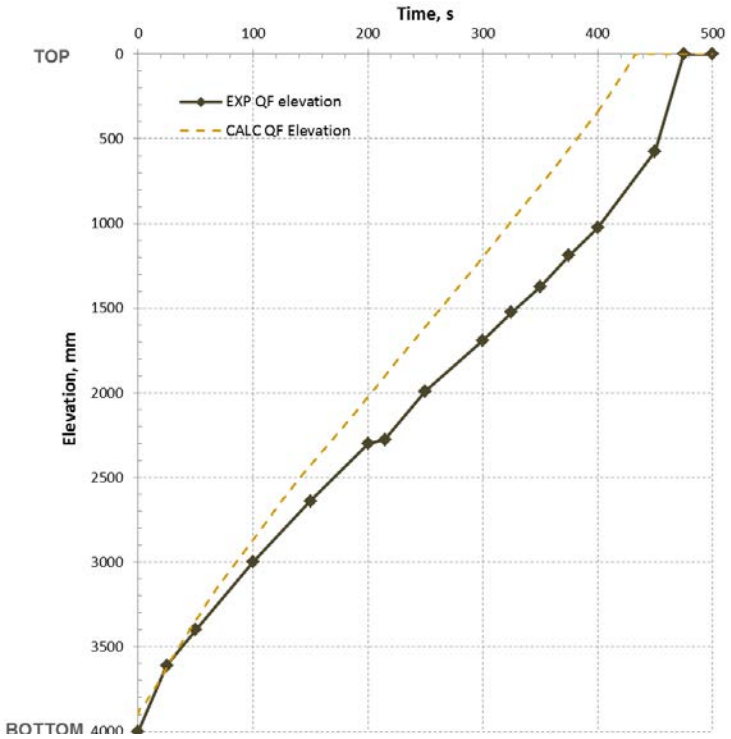

Fig B.5.7 Base case quench front propagation

PCT and bundle quench time

Tab B.5.4 Base case PCT and bundle quench

Institution name	PCT (˚C)	Position (mm)	Bundle quench (s)
CEA	931.	1587.5	429.

Criteria for selection of influential input parameters

The responses and the associated sensitivities chosen for the selection of influential input parameters are those defined in the specifications. They are:

- The maximum cladding temperature at 1680 mm. More precisely cladding temperatures for both values of the parameter, the lower and the higher ones, are compared with the nominal maximum cladding temperature, at the time when the latter occurs, i.e., around 65 s. The drawback of this way of doing is that, for higher times, the differences between nominal and shifted calculations become higher. The advantage is that the same time is considered for all the sensitivity calculations, whatever the input parameter is. The absolute difference between both temperatures, denoted as ΔT_{ref}, is the sensitivity of this response. It is important to note that this difference is only approximately quantified due to the oscillations of the calculated temperatures. An estimation of the accuracy of this difference is roughly 5°C.
- The rewet time at 1680 mm. It is the time when the cladding temperature is lower than the saturation temperature plus 30°C, i.e. lower than 180°C. The absolute difference between both rewet times, denoted as Δt_{rew} and obtained for the higher value and the lower value of the parameter is the sensitivity of this response. Its determination is performed via printouts in the result listing file and is very precise.
- The quench front elevation vs. time. More precisely, the mean relative difference between both quench front elevations, obtained for the higher value and the lower value of the parameter is the sensitivity of this response. It is expressed in % and is denoted as ΔQF. Its determination is not very precise because the relative difference between both quench-front progressions increases vs. time. One can consider that the precision of this response is around ±1% for the low sensitivities, ±2% for the higher ones: for example for the parameter interfacial friction, the sensitivity is 26% ± 2%.

The criteria are defined once the sensitivity calculations are obtained, by looking at the distribution of the sensitivities: ΔT_{ref}, Δt_{rew} and ΔQF. Consequently, 3 groups of parameters are defined for each response, according to the Table B.5.5:

Tab B.5.5 Criteria for selection of influential parameters

	High influence	Medium influence	Low influence
T_{ref}	$\Delta T_{ref} > 120°C$	$40°C < \Delta T_{ref} < 70°C$	$\Delta T_{ref} < 35°C$
t_{rew}	$\Delta t_{rew} > 70$ s	20 s $< \Delta t_{rew} < 35$ s	$\Delta t_{rew} < 14$ s
QF	$\Delta QF > 25\%$	$\Delta QF \approx$ 10-12%	$\Delta QF < 8\%$

But the observation of the time trends: cladding temperature at 1680 mm and quench front elevation, for the nominal calculation and the calculations with the lower value of the parameter and its higher value is the most meaningful means to decide the influence of a given parameter. Such figures are then provided in this document, in addition to the numerical values of ΔT_{ref}, Δt_{rew} and ΔQF.

Selection of parameters

Initial list of parameters

The initial list of parameters is based on the list of the Appendix A of Specifications for the Phase II, with the distinction of Input Global Parameters (IGP), Input Basic Parameters (IBP) and Input Coefficient Parameters (ICP). Concerning the IGP, two parameters are considered for the interphase heat transfers: a multiplier of the interface-liquid heat transfer (qle) and a multiplier of the interface-vapour heat transfer (qve). The IBP are exactly the ones of the Specifications. Only 3 ICP are considered:

- The global rate of entrainment whatever the physical law where it is used: interfacial friction or interface heat transfers (qle and qve). More precisely, in CATHARE, there are 4 rates of entrainment: two for interfacial friction, upstream and downstream from the quench front and two for interface heat transfers (qle and qve), also upstream and downstream from the quench front. In this part of the study, these 4 rates of entrainment are simultaneously shifted, since they represent the same phenomenon.
- The droplet diameter whatever the physical law where it is used: interfacial friction or interface heat transfers (qle and qve). With the same logic as for the rate of entrainment, there are, in CATHARE, 4 droplet diameters. And in the same way as for the rate of entrainment, they are simultaneously shifted in this part of the study.
- The threshold distance used in the heat transfer enhancement just downstream from the quench front, due to the violent boiling and the liquid sputtering. Its reference value is 60 cm.

The other ICP of Appendix A of the Specifications are not considered for the following reasons:

- The spacer grid heat transfer enhancement factor is not modelled in CATHARE.
- Interfacial area: Such a notion is not explicitly described by CATHARE, notably because it would depend on the type of flow (dispersed or with a film for example); consequently the physical models such as interfacial friction or interface heat transfers do not explicitly use interfacial area.

This first series of Input Parameters is given in the Table B.5.6, with their range of variation. These ranges of variation have been given by expert judgment.

Tab B.5.6 Initial list of input parameters

Input Global Parameters		
1	Interface-liquid heat transfer (qle)	0.2 - 5
2	Interface-vapour heat transfer (qve)	0.5 - 2
3	Interfacial friction	0.1 - 10
4	Global wall heat transfer	0.5 - 2
5	Heat transfer related to the very local QF progression (2-D wall conduction: k2)	0.5 - 2
Input Basic Parameters		
1	Pressure	0.99 – 1.01
2	Inlet velocity	0.98 - 1.02
3	Inlet temperature (reference value: see table 2)	±2°C
4	Initial wall temperature (reference value: 800°C)	±10°C
5	Power	0.99 – 1.01
6	NiCr conductivity	0.95 – 1.05
7	NiCr volumetric heat capacity (ρCp)	0.95 – 1.05
8	MgO conductivity	0.8 – 1.2
9	MgO volumetric heat capacity (ρCp)	0.8 – 1.2
10	Hydraulic diameter	0.995 – 1.005
11	Form loss coefficients	0.5 - 2
Input Coefficient Parameters		
1	Rate of entrainment	0.7 – 1.3
2	Droplet diameter	0.5 – 2
3	Threshold distance (reference value: 60 cm)	0.7 – 1.3

Temporary list of Influential Parameters

The following Table B.5.7 gives the sensitivity results for the influential parameters among the first initial list of Table B.5.6. According to the defined criteria, only 6 parameters are influential (high influence or medium influence) for at least one response. In Table B.5.7, high influence is indicated with a dark orange background, and medium influence is indicated with a clear orange background.

Tab B.5.7 Influential parameters among the fi rst series of parameters

Type of para meter	Parameter	Subroutine or keyword	Multiplier MIN	Multiplier MAX	T_{ref} variations [°C]	ΔT_{ref} total variation [°C]	t_{rew} variations [s]	Δt_{rew} total variation [s]	QF variations [%]	ΔQF total variation [%]
IGP	Interface-vapour heat transfer	SP1QVE	0.5	2	+20/-20	40	+3.2/-2.5	5.7	-1.5/+1.5	3
IGP	Interfacial friction	SP1TOI	0.1	10	+12/-54	66	-25.8/+54.4	80.2	+11/-15	26
IGP	Global wall heat transfer	PQPT	0.5	2	+95/-108	203	+57.1/-45.1	102.2	-15.5/+20.5	36
IGP	Very local QF progression (k2)	P1K2FDT	0.5	2	+6/-40	46	+47.6/-57.3	104.9	-15/+30	45
IBP	MgO volumetric heat capacity (ρCp)	FWOMGO.f	0.8	1.2	+20/-13	33	-10.8/+11.1	21.9	+4/-4	8
ICP	Global droplet diameter	SP1DGTOI, SP1DGFDT, SP1DGQLU, SP1DGQLD	0.5	2	-25/+25	50	+7.8/-5.7	13.5	-2.5/+2.5	5

Here are some comments on the presentation of the results of the Table B.5.7:

- The type of parameter is mentioned.
- Excepted for the material properties, all the parameters are modified from the input data deck. The name of the variable of the input deck is given in the table.
- The material properties are modified in the subroutines where they are calculated: the name of the subroutine for the only influential material property (ρCp of MgO) is indicated.
- All the influential parameters are multipliers: their reference value is equal to 1 and is not indicated in the table.

In addition to the response variation corresponding to the MIN value with respect to the nominal value of the parameter (idem for the MAX value of the parameter), the total variation MAX-MIN is also given, for each kind of response.

- The sensitivity results are provided for the 3 responses: T_{ref}, t_{rew} and QF defined in criteria. T_{ref} and t_{rew} are taken at the 1680 mm elevation, not indicated in the table.
- For the QF variation, a negative value means that the QF elevation with the shifted parameter is lower than with the nominal calculation. In other words, the quench front progression is slower.

Figures are more meaningful than a table to show the sensitivity results. For each parameter of Table B.5.7, the cladding temperatures at 1680 mm vs. time and the quench front progressions are presented for the 3 calculations: the nominal one, the calculation with the minimum value of the parameter and the calculation with its maximum value.

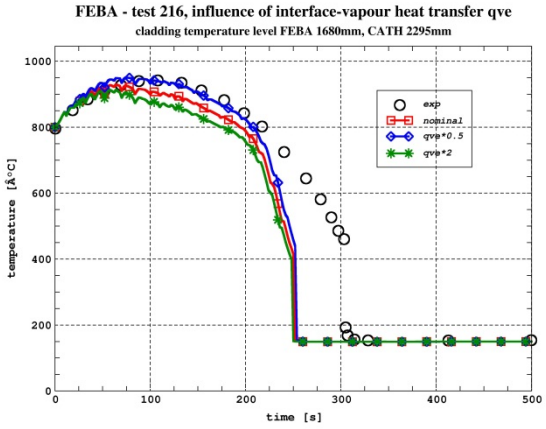

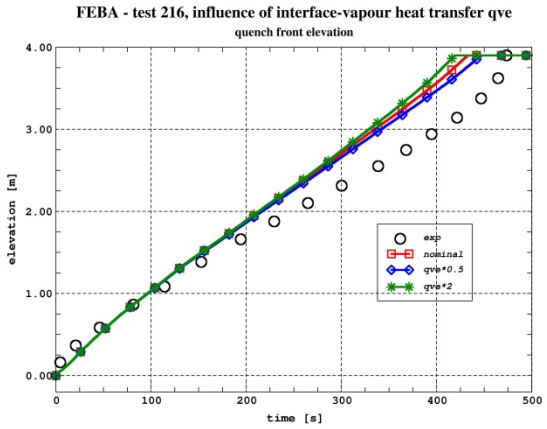

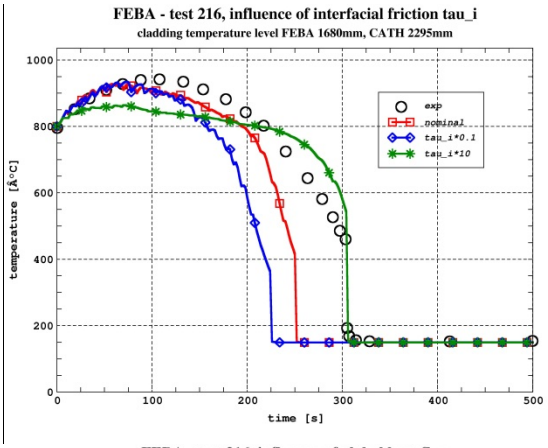
FEBA - test 216, influence of interfacial friction tau_i
cladding temperature level FEBA 1680mm, CATH 2295mm
temperature [°C]
time [s]
exp
nominal
tau_i*0.1
tau_i*10

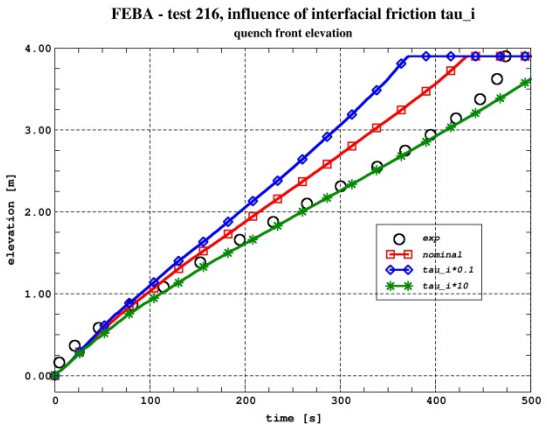
FEBA - test 216, influence of interfacial friction tau_i
quench front elevation
elevation [m]
time [s]
exp
nominal
tau_i*0.1
tau_i*10

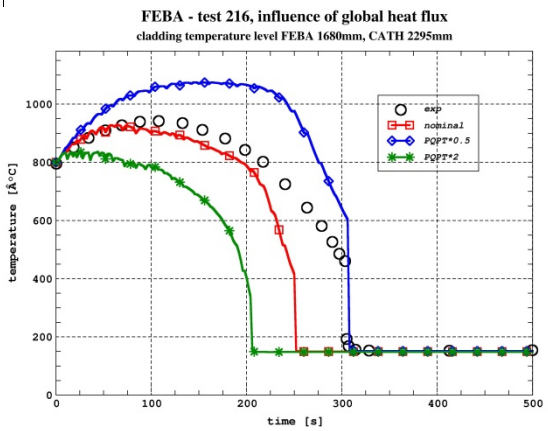
FEBA - test 216, influence of global heat flux
cladding temperature level FEBA 1680mm, CATH 2295mm
temperature [°C]
time [s]
exp
nominal
POPT*0.5
POPT*2

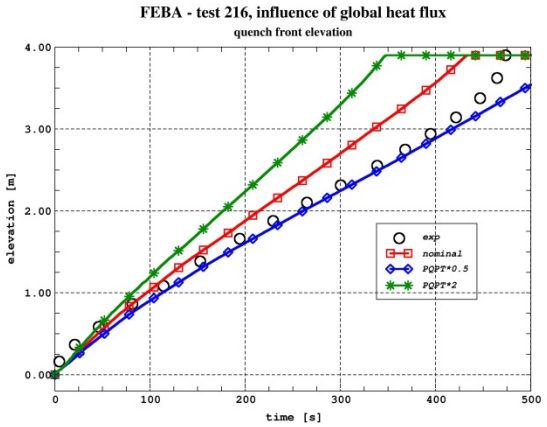
FEBA - test 216, influence of global heat flux
quench front elevation
elevation [m]
time [s]
exp
nominal
POPT*0.5
POPT*2

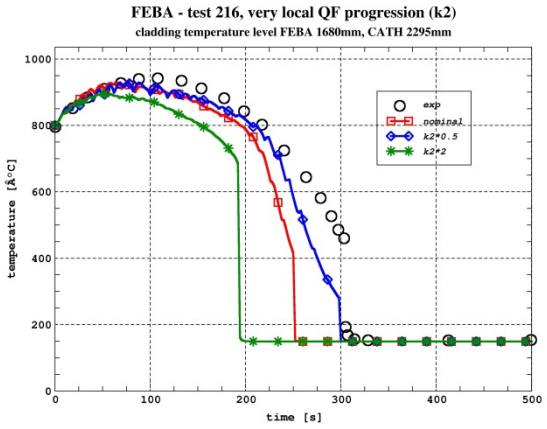
FEBA - test 216, very local QF progression (k2)
cladding temperature level FEBA 1680mm, CATH 2295mm
temperature [°C]
time [s]
exp
nominal
k2*0.5
k2*2

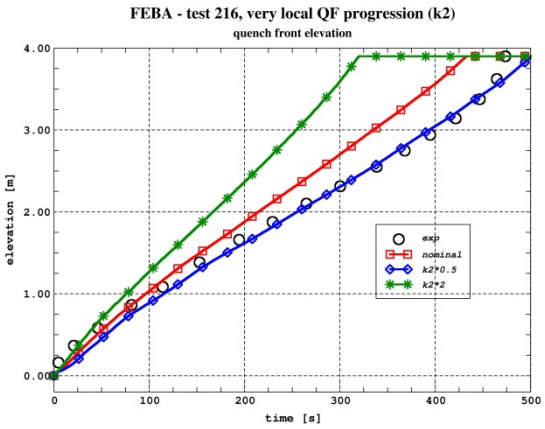
FEBA - test 216, very local QF progression (k2)
quench front elevation
elevation [m]
time [s]
exp
nominal
k2*0.5
k2*2

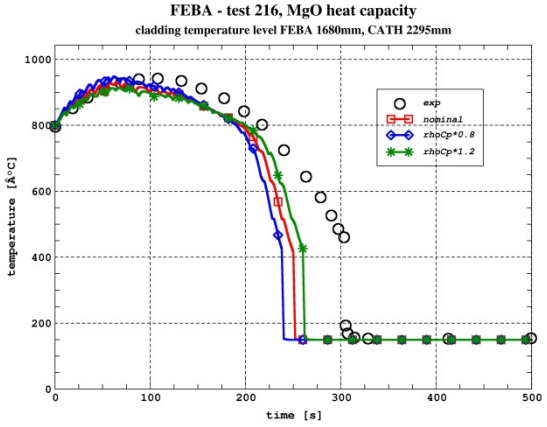
FEBA - test 216, MgO heat capacity
cladding temperature level FEBA 1680mm, CATH 2295mm
temperature [°C]
time [s]
exp
nominal
rhoCp*0.8
rhoCp*1.2

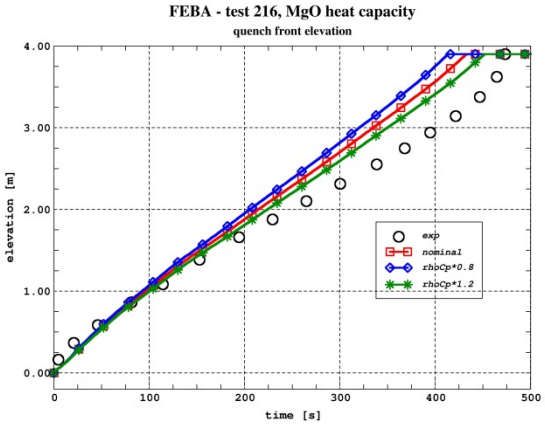
FEBA - test 216, MgO heat capacity
quench front elevation
elevation [m]
time [s]
exp
nominal
rhoCp*0.8
rhoCp*1.2

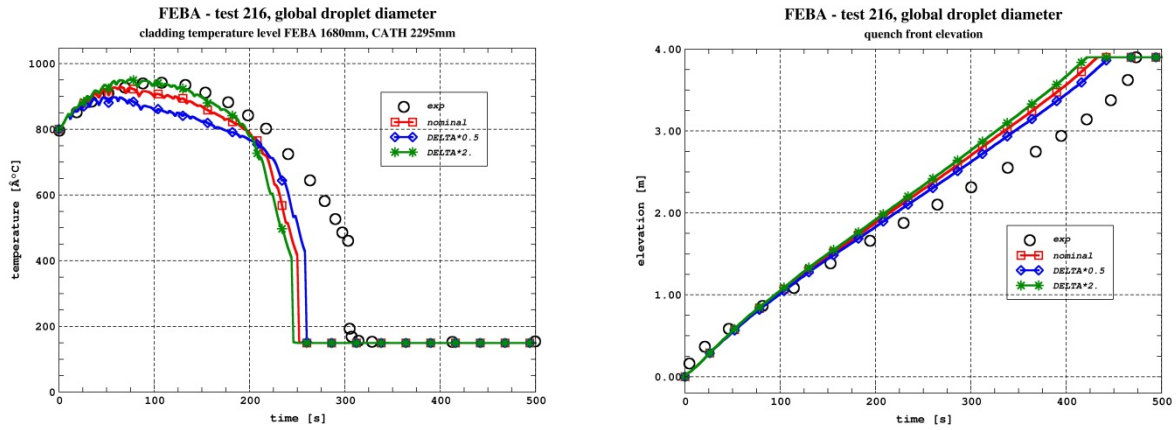

Fig B.5.8 Sensitivity calculation results for the 6 influential parameters of the initial list of Table B.5.6

The Table B.5.7 and the Figure B.5.8 show that the clearly dominant parameters are:

- The interfacial friction SP1TOI;
- The global wall heat transfer PQPT;
- The very local QF progression (k2) P1K2FDT.

The 3 other parameters, which have a medium influence, are:

- The interface-vapour heat transfer SP1QVE;
- The MgO volumetric heat capacity (ρCp);
- The global droplet diameter δ modified by shifting simultaneously SP1DGTOI (δ for interfacial friction upstream from the QF), SP1DGFDT (δ for interfacial friction downstream from the QF), SP1DGQLU (δ for qle/qve upstream from the QF) and SP1DGQLD (δ for qle/qve downstream from the QF).

All the dominant parameters are of IGP type. The other parameters with a medium influence are an IGP, an IBP and an ICP.

However, the opinion of CEA is that these sensitivity results must not be considered as they stand. The arguments for that are explained below.

CEA considerations about the list of Input Parameters to be considered

The Input Basic Parameters IBP

Generally speaking, the nature of the IBP is different from that of the IGP and ICP, since these parameters are not physical models of the CATHARE code. Their uncertainty is known a priori: it should be theoretically given by the experimenters. Consequently, for Phase III of PREMIUM, it seems preferable to impose this uncertainty and not to estimate it, unlike the uncertainty of the IGP and the ICP.

Among the IBP, only the volumetric heat capacity (ρCp) of MgO is influential, but significantly less than the 3 dominant parameters (see figure 2). In addition, its range of variation [0.8; 1.2] is probably too broad. In reality, the uncertainty of Cp is quite low: ±5% according to the Appendix I of Specifications for Phase II on the FEBA material properties. The problem is the estimation of the ρ density, badly known due to an unknown porosity. Consequently it would be better to describe the uncertainty of ρCp of MgO by a bias due to the porosity and a low standard deviation corresponding to the ±5% variation. This bias being unknown and ρCp of MgO having only a medium influence with the [0.8; 1.2] range of variation, CEA decides not to consider it in the Phase III of PREMIUM.

The Input Coefficient Parameters ICP

Considering ICP for an uncertainty study such as Phase III of PREMIUM raises some problems for different reasons.

The first reason is that a given ICP is always dependent on one or several IGP. Let us consider for example the droplet diameter, which is the only ICP rather influential among the considered ones. This parameter depends on two influential IGP: the interfacial friction and the vapour-interface heat transfer (qve). We are going to demonstrate more precisely this affirmation in the next paragraph by considering separately the 4 droplet diameters: SP1DGTOI, SP1DGFDT, SP1DGQLU and SP1DGQLD.

Another example can be taken to show that ICP and IGP are dependent: let us consider the threshold distance used for the heat transfer enhancement just downstream from the quench front, even if it is not a relevant parameter. This parameter is present in the correlation describing this heat transfer enhancement, which is a part of the wall-interface heat transfer physical model, which is itself a part of the IGP global wall heat flux (PQPT). Consequently this threshold distance must not be considered at the same time as PQPT.

The second reason is that the list of the possible ICP is almost endless, and in any case not limited to the parameters of the table 6. For example one could consider the different modes of wall-fluid heat transfers or the different physical models depending if they are taken upstream or downstream from the quench front. By the way, the influence of some of them, not quoted in the Appendix A of the Specifications such as forced convection with vapour, will be estimated in the next paragraph. Other kinds of ICP are the coefficients of the physical models. Considering all the kinds of ICP is impossible, since there is no limitation in their list. And finding a criterion to consider only a given type of ICP seems difficult. Due to this doubt about the completeness of the list of ICP, there is always a risk to forget one or several ones among them.

With these considerations, it becomes obvious that the droplet diameter cannot be retained among the parameters considered for Phase III of PREMIUM. A last reason is that its influence is significantly less than the influence of the 3 dominant parameters (interfacial friction, global wall heat transfer, k2).

The Input Global Parameters IGP

At the light of the former paragraph, considering only IGP could be also a good solution, avoiding dependences. In addition and unlike the ICP, their list is limited. But the risk of such an approach is to consider too general parameters. Indeed the most general IGP are the 7 closure laws involved in the different balances and used in any thermo-hydraulic code, including CATHARE. They are:

For the momentum balance equations:

- Gas: Cg: wall-vapour friction coefficient and τi: interfacial friction;
- Liquid: Cl: wall-liquid friction coefficient and τi: interfacial friction.

For the energy balance equations:

- Gas: qpv: wall-vapour heat transfer and qve: vapour-interface heat transfer;
- Liquid: qpl: wall-liquid heat transfer and qle: liquid-interface heat transfer.

All balances:

- qpi: wall-interface heat transfer via Γ, the interfacial mass transfer.

In case of reflood, one can add:

- k2, parameter related to the very local quench front progression describing the 2-D conduction in the wall (P1K2FDT in the Table B.5.6).

For the Phase II of PREMIUM:

- Cg and Cl have not been considered because they are obviously not influential;
- qle, qve and τi have been considered;
- qpv, qpl and qpi have been merged into a macro-parameter: global wall heat transfer;
- k2 has been considered.

But considering only IGP has an outstanding drawback. Whatever the considered experiment, the closure laws, i.e., the IGP, are the same. It is right for any kind of experiment, even if it is not devoted to the study of reflood. Consequently, for each experiment, uncertainty methods will give different uncertainties for the IGP and the synthesis of all these uncertainties will pose problems.

The method for the selection of the influential parameters proposed by CEA

Consequently, another approach is proposed by CEA for PREMIUM and more generally for any uncertainty determination. For the experiment(s) considered for an uncertainty study, the dominant physical phenomena are listed by expert judgment. After that, the physical models related to these macro phenomena are identified, via expert judgment helped with sensitivity calculations. They can be of IGP type such as interfacial friction. But they can also be of ICP type, such as forced convection with vapour, or interfacial friction downstream from the quench front. The constraint is to not consider together redundant parameters such as global interfacial friction and interfacial friction downstream from the quench front, or global wall heat transfer and forced convection with vapour.

Another constraint for CEA is the limited number of input parameters that the method planned for Phase III, CIRCE, can consider. It is due to the limited number of experimental available responses, but also to the nature of these responses, as explained below for the vapour-interface heat transfer (qve).

For FEBA, the physical phenomena influential on the cladding temperatures and the quench front progression are:

1. All the terms describing the wall-fluid heat transfers, but only downstream the quench front;
2. The mechanical laws controlling the amount of water downstream from the quench front;
3. The parameter related to the very local quench front progression describing the 2-D conduction in the wall, denoted as k2 (P1K2FDT in the Table B.5.6).

For the macro-phenomenon 1, one can consider the different wall heat transfer modes: forced convection with vapour associated with vapour-interface heat transfer, film boiling, liquid and vapour radiation, etc. But it results in too many input parameters for CIRCE. Another possibility is to consider only one global physical model which is the global wall heat transfer, but just downstream from the quench front (denoted as PQFDT), unlike the PQPT parameter considered in the initial list of table 6. Both methods have the advantage to be specific to a reflood experiment but the second one requires considering only one parameter and is preferred. It would have been preferable to consider separately the vapour-interface heat transfer (qve), but this model is especially influential on the vapour temperatures, badly measured in FEBA experiment. Consequently, CEA chooses to include its uncertainty into that of PQFDT, since qve contributes also to the determination of the wall temperature as explained in paragraph below describing wall-to-fluid heat transfer model.

Two interfacial frictions can be considered for the macro-phenomenon 2: the interfacial friction upstream from the quench front of bubble-slug type and the interfacial friction downstream from the quench front of annular with droplet entrainment type. In this case too, both interfacial frictions are more specific of a reflood experiment such as FEBA than only one global interfacial friction.

The macro-phenomenon 3, k2, has been already studied.

Additional sensitivity calculations

As a consequence, some additional sensitivity calculations have been performed to illustrate:

- the former considerations about the final choice of input parameters: the 5 first parameters;
- the rule of the different droplet diameters: the 4 other parameters.

They are presented in the table 8. The range of variation for both kinds of interfacial friction (P1TOB and TOIFDT) is, on purpose, the same as for the global interfacial friction (SP1TOI in Table B.5.6). In the same way, the ranges of variation of 3 heat transfers (PQFDT, PPHCFR and PPHBOR) are also that of the global wall heat transfer of Table B.5.6 (PQPT).

Tab B.5.8 Additional sensitivity calculations

Sensitivity calculations performed for the final choice of the input parameters			
1	Interfacial friction in bubble-slug regime (upstream from the QF)	P1TOB	0.1 - 10
2	Interfacial friction downstream from the QF	TOIFDT	0.1 - 10
3	Global wall heat transfer downstream from the QF	PQFDT	0.5 - 2
4	Forced convection with vapour	PPHCFR	0.5 - 2
5	Film boiling	PPHBOR	0.5 - 2
Sensitivity calculations performed to explain the influence of the droplet diameters			
1	For interfacial friction upstream from the QF	SP1DGTOI	0.5 - 2
2	For interfacial friction downstream from the QF	SP1DGFDT	0.5 - 2
3	For interface heat transfers (qle/qve) upstream from the QF	SP1DGQLU	0.5 - 2
4	For interface heat transfers (qle/qve) downstream from the QF	SP1DGQLD	0.5 - 2

The parameters of this list influential with at least one criterion among the criteria of Table B.5.3 are indicated in the Table B.5.9. The same colour code as in the paragraph on “Temporary list of Influential Parameters” is applied: dark orange for a high influence, clear orange for a medium influence.

The graphs similar to those of Figure B.5.8 are plotted on the following Figure B.5.9.

Tab B.5.9 Additional sensitivity calculations: influential parameters

Parameter	Keyword	Multiplier MIN	Multiplier MAX	T_{ref} variations [°C]	ΔT_{ref} total variation [°C]	t_{rew} variations [s]	Δt_{rew} total variation [s]	QF variations [%]	ΔQF total variation [%]
Interfacial friction in bubble-slug regime (upstream from the QF)	P1TOB	0.1	10	+14/-32	46	+3.1/+5.0	1.9	negligible	<3
Interfacial friction downstream from the QF	TOIFDT	0.1	10	+13/-53	66	-24.7/+48.2	72.9	+12/-14	26
Global wall heat transfer downstream from the QF	PQFDT	0.5	2	+79/-117	196	+59.5 /-45.9	105.4	-16/+21	37
Forced convection with vapour	PPHCFR	0.5	2	+69/-62	131	+13.4/-18.2	31.6	-4.5/+7.5	12
Film boiling	PPHBOR	0.5	2	+13/-17	30	+15.6/-13.9	29.5	-5.5/+5.5	11
Droplet diameter for interfacial friction downstream from the QF	SP1DGFDT	0.5	2	-13/+13	26	+11.9/-8.1	20.0	-4.5/+3.5	8
Droplet diameter for interface heat transfers (qle/qve) downstream from the QF	SP1DGQLD	0.5	2	-21/+22	43	-3.4/+4.4	7.8	+2.3/-2.2	4.5

FEBA - test 216, bubbles-slug tau_i (upstream from the QF)
cladding temperature level FEBA 1680mm, CATH 2295mm

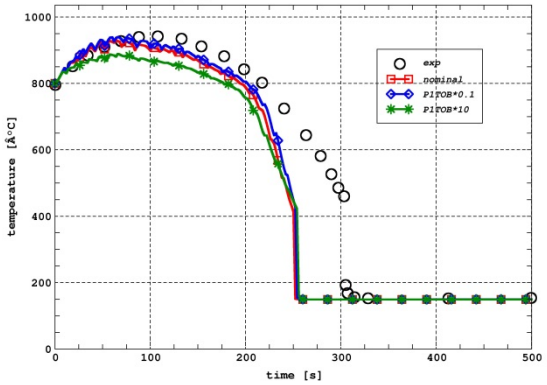

FEBA - test 216, bubbles-slug tau_i (upstream from the QF)
quench front elevation

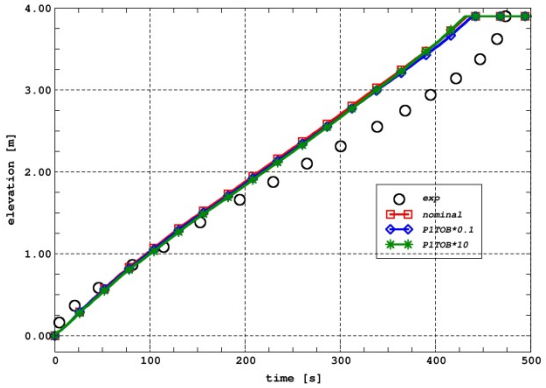

FEBA - test 216, interfacial friction downstream from the QF
cladding temperature level FEBA 1680mm, CATH 2295mm

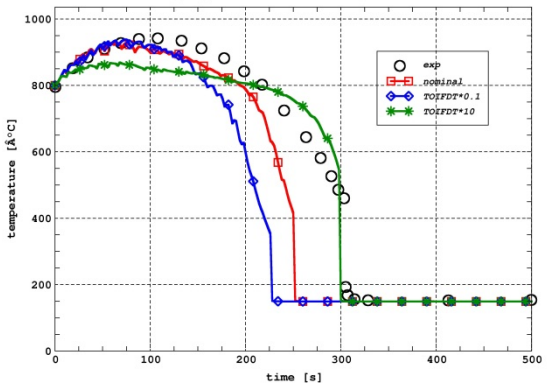

FEBA - test 216, interfacial friction downstream from the QF
quench front elevation

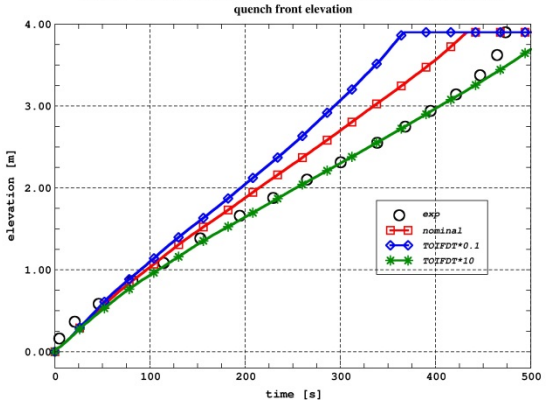

FEBA - test 216, global heat transfer downstream from the QF
cladding temperature level FEBA 1680mm, CATH 2295mm

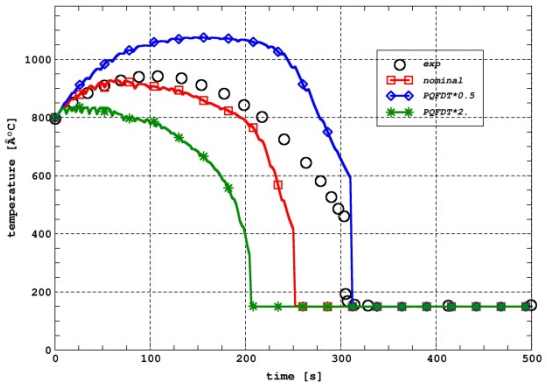

FEBA - test 216, global heat transfer downstream from the QF
quench front elevation

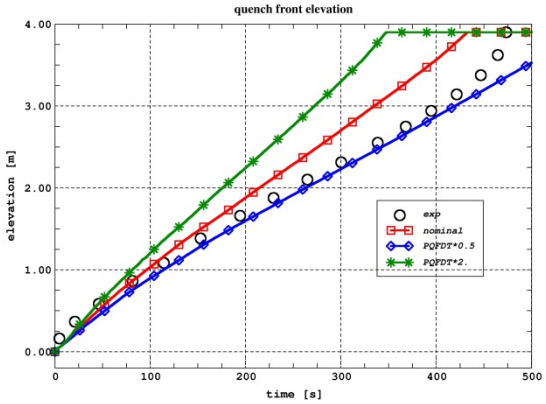

FEBA - test 216, forced convection with vapour
cladding temperature level FEBA 1680mm, CATH 2295mm

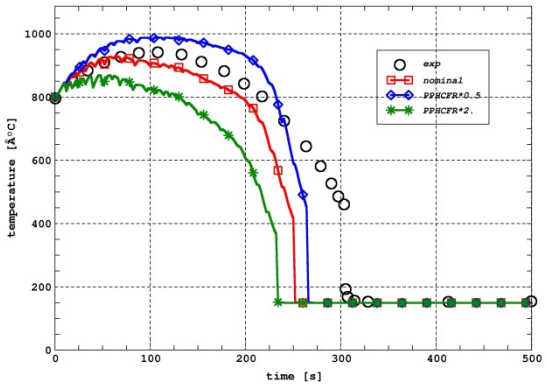

FEBA - test 216, forced convection with vapour
quench front elevation

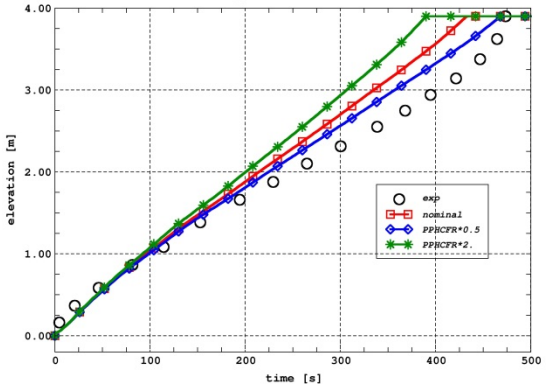

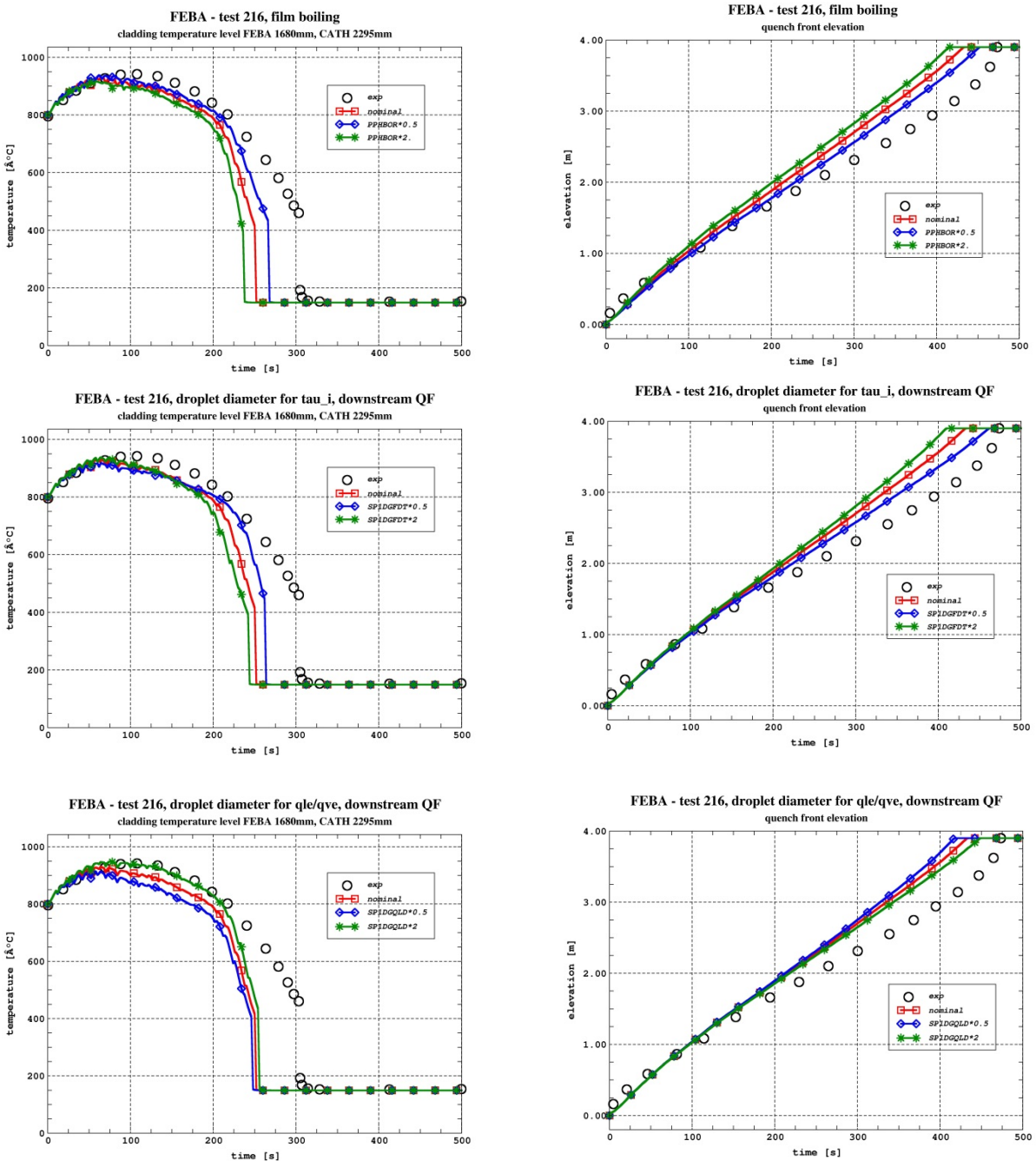

Fig B.5.9 Sensitivity calculation results for the 7 influential parameters of the additional list of Table B.5.8

<u>Comments about the 5 parameters added for the final choice of the input parameters</u>

All of them have either a medium influence (P1TOB and PPHBOR) or a high influence (TOIFDT, PQFDT and PPHCFR). The relevant parameters finally retained for Phase III of PREMIUM are:

- Interfacial friction, but only downstream from the QF (TOIFDT). Its influence is higher by much than the influence of interfacial friction upstream from the QF. And this interfacial friction is specific to reflood, more than the global interfacial friction SP1TOI of the Table B.5.6.
- Global wall heat transfer, but only downstream from the QF (PQFDT). It is also specific to reflood, more than the global wall heat transfer PQPT of the Table B.5.6. Another possibility would have been to consider forced convection with vapour (PPHCFR) instead of this global heat transfer, after checking that the other modes of heat transfer (radiation for example) are not very relevant as it is the case for film boiling (PPHBOR). But PQFDT is more global.

- The k2 correlation describing the 2-D conduction in the very local meshing moving with the quench front (P1K2FDT). This parameter was considered in the initial Table B.5.6.

One can note that only very dominant parameters are retained. It is due to the lack of very numerous and various experimental responses (the cladding temperatures of 6 FEBA tests are the main responses), which obliges a method such as CIRCE to consider few input parameters. Due to this constraint, CEA prefers to consider only global (and specific to the reflood) input parameters. That is why, for instance, the interface-vapour heat transfer (SP1QVE) is not directly considered: its uncertainty will be included into the uncertainty of the global wall heat transfer downstream from the QF, PQFDT. It is justified since the interface-vapour heat transfer is a contributor to the prediction of the wall temperature (cf. next paragraph). With more numerous and more various responses, it would have been possible to consider more parameters, less influential, such as interfacial friction upstream from the QF (P1TOB), interface-vapour heat transfer (SP1QVE) or all the heat transfer modes in dry zone (PPHCFR, PPHBOR, etc.). For example, considering SP1QVE would have been easier if the measurements of vapour temperatures were reliable, what is unfortunately not the case in FEBA.

Comments about the droplet diameters:

Only two droplet diameters among the 4 initial ones have some influence:

- SP1DGFDT (related to TOIFDT: τi downstream from the QF) is influential because TOIFDT is influential. It is preferable to consider only the most global parameter which is TOIFDT.
- SP1DGQLD (related to SP1QLE and SP1QVE: qle/qve downstream from the QF) is influential because qve, the interface-vapour heat transfer, present only downstream from the QF, is influential. In this case too it would be preferable to consider only one global parameter, qve. But, for the FEBA study, the uncertainty of qve will be included into that of PQFDT, as explained above.

Consequently, in the initial list of influential parameters (Table B.5.5), the global droplet diameter was influential due to the influence of SP1DGFDT and SP1DGQLD.

Wall-to-fluid heat transfer model

Independently of reflood, all the different modes of heat transfers with walls are taken into account by CATHARE. The classical 3 zones of the boiling curve are considered:

Zone A: transfers with a wetted wall. The physicals models of CATHARE are:

- Natural and forced convection with liquid in both laminar and turbulent regimes;
- Subcooled and saturated nucleate boiling with criteria for onset of nucleate boiling and net vapour generation;
- Film condensation (with or without non-condensable gases).

Zone C: post dry-out heat transfers. The physical models of CATHARE are:

- Natural and forced convection with gas (or vapour) in both laminar and turbulent regimes;
- Radiation to vapour and liquid;
- Film boiling for inverted annular, inverted-slug and dispersed flows.

The interface-vapour heat transfer (qve) is also involved in the post dry-out heat transfer. Indeed, the wall temperature is determined as much by the wall-vapour heat transfer via (T_w-T_v) as by qve via $(T_v-T_{sat}(P))$.

Zone B: Transition boiling.

Three “dry-out” criteria are used to reach the dry-out of the wall (zones B and C):

- The flow is in pure gas conditions;
- The wall temperature is higher than the minimum stable film temperature;
- The total wall-liquid heat flux is higher than the critical heat flux.

It is important to note that each physical model is unique. No choice among several correlations is proposed to the user, in order to reduce the user effect.

PQPT is defined as the multiplier of the sum of these different heat fluxes with walls.

As already explained in §1.3, some of these physical models are modified in case of reflood. They are:

- Gas (or vapour) convection, natural and forced (PPHCFR);
- Nucleate boiling;
- Film boiling (PPHBOR);
- The transition boiling is suppressed.

Two heat exchange modes are added for reflood (cf. paragraph on adopted models):

- A 2-D conduction wall to fluid heat transfer, performed with a very fine meshing moving with the quench front, denoted as k2 for CATHARE (P1K2FDT). It replaces the transition boiling and the minimum stable film temperature;
- An evaporation flux added to the interface-wall heat transfer, which takes into account the violent boiling and the liquid sputtering just downstream from the quench front. This flux is considered on a given distance, which is SP1DZ0 (reference value: 60 cm).

Downstream from the quench front, all these different fluxes are added in a global wall heat flux the multiplier of which is PQFDT.

Two types of reflood are modelled in CATHARE: bottom up and top down. For the FEBA modelling, only the bottom up reflood is used.

Conclusions

The work performed by CEA for the determination of the input parameters considered in the following Phase III of PREMIUM consists of several parts:

Firstly, the list proposed by the coordinators of Phase II in their specifications is considered with minor modifications. The level of influence (high, medium and low) is estimated via numerical criteria, but as these criteria are somehow too arbitrary, the results of the sensitivity calculations are also shown on figures. The most influential parameters are of IGP type but one IBP and one ICP have a medium influence.

But drawing conclusions from this first list of influential input parameters does not seem satisfactory to CEA. The reasons for that are explained in detail in this document and are briefly recalled below:

- The uncertainty of the IBP has to be imposed and not to be estimated;
- ICP and IGP are redundant and must not be considered together;
- IGP are too general.

An approach not based on IBP, ICP and IGP is proposed: in a first step, the macro phenomena of the considered experiment, FEBA for PREMIUM, are identified by expert judgment. In a second step, the physical models describing these macro phenomena are listed and sensitivity calculations are performed to select the most influential ones.

To illustrate these considerations and to make the final selection of the influential parameters, additional sensitivity calculations are performed by CEA. Taking into account that the method that CEA intends to use for Phase III, CIRCE, can consider only a limited number of parameters, 3 input parameters are finally retained, all of them having a high level of influence:

- Interfacial friction, but only downstream from the quench front(TOIFDT);
- Global wall heat transfer, but only downstream from the quench front (PQFDT);
- The k2 correlation describing the 2-D conduction in the very local meshing moving with the quench front (P1K2FDT).

These parameters take into account the specificity of the reflood. The uncertainty of the interface-vapour heat transfer (medium influence) will be included into that of PQFDT. A conclusion of the CEA contribution to Phase II is that its final list of input parameters is the result of a careful consideration, which is an important part of any uncertainty determination study.

In addition, the issue of the ICP dependent on IGP is addressed via the example of the droplet diameter. One shows that this ICP is rather influential because of the influence of both IGP: interfacial friction and interface-vapour heat transfer.

B.6 IRSN (France) results

Model description

Information about the code version and the software platform that has been used for the calculations of FEBA 216:

Tab B.6.1 IRSN code and software platform

Institution name	Code version	Software platform
IRSN	CATHARE 2 V2.5_2 mod8.1	Unix

Nodalization and basic geometrical properties

The circuit is modelled by one single 1D component representing the core bundle (heated part, 3900 mm) with only 1 heat rod, 2 boundary conditions at the inlet (velocity) and at the outlet (pressure). The thick-wall housing is modelled (thickness is 6.5 mm) whereas unheated part of rods, lower and upper plenum are not modelled.

The 1D component is composed of 39 meshes in the core and each vertical mesh is 100 mm height:

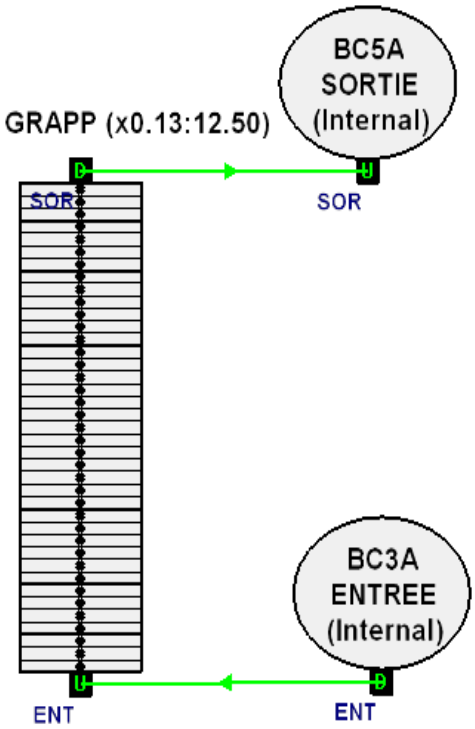

Fig B.6.1 FEBA nodalization

The mean hydraulic diameter of the bundle is determined as the following way:

- Total wet perimeter of the section: P = 1158/25 = 46.3 mm (wall friction perimeter);
- Total bundle flow section: S = 3893/25 = 155.7 mm²;
- The mean hydraulic diameter of the bundle is: Dhmoy = 4S/P = 13.44 mm. This hydraulic diameter is applied in all the core meshes.

Thermal properties of the materials (Nichrome Ni Cr 80 20 for cladding and heating elements, Magnesium oxide as a filler and insulator material in the fuel rod simulator and the V2A Chrome Nickel Steel for the test section housing) are obtained by a linear or a polynomial regression from FEBA data given by GRS.

A constant pressure form loss coefficient of 0.5 is imposed through the core bundle at each vector node of the axial component. Friction loss along the core is directly calculated by the code using the wall friction perimeter of 1158 mm. Particular loss coefficients at the position of the spacer grids are not considered.

Boundary and initial conditions

The boundary and initial conditions applied to the model are described below:

Tab B.6.2 Heat-up period

HEAT UP PERIOD	
Parameter	**Value**
Low rod Power	6%
Initial Outlet Pressure	4.1 Bar
Cladding Temperature	787°C

Tab B.6.3 Test run conditions

TEST RUN	
Parameter	**Value**
System Pressure	4.1 Bar
Bundle Power	200 kW
Decay Heat	120% ANS
Flooding Velocity	3.8 cm/s
Flooding Temperature	63°C (0s) 37°C (end)

Adopted models (flags)

Standard CATHARE code with reflooding model is used, taking into account the radial and axial conduction in the vicinity of the quench front with a meshing refinement.

Assumptions and steady-state achievement

A steady state is obtained with a zero flow (actually 1.E-5 for numerical reasons) and a zero power. The pressure is imposed at the top of the bundle.

The heat-up phase is calculated with a low steam flow and a reduced power. The transient begins when the experimental initial clad temperature at 1.625 m is reached. The reduced power (6% in this test) is adjusted in order to reach the experimental housing initial temperature at the beginning of the transient (the lower the power, the closer the bundle and housing temperatures). The heat exchanges between bundle and housing are mainly due to radiation during this phase.

We present on the following graph the comparison of measured and calculated axial temperature distribution of heater rods surface and housing internal wall at the instant immediately prior to start of transient.

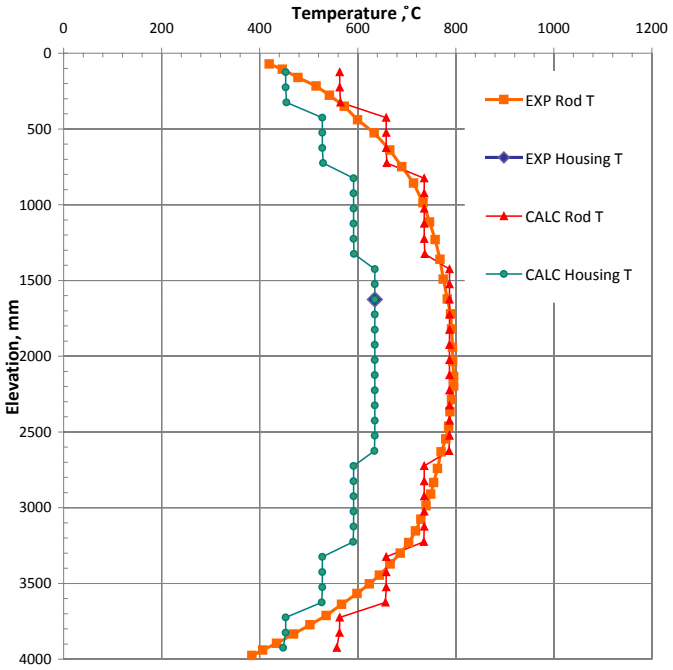

Fig B.6.2 Steady-state temperature profile

For the same peaking factor, the experimental results show a higher temperature (20 to 40 °C) in the lower part of the device where the measurement locations are closer to the adjacent higher power zone. The CATHARE results are symmetrical (same temperature for the same linear power) because there is no axial conduction calculation during this pre-reflood phase. Experimental axial conduction can also explain the overestimation of the calculated temperatures at the very bottom of the device.

Base case results

After performing the reference case calculation, the comparison of the calculated and experimental results is given in series of figures for FEBA test 216.

Figures of all (exp-calc) responses

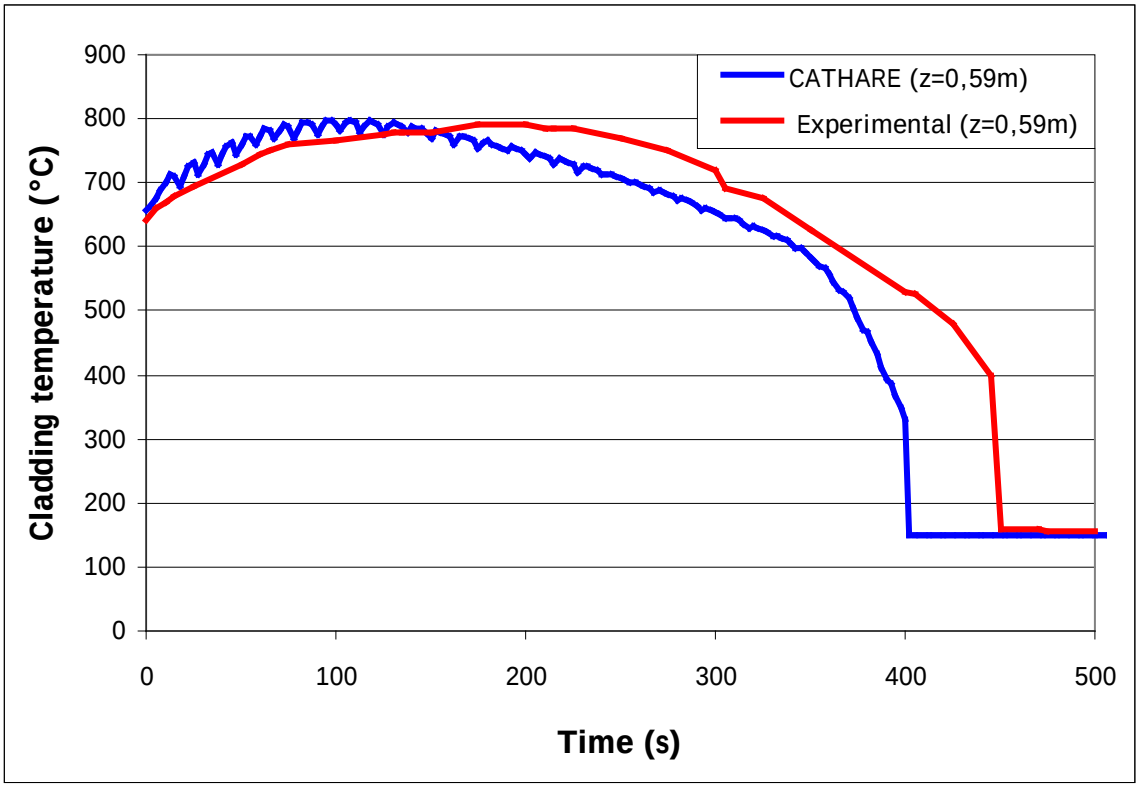

Fig B.6.3 Heater rod surface temperature corresponding to 12b2 experimental measurement

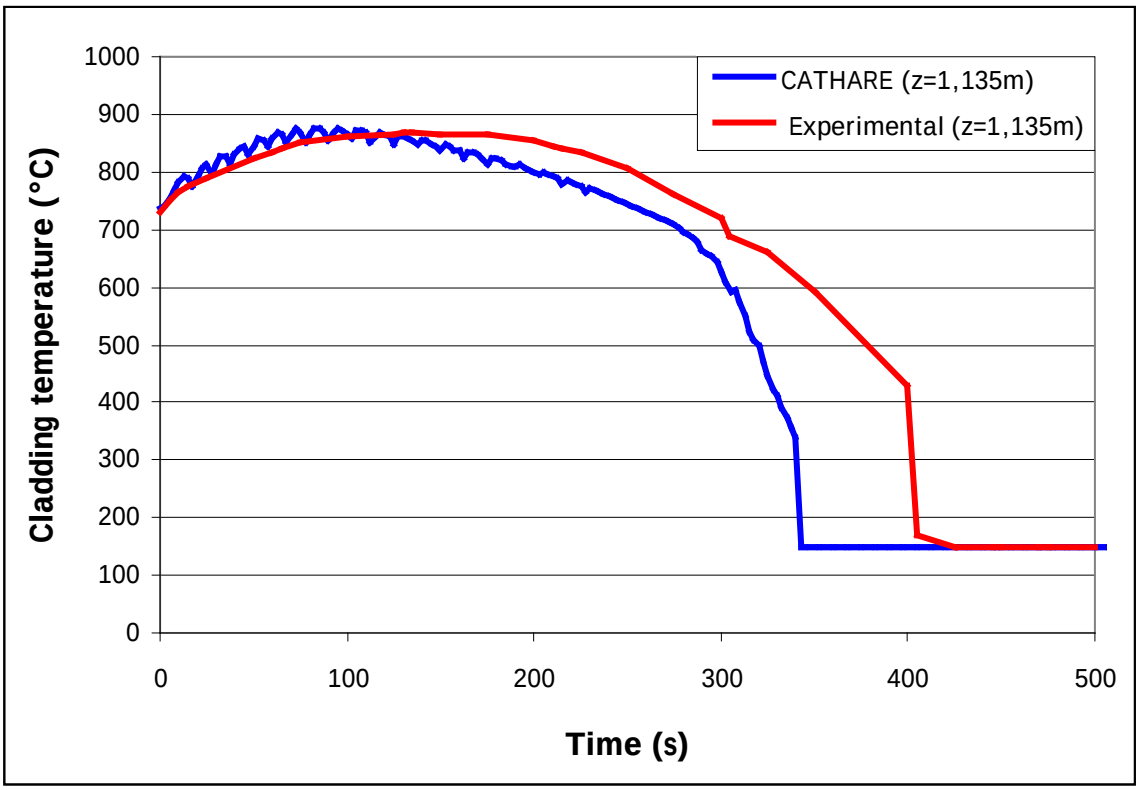

Fig B.6.4 Heater rod surface temperature corresponding to 12b3 experimental measurement

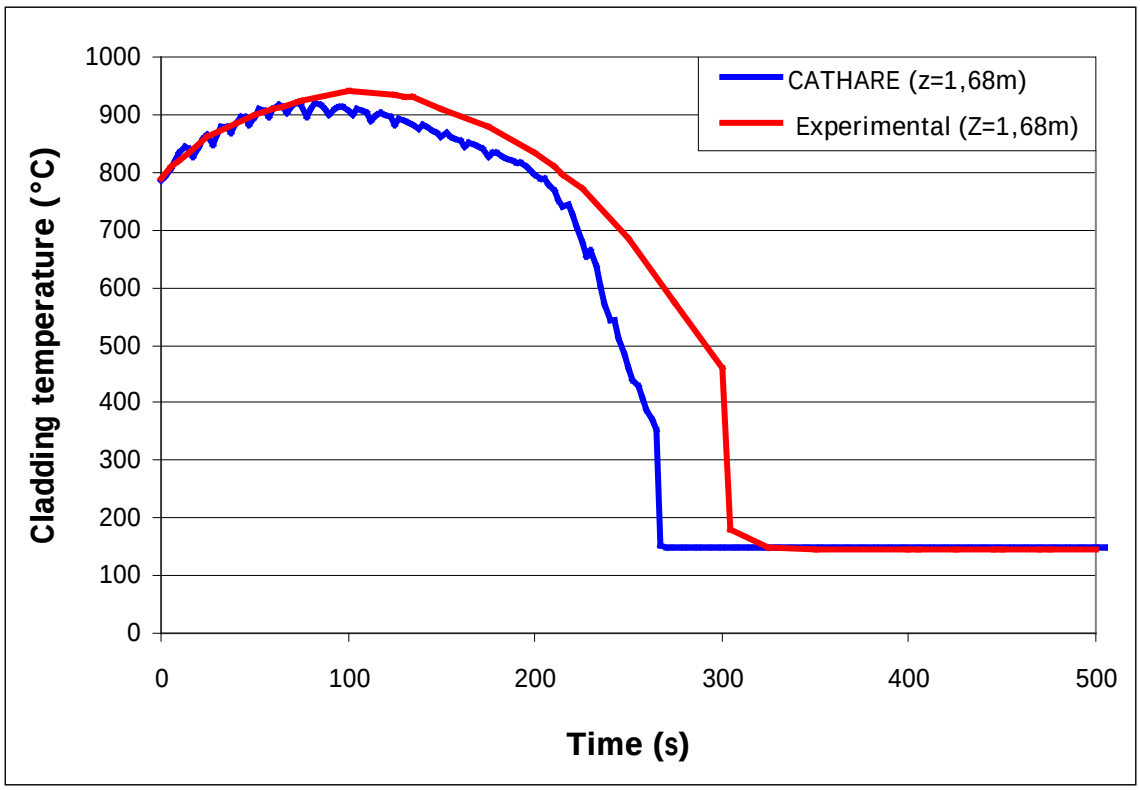

Fig B.6.5 Heater rod surface temperature corresponding to 12b4 experimental measurement

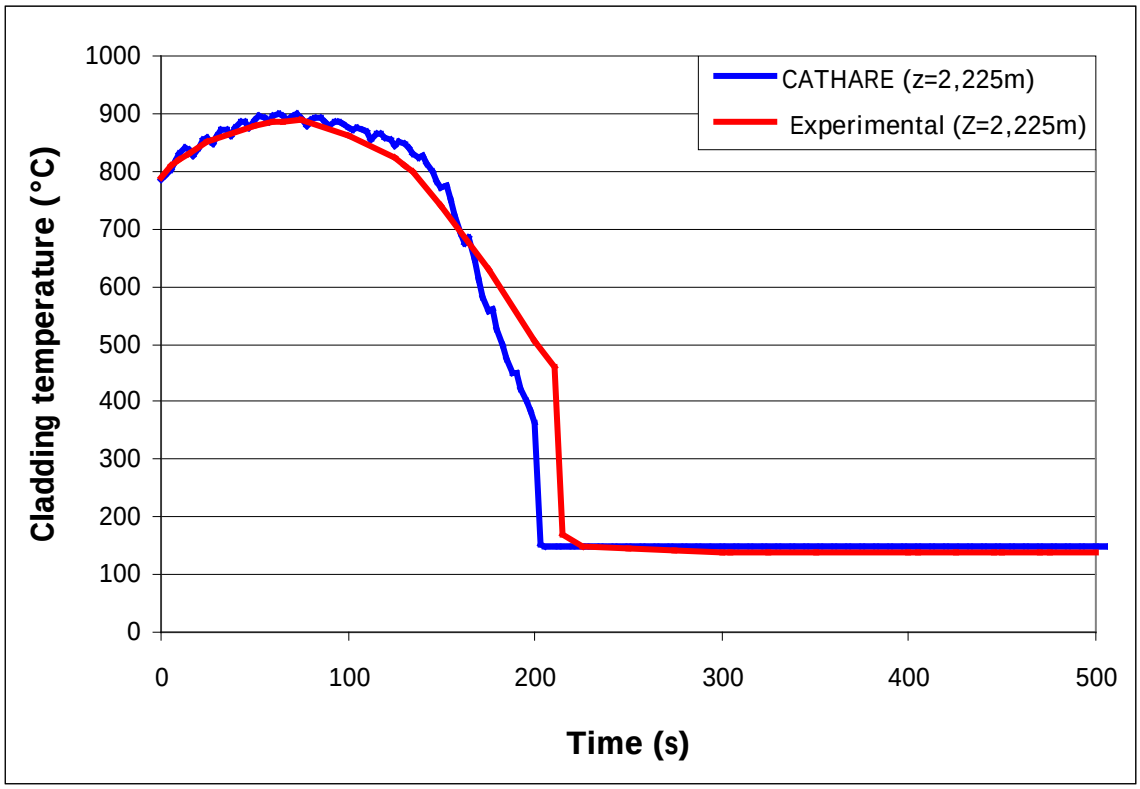

Fig B.6.6 Heater rod surface temperature corresponding to 18a1 experimental measurement

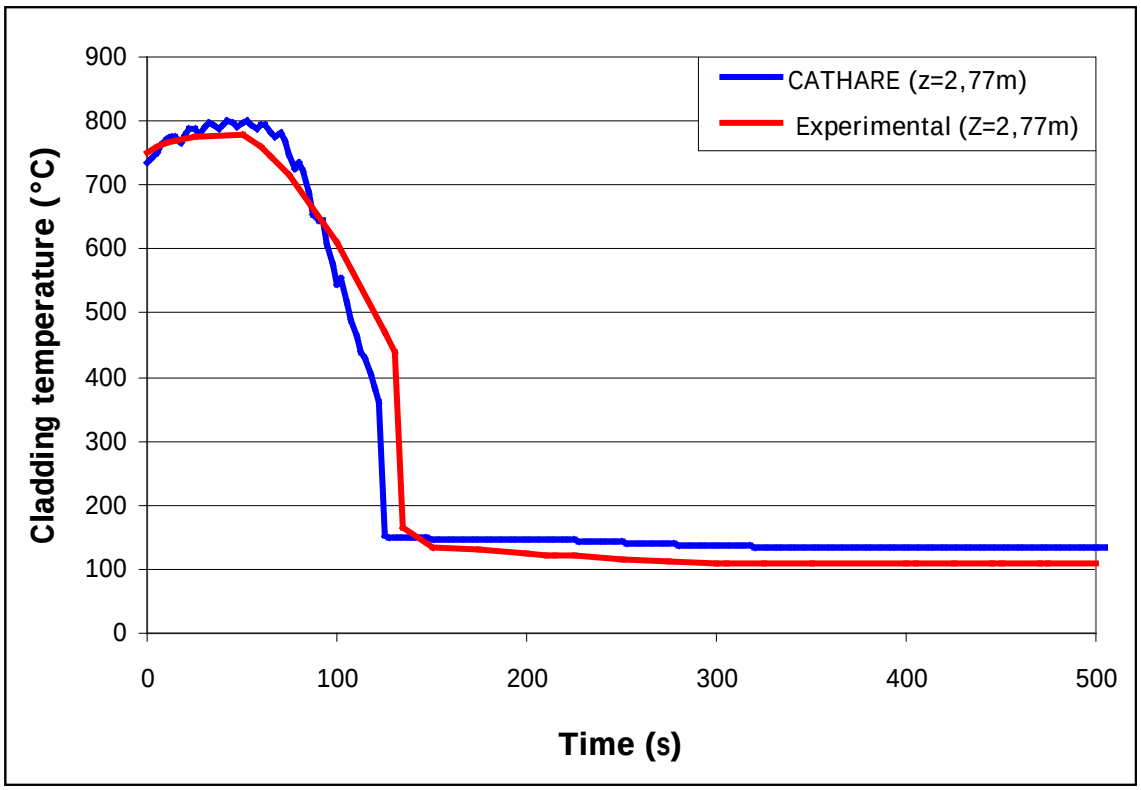

Fig B.6.7 Heater rod surface temperature corresponding to 18a2 experimental measurement

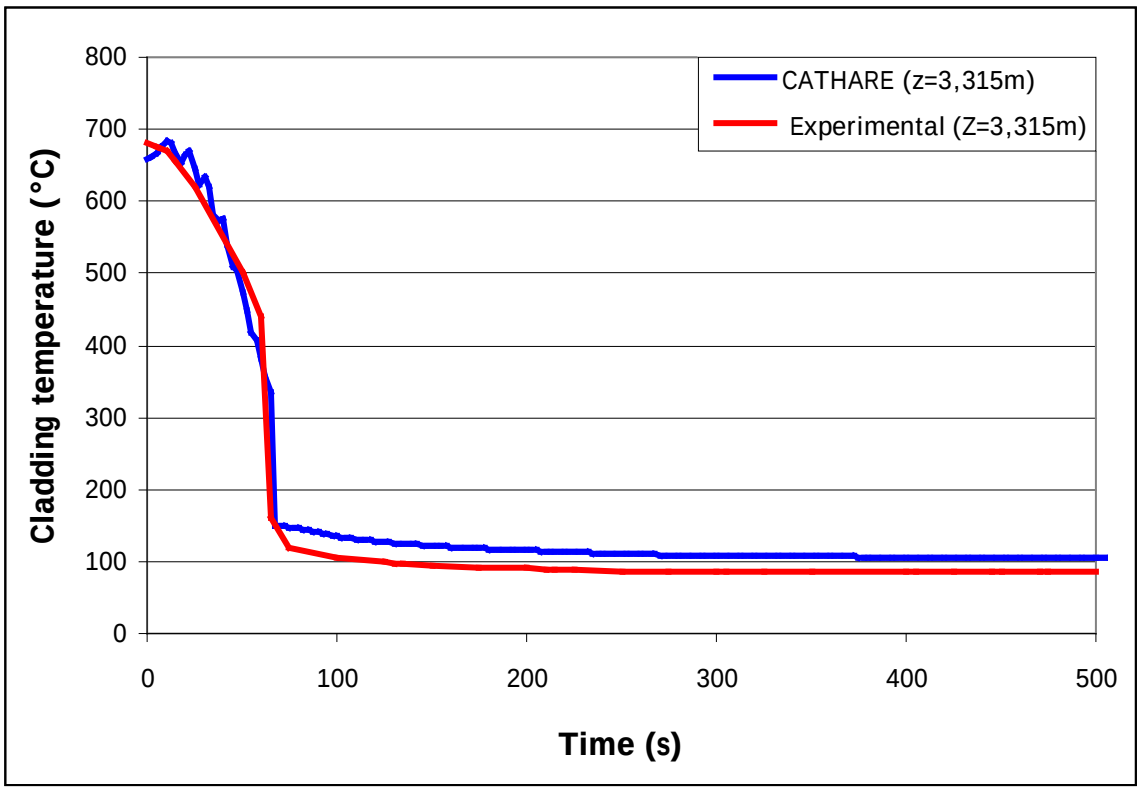

Fig B.6.8 Heater rod surface temperature corresponding to 18a3 experimental measurement

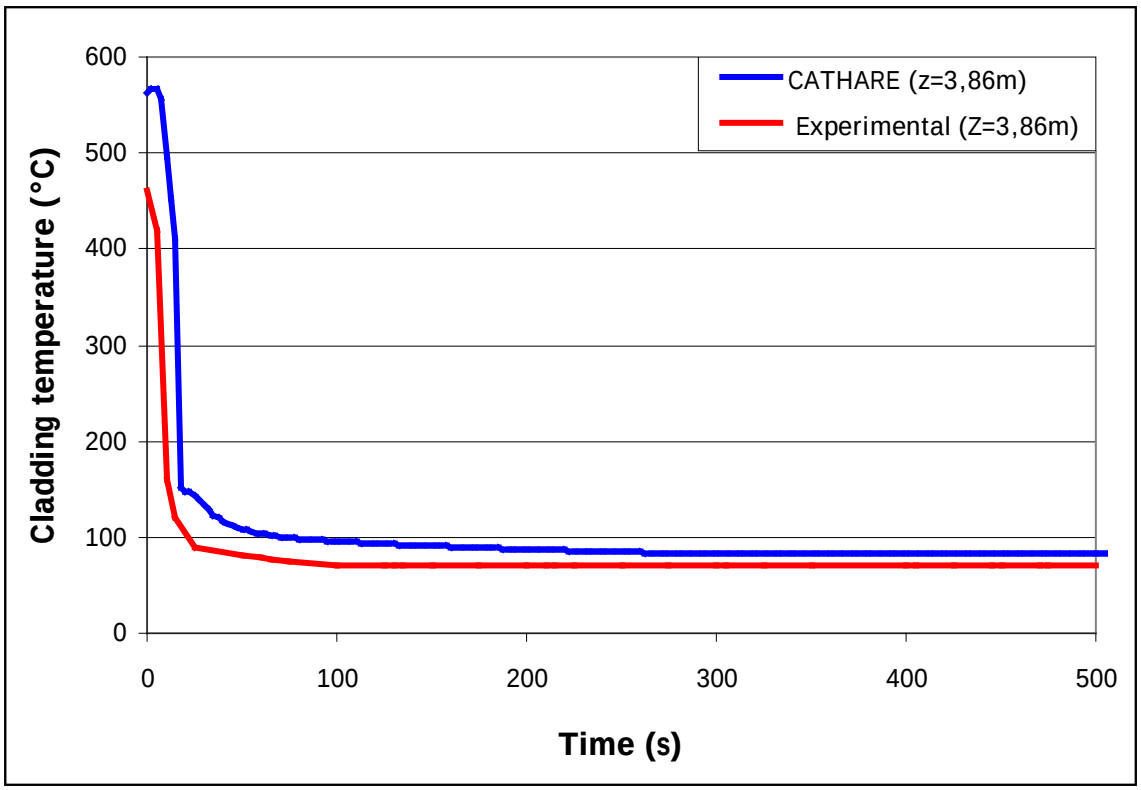

Fig B.6.9 Heater rod surface temperature corresponding to 18a4 experimental measurement

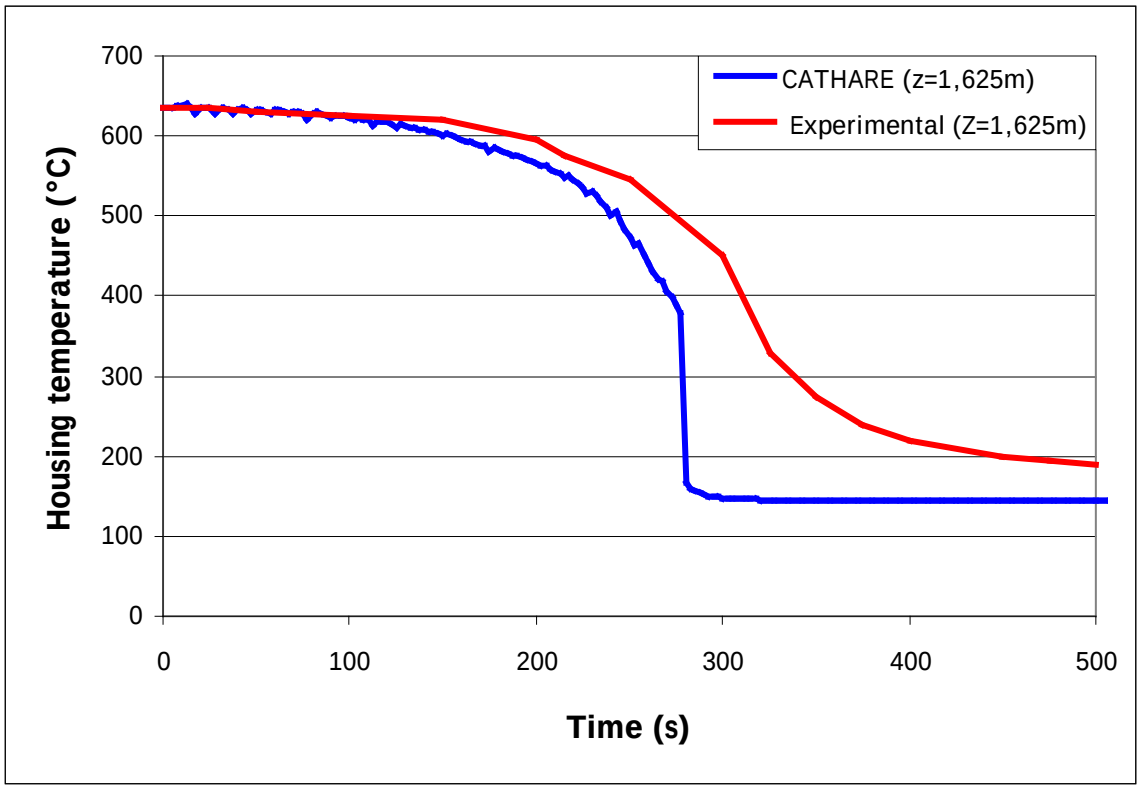

Fig B.6.10 Housing temperature at elevation 1625 mm

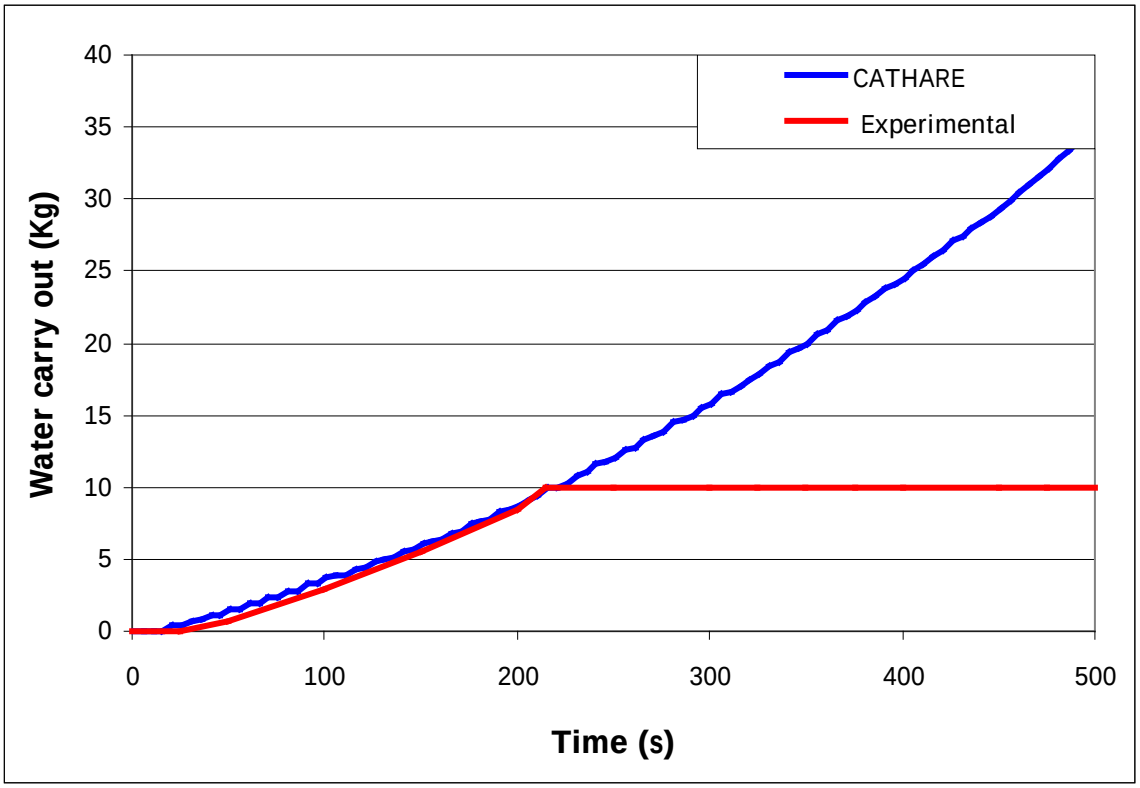

Fig B.6.11 Liquid carryover

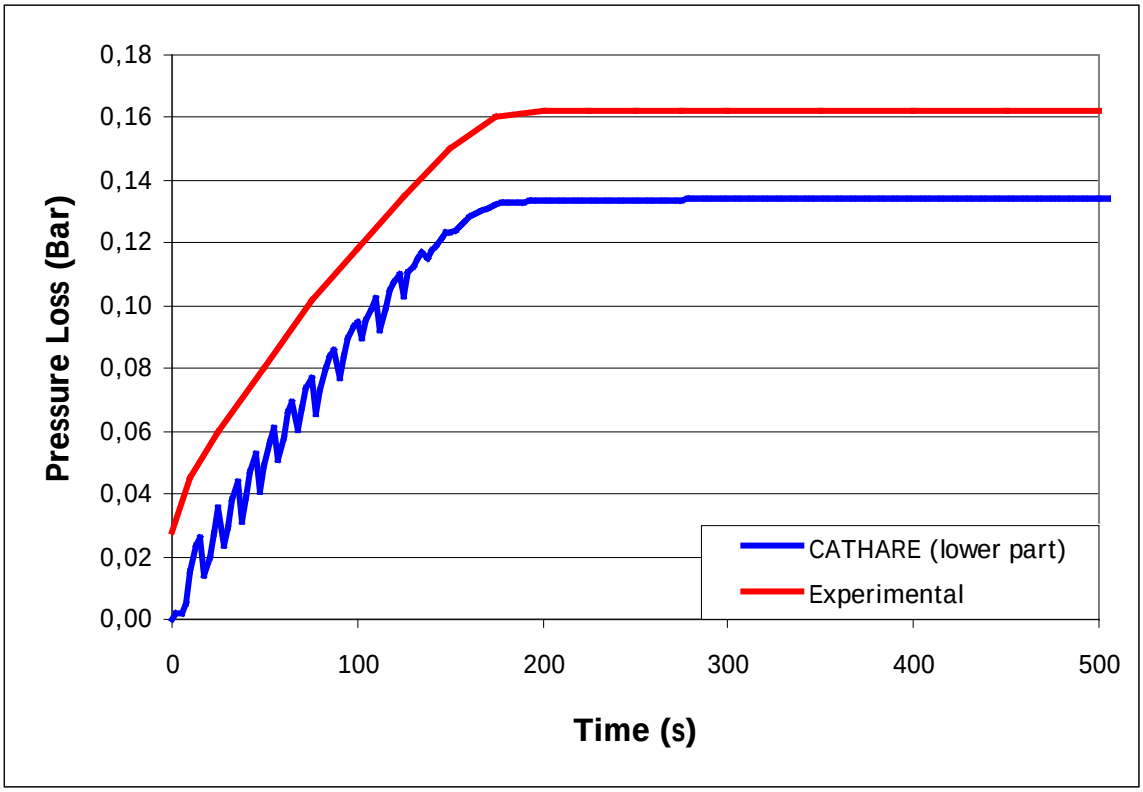

Fig B.6.12 Pressure drop at the lower part

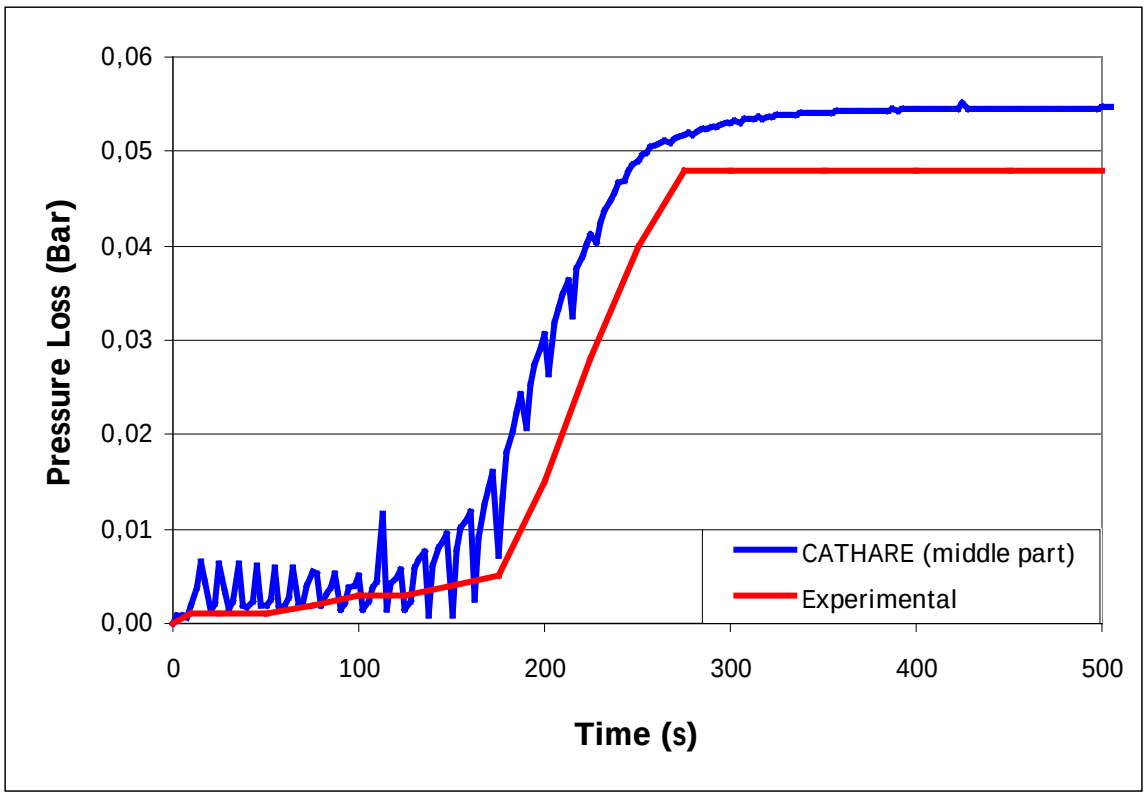

Fig B.6.13 Pressure drop at the middle part

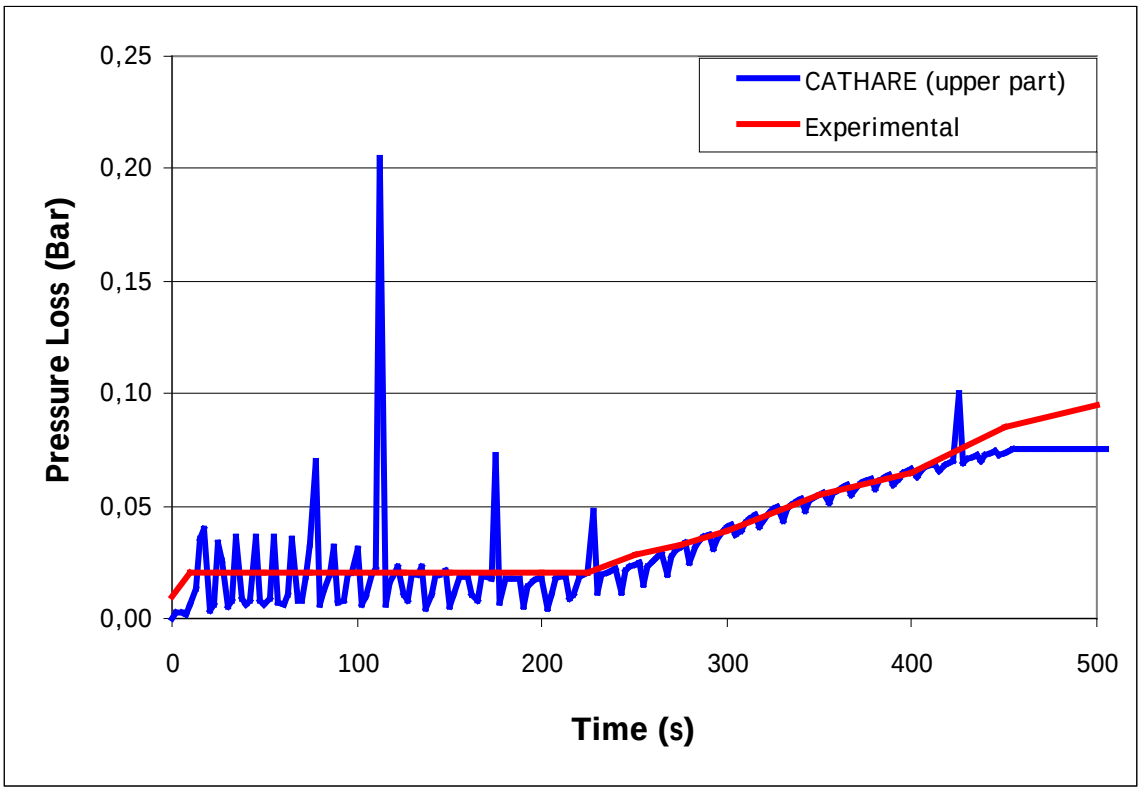

Fig B.6.14 Pressure drop at the upper part

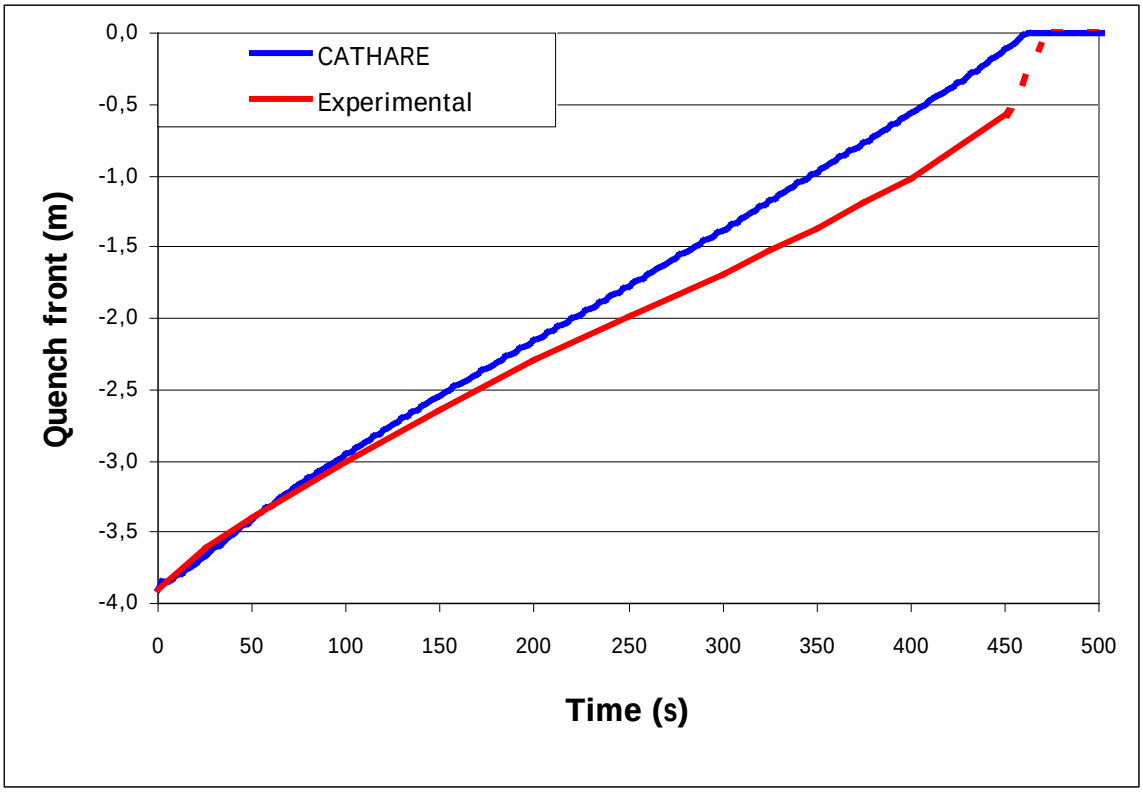

Fig B.6.15 Quench from elevation vs. time

It should be noted that the experimental pressure loss measure includes a height of unheated rods, which is not modelled with CATHARE, leading to the gap of 0.03 bar on the previous figure.

The uppermost (level 0 m) of the experimental quench time corresponds to an unheated part of the rods, which is not modelled with CATHARE.

CATHARE calculations results are roughly in agreement with experimental ones. At the beginning of the transient (from bottom to 2.225 m), the reflooding phase is rather well predicted by CATHARE (maximum value and trend of the cladding temperature, time of rewet and quench front). However, Figures in relation to locations 0.59, 1.135 m and 1.68 m show that the wall temperatures predicted by the code begin to decrease when they continue to increase according to the experimental data. The calculated quench front progresses too fast compared to the experimental data.

PCT and bundle quench time

Tab B.6.4 Base case PCT and bundle quench

Institution name	PCT (°C)	Position (mm)	Bundle quench (s)
IRSN	925	1500	462

Criteria for selection of influential input parameters

An initial list of input parameters has been selected (see following paragraph) by expert judgment. A sensitivity analysis have been performed with a OAT (One-At-a-Time) sampling by changing one input parameter at a time (to its extreme value in the range of variation) and keeping all other input parameters fixed to their best-estimate values.

The two relevant responses for reflood considered in this study are:

- Heater rod surface temperature at location Z=1.68 m;
- Rewet time (time when abrupt change occurs in the rod surface temperature) at location Z=1.68 m.

Two criteria have been used for selection of influential input parameters:

- The absolute value of variation in heater rod surface temperature is $\Delta \mathbf{T_{clad}(Z)=50°C}$;
- The variation in rewet time is $\Delta \mathbf{t_{rew}(Z)=\pm 10\%}$.

It was decided to select the influent IGP parameters rather than the ICP ones, e.g. the global heat transfer rather than the droplet diameter which is one of the parameters of the heat transfer correlation.

The possibility of comparison between results of different codes seems thus higher considering global parameters (correlations) rather than parameters which are coefficients of these correlations.

Besides, it seems easier to understand the effect on the physical results of the code, when modifying global parameters.

Selection of parameters

Initial list of parameters

The following table presents the initial list of input parameters considered as potentially influential for reflood-related phenomena. These input parameters are classified according to the definitions provided in specifications for Phase II (IGP: Input Global Parameter - ICP: Input Coefficient Parameter – IBP: Input Basic Parameter).

Tab B.6.5 Initial list of input parameters

Type	Name (CATHARE)	Parameter Explanation	Uncertainty Range		
			Ref	Min	Max
IGP	SP1QLE	Liquid-interface heat transfer (total)	1	0.5	2
	SP1QVE	Vapour-interface heat transfer (total)	1	0.5	2
	TOIFDT	Interfacial friction downstream quench front	1	0.25	4.0
	SP1ETO	Entrainment rate (for Toi)	1	0.7	1.3
	PQFDT	Wall-fluid global heat transfer downstream quench front	1	0.5	3
	P1K2FDT	K2 reflood parameter (2D conduction near quench front)	1	0.5	2
ICP	SP1CG	Vapour-wall friction	1	0.8	1.9
	SP1CLR	Liquid-wall friction (reflooding)	1	0.8	1.9
	SP1DGQVE	Droplets diameter (for QVE)	1	0.5	2
	SP1DGTOI	Droplet diameter upstream quench front (for Toi)	1	0.5	2
	SP1DGFDT	Droplet diameter downstream quench front (for Toi)	1	0.5	2
	DTMFS	Minimum temperature of stable film boiling	0	-42°C	60°C

Tab B.6.6 Initial list of input parameters (continue)

Type	Name (CATHARE)	Parameter Explanation	Uncertainty Range		
			Ref	Min	Max
IBP	XPOUT	Pressure	1	0.95	1.05
	XVINJ	Mass flux	1	0.95	1.05
	XTPINIT	Initial wall temperature	1	0.98	1.02
	XTINJ	Fluid temperature	1	0.95	1.05
	XPUISS	Power density	1	0.98	1.02
	XTOPHECO	Tophet thermal conductivity	1	0.95	1.05
	XTOPHECP	Tophet heat capacity	1	0.95	1.05
	XMGOCO	MgO thermal conductivity	1	0.8	1.2
	XMGOCP	MgO heat capacity	1	0.95	1.05
	XDIAMH	Hydraulic diameter	1	0.95	1.05
	XDP	Pressure form loss coefficients	1	0.5	2

Final list of Influential Parameters

The following table presents the more influential input parameters according to the criteria described in section 3, for FEBA test 216.

Tab B.6.7 Final list of influential input parameters

Parameter	Subroutine	Fortran variable / Keyword	Multiplier REF / REF value	Multiplier MIN	Multiplier MAX	T_{clad} variation [°C]	Position [mm]	t_{rew} variation [s]	Position [mm]
Wall-fluid global Heat Transfer downstream quench front	Data Deck	PQFDT	1.0	0.5	3.0	**+144 / −97**	1680	**+66 / −81**	1680
K2 reflood parameter (2D conduction near quench front)	Data Deck	P1K2FDT	1.0	0.5	2.0	*+1 / −18*	1680	**+37 / −59**	1680
Interfacial friction downstream quench front	Data Deck	TOIFDT	1.0	0.25	4.0	**+20 / −32**	1680	*-21 / +23*	1680

Both responses (cladding temperature – nominal value of 921 °C – and rewet time – nominal value of 270 s – at 1.68m) are mainly sensitive to the wall-fluid global heat transfer downstream quench front (PQFDT) which can be considered as the more relevant parameter. The K2 reflood parameter (P1K2FDT) is mainly influential for the rewet time (Δt_{rew}=±10%) whereas the Interfacial friction downstream quench front (TOIFDT) mainly for the heater rod surface temperature (ΔT_{clad}=50°C).

Conclusions

The modelling description and the reference calculation results of FEBA test 216 with CATHARE code have been presented. Numerical results are in agreement with experimental data in spite of an early reflooding (especially at locations from 0.59 to 1.68) and a slight under-estimation of the maximum cladding temperature in the vicinity of 1.68m (location of the global maximum).

A sensitivity analysis has permitted to select 3 influential input parameters that will be used in Phase-III of the benchmark:

- Wall-fluid global heat transfer downstream quench front (PQFDT);
- K2 axial conduction model near quench front parameter (P1K2FDT);
- Interfacial friction downstream quench front (TOIFDT).

At location 1.68m, the heater rod surface temperature is essentially sensitive to PQFDT and TOIFDT, whereas the rewet time is to PQFDT and K2.

B.7 GRS (Germany) results

Model description

Tab B.7.1 GRS code and software platform

Institution name	Code version	Software platform
GRS	ATHLET 2.2B	Unix

Nodalization and basic geometrical properties

The thermal-hydraulic channel of the test section is modelled as 1-D object (PIPE in ATHLET nomenclature) divided into 23 control volumes (see Fig. 1). The total length of the channel is 4.191 m. The modelled channel begins shortly below the pressure tap for pressure drop measurement. The channel ends at the outlet from the upper core plate. The first control volume is unheated.

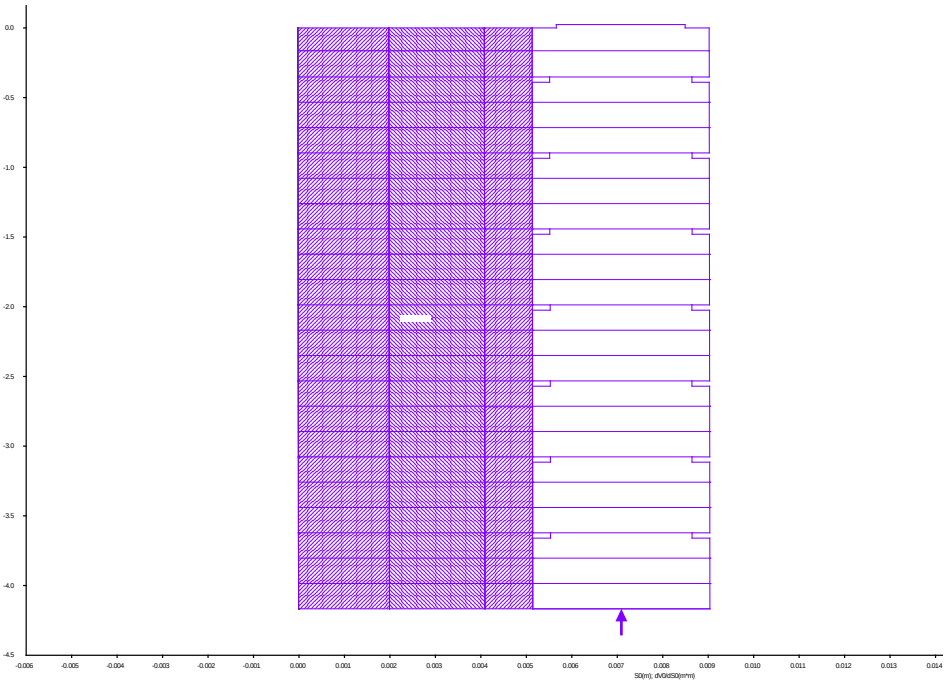

Fig B.7.1 Spatial discretization of T-H channel and heater rod

The inlet conditions at the bottom of the channel are modelled as FILL (G, h boundary condition). The outlet plenum of the test section is modelled as time-dependent volume (TDV – p, h boundary condition).

The rod simulators are modelled as heated rods divided into 23 axial nodes according to the thermal-hydraulic channel nodalization. The heated length is 3.9 m. the first node is unheated. The last node is heated at the part of its length.

The model of the heater rod consists of three radial zones:

- Inner zone: filler – MgO
- Insulator – MgO
- Cladding – Nichrom

In the thermal-hydraulic channel the grid spacer geometry is modelled. It means that at the level of a grid spacer the channel cross-section area decreases. The cross- section area of the channel is 0.003893 m². The cross section area at the level of a grid spacer is 0.003115 m². The hydraulic diameter of the channel is 13.47 mm. At the level of a grid spacer the hydraulic diameter has been determined as 9.64 mm. The hydraulic diameter of the upper core plate is 10 mm.

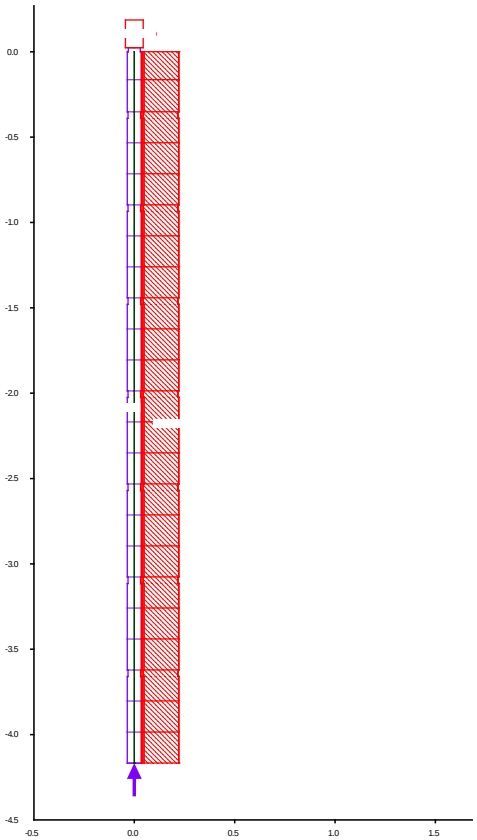

Fig B.7.2 FEBA test section consisting of T-H channel and housing with isolation

Boundary and initial conditions

System pressure is 4.12 bar and inlet mass flow is 0.147 kg/s. They are constant during the whole test run. The inlet temperature varies according to the experimental measurement.

Adopted models (flags)

For the analyses the 5 balance equation model with relative drift velocity has been applied.

Assumptions and steady-state achievement

In ATHLET the temperature distribution in the heat slabs cannot be given as initial condition. The axial and radial temperature distribution has to be obtained within ATHLET steady state iteration procedure. For this purpose the axial temperature distribution in the middle of the heater rod has been defined. It was assumed to be similar to the measured cladding axial temperature distribution. Additionally, a low power lever according to the experimental procedure and inlet steam mass flow resulting in steam velocity about 3.8 cm/s has been assumed at the start of the test run. The assumed inlet and boundary conditions were:

- Inlet steam mass flow: 0.00147 m/s
- Inlet steam temperature: 66 °C
- Bundle power: 25 kW

The housing as well as insulator is modelled according to the test facility description. The environment temperature was assumed as 27 °C.

The temperature distribution in the heater rod and in the housing, and thermal-hydraulic parameters in the channel have been obtained within the steady-state iteration procedure on the basis of the assumed initial and boundary conditions.

The cladding temperature distribution equivalent with the measured one could be obtained after a few manual iterations with correction of the temperature distribution in the middle of the heater rod.

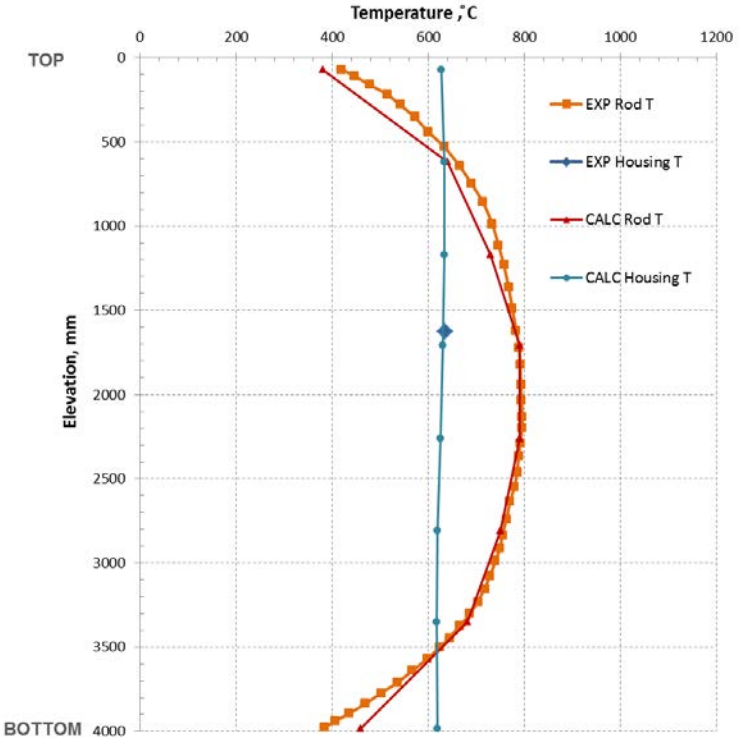

Fig B.7.3 Steady-state temperature profile

Base case results

Figures of all (exp-calc) responses

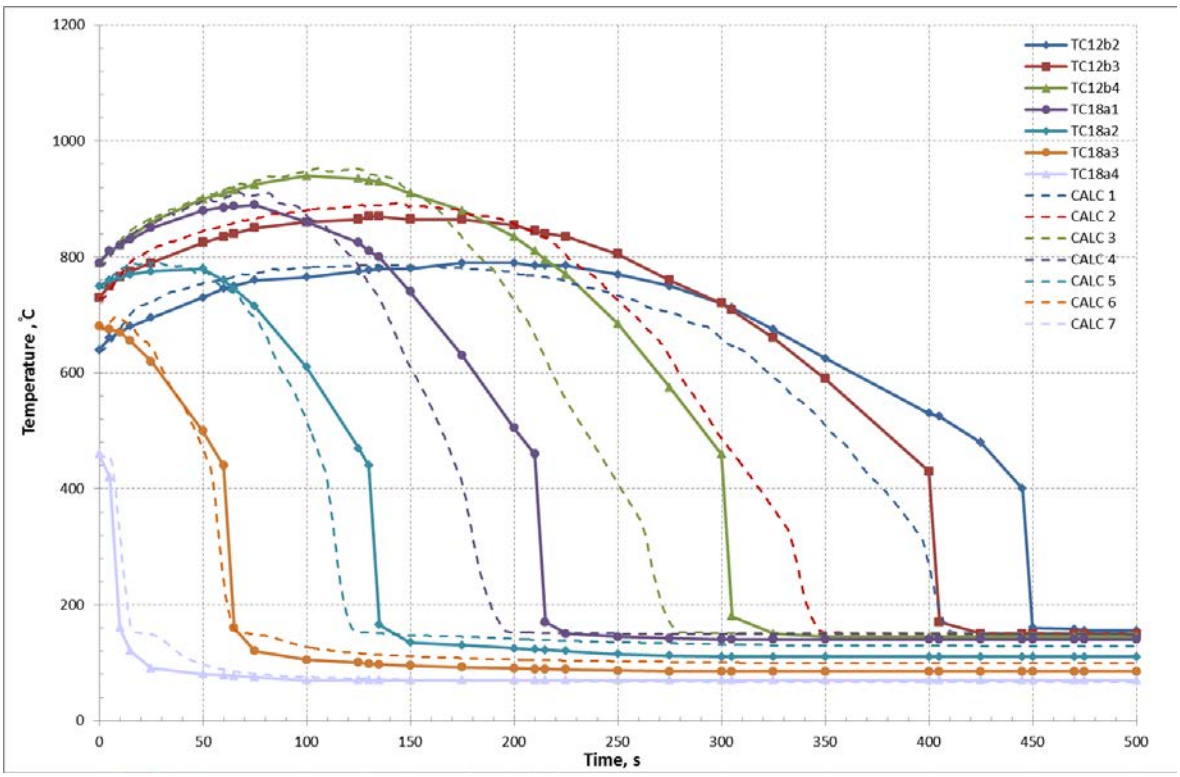

Fig B.7.4 Base case cladding temperatures

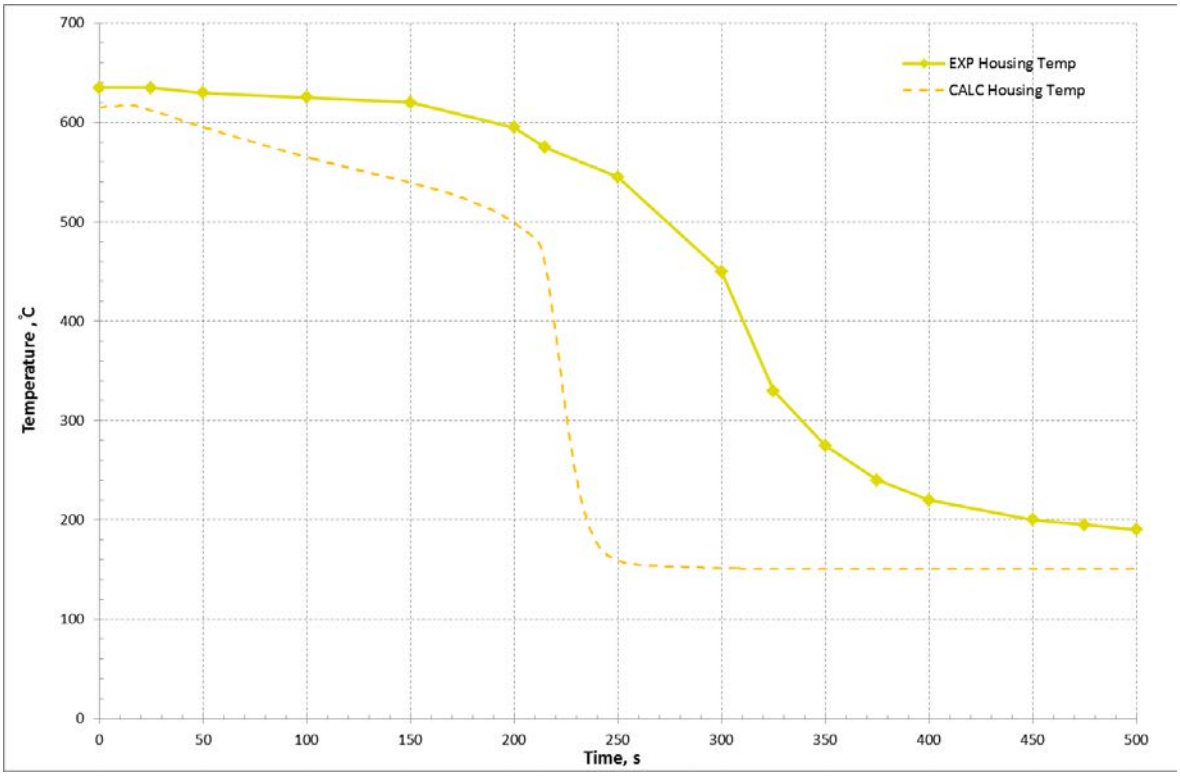

Fig B.7.5 Base case housing temperature

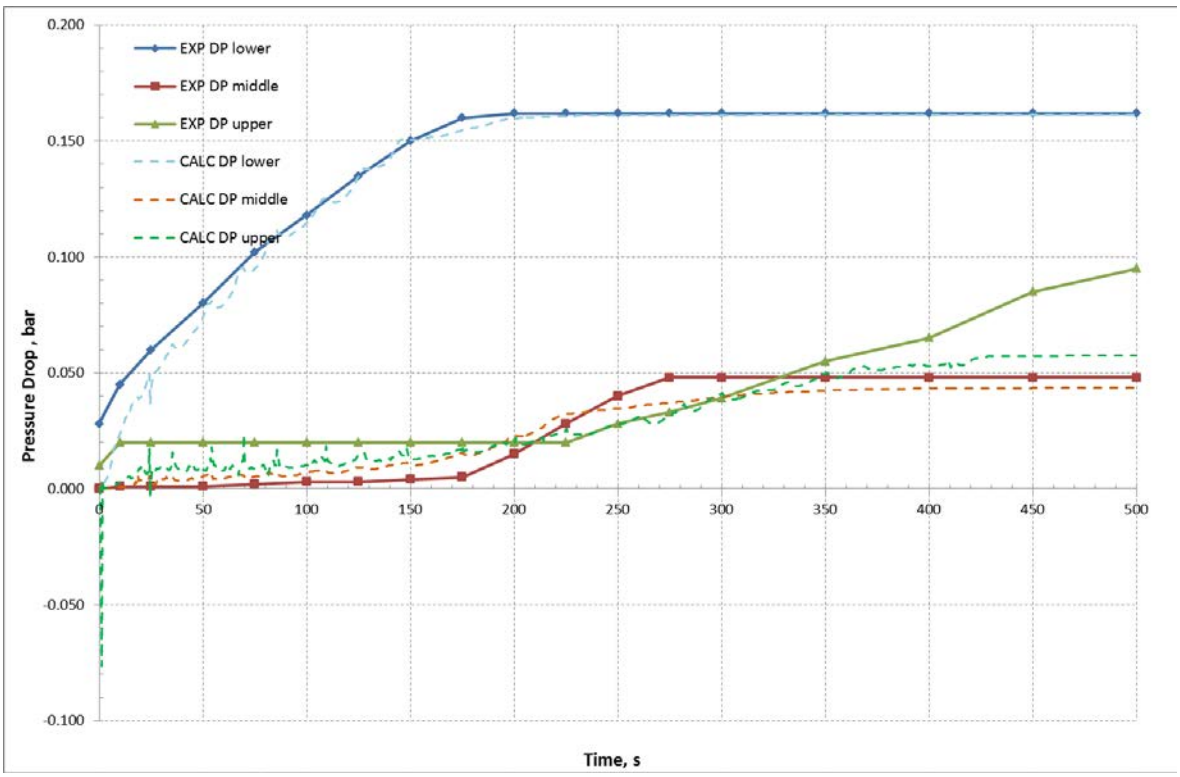

Fig B.7.6 Base case pressure drops

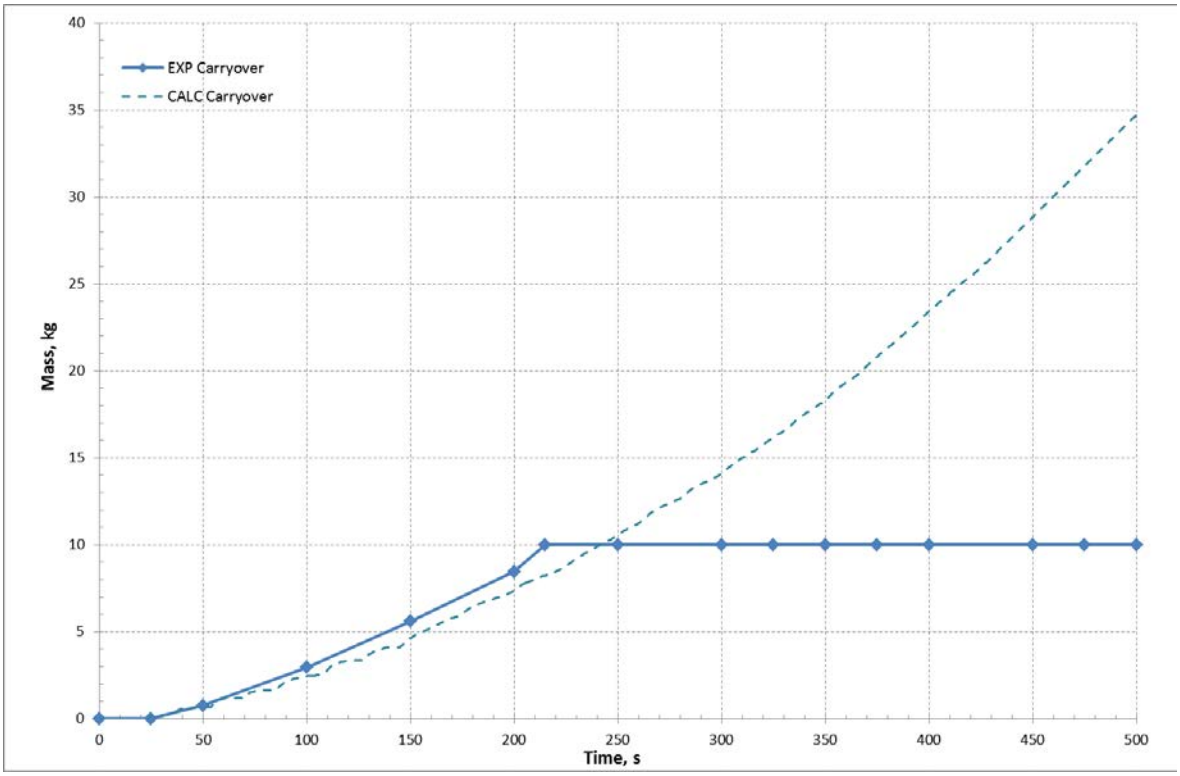

Fig B.7.7 Base case liquid carryover

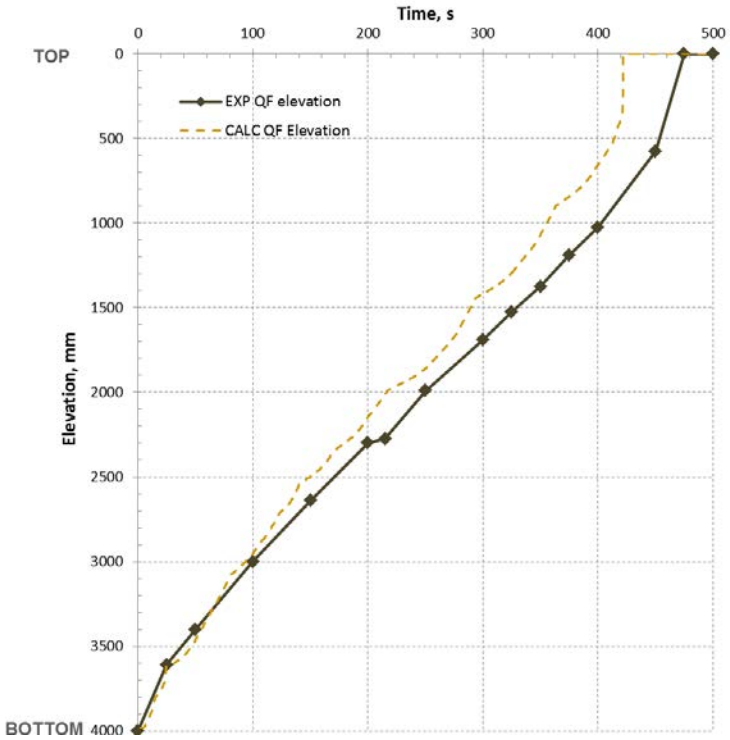

Fig B.7.8 Base case quench front propagation

PCT and bundle quench time

Tab B.7.2 Base case PCT and bundle quench

Institution name	PCT (˚C)	Position (mm)	Bundle quench (s)
GRS	958	1680	422

Criteria for selection of influential input parameters

The selected criterion was the difference of the position of the quench front 300 sec after start of the transient.

Selection of parameters

The results of the parameter sensitivity investigation are shown in the following table

Tab B.7.3 Initial list of input parameters

Par. No	Parameter description	Parameter name	Reference value	Variation range		Resulting quench front variation, mm
				Min	Max	
1	Relative velocity in bundle - multiplier	ODBUN	1.0	0.3	1.0	-1016
2	Heat transfer at quench front	CQHTWB	10^5 W/m²K	10^5	10^6	-200
3	Water entrainment - multiplier	OENBUN	1.0	0.5	2.0	-278
4	Forced convection to steam – multiplier	OHVFC	1.0	0.85	1.25	-123
5	Film boiling – multiplier	OHWFB	1.0	0.65	1.3	-81
6	Inlet temperature	TINL	660°C	660°C	710°C	48
7	Quench front modelling		Yes	No	Yes	950
8	HTC MgO – Cladding interface		10^5 1/m²K	10^4	10^5	7
9	Grid spacers geometry		Yes	No	Yes	-69
10	Wall friction	LAMBDA	0.015	0.015	0.02	~0
11	HTC housing – isolation interface		100 1/m²K	10	1000	57
12	Two phase flow multiplier - pressure	OFI2V	1.0	0.2	1.0	1
13	No of droplets in evaporation model	ZT	10^9 1/m³	10^9	10^{10}	-90
14	Housing quench front modelling		Yes	No	Yes	-22
15	HTC: steam	OHWNB	1.0	0.8	1.2	-32

Wall-to-fluid heat transfer model

In the code ATHLET by quench modelling heat transfer model as well as specific model for reflooding are applied.

The quench front model determines the current quench front position. It defines the boarding between dry position (film boiling or forced convection to steam) and wet position (transition boiling or nucleate boiling). In the ATHLET heat transfer correlation logic the critical heat flux is used to distinguish between nucleate boiling heat transfer and transition boiling.

The quench front model in ATHLET is an algebraic model which determines the quench front propagation in the existing nodalization on the basis of quench front velocity (the main output of the quench front model) and current integration time step. The heat transfer in the control volume with quench front is calculated on the basis of length weighted average of heat transfer coefficients on rewetted and dry side of the quench front.

In ATHLET for nucleate boiling conditions the Chen correlation /3/ is applied. For film boiling conditions the heat transfer correlation can be chosen between three programmed correlations:

- Modified Dougall-Rohsenow correlation/4/
- Groeneveld 5.9 correlation /5/
- Condie-Bengson IV correlation /6/

The default correlation in ATHLET is the modified Dougall-Rohsenow correlation and this correlation has been applied in the FEBA experiment simulation.

For the transition boiling a cosine shape interpolation between nucleate boiling and film boiling is applied.

The detailed description of the heat transfer modelling in ATHLET can be found in the code description /7/.

Conclusions

Parameters 1, 2 and 3 are decided to be investigated in the Phase III. Parameters 4, 5 and 13 are taken into account as the peak cladding temperature is of importance. For quench front propagation they seem to be not so important. They influence will be investigated farther by other test runs. Parameters 7, 9 and 14 will be fixed and used as in the reference run. The remaining parameters seem to be negligible and they are going to be neglected.

B.8 KIT (Germany) results

Model description

Tab B.8.1 KIT code and software platform

Institution name	Code version	Software platform
Karlsruhe Institute of Technology	TRACE Version 5 Patch 3	Windows 7 with an Intel(R) Core™ i5 CPU 650 @3.20 GHz, 64 bit and 4 GB RAM

Nodalization and basic geometrical properties

The TRACE model consists of 1 CHAN component which models the assembly, 1 FILL component which serves as input and boundary condition for temperature and mass flow rate (velocity) and 1 BREAK component to represent the pressure boundary condition. The CHAN component is subdivided in 43 axial cells for the fluid domain (10 cm cell length) and of 123 axial cells for the wall domain (3.33 cm cell length). In addition, the 5x5 array is modelled , including also the bundle box. The bundle employs 7 spacer grids which have been modelled by activating the spacer grid model in order to account for the heat transfer enhancement in the vicinity of the spacers. Main geometrical parameters are gathered in Table B.8.2.

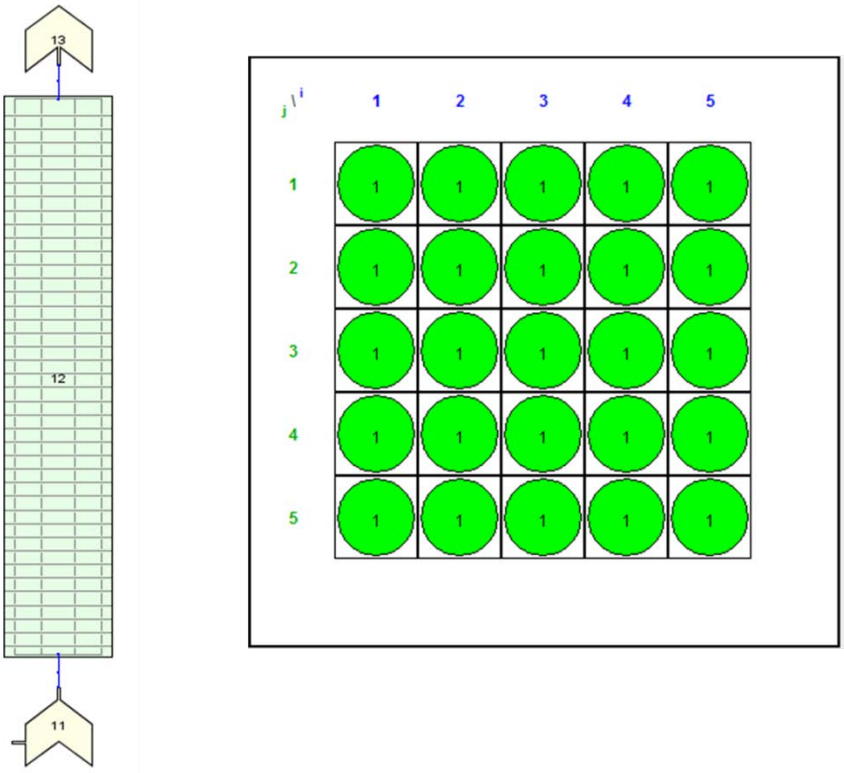

Fig B.8.1 Axial and radial nodalization of the FEBA assembly with TRACE

Tab B.8.2 Main geometrical data of the FEBA assembly model

Parameter	Value
No. of cells – fluid	43
No. of cells – wall	123
Cell length – fluid	1 x 7.5 cm + 41 x 10 cm + 1 x 13.5 cm
Cell length – wall	3.33 cm
Total length	4.114 m
Flow area	3.89319E-10 m²
Hydraulic diameter	13.47 mm
No. of spacers	7
Spacer positions (from bottom)	397, 961, 1525, 2089, 2653, 3217, 3718 mm
Spacer blockage ratio	20 %
No. of rods	25
Rod outer diameter	10.75 mm
pitch-to-diameter	1.33
Box width	0.314 m
Box thickness	6.5 mm

Boundary and initial conditions

The considered boundary conditions have been extracted from the original FEBA report by means of vector plot extractions. The flooding velocity, the inlet temperature, the system pressure and the assembly power are plotted in Figure B.8.2. The axial power profile is according to the specification and is depicted in Figure B.8.3.

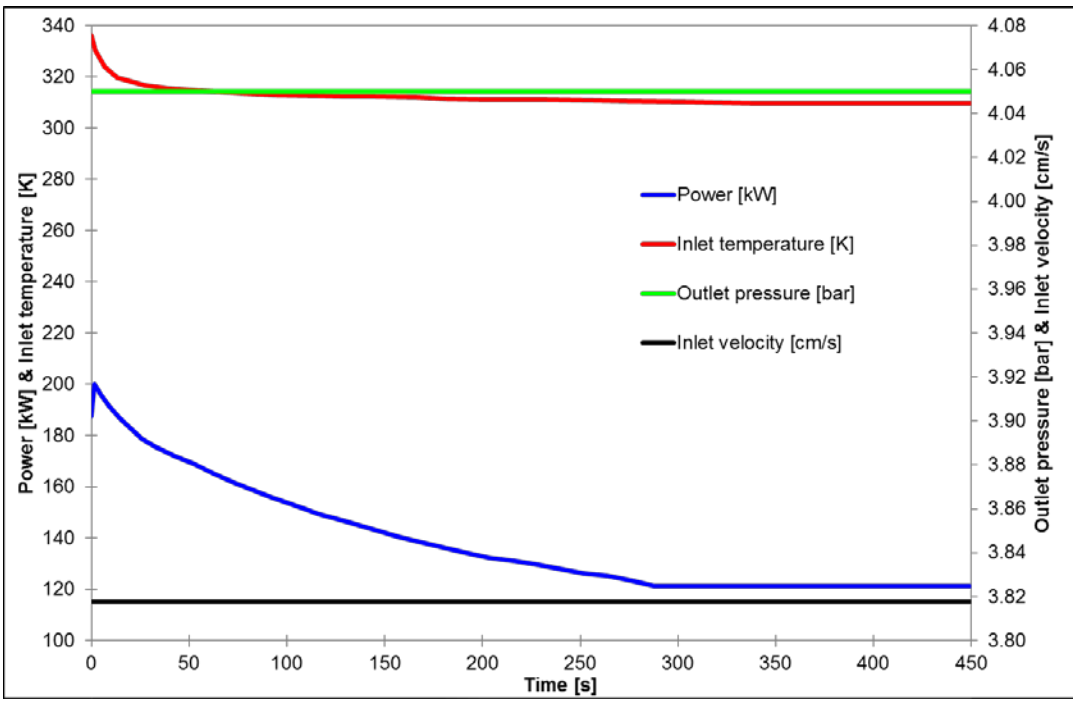

Fig B.8.2 Input and boundary conditions for FEBA test case 216

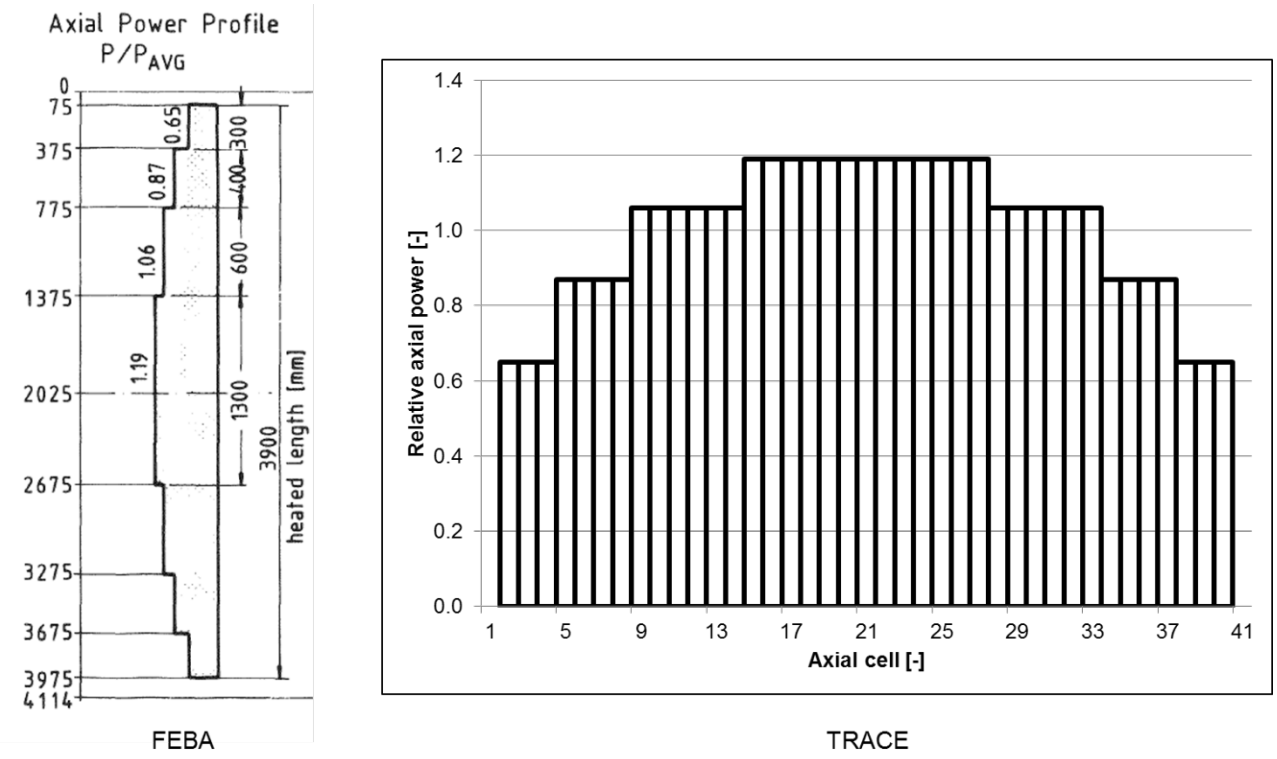

Fig B.8.3 FEBA and TRACE power profile in axial direction

Adopted models (flags)

No special flag has been set in order to perform the transients. One major difference to the original TRACE version is that a bias has been removed from the source code. That bias has been introduced by the TRACE developers in order to somehow guarantee that the peak cladding temperature during LOCA is not under estimated /8/. But since the purpose of this study is to analysis the experiment and not a LWR related transient, the bias has been removed. The model of concern is the two-phase flow enhancement factor during dispersed flow film boiling. The correlation in the original paper /9/ writes as follows,

$$F_{2\Phi\ \text{enhancement}} = \text{MAX}\left\{\left[1 + 25 \cdot \frac{(1-\alpha)\cdot \text{Gr}_{2\Phi}}{\text{Re}^2}\right]^{0.5}, 5\right\} \quad (1)$$

The TRACE developers replace the 25 with 100. That has been undone in order to have an unbiased TRACE version. For the sake of understanding, the correlation is given below along with the reasoning of the code developers.

"…Equation (…) does a reasonable job of correlating the "low quality" data but caused the peak clad temperature in reflood simulations to be under-predicted. Therefore, the magnitude of the enhancement factor was reduced…"…As expected, the majority of the data points are under predicted because the TRACE model was given a conservative bias to avoid under-predicting the peak clad temperature during reflood…"…Also, to eliminate unreasonably large values for this enhancement factor at low Reynolds no. conditions, is limited to have a value no greater than 5…"

We are aware that other bias might be hidden somewhere in the TRACE source code since TRACE always over estimates the cladding temperature.

Assumptions and steady-state achievement

No special assumption is considered. The calculation was performed directly as transient without performing a steady state run prior to this.

Base case results

Figures of all (exp-calc) responses

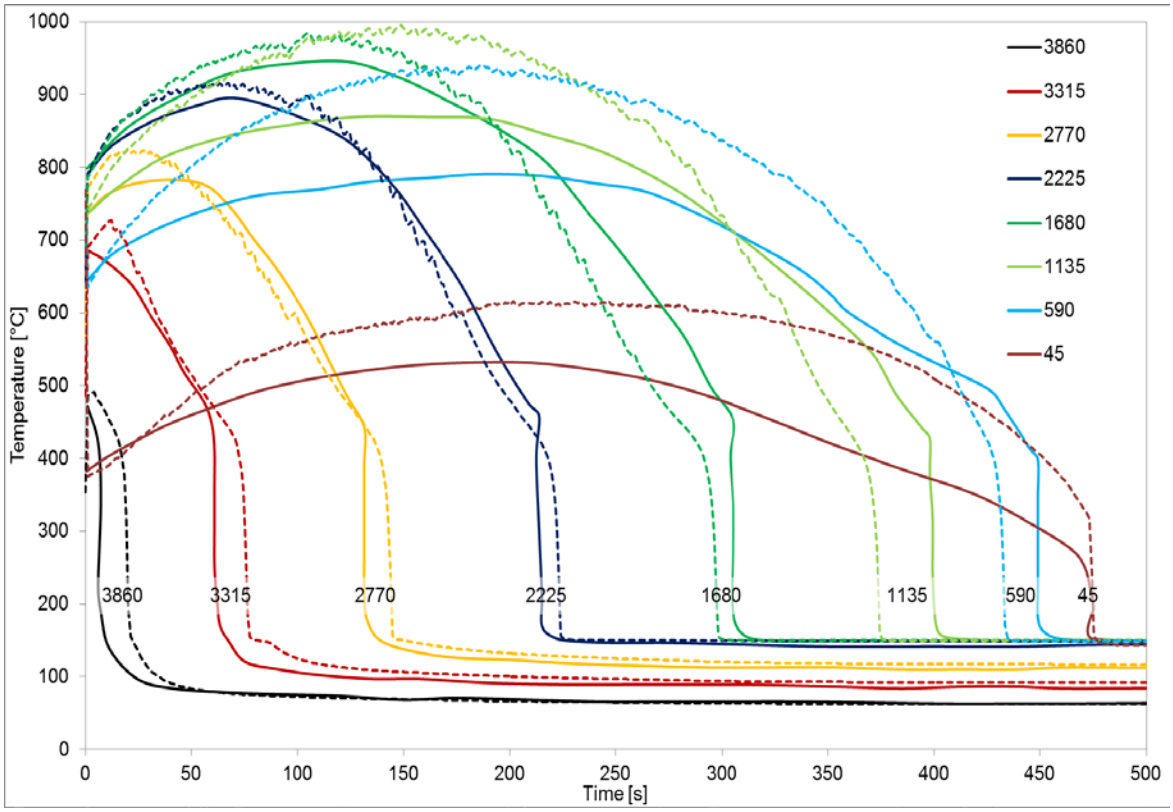

Fig B.8.4 Cladding temperatures as a function of time (solid line = experiment; broken line = TRACE)

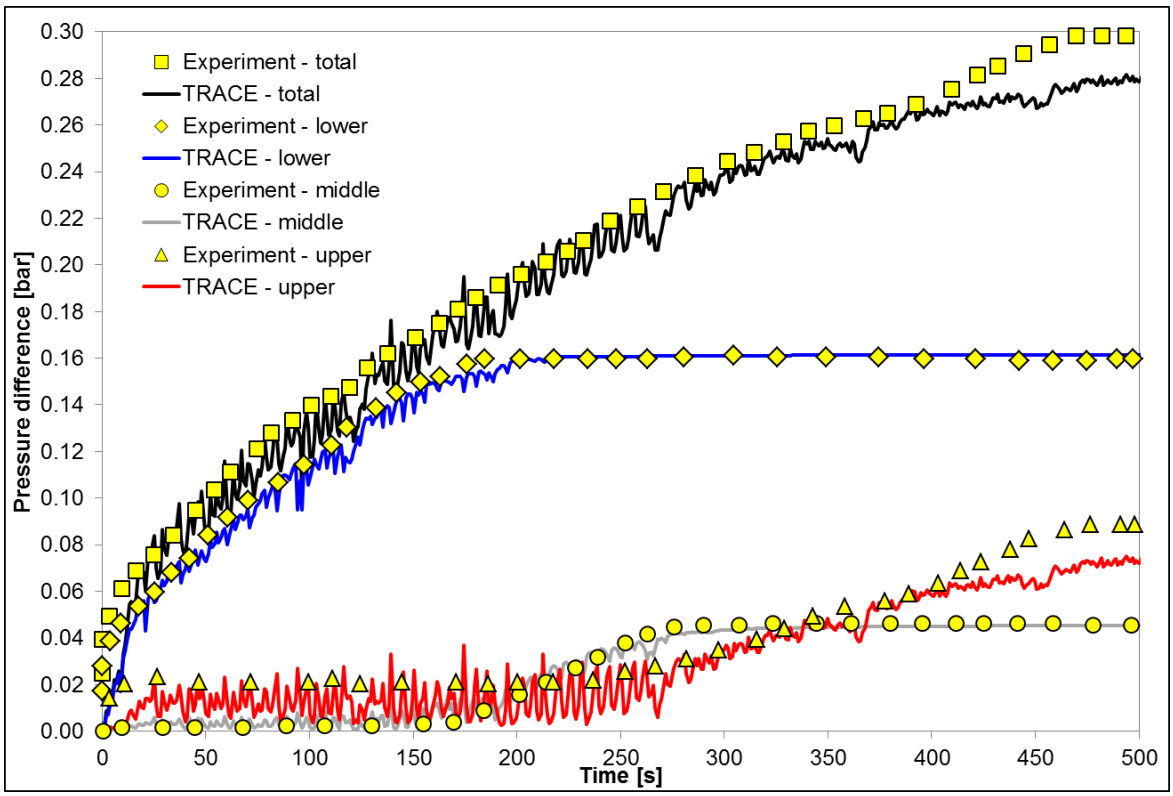

Fig B.8.5 Pressure drop as a function of time

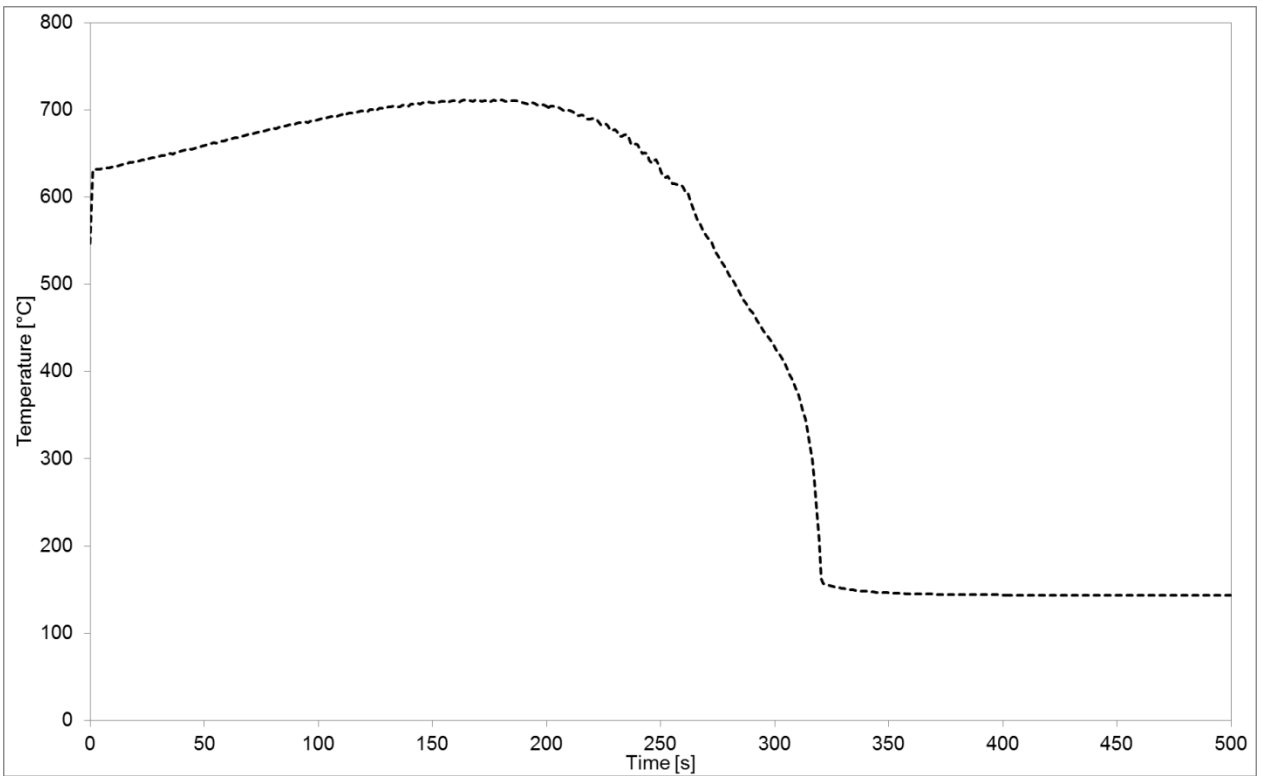

Fig B.8.6 Calculated housing temperatures as a function of time

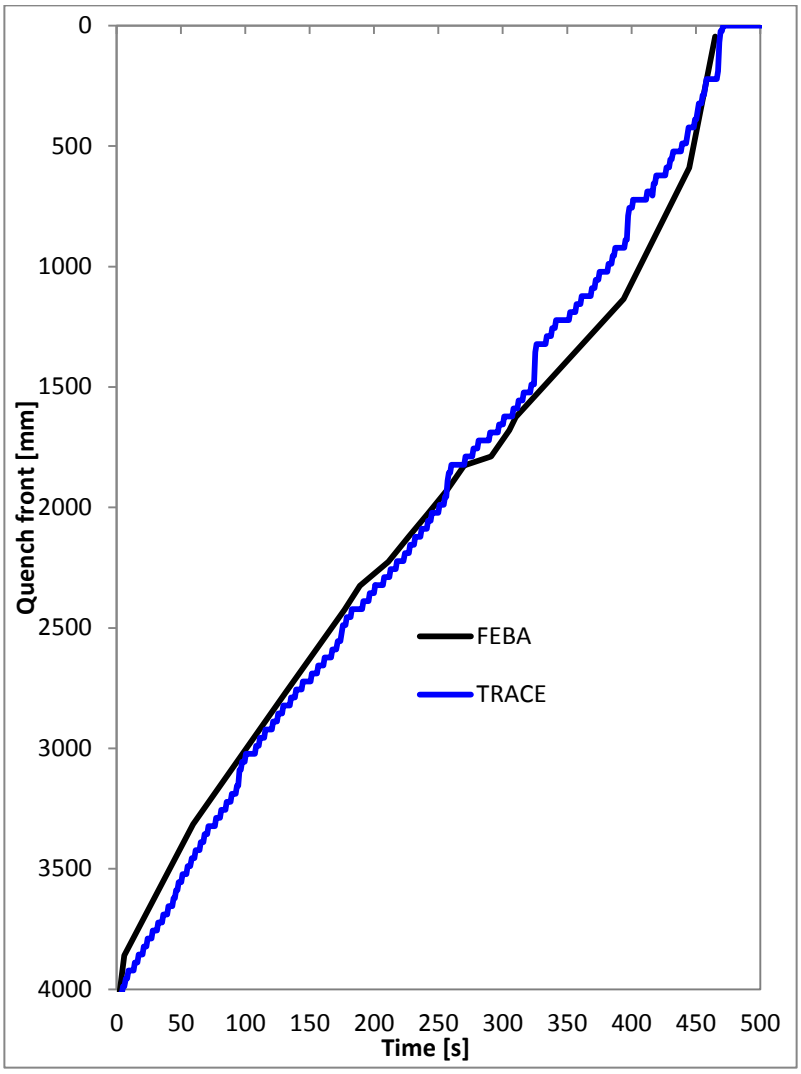

Fig B.8.7 Quench front propagation

PCT and bundle quench time

Tab B.8.3 Base case PCT and bundle quench

Institution name	PCT (˚C)	Position (mm)	Bundle quench (s)
KIT INR	491.01	590	21.1
	727.23	1135	78.3
	823.07	1680	145.6
	910.97	2225	223.9
	974.69	2770	297.2
	978.34	3315	361.3
	923.98	3860	430.3

Criteria for selection of influential input parameters

A reference calculation was performed with the purpose to identify the models which will be called in TRACE. Based on the outcome, as much as possible parameters have been selected in order to get a wider overview on the general influence of the parameters and the models itself. With the help of the additional modules we use for the regular uncertainty study, I added a multiplier to all of these models at once and I submitted than the corresponding number of runs. Where during each run only one multiplier is changed from 1.0 to its maximum value. The remaining ones are 1.0. The same was done with their minimal values. In some cases the parameters in the models have been changed directly. An example is parameter no. 21, the bundle correction factor during post CHF reflood. The Nusselt number is calculated for pipe geometry and afterwards multiplied with the bundle correction factor. This value is 1.3 in the original TRACE version. During phase II, that parameter is changed to 1.2 and 1.4. The procedure is identical to the other non-multipliers. In general, all parameters having a 1.0 as reference are multipliers.

Selection of parameters

Initial list of parameters

The initial list contains more than 50 parameters. The intention of having that much parameter is to identify to which extend a change of these parameters will provoke a change in the maximum cladding temperature and the time of rewet. In order to make the comparison between different codes easier, some of the parameters are grouped together (parameters 51 to 56). These parameters contain then the uncertainty of several parameters which is in the simplest case the product of the single uncertainties.

For instance, the uncertainty for the heat transfer coefficient of the dispersed flow film boiling (parameter 53) contains the uncertainty of: thermo physical properties, wall-to-fluid heat transfer, interfacial heat transfer, variable properties effect (taking into account the difference between bulk and wall properties), entrance length effects, etc.

The uncertainties have been taken from the original papers or from comparison with experimental data, recommendations or they have been adopted from other benchmark participants.

Tab B.8.4 Initial list of input parameters

No.	Parameter	Reference	Max	Min	Typ
1	Density (liquid)	1.0000	1.0100	0.9900	IBP
2	Specific heat (liquid)	1.0000	1.0100	0.9900	IBP
3	Thermal conductivity (liquid)	1.0000	1.0250	0.9750	IBP
4	Dynamic viscosity (liquid)	1.0000	1.0200	0.9800	IBP
5	Density (vapour)	1.0000	1.0100	0.9900	IBP
6	Specific heat (vapour)	1.0000	1.0100	0.9900	IBP
7	Thermal conductivity (vapour)	1.0000	1.0250	0.9750	IBP
8	Dynamic viscosity (vapour)	1.0000	1.0200	0.9800	IBP
9	Nusselt laminar (vapour)	1.0000	1.0800	0.9200	IGP
10	Nusselt turbulent (vapour)	1.0000	1.0800	0.9200	IGP
11	Variable property effect (vapour)	1.0000	1.0400	0.9600	ICP
12	Entrance length effect (vapour)	1.0000	1.0500	0.9500	ICP
13	Nusselt laminar (liquid)	1.0000	1.0800	0.9200	IGP
14	Nusselt turbulent (liquid)	1.0000	1.0800	0.9200	IGP
15	Nusselt NC (liquid)	1.0000	1.0800	0.9200	IGP
16	Variable property effect (liquid)	1.0000	1.0400	0.9600	ICP
17	2P flow enhancement factor	1.0000	1.1500	0.8500	ICP
18	Vapour film thickness	1.0000	1.1000	0.9000	ICP
19	Non-dimensional film thickness	1.0000	1.1000	0.9000	ICP
20	Nusselt wall-to-interface	1.0000	1.1000	0.9000	IGP
21	Bundle correction factor	1.3000	1.4000	1.2000	ICP
22	Emissivity (liquid)	0.9600	0.9980	0.9500	ICP
23	Nusselt interface (liquid)	100.0000	300.0000	100.0000	ICP
24	Terminal velocity	1.0000	1.0500	0.9500	ICP
25	Nusselt droplet I	0.5700	0.6020	0.5380	ICP
26	Nusselt droplet II	0.7000	0.7620	0.6380	ICP
27	Droplet diameter	1.0000	1.1500	0.8500	ICP
28	Drag coeff. annular flow	1.0000	1.1000	0.9000	IGP
29	Drag coeff. slug flow	1.0000	1.1000	0.9000	IGP
30	Drag coeff. dispersed flow	1.0000	1.1000	0.9000	IGP
31	Interfacial friction bubbly flow	1.0000	1.1000	0.9000	IGP
32	Interfacial friction annular mist	1.0000	1.1000	0.9000	IGP
33	Film friction annular flow	1.0000	1.1000	0.9000	IGP
34	Wall-to-fluid friction	1.0000	1.0500	0.9500	IGP
35	Spacer enhancement HTC	1.0000	1.1500	0.8500	IGP
36	Form loss coeff. spacer	1.0000	1.2000	0.8000	IBP
37	Thermal conductivity Nichrome	1.0000	1.0500	0.9500	IBP
38	Specific heat Nichrome	1.0000	1.0500	0.9500	IBP
39	Thermal conductivity MgO	1.0000	1.0500	0.9500	IBP
40	Specific heat MgO	1.0000	1.0500	0.9500	IBP
41	Emissivity (wall)	0.7000	0.8000	0.6000	IBP
42	Spacer vane blockage	0.2000	0.3000	0.0000	IBP

43	Inlet velocity	1.0000	1.0100	0.9900	IBP
44	Inlet temperature	1.0000	1.0050	0.9950	IBP
45	Wall roughness	2.50E-06	1.00E-05	1.00E-06	IBP
46	Hydraulic diameter	1.0000	1.0100	0.9900	IBP
47	Initial housing temperature	0.0000	5.0000	-5.0000	IBP
48	Initial pin temperature	0.0000	5.0000	-5.0000	IBP
49	Outlet pressure	1.0000	1.0100	0.9900	IBP
50	Assembly power	1.0000	1.1000	0.9000	IBP
51	HTC vapour	1.0000	1.2400	0.8000	IGP
52	HTC liquid	1.0000	1.1800	0.8400	IGP
53	HTC DFFB	1.0000	1.4300	0.6800	IGP
54	HTC IAFB	1.0000	1.4300	0.6800	IGP
55	HTC interfacial	1.0000	1.2500	0.7500	IGP
56	Drag coeff. interfacial	1.0000	1.1500	0.8500	IGP

Tab B.8.5 Results at 12b4 (1680 mm) with maximum values

No.	Parameter	Tclad [K]	tQuench [t]	ΔT	Δt
0	Reference solution	974.69	297.21	-	-
1	Density (liquid)	973.52	294.16	-1.17	-3.04
2	Specific heat (liquid)	974.53	296.19	-0.16	-1.01
3	Thermal conductivity (liquid)	975.02	296.18	0.33	-1.02
4	Dynamic viscosity (liquid)	974.08	296.24	-0.61	-0.96
5	Density (vapour)	975.13	296.17	0.44	-1.03
6	Specific heat (vapour)	974.41	296.20	-0.28	-1.00
7	Thermal conductivity (vapour)	970.89	294.18	-3.80	-3.02
8	Dynamic viscosity (vapour)	977.50	297.23	2.81	0.03
9	Nusselt laminar (vapour)	971.58	293.25	-3.11	-3.95
10	Nusselt turbulent (vapour)	971.08	296.13	-3.61	-1.07
11	Variable property effect (vapour)	972.95	296.20	-1.74	-1.00
12	Entrance length effect (vapour)	972.49	296.15	-2.20	-1.05
13	Nusselt laminar (liquid)	974.71	296.18	0.02	-1.02
14	Nusselt turbulent (liquid)	972.42	295.16	-2.27	-2.04
15	Nusselt NC (liquid)	974.69	296.17	0.00	-1.03
16	Variable property effect (liquid)	975.32	296.26	0.63	-0.94
17	2P flow enhancement factor	966.59	292.18	-8.10	-5.02
18	Vapour film thickness	969.80	297.18	-4.89	-0.02
19	Non-dimensional film thickness	972.89	291.20	-1.80	-6.00
20	Nusselt wall-to-interface	970.69	289.24	-4.00	-7.96
21	Bundle correction factor	972.23	290.19	-2.46	-7.01
22	Emissivity (liquid)	973.86	295.27	-0.83	-1.93
23	Nusselt interface (liquid)	976.42	296.26	1.73	-0.94
24	Terminal velocity	974.29	296.18	-0.40	-1.02
25	Nusselt droplet I	972.52	296.17	-2.17	-1.03
26	Nusselt droplet II	976.43	296.24	1.74	-0.96
27	Droplet diameter	976.75	294.23	2.06	-2.97

28	Drag coeff. annular flow	974.96	299.21	0.27	2.01
29	Drag coeff. slug flow	981.12	298.27	6.43	1.07
30	Drag coeff. dispersed flow	975.92	297.17	1.23	-0.03
31	Interfacial friction bubbly flow	976.71	296.27	2.02	-0.93
32	Interfacial friction annular mist	975.03	296.19	0.34	-1.01
33	Film friction annular flow	975.42	296.22	0.73	-0.98
34	Wall-to-fluid friction	975.24	296.25	0.55	-0.95
35	Spacer enhancement HTC	962.90	274.08	-11.79	-23.12
36	Form loss coeff. spacer	974.69	296.17	0.00	-1.03
37	Thermal conductivity Nichrome	976.93	297.23	2.24	0.03
38	Specific heat Nichrome	972.31	299.20	-2.38	2.00
39	Thermal conductivity MgO	976.57	296.24	1.88	-0.96
40	Specific heat MgO	969.48	301.32	-5.21	4.12
41	Emissivity (wall)	971.38	294.19	-3.31	-3.01
42	Spacer vane blockage	968.73	292.19	-5.96	-5.01
43	Inlet velocity	973.32	294.17	-1.37	-3.03
44	Inlet temperature	976.10	297.26	1.41	0.06
45	Wall roughness	974.58	296.22	-0.11	-0.98
46	Hydraulic diameter	968.89	290.17	-5.80	-7.03
47	Initial housing temperature	976.89	297.29	2.20	0.09
48	Initial pin temperature	978.97	296.23	4.28	-0.97
49	Outlet pressure	975.43	295.24	0.74	-1.96
50	Assembly power	1009.10	315.30	34.41	18.10
51	HTC vapour	976.04	289.00	-12.68	-8.20
52	HTC liquid	973.70	295.12	-0.27	-2.08
53	HTC DFFB	974.69	296.17	-20.60	-1.03
54	HTC IAFB	971.26	291.23	-2.80	-5.97
55	HTC interfacial	993.54	294.20	-16.69	-3.00
56	Interfacial drag coeff.	958.48	303.27	7.54	6.07

Tab B.8.6 Results at 12b4 (1680 mm) with minimum values

No.	Parameter	Tclad [K]	tQuench [t]	ΔT	Δt
0	Reference solution	974.69	297.21	-	-
1	Density (liquid)	976.62	298.18	1.93	0.98
2	Specific heat (liquid)	975.92	296.32	1.23	-0.88
3	Thermal conductivity (liquid)	975.14	296.22	0.45	-0.98
4	Dynamic viscosity (liquid)	975.27	296.14	0.58	-1.06
5	Density (vapour)	975.13	296.17	0.44	-1.03
6	Specific heat (vapour)	974.41	296.20	-0.28	-1.00
7	Thermal conductivity (vapour)	972.95	299.21	-1.74	2.01
8	Dynamic viscosity (vapour)	973.93	295.18	-0.76	-2.02
9	Nusselt laminar (vapour)	973.53	299.15	-1.16	1.95
10	Nusselt turbulent (vapour)	975.76	296.27	1.07	-0.93
11	Variable property effect (vapour)	975.60	296.19	0.91	-1.01
12	Entrance length effect (vapour)	974.95	296.24	0.26	-0.96

13	Nusselt laminar (liquid)	974.79	296.13	0.10	-1.07
14	Nusselt turbulent (liquid)	976.07	296.27	1.38	-0.93
15	Nusselt NC (liquid)	974.69	296.17	0.00	-1.03
16	Variable property effect (liquid)	974.92	296.20	0.23	-1.00
17	2P flow enhancement factor	970.73	295.16	-3.96	-2.04
18	Vapour film thickness	972.72	293.12	-1.97	-4.08
19	Non-dimensional film thickness	968.13	301.17	-6.56	3.97
20	Nusselt wall-to-interface	969.19	302.33	-5.50	5.13
21	Bundle correction factor	970.68	301.34	-4.01	4.14
22	Emissivity (liquid)	974.74	296.10	0.05	-1.10
23	Nusselt interface (liquid)	974.69	296.17	0.00	-1.03
24	Terminal velocity	975.66	296.20	0.97	-1.00
25	Nusselt droplet I	977.32	297.24	2.63	0.04
26	Nusselt droplet II	973.38	296.21	-1.31	-0.99
27	Droplet diameter	969.88	299.16	-4.81	1.96
28	Drag coeff. annular flow	973.70	292.21	-0.99	-4.99
29	Drag coeff. slug flow	968.83	294.22	-5.86	-2.98
30	Drag coeff. dispersed flow	974.23	296.14	-0.46	-1.06
31	Interfacial friction bubbly flow	974.46	296.25	-0.23	-0.95
32	Interfacial friction annular mist	974.53	296.22	-0.16	-0.98
33	Film friction annular flow	974.86	296.23	0.17	-0.97
34	Wall-to-fluid friction	974.42	296.27	-0.27	-0.93
35	Spacer enhancement HTC	960.49	289.19	-14.20	-8.01
36	Form loss coeff. spacer	974.69	296.17	0.00	-1.03
37	Thermal conductivity Nichrome	974.85	296.28	0.16	-0.92
38	Specific heat Nichrome	974.34	293.19	-0.35	-4.01
39	Thermal conductivity MgO	974.42	296.22	-0.27	-0.98
40	Specific heat MgO	975.11	290.23	0.42	-6.97
41	Emissivity (wall)	972.16	299.28	-2.53	2.08
42	Spacer vane blockage	975.92	296.14	1.23	-1.06
43	Inlet velocity	977.42	298.27	2.73	1.07
44	Inlet temperature	975.65	294.33	0.96	-2.87
45	Wall roughness	975.50	296.27	0.81	-0.93
46	Hydraulic diameter	979.23	302.26	4.54	5.06
47	Initial housing temperature	974.39	296.23	-0.30	-0.97
48	Initial pin temperature	972.00	296.27	-2.69	-0.93
49	Outlet pressure	976.05	297.25	1.36	0.05
50	Assembly power	937.05	274.15	-37.64	-23.05
51	HTC vapour	976.04	296.12	1.35	-1.08
52	HTC liquid	973.70	295.26	-0.99	-1.94
53	HTC DFFB	981.09	296.17	6.40	-1.03
54	HTC IAFB	972.03	299.26	-2.66	2.06
55	HTC interfacial	993.54	299.22	18.85	2.02
56	Interfacial drag coeff.	958.48	285.23	-16.21	-11.97

As it can be seen neither of these changes provoked the temperature to change by at least ± 50 K or to change the time of rewet by ± 10 %. One reason is related to the definition of the uncertain range of the

considered parameters. An increase of the range will result in a more pronounced change between reference and minimum/maximum.

The chosen uncertainty range is realistic and is based, among others on the comparison between experimental data and the considered models. One has to keep also in mind that some of these parameters are not independent from the others. In case one reduces e.g. the interfacial friction to zero, one implies that the vapour and the liquid would be perfectly separated which is not possible with system codes. on the other side an artificially increased friction would mean that both phase have almost the same velocity which might be wrong from the physical point of view.

One thing which can be seen from the tables is that in some cases the variation is negative no matter whether the corresponding parameter was increased or decreased. The logic mind would say that if an increase of the input parameter causes an increase of the output parameter, a decrease would be followed by a decrease. One has to keep in mind that the physical models and their implementation into the whole system is not straight forward. TRACE employs a lot of routines and the system is more like a nested loop. Sometimes several parameters will be calculated and the maximum/minimum of them will be used. In case the considered parameter is neither the smallest nor the largest one, a change of it might not result in a varying output parameter.

In addition, in order to calculate one parameter, others are needed which might depend on the actual one, iteration loops, etc. Therefore, that strange behaviour can, to some extent, be explained.

Final list of Influential Parameters

The final list contains 7 parameters. The most of them should be also available in other codes. The HTC for dispersed flow film boiling and inverted annular film boiling are from post CHF heat transfer regimes. In both cases a liquid and a vapour value is calculated and then depending on parameters like void, radiation enclosure, etc. a weighting is performed. The HTC for liquid and vapour are the ones for single and pre-CHF two phase flow.

Tab B.8.7 Final list of influential input parameters

Parameter	Subroutine	Fortran variable / Key word	Multiplier REF / REF value	Multiplier MIN	Multiplier MAX	T_{clad} variation [°C]	Position [mm]	t_{rew} variation [s]	Position [mm]
2P flow enhancement factor	REFLOOD	tpEnh	1.0	0.85	1.15	-4.0/ -8.1	1680	-2.0/ -5.0	1680
Spacer grid enhancement	Spacer Grid Crunch	f	1.0	0.85	1.15	-14.0/ -11.8	1680	-8.0/ -23.1	1680
Assembly power	INPUT	rpwtbr	1.0	0.90	1.10	-37.6/ +34.4	1680	-23.1/ +18.1	1680
HTC vapour	REFLOOD	hvWall	1.0	0.80	1.24	+1.4/ -12.7	1680	-1.1/ -8.2	1680
HTC DFFB	REFLOOD	hvWall/ hlWall	1.0	0.68	1.48	+6.4/ -20.6	1680	-1.0/ -1.0	1680
HTC interface	REFLOOD	hvAi/ hlAi	1.0	0.75	1.25	+18.9/ -16.7	1680	+2.0/ -3.0	1680
Interfacial drag coefficient	REFLOOD	ci	1.0	0.85	1.15	-16.2/ +7.5	1680	-12.0/ +6.1	1680

Wall-to-fluid heat transfer model

In order to understand the TRACE selection with respect to the heat transfer the following two flowcharts are taken from the TRACE theory manual /8/ and shown hear.

During the investigations it turned out that the post-CHF heat transfer regime dispersed flow film boiling is the most used one. The calculation of the heat transfer coefficient for DFFB requires the calculation of the single phase heat transfer coefficient and a two phase flow correction coefficient. The models are depicted in the following.

$$\mathrm{Nu}_{\mathrm{laminar}} = \mathrm{MAX}\left(\mathrm{Nu}_{\mathrm{Kim\ \&\ Li}}, \mathrm{Nu}_{\mathrm{El-Genk,\ laminar}}\right) \tag{2}$$

$$\mathrm{Nu}_{\mathrm{Kim\ \&\ Li}} = -5.6605 \cdot \left(\frac{p}{d}\right)^2 + 31.061 \cdot \left(\frac{p}{d}\right) - 24.473 \tag{3}$$

$$0 < \mathrm{Re} < 250;\ 1.1 < \left(\frac{p}{d}\right) < 2.0$$

$$\mathrm{Nu}_{\mathrm{El-Genk,\ laminar}} = A \cdot \mathrm{Re}^{B} \cdot \mathrm{Pr}^{0.33} \tag{4}$$

$$A = 2.97 - 1.76 \cdot \left(\frac{p}{d}\right);\ \mathrm{B} = 0.56 \cdot \left(\frac{p}{d}\right) - 0.3$$

$$250 < \mathrm{Re} < 30000;\ 3 < \mathrm{Pr} < 9;\ 1.25 < \left(\frac{p}{d}\right) < 1.5$$

$$\mathrm{Nu} = \mathrm{MAX}(\mathrm{Nu}_{\mathrm{laminar}}, \mathrm{Nu}_{\mathrm{turbulent}}) \tag{5}$$

$$\mathrm{Nu}_{\mathrm{El-Genk,\ turbulent}} = C \cdot \mathrm{Re}^{0.8} \cdot \mathrm{Pr}^{0.33} \tag{6}$$

$$C = 0.028 \cdot \left(\frac{p}{d}\right) - 0.006$$

$$\mathrm{Nu}_{\mathrm{turbulent}} = \mathrm{Nu}_{\mathrm{El-Genk,\ turbulent}} \cdot F_{\mathrm{var.\ vap.\ prop.\ effect}} \tag{7}$$

$$F_{\mathrm{var.\ vap.\ prop.\ effect}} = \left(\frac{T_{\mathrm{wall}}}{T_{\mathrm{vapor}}}\right)^{n} \tag{8}$$

$$n = \begin{cases} -\left[\log\left(\frac{T_{\mathrm{wall}}}{T_{\mathrm{vapor}}}\right)\right]^{0.25} + 0.3 & , \quad T_{\mathrm{wall}} \geq T_{\mathrm{vapor}} \\ -0.36 & , \quad T_{\mathrm{wall}} < T_{\mathrm{vapor}} \end{cases}$$

$$\mathrm{Nu}_{\mathrm{turbulent}} = \mathrm{Nu}_{\mathrm{turbulent}} \cdot F_{\mathrm{entrance\ length\ \ effect}} \tag{9}$$

$$F_{\mathrm{entrance\ length\ effect}} = 1 + \frac{2.4254}{\left(\frac{l}{d}\right)^{0.676}} \tag{10}$$

$$HTC = \frac{\mathrm{Nu} \cdot k}{d} \tag{11}$$

$$HTC = HTC \cdot F_{2\Phi\ \mathrm{enhancement}} \tag{12}$$

$$F_{2\Phi\ \text{enhancement}} = \left[1 + 100 \cdot \frac{(1-\alpha)\cdot \mathrm{Gr}_{2\Phi}}{\mathrm{Re}^2}\right]^{0.5} \quad (13)$$

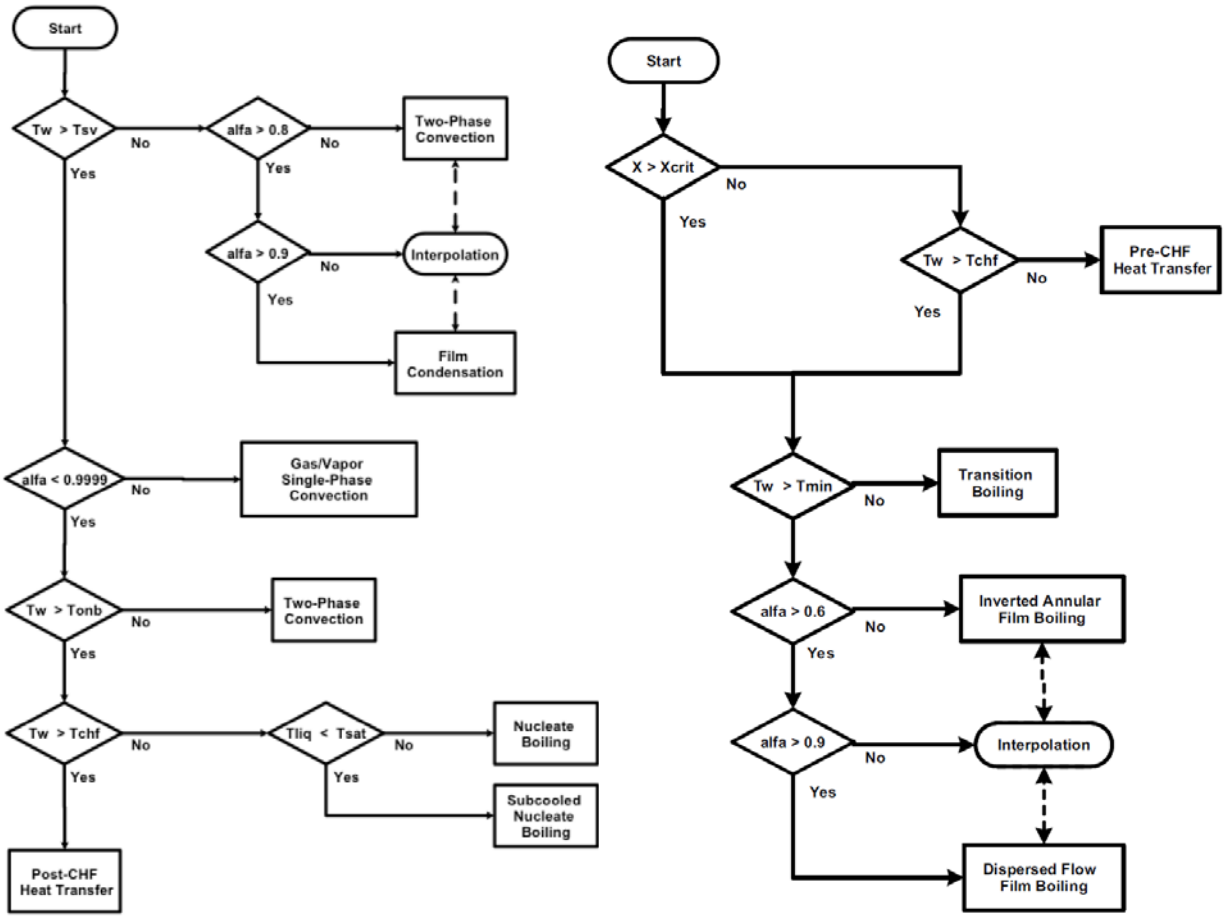

Fig B.8.8 Pre-CHF (left) and Post-CHF (right) heat transfer selection logic

Conclusions

The comparison between the experimental data and the predictions show a very good agreement based on the presented results TRACE qualifies for further investigations related to phase III without performing modelling improvements (input deck) or physical model improvements (source code). The final list of influential input parameters presented in Table B.8.7 will be considered for phase III.

In case the discussion with other benchmark participants, based on the presented results, indicates a necessary change of the parameters of their range (smaller or wider), the analysis can be performed again without spending too much time since everything is, more or loss, automatized.

B.9 UNIPI (Italy) results

Model description

Tab B.9.1 UNIPI code and software platform

Institution name	Code version	Software platform
GRNSPG/UNIPI	RELAP5 Mod3.3 patch3	Linux Ubuntu 32-bit

Nodalization and basic geometrical properties

1-D nodalization has been developed to model the FEBA test section. The model consists of the heated part of test section (pipe 110), lower (branch 100) and upper plena (branch 120). The heater rods are modelled with a single heat structure component with power profile imposed as in experiment specifications. The housing is modelled with a heat structure, isolated on the external side.

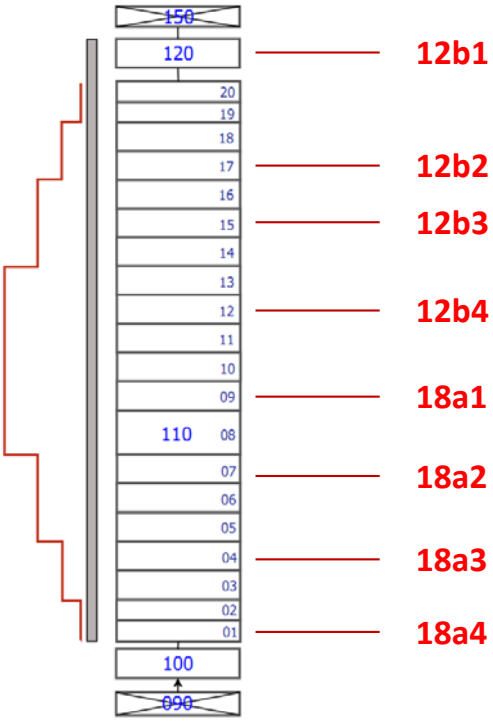

Fig B.9.1 FEBA nodalization

The model is characterized by the following parameters:

- Total height/length of 4.322 m (including 3.9 m of heated length);
- The heated length is modelled with 20 hydraulic nodes
- Flow area $3.893 \cdot 10^{-3}$ m^2
- Hydraulic diameter $1.347 \cdot 10^{-2}$ m
- Wall roughness $2.0 \cdot 10^{-5}$
- Spacer grid are simulated by assignment of pressure loss coefficients K_{loss}=0.2 at the corresponding junctions (flow area and hydraulic diameter maintained as for the rest of the bundle)
- The upper grid plate is simulated by flow area and hydraulic diameter corresponding to the 36 10mm holes at the junction between the pipe 100 (heated part) and branch 120 (upper plenum)
- Total heat transfer area of the heated part of heater rods 9.034 m^2
- Maximum linear heat rate 2.44 kW/m
- The additional boundary options using 9-word format have been specified for heat structure representing heater rods such as heated diameter, heated length forward/reverse, grid spacer length forward/reverse, etc.

Boundary and initial conditions

The boundary conditions to the model have been applied by means of time-dependent volume and time-dependent junction components:

- Pressure has been imposed by time-dependent volume 150
- Flooding coolant temperature has been imposed by time-dependent volume 90
- Flooding velocity has been imposed by time-dependent junction 95 (connecting tmdpvol 90 and branch 100)
- Power has been imposed to the corresponding heat structure by means of general table with specified power curve
- Heat losses were not simulated by the model

The model has been initialized at "cold" conditions:

- Pressure at 4.1 bar
- Hydraulic nodes filled with vapour at saturation temperature
- No flow imposed in the nodes and boundary conditions
- Heater rod heat structure meshes initialized at vapour temperature (420 K)

Adopted models (flags)

The following specific RELAP5 models were activated for hydrodynamic and heat transfer processes:

- Bundle interphase friction model has been activated in the hydraulic nodes of the heated part by setting flag b=1;
- "Reflood" model has been activated in the heat structure representing the heater rods;
- "Vertical bundle without cross flow" heat transfer mode has been set at the boundary of the heat structure representing the heater rods.

Radiation heat transfer has not been modelled explicitly, but radiation heat transfer from heater rod surface to liquid droplets is taken into account by additive term to the film boiling coefficient to liquid in special RELAP5 reflood model.

Assumptions and steady-state achievement

Since the model has been initialized at "cold" conditions, the heat-up conditioning phase has been simulated in order to reach the Start of Transient (SoT) conditions.

A power of 40 kW has been supplied to the heater rods until the temperature in the heat structure, where the maximum steady-state value observed in experiment, reached the experimental value minus 5K. Then the calculation proceeded at quasi-steady-state conditions with 0.5 kW power until the temperature in the mentioned heat structure reached the experimental value. At this point the SoT conditions were achieved. The obtained axial temperature distribution in heater rods and housing are provided in the Figure below.

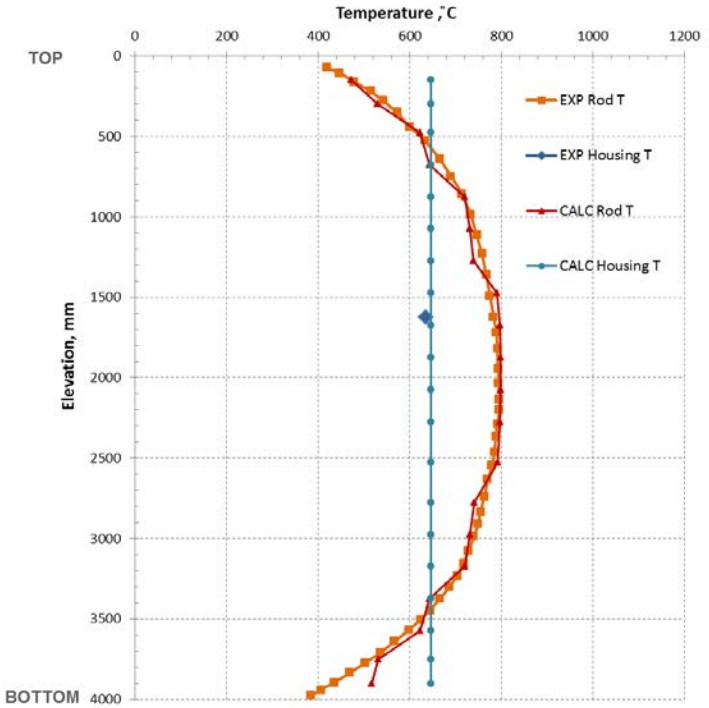

Fig B.9.2 Steady-state temperature profile

Base case results

The obtained reference case calculation results are presented at the following figures. The PCT is underestimated by the code and the rewet time at different elevations (quench front propagation) is anticipated in calculation with respect to the experimental data.

Figures of all (exp-calc) responses

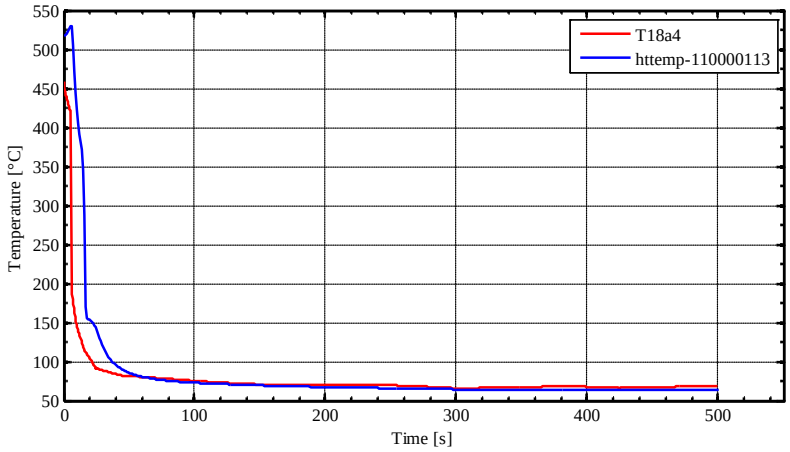

Fig B.9.3 Base case calculation of cladding temperature at T18a4

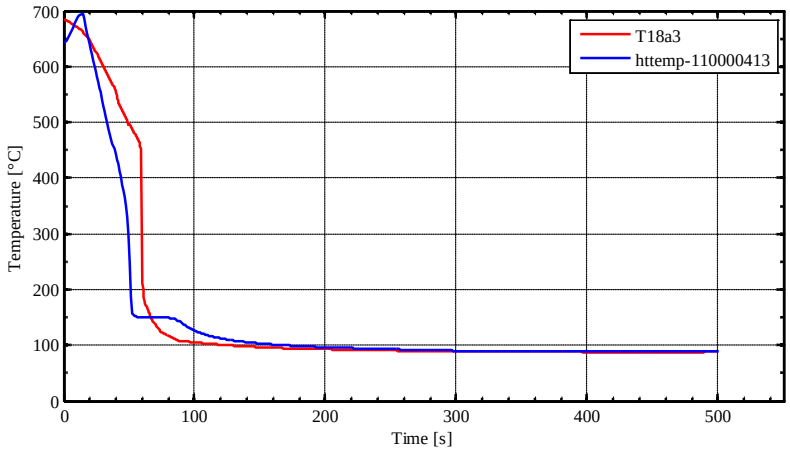

Fig B.9.4 Base case calculation of cladding temperature at T18a3

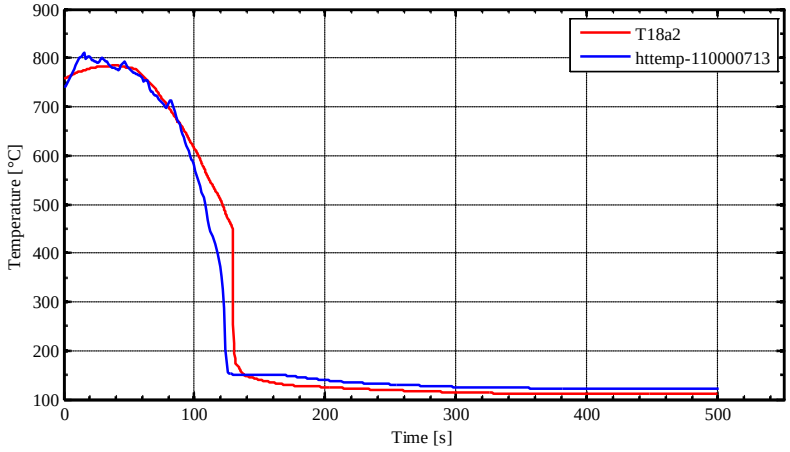

Fig B.9.5 Base case calculation of cladding temperature at T18a2

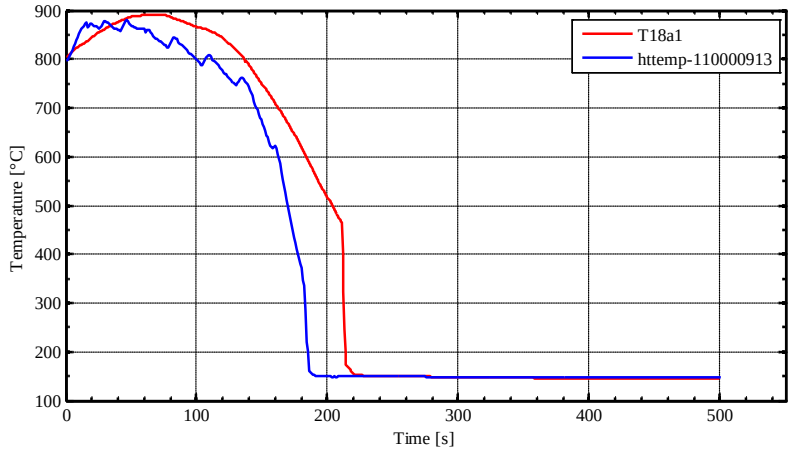

Fig B.9.6 Base case calculation of cladding temperature at T18a1

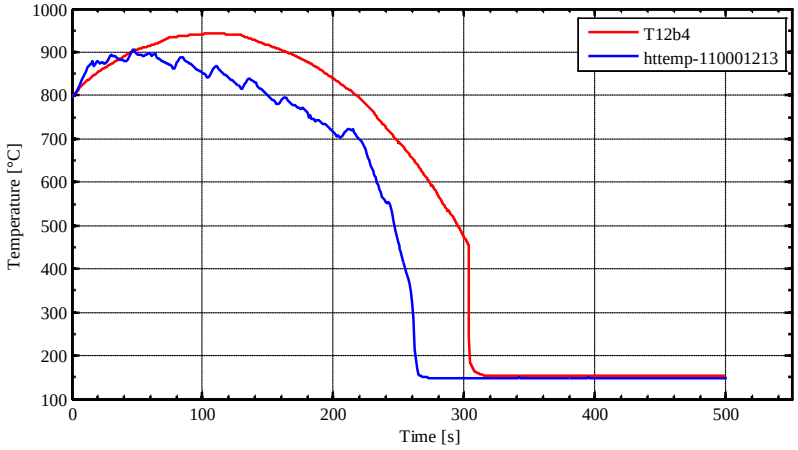

Fig B.9.7 Base case calculation of cladding temperature at T12b4

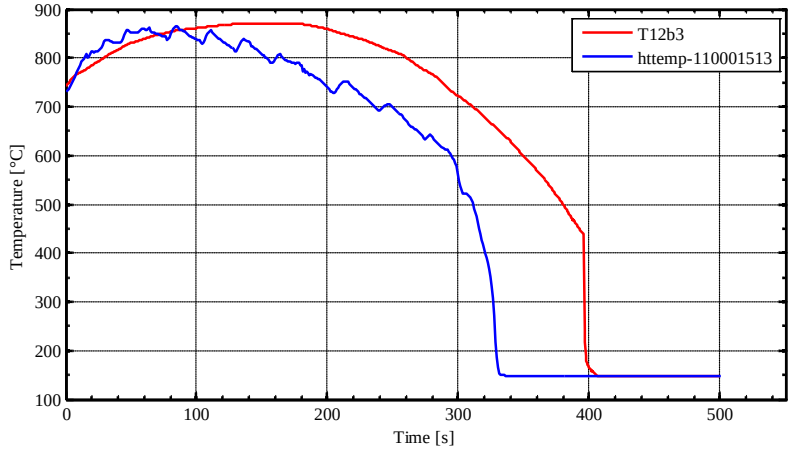

Fig B.9.8 Base case calculation of cladding temperature at T12b3

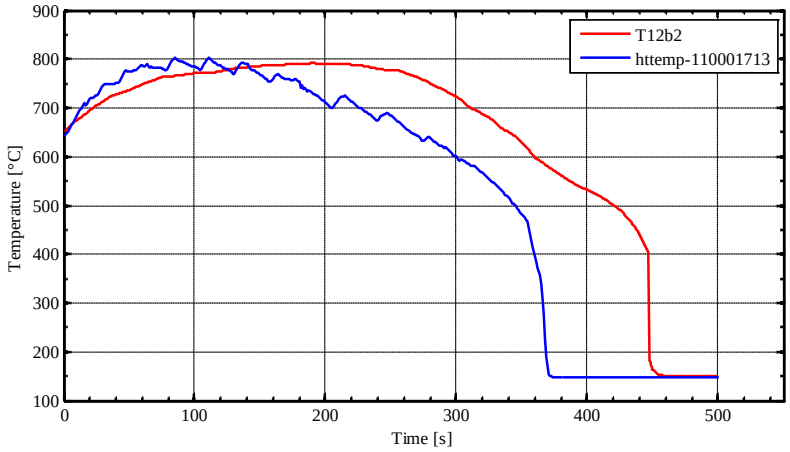

Fig B.9.9 Base case calculation of cladding temperature at T12b2

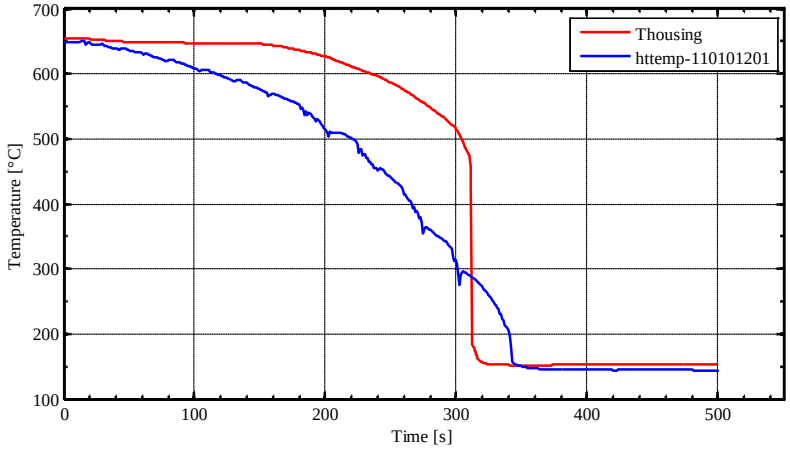

Fig B.9.10 Base case calculation of housing temperature at 1625mm

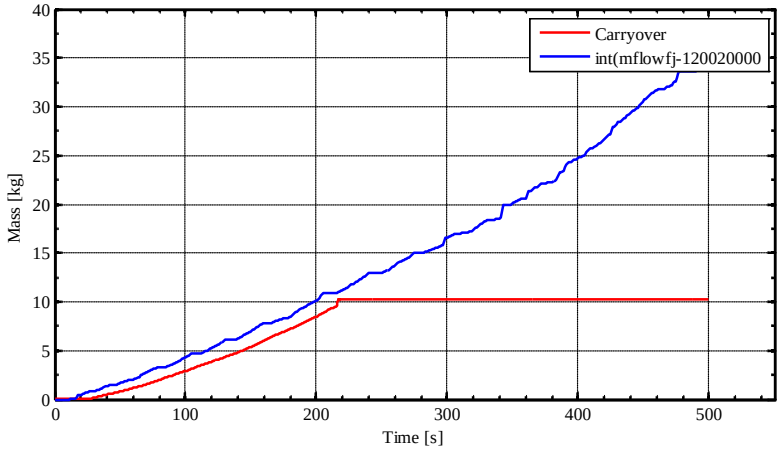

Fig B.9.11 Base case calculation of liquid carryover

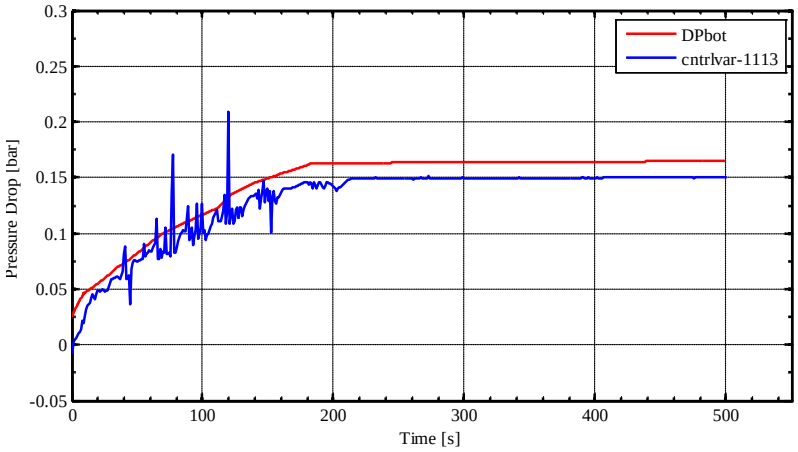

Fig B.9.12 Base case calculation of bottom pressure drop

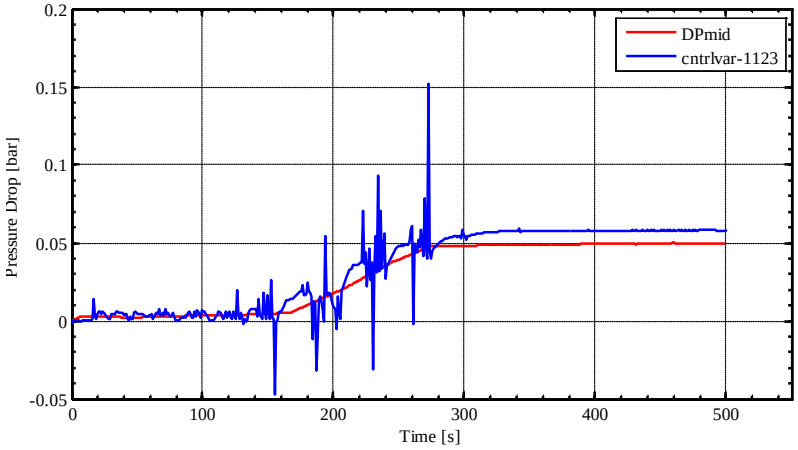

Fig B.9.13 Base case calculation of middle pressure drop

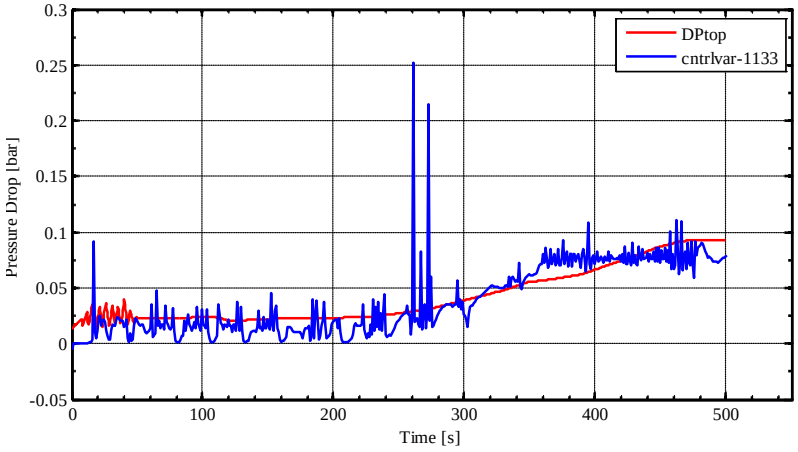

Fig B.9.14 Base case calculation of top pressure drop

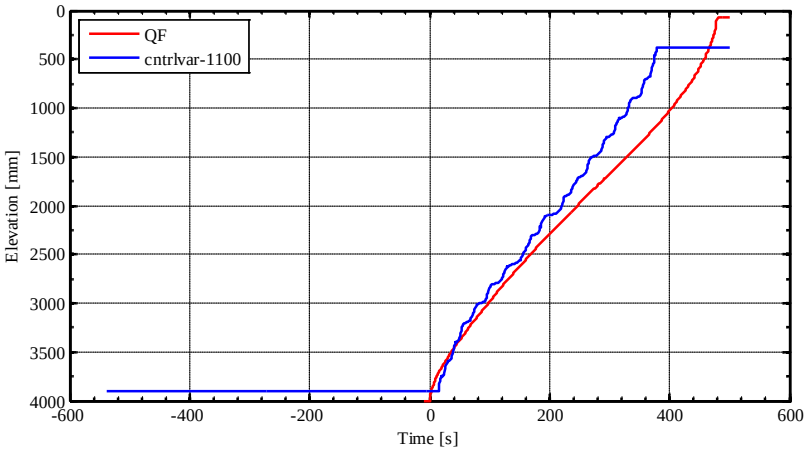

Fig B.9.15 Base case calculation of quench front propagation

PCT and bundle quench time

Tab B.9.2 Base case PCT and bundle quench

Institution name	PCT (°C)	Position (mm)	Bundle quench (s)
GRNSPG/UNIPI	908	1680mm	378

Criteria for selection of influential input parameters

The set of criteria, proposed by GRNSP/UNIPI in the Specifications for the Phase II of the PREMIUM benchmark were adopted to identify the influential input parameters.

An influential IP has to be such that its extreme value in the range of variation causes the following change in the either of two main reflood responses (at least one out of two criteria should be fulfilled)

- The absolute value of variation in rod surface temperature T_{clad} is $\mathbf{\Delta T_{ref} = 50K}$
- The variation in rewet time t_{rew} is $\mathbf{\Delta t_{rew} = 10\%}$

Additional criteria (3-6), provided in Specifications, were also applied in order to ensure the "realism" of selected influential input parameters.

Selection of parameters

Initial list of parameters

The Sample List provided in Appendix A of Specifications for the Phase II has been used as an initial list of parameters for analysis. Moreover, some other parameters have been added to the initial list after thorough analysis of the corresponding RELAP5 code subroutines.

Tab B.9.3 Initial list of input parameters

Input Basic Parameter	
1	Pressure
2	Flooding velocity
3	Fluid temperature
4	Ni Cr Thermal conductivity
5	Ni Cr Heat capacity
6	MgO Thermal conductivity
7	MgO Heat capacity
8	Housing initial temperature
9	Power
10	Grid pressure loss coefficient
Input Global Parameter	
1	Film boiling heat transfer coefficient
2	Transition boiling heat transfer coefficient
3	Junction interface friction coefficient
4	Effective interface friction coefficient
5	Interphase heat transfer
Input Coefficient Parameter	
1	Droplet Weber (critical) number
2	Minimum droplet diameter
3	Quench front threshold distances for HTC transitions

Final list of Influential Parameters

After the performing a sensitivity analysis of calculation with singe-parameter variation from the initial list of parameters and applying the criteria for identification of influential input parameters, the final list of parameters has been defined. The list is presented in the following table together with the variation range of the selected parameters and corresponding variations of responses of interest (cladding temperature and time of rewet) at selected elevations.

Tab B.9.4 Final list of influential input parameters

Parameter	Subroutine	Fortran variable / Key word	Multiplier REF / REF value	Multiplier MIN	Multiplier MAX	T_{clad} variation [°C]	Position [mm]	t_{rew} variation [s]	Position [mm]
Film boiling wall-to-liquid HTC	PSTDNB	hfb	1.0	0.5	3.0	+13 / -34	1680	+58 / -62	1680
Film boiling wall-to-vapour HTC	PSTDNB	hv	1.0	0.65	4.0	+59 / -44	1680	0 / -30	675
Junction interphase drag for bubbles and droplets	FIDIS2	fic	1.0	0.5	1.5	-15 / +15	1680	-46 / +40	1680
Resulting interphase friction at junctions	PHATNJ	fij	1.0	0.5	1.5	-12 / +11	1680	-55 / +45	1680
Interphase heat transfer in dispersed flow for dry wall	DISPDRYHIF	hifc, higc, hgfc	1.0	0.2/1/	5.0/1/	+79 / -56	675	+31 / -85	675
Minimum droplet diameter/2/	FIDIS2 & FIDISV	dcon(2)	1.5 mm	0.7 mm	2.5 mm	0 / 0	675	+55 / -48	675

/1/ The multiplier has been simultaneously applied for all three partitions of the interphase heat transfer
/2/ The multiplier has been simultaneously applied in both subroutines

Wall-to-fluid heat transfer model

The RELAP5 reflood heat transfer model has been designed specifically for the reflood process which normally occurs at low flow and low pressure (see Section 4.4 of RELAP5 manual Volume 4 for details). Besides adding an axial heat conduction model in the heat structures, changes occur in transition and film boiling heat transfer coefficients, both with and without the hydraulic bundle flag activated, when reflood is active.

A modified Weismann correlation replaces the Chen transition boiling correlation. The correlation is

$$h_w = h_{max}(e^{-0.02\Delta T_{wchf}}) + 4500\left(\frac{G}{G_R}\right)^{0.2}(e^{-0.012\Delta T_{wchf}})$$

where

$h_{max} = \dfrac{0.5\ CHF}{\Delta T_{chf}}$

CHF = critical heat flux

$\Delta T_{wchf} = \max[3, \min(40, T_w - T_{spt})]$

$\Delta T_{chf} = \max(0, T_w - T_{spt})$

G = total mass flux

$G_R = 67.8\ kg/m^2s$

Code use of the Weismann correlation also depends on the distance from the point in question to the quench front position.

The transition boiling heat transfer coefficient to vapour comes from a call to the DITTUS subroutine. This coefficient is then void fraction ramped so that it goes to zero as the void fraction goes to zero.

The film boiling heat transfer coefficient to liquid h_{fFB} uses the maximum of a film coefficient, h_{FBB}, and a Forslund-Rohenow coefficient, h_{FR}. The film coefficient is given by

$$h_{FBB} = [1400 - 1880\min(0.05, z_{QF})]\min(0.999 - \alpha_g, 0.5) + h_{FBGR}(1 - \alpha_g)^{0.5}$$

where h_{FBGR} is a modified Bromley correlation

$$h_{FBGR} = 0.62\left\{\frac{gk_g^3\rho_g(\rho_f - \rho_g)[h_{fg} + 0.5(T_w - T_{spt})C_{pf}]}{\max(0.005, z_{QF})\mu_g(T_w - T_{spt})}\right\}^{0.25}$$

The Forslund-Rohsenow correlation coefficient is given by

$$h_{FR} = h1\left\{\frac{g\rho_g\rho_f h_{fg}k^3}{\left[(T_w - T_{spt})\mu_g d\left(\frac{\pi}{6}\right)^{\frac{1}{3}}\right]}\right\}^{0.25}$$

where

$h1 = 0.4\left(\dfrac{\pi}{4}\right)\left[\dfrac{6(0.999 - \alpha_g)}{\pi}\right]^{2/3}$

Radiation to droplets is added to the final film boiling coefficient to liquid, h_{fFB}. The final value is multiplied times $T_w - T_{spt}$ to get the heat flux to liquid. The heat flux to vapour is the same as the transition boiling value.

Interfacial heat transfer and interfacial drag are also modified when reflood is active. The interfacial area is changed in a control volume next to a heat structure with “reflood” activated. The wet wall droplet size maximum was reduced from 2.5 mm to 1.5 mm. The dry wall Weber number was reduced from 12 mm to 3 mm. Some other modifications have been introduced to the logic for deciding whether the wall was wet or dry.

Conclusions

At the conclusion of the performed analysis, the parameter "Junction interphase drag for bubbles and droplets" from Table B.9.4 has been discarded from the following application to the Phase III since it is covered by parameter "Resulting interphase friction at junctions". Therefore, totally 5 input parameters will be considered in the Phase III:

- Film boiling wall-to-liquid HTC
- Film boiling wall-to-vapour HTC
- Resulting interphase friction at junctions
- Interphase heat transfer in dispersed flow for dry wall
- Minimum droplet diameter.

B.10 KAERI (Rep. of Korea) results

Model description

MARS-KS1.3 code has been used on Intel Quad CPU 2.66GHz PC with WINDOW XP operation system.

Tab B.10.1 KAERI code and software platform

Institution name	Code version	Software platform
KAERI	MARS-KS1.3(COBRA-TF Module)	WINDOW XP

Nodalization and basic geometrical properties

The FEBA test is divided equally in 26 nodes for MARS-KS 1.3 (COBRA-TF Module) model. In this model, the test section is connected with lower plenum and upper plenum by two pipes 150 and 250 corresponding as shown in Figure 1. The grid spacer elevations in this figure are at 7 nodes (3, 7, 10, 14, 18, 21 and 25 node number from the bottom of the test section). In the cross section of FEBA test, due to the asymmetric geometry, the modelled section is only $1/8^{th}$ rod bundle of FEBA test with one equivalent heater rod (of 3.125 rods) and one single channel as shown in Figure 2. The wall of housing is also modelled as insulated heat slab.

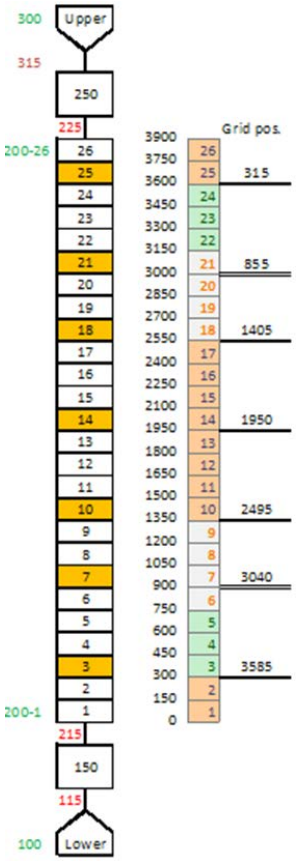

Fig B.10.1 Modelling for FEBA test

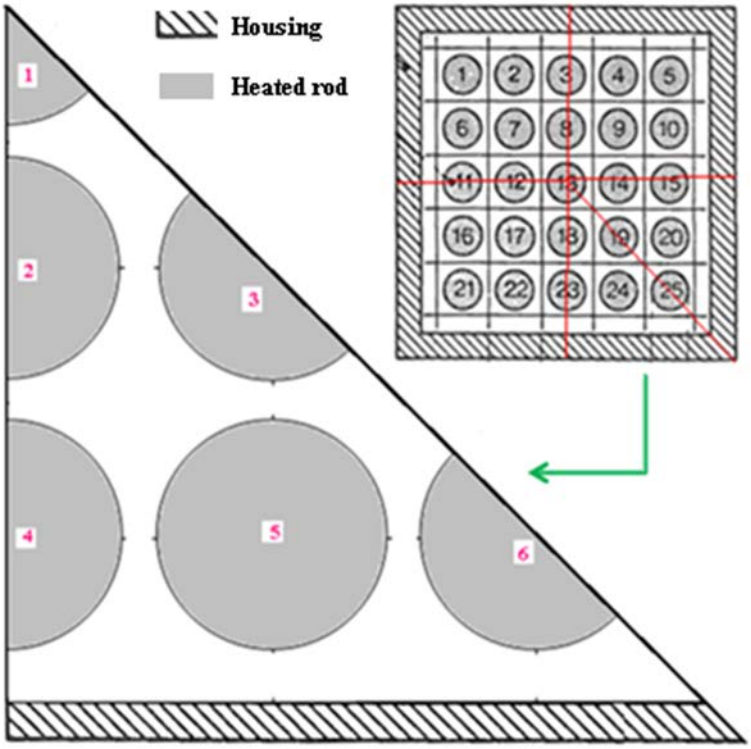

Fig B.10.2 The cross-section model of 1/8 FEBA test

The detail information such as flow area, hydraulic diameter (D_h), etc., related to the testing section model is specified in Table 1. From bottom of the rod bundle, considered that the heater rod includes two parts (unheated lower and heated parts).

Tab B.10.2 Main geometrical parameter of MARS 3D model

Test section	Length	Flow area	Dh	Wall roughness	Total heat transfer area	Max. linear heat rate
Unit	**m**	**m^2**	**m**		**m^2**	**kW/m**
Heater part	3.90	0.00393	0.01344	1.00E-05	3.29258	1.9945
Unheated lower part	0.15	0.00393	0.01344	1.00E-05	0.1266	0.0

Boundary and initial conditions

The boundary and initial conditions such as system pressure, feed water temperature, flooding mass flow rate, maximum power and heat loss for the chosen 216 test in Series I are listed in Table B.10.3. In this calculation, heat loss through the wall was not modelled and there is no heat loss through the housing.

Tab B.10.3 Boundary conditions for test 216

Parameter	Sys. Pressure	Feed water Temp.	Flooding flow rate	Heat losses
Unit	**bar**	**^{0}C**	**kg/s**	**W**
Value	4.1	48 (keep constant in 30s (0-30s)) 37 (linearly decrease (30-600s))	0.0184	0.0

The power B.C. curve is showed in “power B.C curve.txt” with the linear heat generation value, 1.9945 (kW/m).

Figure B.10.3 shows the initial cladding and housing temperatures (using the reference elevation 0.0 m at the top of housing). Because the preheating procedures of all FEBA experiments are similar, we assumed that the initial housing temperatures are similar to test 223.

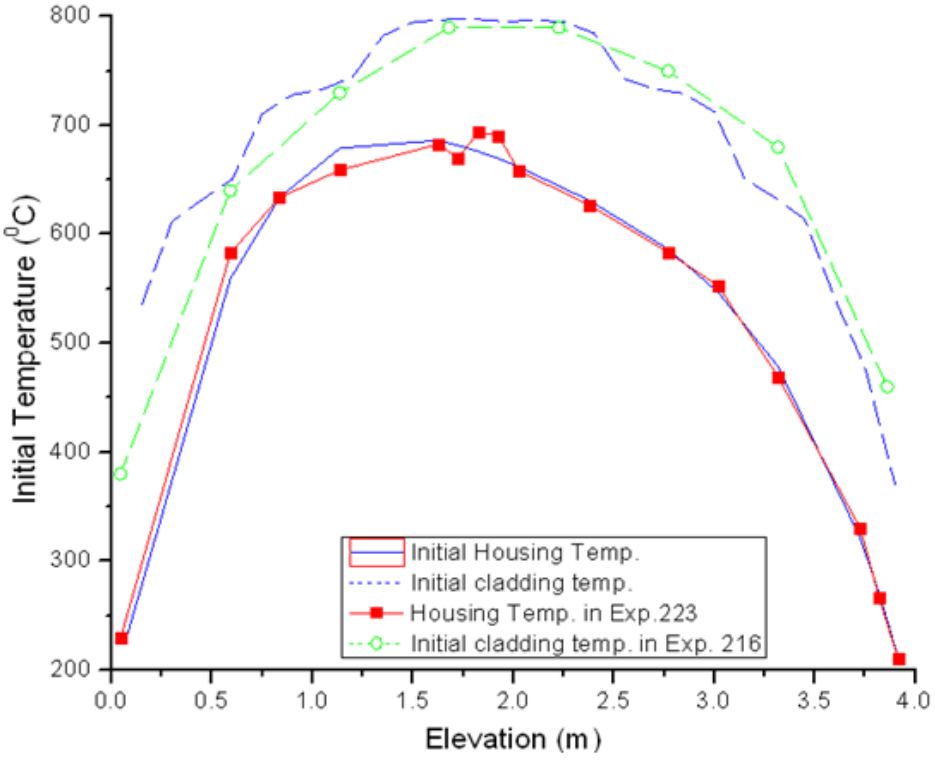

Fig B.10.3 Housing and cladding initial temperatures in comparison with exp data

Adopted models (flags)

In considering the grid space effects, models regarding spacer model were activated in MARS-KS 1.3 (COBRA-TF Module) code:

- Flag for grid quench front model (setting optional flag to activate)
- Flag for grid convective enhancement model (setting optional flag to activate)
- And flag for two-phase enhancement of dispersed flow heat transfer. (setting optional flag to activate)

In MARS calculations, the radiation has not been taken into account.

Assumptions and steady-state achievement

In MARS-KS 1.3 COBRA-TF model, it is not easy to do simulate the steady state as the performed experiment procedure due to the long running time. In order to reach the initial constant temperatures of heater rod cladding, after 790s heating period at low power until reaching the initial temperature, those initial temperatures are kept almost constant in 80 s, it means until 870s. Because of an added lower pipe in order to connect from time dependent volume to 1D part with 3D section, the time constant that the liquid need to be filled in lower volume is 6.0 s. So that the heating time using MARS-KS 1.3 (COBRA-TF Module) is about 870 s. And the feed water is injected 6.0 s earlier in order to fill the lower plenum.

Base case results

Figures of all (exp-calc) responses

The comparison of experimental measurement and calculated cladding temperatures are showed in the figures from Figure B.10.4 to Figure B.10.14. The comparison of heater rod surface temperature corresponding to 12b2, 12b3 and 12b4 in the experimental data (in degree Celsius):

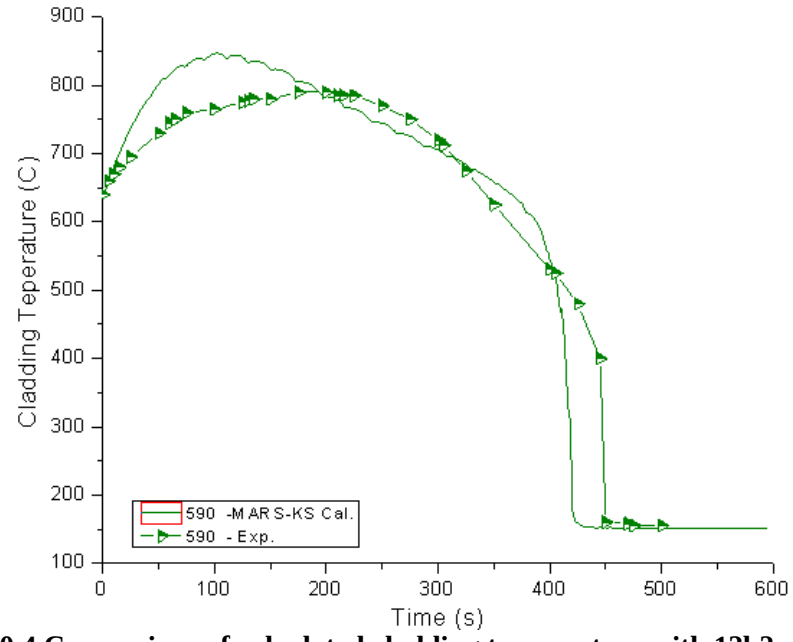

Fig B.10.4 Comparison of calculated cladding temperature with 12b2 exp. data

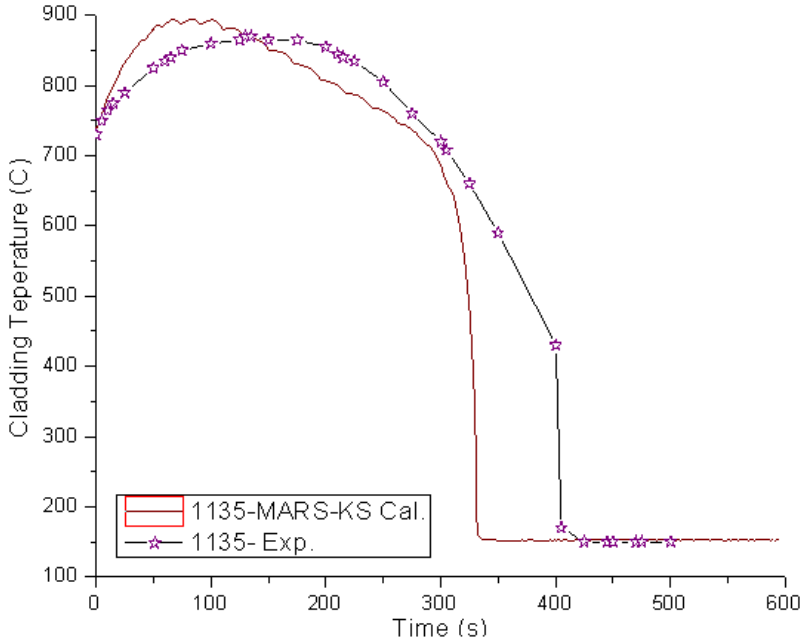

Figure 5.

Figure 6.Fig B.10.5 Comparison of calculated cladding temperature with 12b3 exp. data

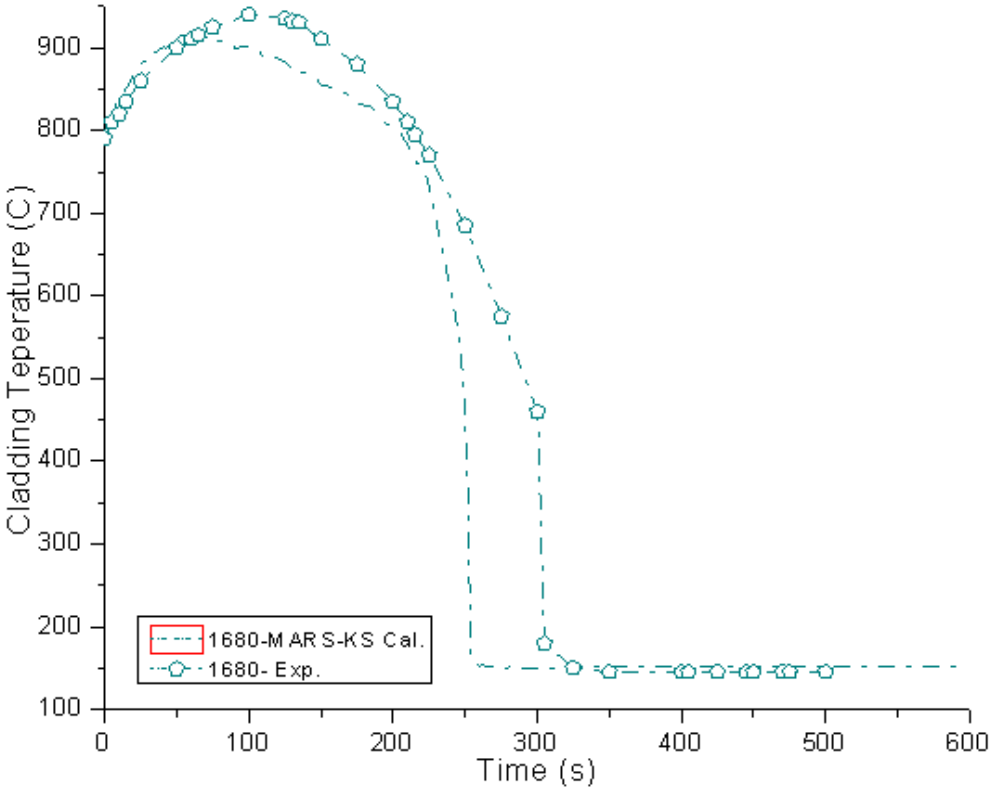

Fig B.10.6 Comparison of calculated cladding temperature with 12b4 exp. data

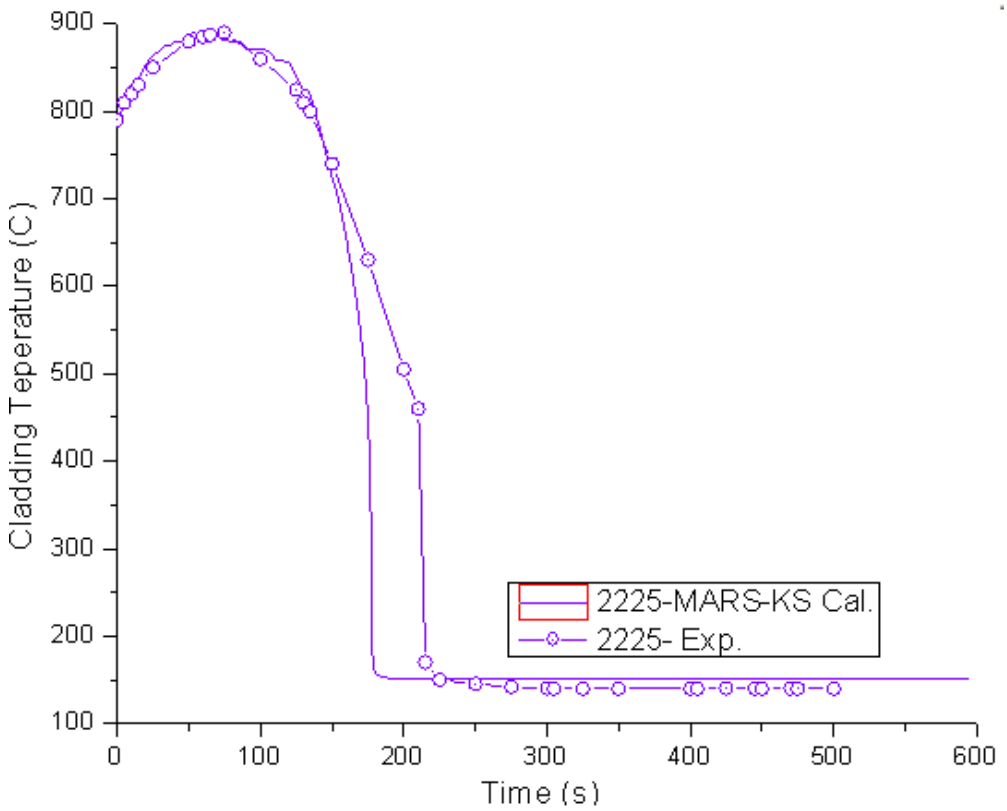

Fig B.10.7 Comparison of calculated cladding temperature with 12a1 exp. data

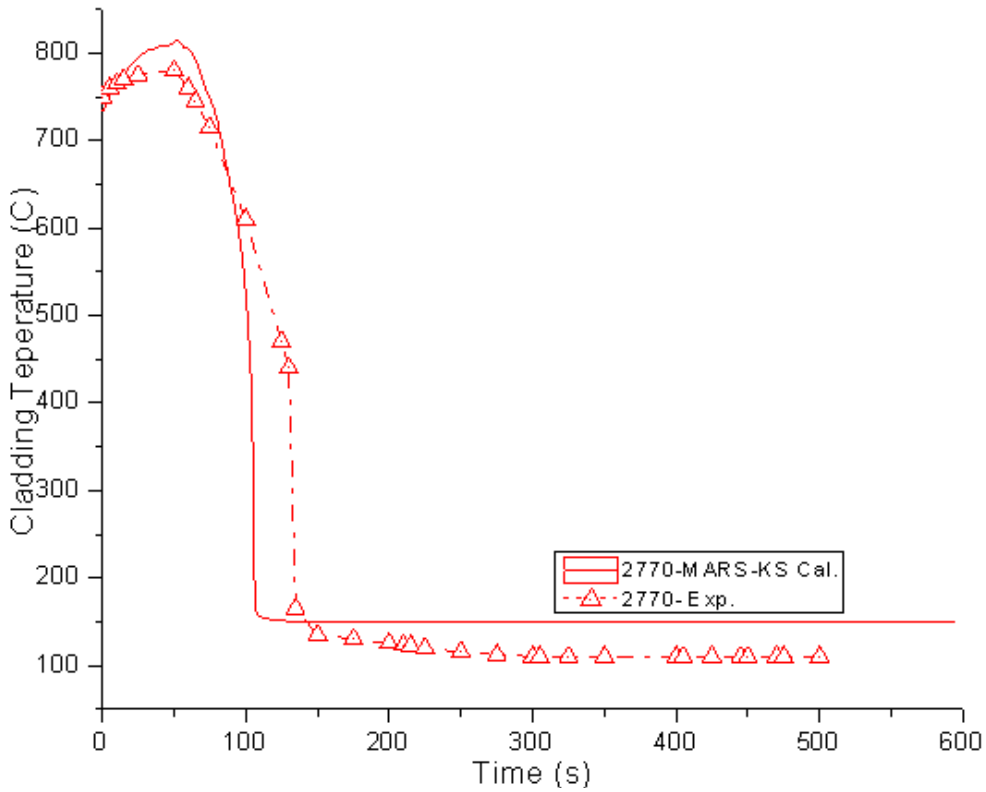

Fig B.10.8 Comparison of calculated cladding temperature with 12a2 exp. data

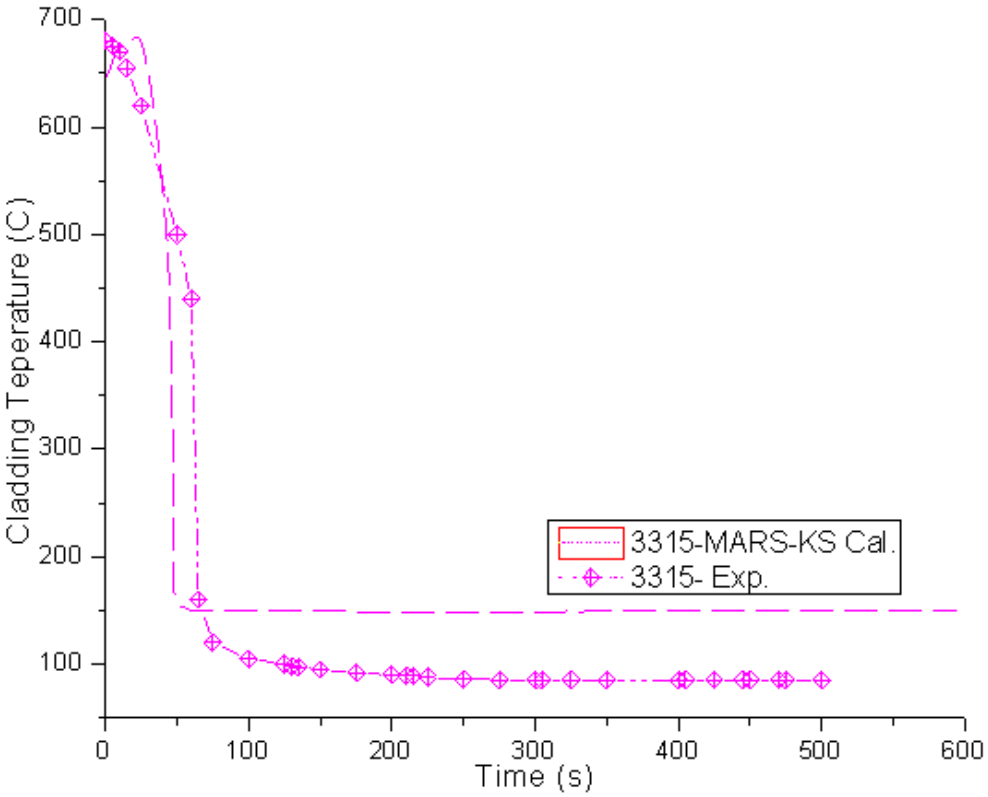

Fig B.10.9 Comparison of calculated cladding temperature with 12a3 exp. data

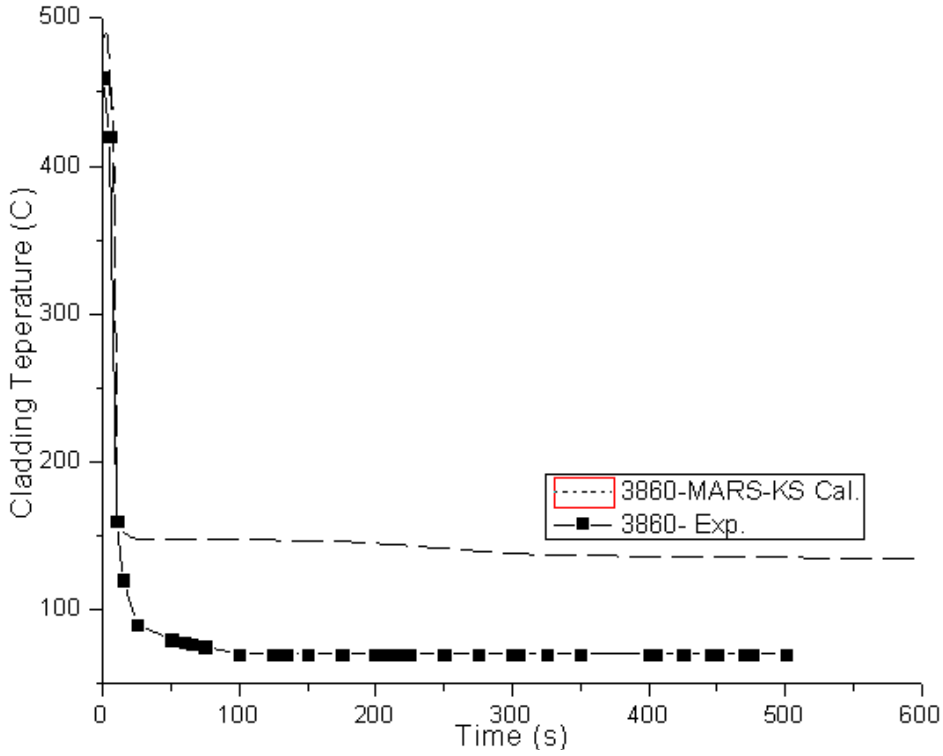

Fig B.10.10 Comparison of calculated cladding temperature with 12a4 exp. data

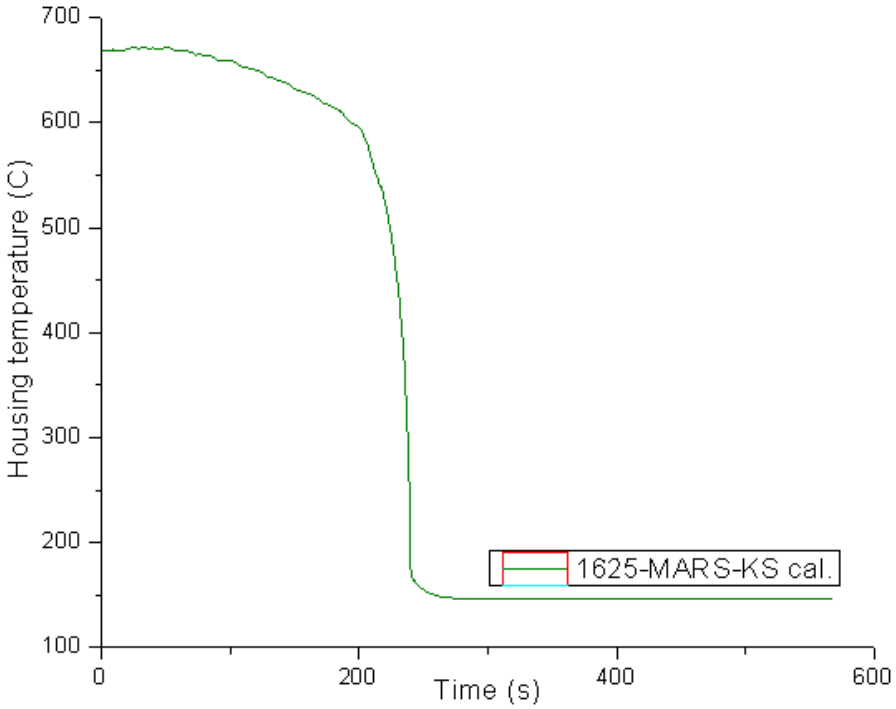

Fig B.10.11 Calculated housing temperature at elevation of 1625mm

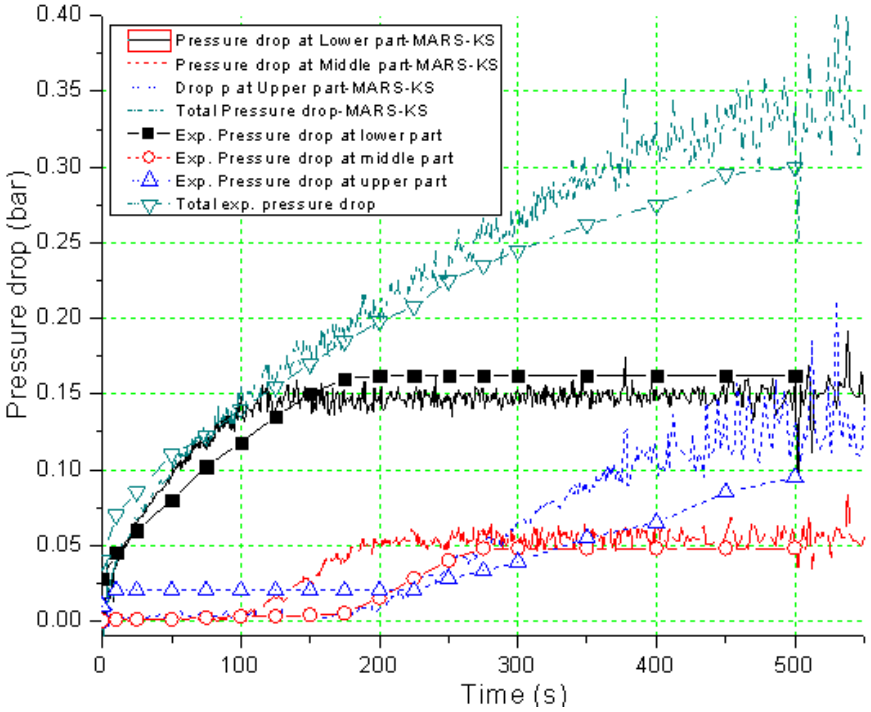

Fig B.10.12 Cal. Pressure drop at lower, middle and upper parts in comparison with exp. data

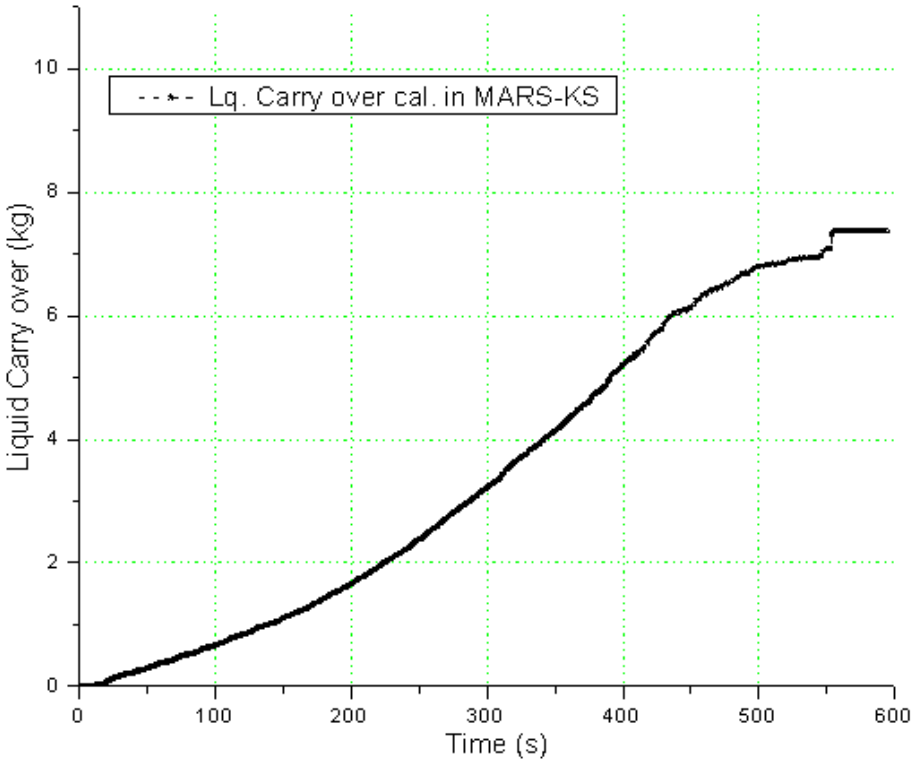

Fig B.10.13 The entrained liquid carry over calculated by MARS-KS (COBRA-TF module)

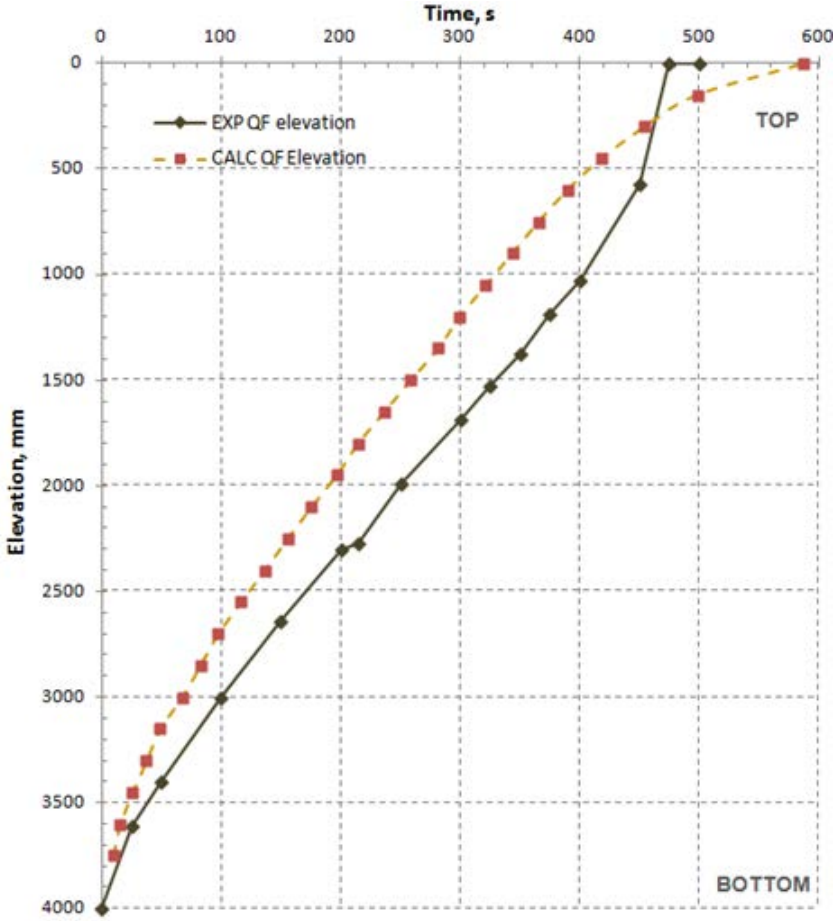

Fig B.10.14 Comparison of quenching front elevation versus time

PCT and bundle quench time

Tab B.10.4 Base case PCT and bundle quench

Institution name	PCT (°C)	Position (mm)	Bundle quench (s)
KAERI	921.3	1500	587.5

Criteria for selection of influential input parameters

Two criteria have been chosen to get the influential parameters for MARS-KS1.3 (COBRA-TF Module). Assuming the effect of time step size or nodalization will be less than 10 deg-C, the PCT criteria has been chosen as 10 deg-C. The criteria of rewetting time has been chosen as 10 second which is a typical transition time from minimum temperature to saturation time.

- Criterion #1: The absolute value of variation in rod surface temperature Tclad, ΔT_{ref} = 10 deg-C at elevation 1500 mm
- Criterion #2: The variation in rewet time trew Δt_{rew} =10 second at elevation 1500 mm

Selection of parameters

Initial list of parameters

The listed initial parameters in the Table B.10.5 are the potential input parameters having the influence to the reflood-related phenomena.

Tab B.10.5 Parameters with potential influence of MARS-KS 1.3 (COBRA-TF Module)

#	ID	Input Basic Parameter (IBP)
1	IP23	Feed water temperature
2	IP24	Flooding Velocity
3	IP25	Pressure
4	IP26	Conductivity of MgO
5	IP27	Heat capacity of MgO
6	IP28	Decay power (Heater Power)
7	IP29	Spacer Grid Blockage Ratio
#	ID	Input Global Parameter (IGP)
1	IP1	Liquid turbulent HT correlation
2	IP2	Liquid laminar HT correlation
3	IP3	Chen nuclear boiling correlation
4	IP4	T_{CHF} (depends on Q_{NB}&Q_{CHF}) of Biasi, Zuber CHF correlation
5	IP6	T_{min} (Boerrenson coefficient correlation)
6	IP7	Modified Bromley correlation
7	IP8	Grid heat transfer enhancement
8	IP9	Vapour turbulent heat transfer
9	IP10	Vapour FLETCH SEASET correlation
10	IP11	Droplet two phase enhancement
11	IP12	Drag coefficient Cd for bubbly flow
12	IP13	Droplet friction factor (Cd of small and large drops)
13	IP15	Interfacial HT model coefficient for subcooled liquid of bubbly flow
14	IP16	Critical We number of bubbly flow in interfacial area of bubble model
15	IP17	Interfacial HT model for supper heated vapour of inverted annulus flow regime
16	IP18	Interfacial HT model for subcooled liquid of inverted annulus flow regime
17	IP19	Interfacial surface area of inverted annulus flow regime
18	IP20	Hot wall flow regime criteria
19	IP22	Interfacial HT model of Droplet
#	ID	Input Coefficient Parameter (ICP)
1	IP5	Drop evaporation efficiency of transition boiling heat transfer
2	IP14	Droplet breakup efficiency

Final list of Influential Parameters

In order to perform the sensitivity analysis, the reference case has been chosen at the elevation of 1500 mm in which PCT occurred (using the same reference value of 0.0 mm on the top of housing). The values of PCT and quenching time of the reference elevation are 921.3 degree Celsius and 281.4 second respectively. Sensitivity analyses were performed using the minimum /maximum values of initial list of 29 parameters. The variations of PCT and quenching time from reference case have been plotted as Figures B.10.15 and 16.

According to sensitivity analysis and criteria 1 and 2 (related to PCT and rewet time), the final list of selected parameters for further analysis are determined as Table B.10.6.

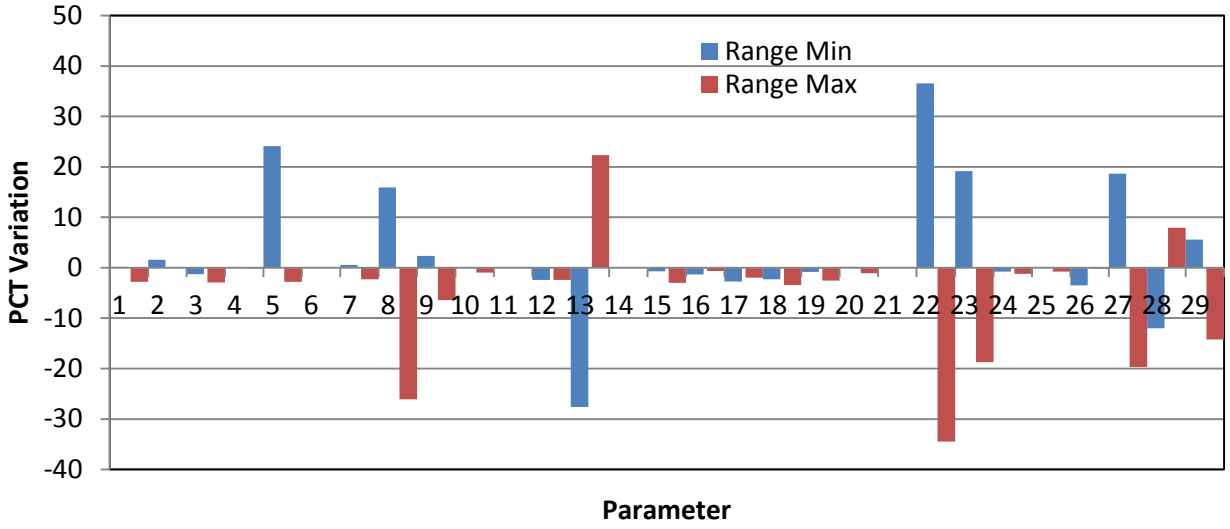

Fig B.10.15 PCT sensitivity results at 1500 mm elevation for 29 parameter analysis

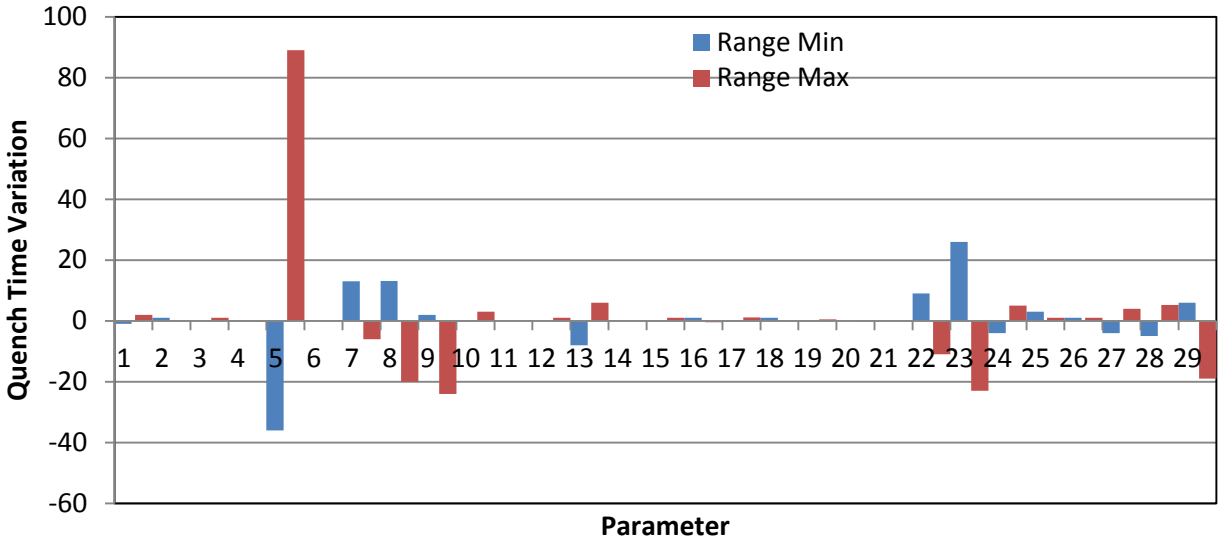

Fig B.10.16 Quench time sensitivity results at 1500 mm elevation for 29 parameter analysis

Tab B.10.6 The selected parameters for further analysis in MARS-KS 1.3 (COBRA-TF Module)

No(ID1[1)]/ID2[2)])	Parameter	Sub-routine	Variable	Multiplier REF /REF value		Multiplier		T_{clad} variation [°C]	t_{rew} variation [s]	Position [mm]
						Min	Max			
1(ICP1/IP5)	Drop evaporation efficiency of transition boiling heat transfer	hcool	Exponent term of effn	IP5	1.0	0.5	1.5[3)]	+24.1/-2.8	+89.0/-36.0	1500
2 (IGP6/IP7)	Modified Bromley Correlations	hcool	hfb	IP7	1.0	0.75	1.25	+0.6/-2.3	+13.0/-6.0	1500
3 (IGP7/IP8)	Grid Heat Transfer enhancement	boiling	spvmg	IP8	1.0	0.5	2.0	+16/-26	+13.0/-20.0	1500
4 (IGP8/IP9)	Vapour Turbulent HT Correlation	boiling	Constant value (0.023D0) of variable spvn	IP9	1.0	0.9	1.1	+2.3/-6.5	+2.0/-24.0	1500
5 (IGP12/IP13)	Droplet friction factor	intfr	cds,cdd	IP13	1.0	0.5	2.0	+22.3/-27.6	+6.0/-8.0	1500
6 (IGP19/IP22)	Interfacial HT model of Droplet	intfr	hascld	IP22	1.0	0.5	2.0	+36.5/-34.5	+9.0/-11.0	1500
7 (IBP2/IP24)	Flooding velocity			IP23	1.0	0.9	1.1	+19.2/-18.8	+26.0/-23.0	1500
8 (IBP5/IP27)	Heat capacity (MgO)			IP27	1.0	0.9	1.1	+1.7/-19.7	+4/-4	1500
9 (IBP6/IP28)	Heater Power			IP28	1.0	0.98	1.02	-12.0/+7.9	-5.0/5.3	1500
10 (IBP7/IP29)	Spacer grid blockage ratio			IP29	1.0	0.5	2.0	5.6/-14.2	6.0/-19.0	1500

1) ID1 : identification number according to input category of table 3
2) ID2: serial number of parameter for sensitivity analysis input of MARS
3) maximum value for parameter is considered as 2.0 , but it has been chosen as 1.5 because of the unexpected calculation error

Wall-to-fluid heat transfer model

The heat transfer package consists of a library of heat transfer correlations and a selection logic algorithm. Together these produce a continuous boiling curve that is used to determine the phasic heat fluxes. To define the boiling curve, it is necessary to know the surface temperature at which CHF occurs. An iterative procedure is used to find the wall temperature at which the heat flux from the Chen nucleate boiling correlation is equal to the critical heat flux. The transition boiling regime is bounded by the CHF point (below which the wall is continuously wetted and nucleate boiling exists) and the minimum stable film boiling point (above which the liquid cannot wet the wall and film boiling exists).

The minimum film boiling temperature is specified as the larger of either Equation or that given by Henry's modification of the Berenson correlation. Since there is no consensus on a correlation to use for the transition boiling region, it is assumed that the transition boiling is composed of both liquid contact (wet wall) and film boiling (dry wall) heat transfer, as follows:

$$q''_{TB} = q''_{WET} + q''_{FB}$$

The wet heat transfer is based on the drop deposition model of Ganic and Hanratty:

$$q''_{WET} = S''_{DE} h_{fg} \eta$$

Where S''_{DE} = drop migration rate towards wall and drop evaporation efficiency, η, is approximated by

$$\eta = \exp\left[1 - \left(\frac{T_W}{T_f}\right)^2\right]$$

Heat transfer in the film boiling region is assumed to result from one of two mechanisms: Dispersed flow film boiling (DFFB) or inverted annular film boiling (IAFB). Dispersed flow film boiling is selected if the void fraction is greater than 0.8. It is treated by a "two step" method where the dominant heat transfer mode is forced convection to superheated steam. The steam superheat is then determined by the interfacial heat transfer rate to the entrained droplets as part of the hydrodynamic solution. Heat flux due to wall-droplet radiation and droplet impingement is superimposed upon the vapour convective heat flux. The total heat flux is:

$$q''_{DFFB} = q''_{FCB} + q''_{R} + q''_{W-D}$$

where q''_{FCB} = vapour convective heat transfer
q''_{R} = wall-drop radiation heat flux
q''_{W-D} = drop impingement heat flux

Heat transfer due to droplets striking the wall is evaluated using the Forslund-Rohsenow equation. The radiative heat transfer is calculated using the model developed by Sun, Gonzalez and Tien et al. When the void fraction is less than 0.6, inverted annular film boiling is assumed to occur. The heat flux for this regime is computed from the larger of either, or the value calculated for dispersed flow film boiling, or the value from the modified Bromley correlation.

$$q''_{IAFB} = q''_{BROM} + q''_{R} + q''_{W-D}$$

At intermediate void fractions ($0.9 > \alpha > 0.4$), the heat flux is interpolated between the values for inverted annular and dispersed flow film boiling.

The spacer grid heat transfer model originally developed for BART code has been adapted for COBRA-TF. Three spacer grid heat transfer model has been included; Convective enhancement, grid rewet and droplet breakup. The convective enhancement correlation of local Nusselt numbers at and downstream of grids is expressed by Yao and Hochreiter.

$$\frac{Nu_x}{Nu_o} = 1 + 5.55\, a_r^2 \exp\left(-0.13 \frac{x}{D_H}\right)$$

COBRA-TF use a simple two-region model as a complicated grid rewet model. The heat balance is used to determine the transient temperature response of the two regions. The small drop field was added to calculate the evaporation rate of the shattered drop fragment. The mass source of shattered droplets generated by droplet breakup is expressed of the entrainment drop flow rate and the grid blockage area.

$$\dot{m}_{DB} = \eta_e \left(\frac{A_G}{A_c}\right) (\dot{m}_e + \dot{m}_{SD})$$

where $\dot{m}_{DB}$ = droplet break-up rate
$\dot{m}_e$ = entrainment flow rate
$\dot{m}_{SD}$ = small drop flow rate

During quenching, the entire boiling curve—from film boiling through transition boiling and critical heat flux to nucleate boiling—can be encompassed by one hydrodynamic mesh cell. A fine mesh-rezoning technique is employed in the COBRATF module to surmount these difficulties. Fine mesh heat transfer cells with axial and radial conduction are superimposed upon the coarse hydrodynamic mesh spacing, and a boiling heat transfer package is applied to each node.

Conclusions

The important parameters were selected by subjective criteria and sensitivity results. The sensitivity results are also based on the subjective decision of uncertainty range of input parameter. The most important parameter such as gap conductance and Zircaloy metal-water reactions were not considered since the FEBA experiment with stainless steel clad and electric heaters will be used in phase-III works. The uncertainty of decay power model, which is usually known as more than ±6%, has been treated as only ±2% uncertainty of electric power measurement. The COBRA-TF spacer grid models are so complicated that the overall grid effects have been considered as a blockage ratio which can be handled by input parameter.

Although the selected parameters are not sufficient to quantify reflood uncertainty for the plant application, the parameters listed in table 4 can be used for experimental facility. The following parameters in table 5 are selected as a final parameter list for the phase-III work.

1) Drop evaporation efficiency of transition boiling heat transfer (Transition Boiling Heat Transfer)
2) Modified Bromley Correlations (Film Boiling Heat Transfer)
3) Grid Heat Transfer enhancement (Convective Heat Transfer Enhancement of Grid)
4) Vapour Turbulent HT Correlation (Droplet Enhancement of Vapour Heat Transfer)
5) Droplet friction factor (Interfacial Friction of DFFB)
6) Interfacial HT model of Droplet(Interfacial Heat Transfer of DFFB)
7) Flooding velocity
8) Heat capacity (MgO)
9) Heater Power
10) Spacer grid blockage ratio

B.11. KINS (Rep. of Korea) results

Model description

The latest version of MARS code (MARS-KS-003) is used, which has the different reflood model compared to the previous version. Also, it has modified only for PREMIUM purpose to handle the input multipliers.

Tab B.11.1 KINS code and software platform

Institution name	Code version	Software platform
KINS	MARS-KS-003, PREMIUM version	PC 2.93GHz, Windows 7

Nodalization and basic geometrical properties

- Nodalization

  The figure below shows the MARS nodalization for FEBA test facility. The heated part is modelled by the pipe component with 39 sub volumes. The rod bundle is simulated as a heat structure with 39 axial nodes and 8 radial mesh points for bundle.

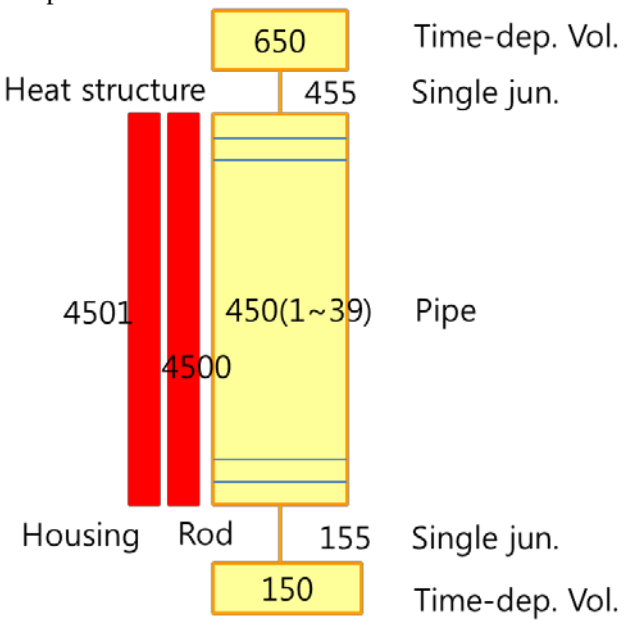

Fig B.11.1 FEBA nodalization

- Total height/length (including heated part and unheated part if modelled); 3.9 m (heated part)
- Heated part flow area, hydraulic diameter, wall roughness (or analogue for distributed friction calculation);

Tab B.11.2 MARS-KS model volume properties

Vol. No	Flow area (m^2)	Hydraulic diameter (m)	Wall roughness (m)
450-1 (bottom)	3.893E-3	1.3444E-02	1.0000E-05
2	3.893E-3	1.3444E-02	1.0000E-05
3	3.893E-3	1.3444E-02	1.0000E-05
4	3.893E-3	9.3170E-03	1.0000E-05
5	3.893E-3	1.3444E-02	1.0000E-05
6	3.893E-3	1.3444E-02	1.0000E-05
7	3.893E-3	1.3444E-02	1.0000E-05
8	3.893E-3	1.3444E-02	1.0000E-05
9	3.893E-3	9.3170E-03	1.0000E-05
10	3.893E-3	1.3444E-02	1.0000E-05
11	3.893E-3	1.3444E-02	1.0000E-05
12	3.893E-3	1.3444E-02	1.0000E-05
13	3.893E-3	1.3444E-02	1.0000E-05
14	3.893E-3	1.3444E-02	1.0000E-05
15	3.893E-3	9.3170E-03	1.0000E-05
16	3.893E-3	1.3444E-02	1.0000E-05
17	3.893E-3	1.3444E-02	1.0000E-05
18	3.893E-3	1.3444E-02	1.0000E-05
19	3.893E-3	1.3444E-02	1.0000E-05
20	3.893E-3	9.3170E-03	1.0000E-05
21	3.893E-3	1.3444E-02	1.0000E-05
22	3.893E-3	1.3444E-02	1.0000E-05
23	3.893E-3	1.3444E-02	1.0000E-05
24	3.893E-3	1.3444E-02	1.0000E-05
25	3.893E-3	9.3170E-03	1.0000E-05
26	3.893E-3	1.3444E-02	1.0000E-05
27	3.893E-3	1.3444E-02	1.0000E-05
28	3.893E-3	1.3444E-02	1.0000E-05
29	3.893E-3	1.3444E-02	1.0000E-05
30	3.893E-3	1.3444E-02	1.0000E-05
31	3.893E-3	9.3170E-03	1.0000E-05
32	3.893E-3	1.3444E-02	1.0000E-05
33	3.893E-3	1.3444E-02	1.0000E-05
34	3.893E-3	1.3444E-02	1.0000E-05
35	3.893E-3	1.3444E-02	1.0000E-05
36	3.893E-3	9.3170E-03	1.0000E-05
37	3.893E-3	1.3444E-02	1.0000E-05
38	3.893E-3	1.3444E-02	1.0000E-05
39 (top)	3.893E-3	1.3444E-02	1.0000E-05

- Flow area, hydraulic diameter and energy/pressure loss coefficients at the position of the spacer grids;

Tab B.11.3 MARS-KS model junction properties

Junction. No	Junction area (m^2)	Junction diameter (m)	Loss coefficient
450-1 (bot)	3.893E-3	1.3444E-02	0.0
2	3.893E-3	1.3444E-02	0.0
3	2.920E-3	9.3170E-03	1.14E+00
4	3.893E-3	1.3444E-02	0.0
5	3.893E-3	1.3444E-02	0.0
6	3.893E-3	1.3444E-02	0.0
7	3.893E-3	1.3444E-02	0.0
8	3.893E-3	1.3444E-02	0.0
9	2.920E-3	9.3170E-03	1.14E+00
10	3.893E-3	1.3444E-02	0.0
11	3.893E-3	1.3444E-02	0.0
12	3.893E-3	1.3444E-02	0.0
13	3.893E-3	1.3444E-02	0.0
14	2.920E-3	9.3170E-03	1.14E+00
15	3.893E-3	1.3444E-02	0.0
16	3.893E-3	1.3444E-02	0.0
17	3.893E-3	1.3444E-02	0.0
18	3.893E-3	1.3444E-02	0.0
19	3.893E-3	1.3444E-02	0.0
20	2.920E-3	9.3170E-03	1.14E+00
21	3.893E-3	1.3444E-02	0.0
22	3.893E-3	1.3444E-02	0.0
23	3.893E-3	1.3444E-02	0.0
24	3.893E-3	1.3444E-02	0.0
25	2.920E-3	9.3170E-03	1.14E+00
26	3.893E-3	1.3444E-02	0.0
27	3.893E-3	1.3444E-02	0.0
28	3.893E-3	1.3444E-02	0.0
29	3.893E-3	9.3170E-03	0.0
30	2.920E-3	9.3170E-03	1.14E+00
31	3.893E-3	1.3444E-02	0.0
32	3.893E-3	1.3444E-02	0.0
33	3.893E-3	1.3444E-02	0.0
34	3.893E-3	1.3444E-02	0.0
35	3.893E-3	9.3170E-03	0.0
36	2.920E-3	9.3170E-03	1.14E+00
37	3.893E-3	1.3444E-02	0.0
38 (top)	3.893E-3	1.3444E-02	0.0

- Total heat transfer area of the heater rods; 3.2928 m^2 (=2πx(10.75/2/1000)x3.9x25)

- Maximum linear heat rate; 23.8 W/cm

Boundary and initial conditions

The following boundary and initial conditions are assumed in the calculation.

- Pressure: 410 kPa
- Flooding temperature:

Tab B.11.4 Flooding temperature

Time(sec)	Temp.(K)
0	333.
20	318.
50	315.
100	313.
900	310.

- Flooding velocity or mass flow rate: 3.8 cm/s
- Power: 195 kW
- Heat losses: No heat losses are assumed

Adopted models (flags)

The rod bundle interphase friction model will be applied in the hydraulic nodes of the heated part.

The radiation has not been taken into account in this calculation.

Assumptions and steady-state achievement

The initializing state was achieved when the heater surface temperatures reached at the temperature of experiment. The FABA rods are heated with bundle power 40 kW for 700 seconds before transient calculation.

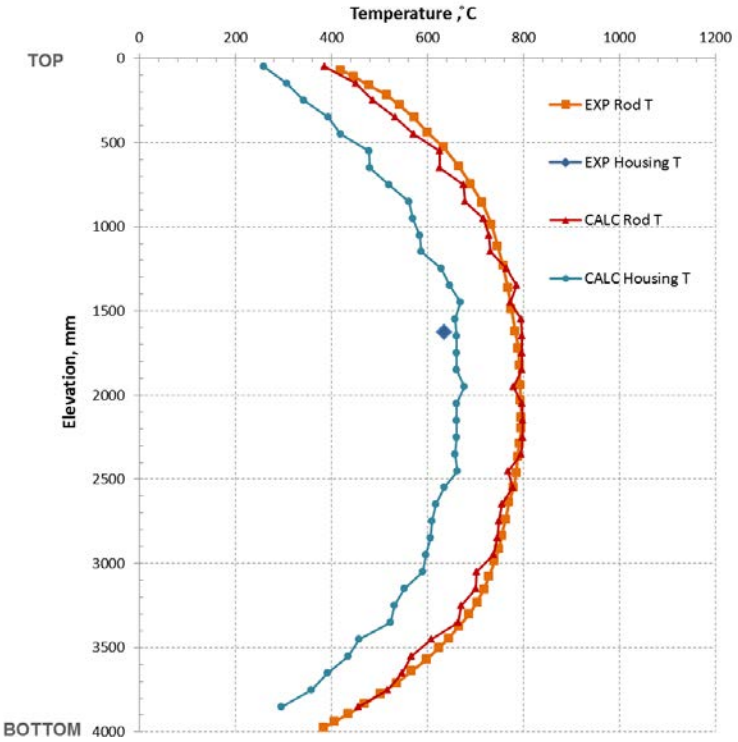

Fig B.11.2 Steady-state temperature profile

Base case results

Figures of all (exp-calc) responses

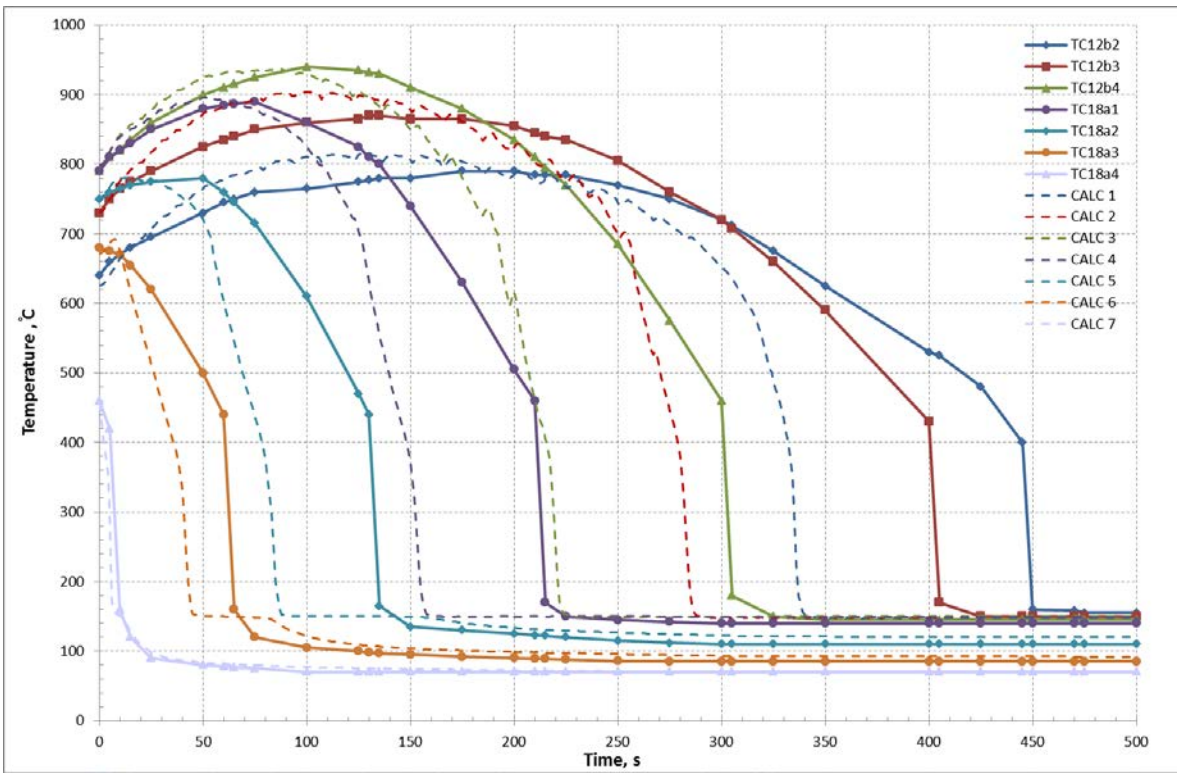

Fig B.11.3 Base case cladding temperatures

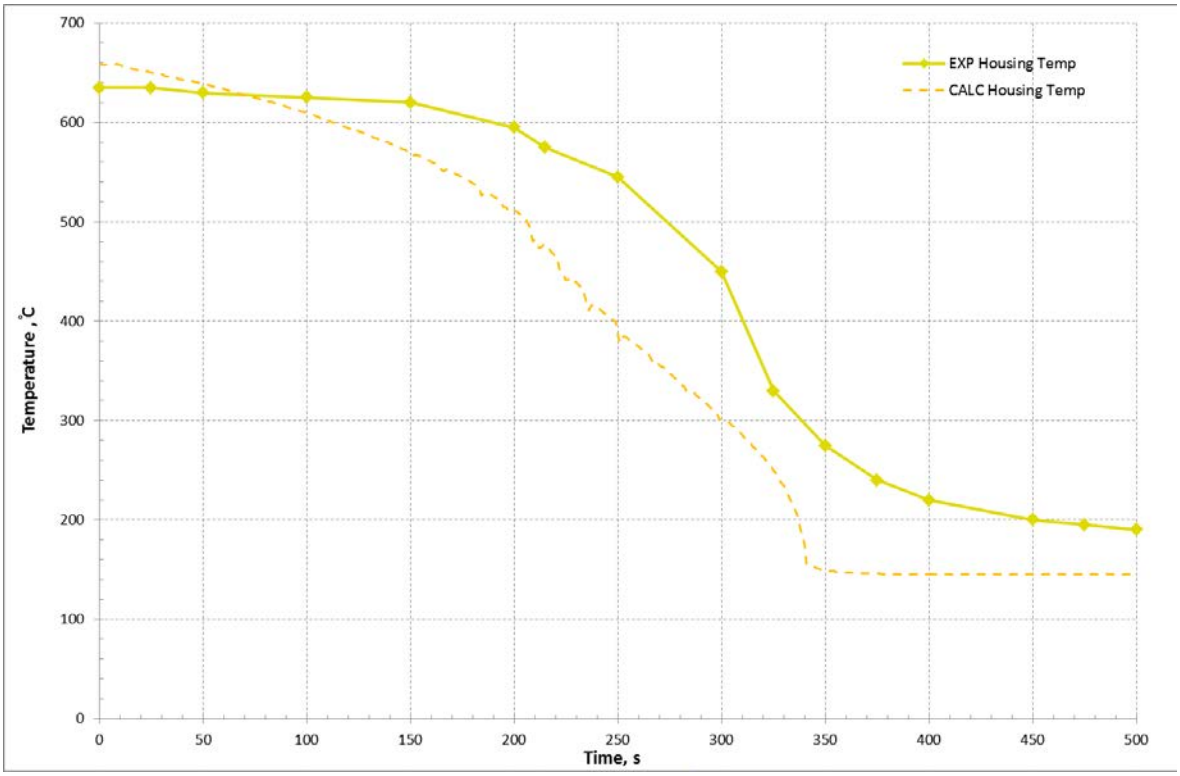

Fig B.11.4 Base case housing temperature

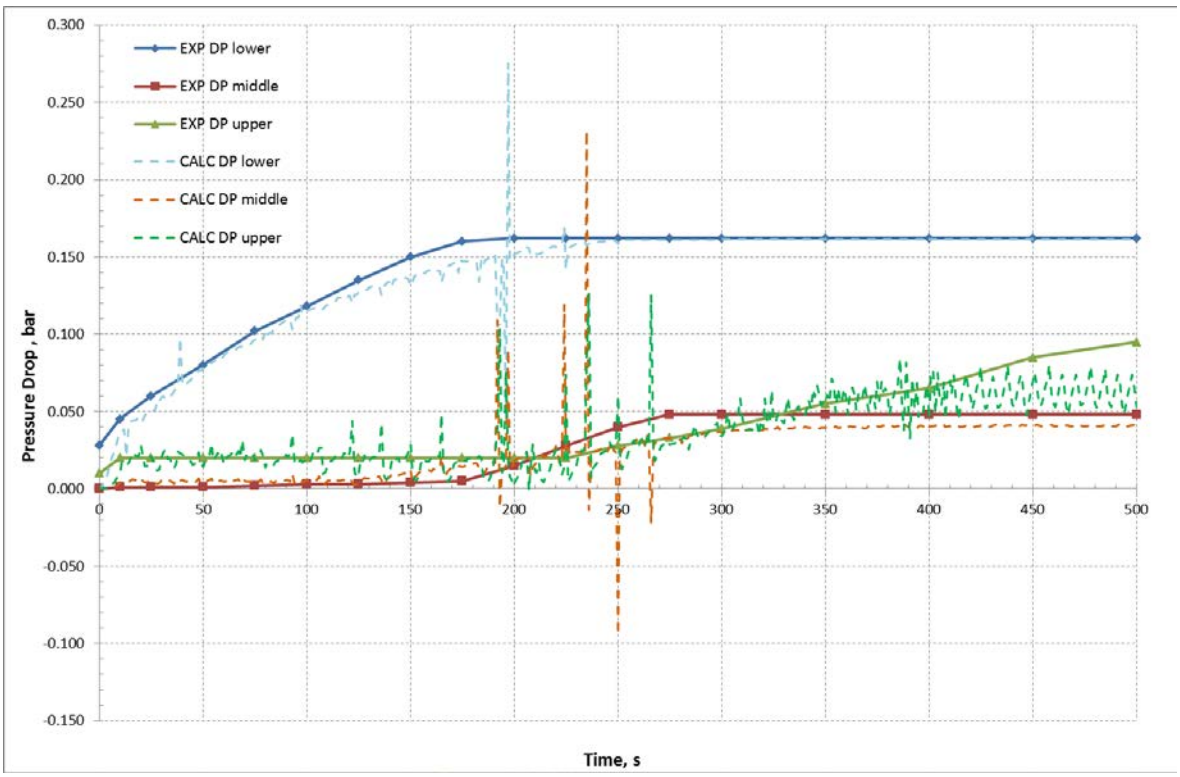

Fig B.11.5 Base case pressure drops

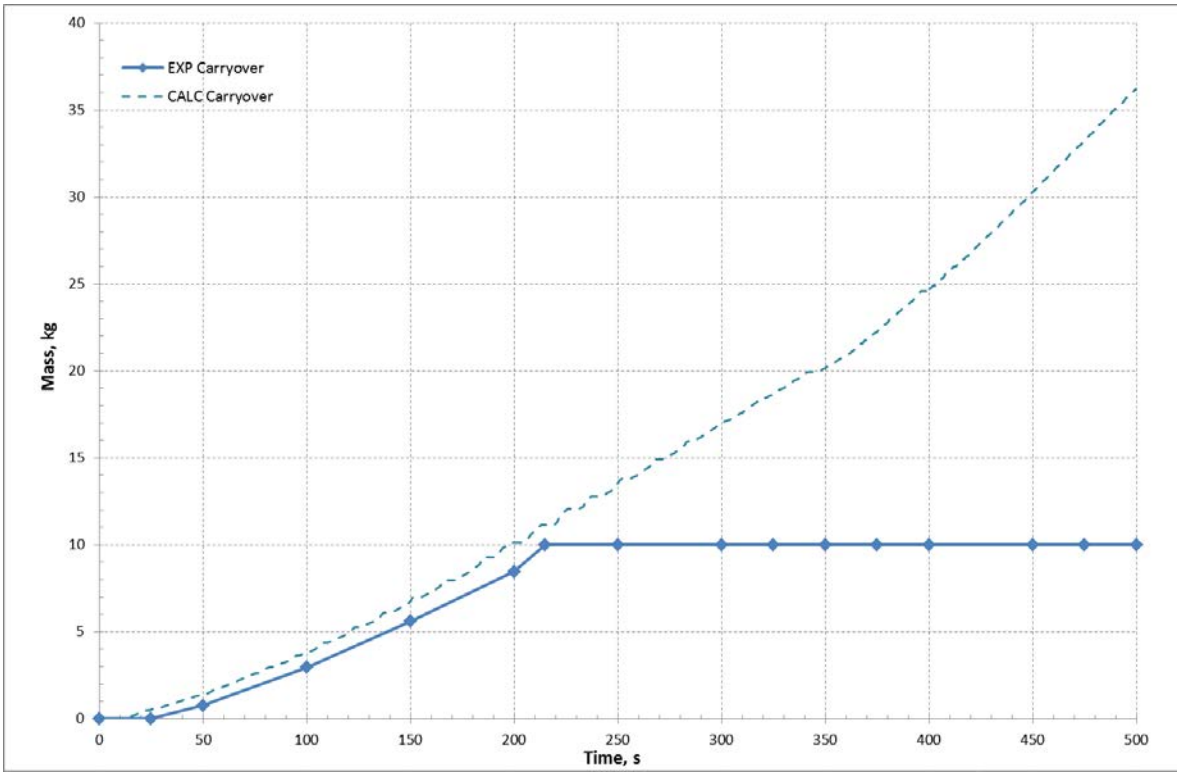

Fig B.11.6 Base case liquid carryover

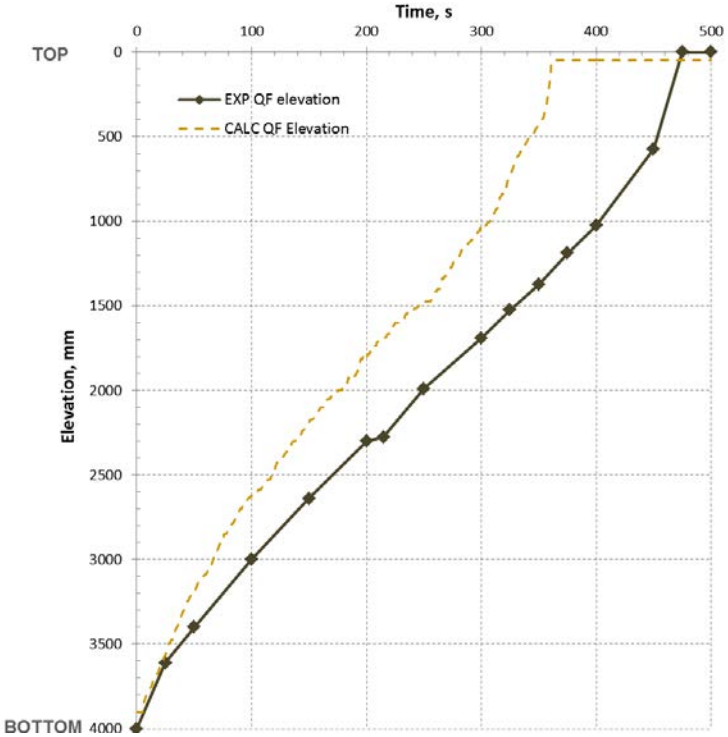

Fig B.11.7 Base case quench front propagation

PCT and bundle quench time

Tab B.11.5 Base case PCT and bundle quench

Institution name	PCT (˚C)	Position (mm)	Bundle quench (s)
KINS	946.1	1425	192

Criteria for selection of influential input parameters

The criteria for selection of influential input parameter were basically determined in accordance with the specifications for Phase II of the PREMIUM benchmark. However, it is not easy to clearly select the rewet time during transients for FEBA experiment. So, the quenching time at the elevation corresponding to maximum rod surface temperature is considered as one of criteria, which is defined as the time when $T_{clad} \leq T_{sat} + 30$ K.

An influential IP should satisfy that either of two reflood response (rod surface temperature or quenching time) shows the following large change at its extreme value in the range of input variation:

- The absolute value of variation in rod surface temperature is ΔT_{ref}= 30K
- The variation in quenching time is Δt_{quench}= 7%

Selection of parameters

Initial list of parameters

Twenty-one input parameters are initially considered as potentially influential for reflood-related phenomena base on Rod Bundle Heat Transfer (RBHT) programme of USNRC.

Tab B.11.6 Initial list of input parameters

Input Basic Parameter	
1	ANS decay model
2	Heater(MgO) thermal conductivity
3	Heater(MgO) heat capacity
4	Cladding(Ni Cr) thermal conductivity
5	Cladding(Ni Cr) heat capacity
Input Global Parameter	
1	Chen nucleate boiling heat transfer coefficient
2	AECL CHF lookup table
3	Pool boiling CHF(Zuber)
4	Modified Weismann correlation
5	Bromley void weighted QF heat transfer
6	Forslund-Rohsenow equation
7	Droplet enhancement factor
8	Interfacial drag for bubbly flow
9	Ishii-Mishama entrainment
10	Interfacial HT of subcooled liquid
11	Interfacial HT of drop-steam
Input Coefficient Parameter	
1	Convection to superheated vapour (turbulent, laminar, natural convection)
2	Weber number
3	Interfacial area of Inverted annular (roughness)
4	Dry/wet wall criteria
5	Transition criteria for void fraction

Final list of Influential Parameters

Tab B.11.7 Final list of influential input parameters

Parameter	Module::Subroutine	Fortran variable / Keyword	Multiplier REF / REF value	Multiplier MIN	Multiplier MAX	T_{clad} variation [°C]	Position [mm]	T_{que} variation [s]	Position [mm]
Convection to superheated vapour (linear interpolation between Reynold number 3000 and 10000)	WallHeatTransfer::SinglePhase	htcoef	1.0/3000.	0.5	1.5	+68.7/-37.2	1425	-	-
Weber number	InterphaseDrag::BubbleDropDrag	web(3)	1.0/4.0	0.5	2.0	-	-	+17/-21	1425
Dry/wet wall criteria ($T_g = T_{sat}$+30°C) for inverted annular flow	InterphaseHTC::GteInterphaseHTC	Constant value(30.0)	1.0/30.	0.5	2.0	+0.32/-31.2	1425	+13/-90	1425
Interfacial heat transfer of drop-steam (TRACE blowing factor)	InterphaseHTC::GteInterphaseHTC	blow_f	1.0	0.5	2.0	+29.4/-44.78	1425	-	-

Wall-to-fluid heat transfer model

The original MARS code (MARS-KS-003) reflood model has been improved. The model proposed by Bajorek and Young is incorporated for the dispersed flow film boiling (DFFB) wall heat transfer. Both space grid and droplet enhancement models are included in this model.

$$h_{cwv} = F_{grid}\, F_{2\phi}[F_{lt}\, h_{lam} + (1 - F_{lt})h_{tur}]$$

where F_{grid} is space grid effect, $F_{2\Phi}$ is droplet enhancement factor, and F_{lt} is a linear function that has a value of 1.0 at Re=3000 and a value of 0.0 at Re=10000.

Inverted annular film boiling (IAFB) is modelled by using the original PSI model, which uses the maximum of a film coefficient and a Forslund-Rohsenow coefficient. The flow transition between the DFFB and IABF, is modelled using the TRACE code interpolation. The assessment calculations were performed for FLECHT-SEASET and RBHT tests.

Conclusions

Twenty-one input parameters are initially considered as potentially influential for reflood-related phenomena, which were derived from the highly ranked parameters based on Rod Bundle Heat Transfer (RBHT) programme Phenomena Identification and Ranking Table (PIRT) of USNRC. The sensitivity analysis shows that four influential parameters are dominant in accordance with the selection criteria. They will be used in the Phase III of PREMIUM.

B.12 OKBM (Russian Federation) results

Model description

Tab B.12.1 OKBM code and software platform

Institution name	Code version	Software platform
Afrikantov OKB Mechanical Engineering (OKBM) Nizhniy Novgorod, Russia	RELAP/SCDAPSIM/MOD3.4	Windows XP

Nodalization and basic geometrical properties

Input model for RELAP code is a simple single-channel model containing (see nodalization diagram in Figure B.12.1):

- inlet time-dependent volume;
- inlet time-dependent junction;
- pipe component (No. 20) simulating the test section, including lower and upper chambers;
- outlet single junction;
- outlet time-dependent volume;
- heat structure simulating all 25 heater rods;
- heat structure simulating bundle shroud (housing).

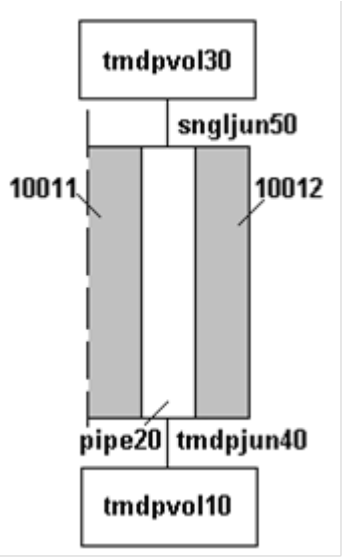

Fig B.12.1 FEBA test section nodalization diagram

Main geometrical parameters of the pipe 20 component:

- Total length 4.165 m
- Heated length 3.900 m
- Lower chamber: flow area 6.162E-3 m2 (area inside square shroud), length 0.14 m
- Upper chamber: flow area 3.893E-3 m2 (same as in the bundle), length 0.125 m
- Rod bundle: flow area 3.893E-3 m2, hydraulic diameter 0.01344 m, wall roughness 1.E-6 m;
- Number of axial nodes 41: 1 for lower chamber, 1 for upper chamber, 39x0.1m equal nodes for heated part
- Flow area and hydraulic diameter at the position of the spacer grids is the same as in the whole bundle, local pressure loss coefficients are 0.6, grids are slightly “shifted” to the nearest junction;
- Outlet single junction: flow area 2.827E-3 m2, hydraulic diameter 0.01 m – simulates upper grid
- Total heat transfer area of the heater rods calculated by the code from the input geometry: 25*Pi*0.01075m*3.9m=3.293 m2; shroud HT area is 4*0.0785m*3.9m=1.2246m2
- Heat structures axial nodalization corresponds to that of the hydraulic channel;
- Heat capacity of the grids neglected;

- Maximum linear heat rate is 2.44 kW/m – corresponds to axial peaking factor of 1.19 and maximum power 200 kW;
- Variation of local power due to dependence of the electrical resistance on temperature is taken into account although it is not strong.

Boundary and initial conditions

The following boundary conditions are applied:

- Outlet pressure – tmdpvol 30
- Flooding water temperature - tmdpvol 10
- Flooding velocity – tmdpjun 40
- Power – internal power source in heater rod heat structure
  - Time histories of the above parameters were digitized from the curves presented in "FEBA desc3" file distributed after kick-off meeting in Paris
- Heat losses not modelled
- Housing heat capacity increased to account for possible energy stored in structural elements (flanges etc.)

Adopted models (flags)

- Bundle interphase friction model has been activated in the hydraulic nodes of the heated part by setting flag b=1.
- "Vertical bundle without cross-flow" heat transfer mode has been set at the boundary of the heat structure representing the heater rods (BC type 110).
- CCFL model is not used, all other models used by default
- Thermal radiation between heater rods and housing is not taken into account

Assumptions and steady-state achievement

To obtain the initial conditions of the FEBA-216 test, code was run in "steady-state" mode at low power (10 kW) and no-flow conditions with experimental values of temperatures input for heater rods. Housing temperature distribution was calculated by the code. Reaching the "steady-state" according to the code internal criteria was considered acceptable, although some increase of rod cladding temperatures in the bundle lower part took place. This approach was used since the available information on the initial steady state was insufficient.

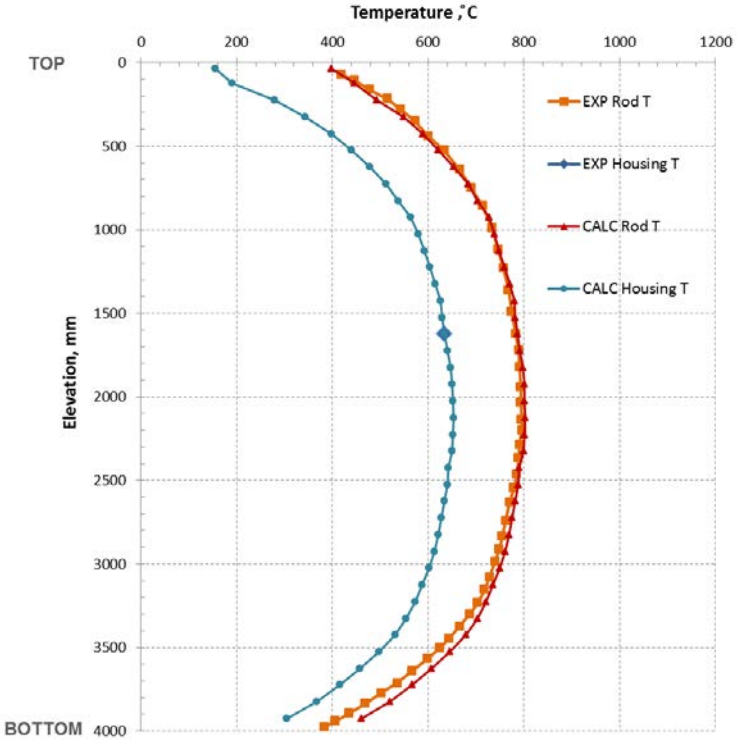

Fig B.12.2 Steady-state temperature profile

Base case results

Figures of all (exp-calc) responses

Comparison of experimental measurements and calculated parameters is presented in figures below. Elevations are used as specified for the experiment, i.e., 0 mm corresponds to the top end of the housing.

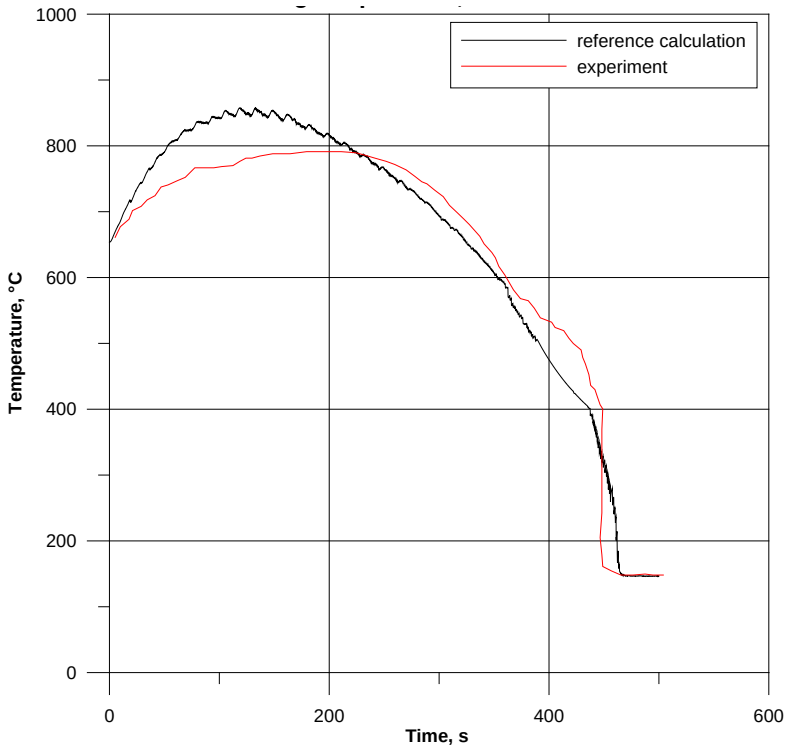

Fig B.12.3 Heater rod surface temperature corresponding to 12b2 experimental measurement

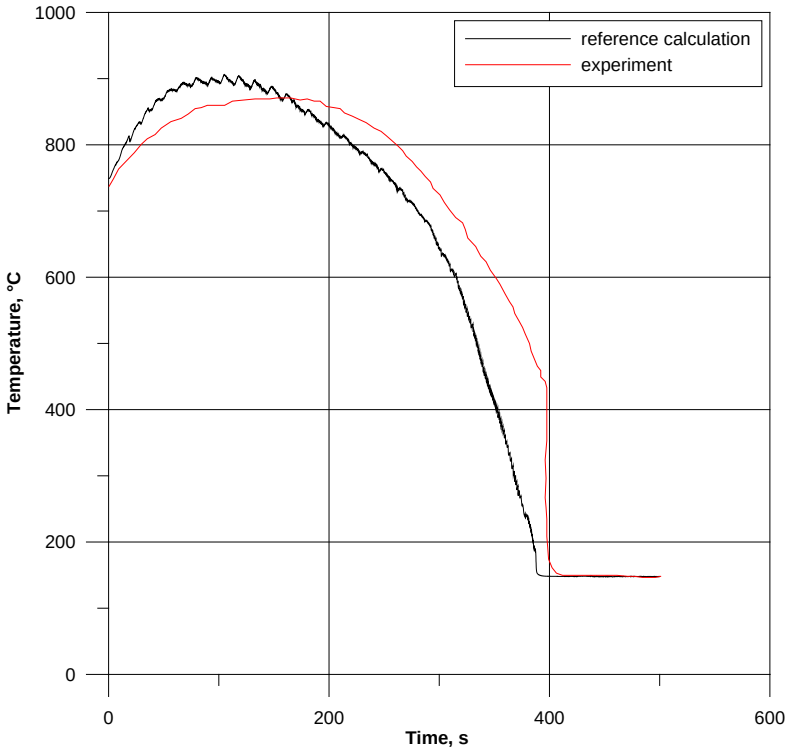

Fig B.12.4 Heater rod surface temperature corresponding to 12b3 experimental measurement

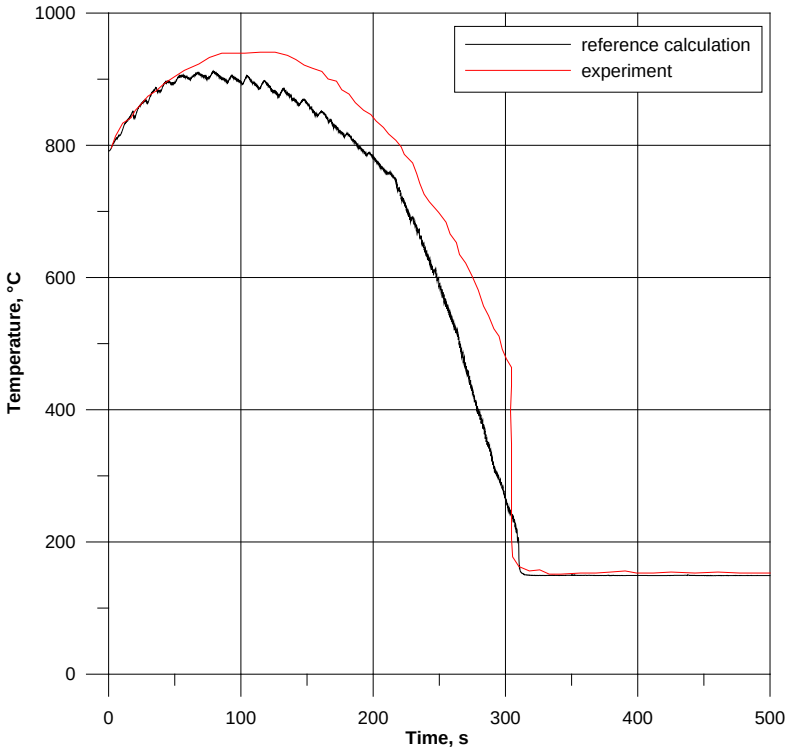

Fig B.12.5 Heater rod surface temperature corresponding to 12b4 experimental measurement

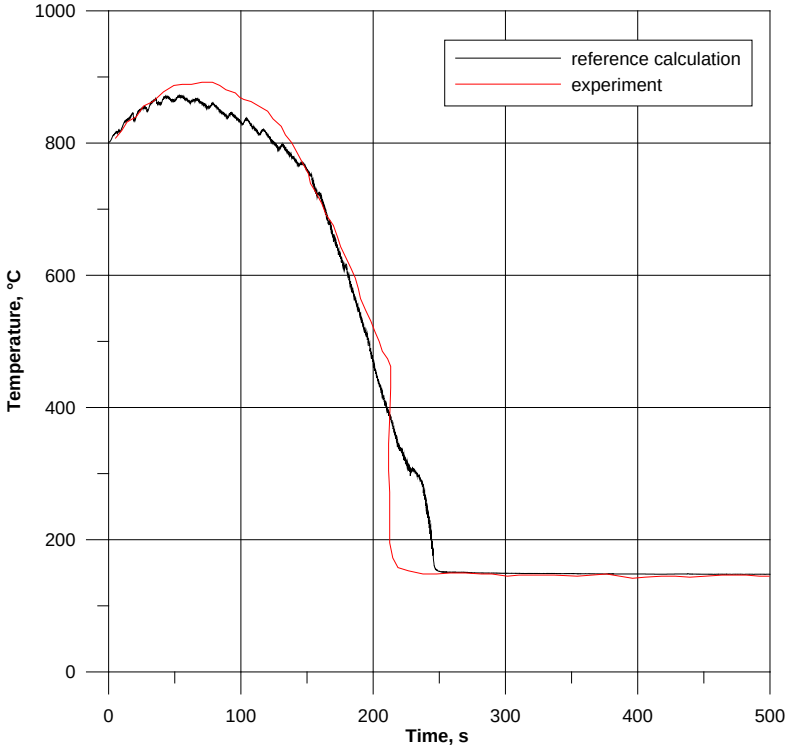

Fig B.12.6 Heater rod surface temperature corresponding to 18a1 experimental measurement

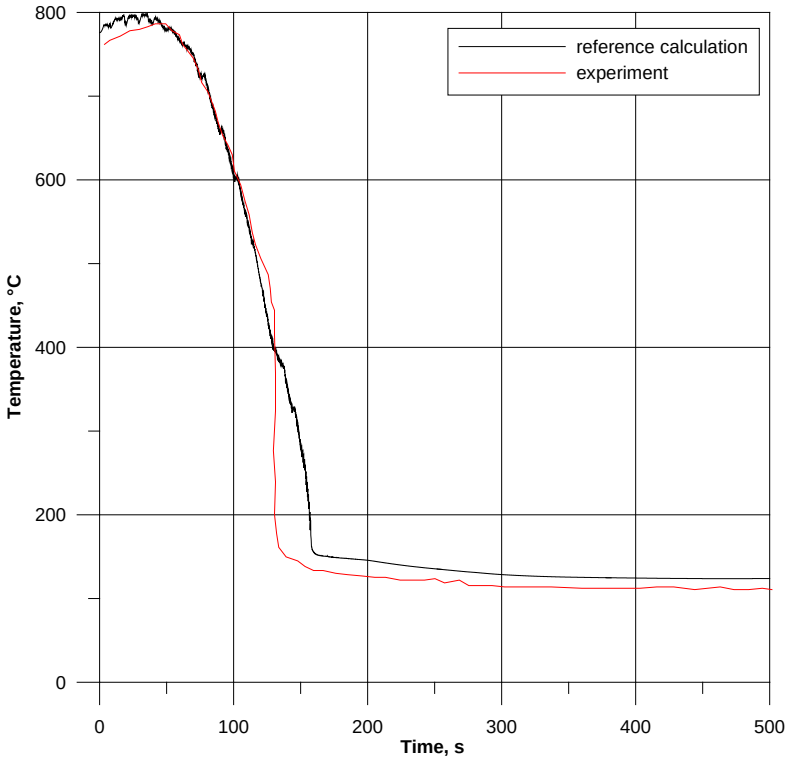

Fig B.12.7 Heater rod surface temperature corresponding to 18a2 experimental measurement

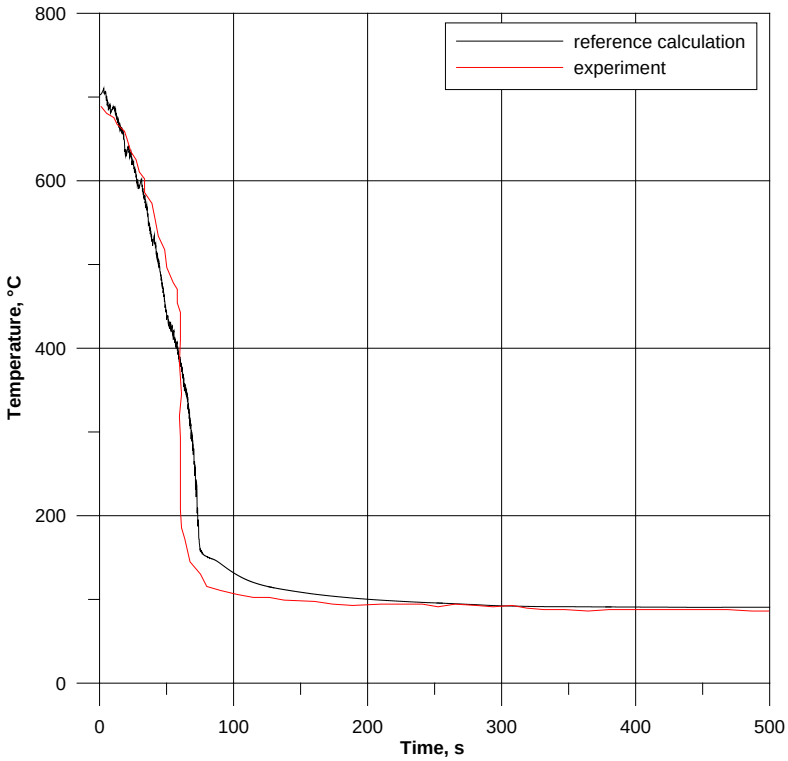

Fig B.12.8 Heater rod surface temperature corresponding to 18a3 experimental measurement

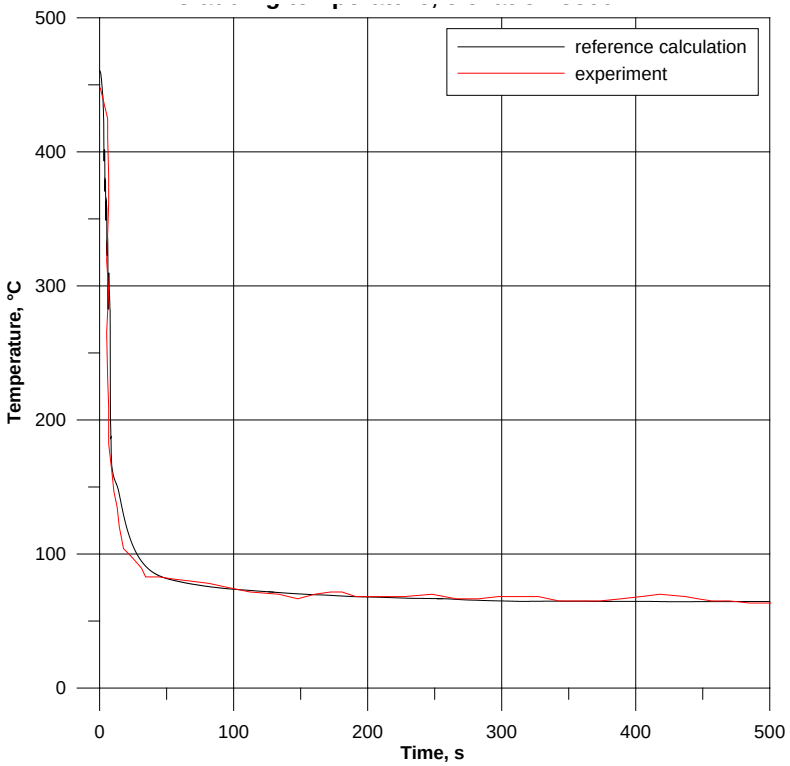

Fig B.12.9 Heater rod surface temperature corresponding to 18a4 experimental measurement

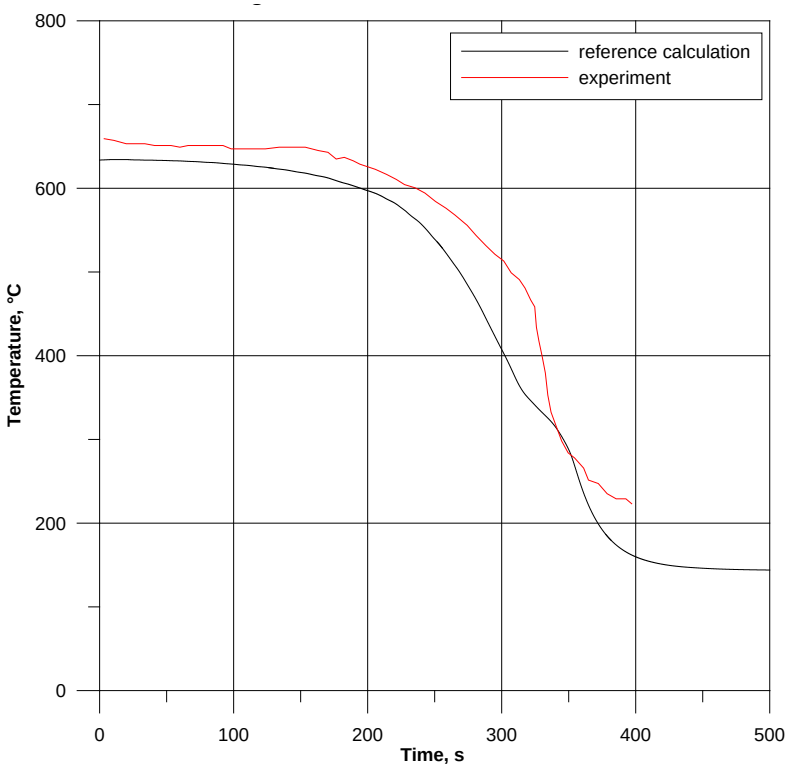

Fig B.12.10 Housing temperature at elevation 1625 mm

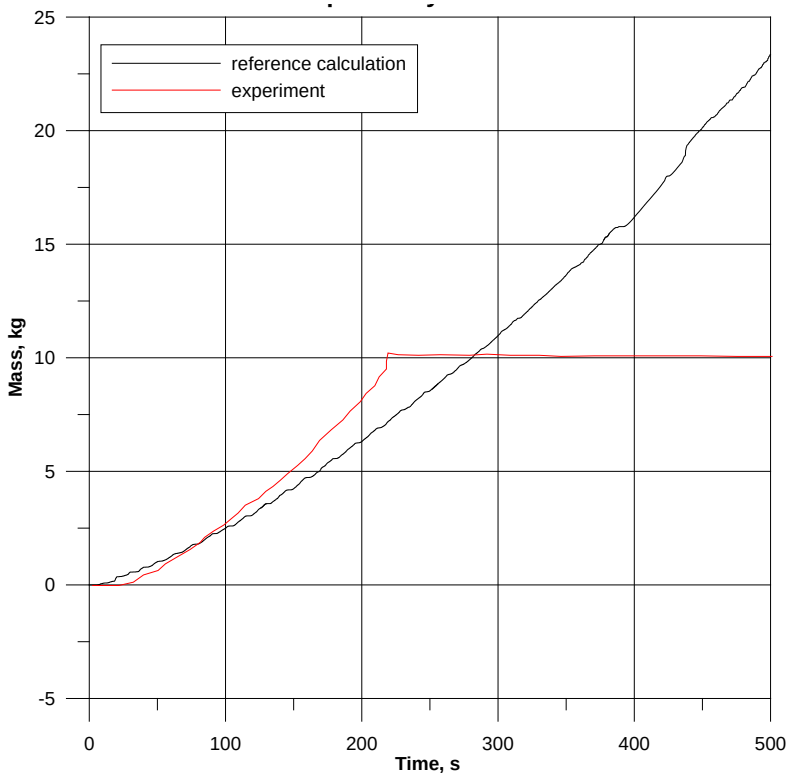

Fig B.12.11 Liquid carryover

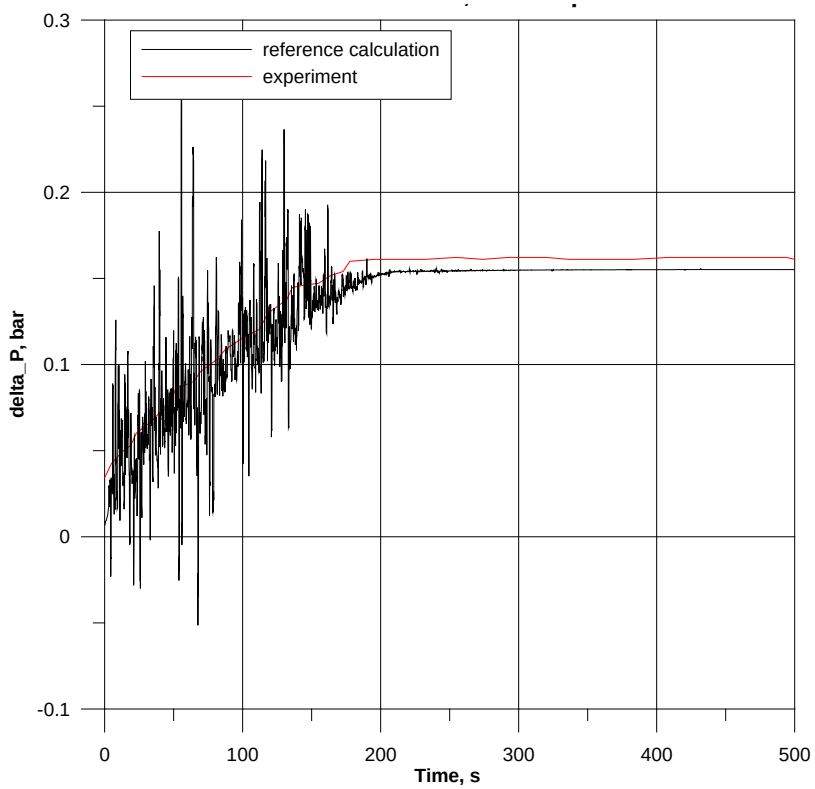

Fig B.12.12 Pressure drop in the bundle lower part

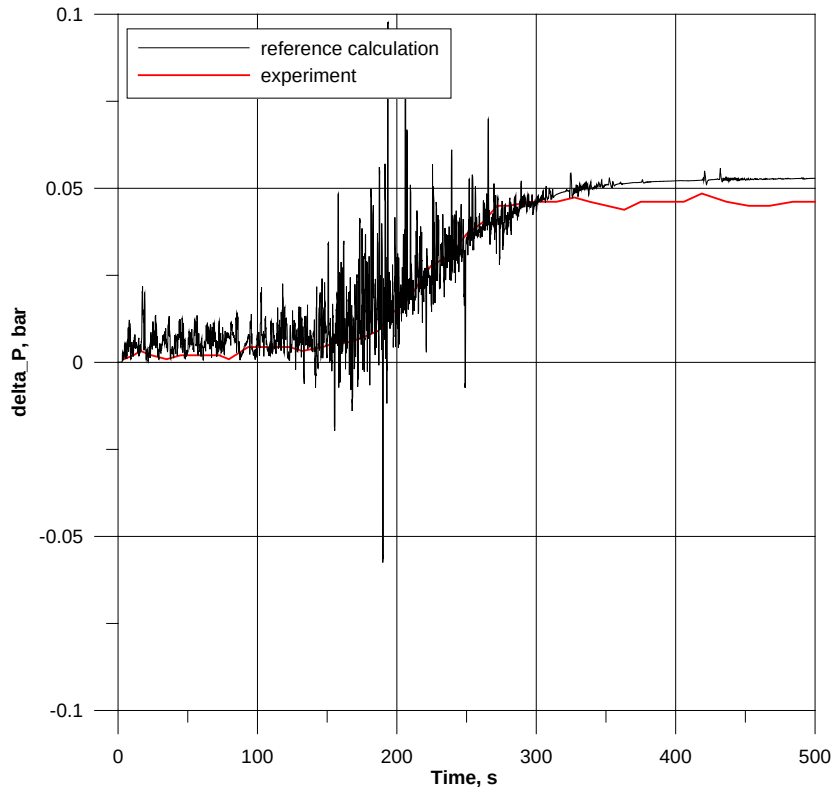

Fig B.12.13 Pressure drop in the bundle middle part

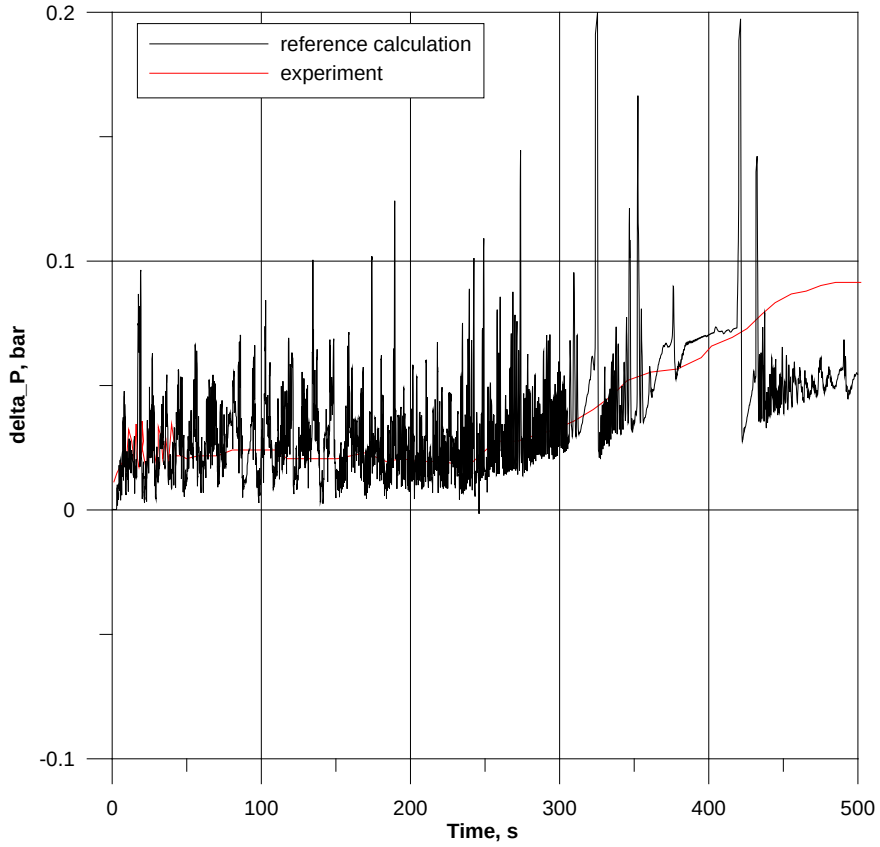

Fig B.12.14 Pressure drop in the bundle top part

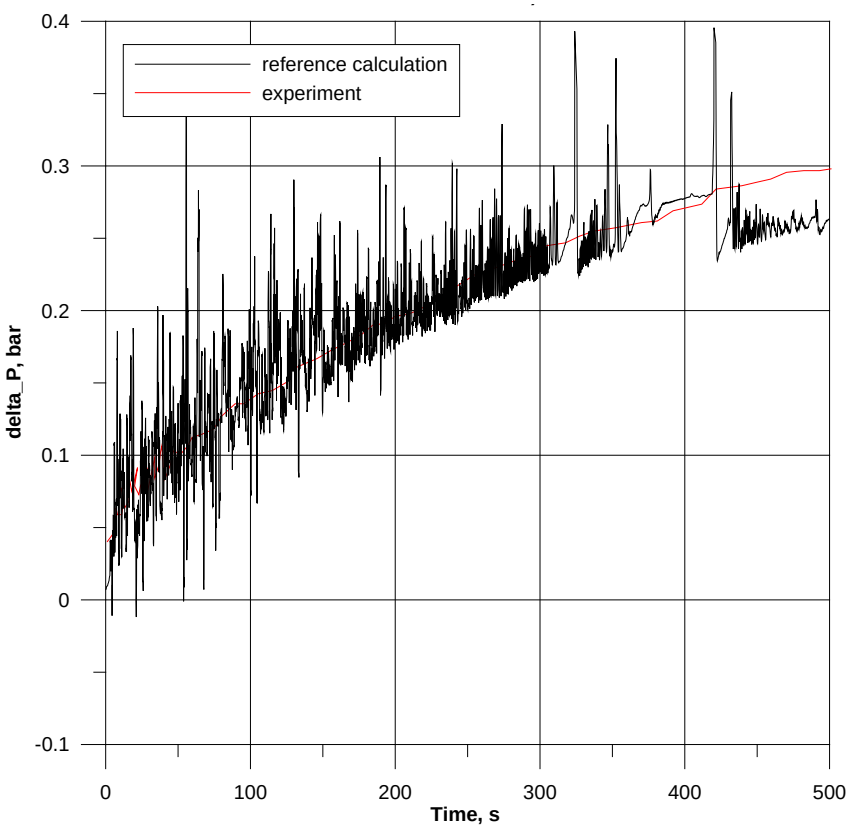

Fig B.12.15 Total bundle pressure drop

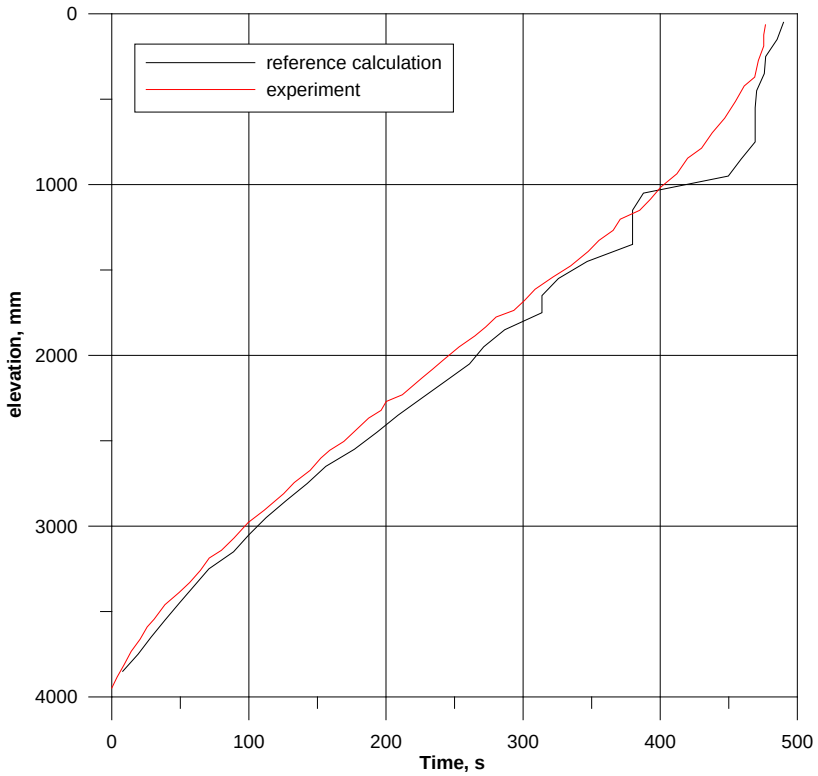

Fig B.12.16 Quench front elevation

PCT and bundle quench time

Tab B.12.2 Base case PCT and bundle quench

Institution name	PCT (°C)	Position (mm)	Bundle quench (s)
OKBM	915	1575-1675 (1625)	489

Criteria for selection of influential input parameters

Criteria from the Phase II Specifications were used for selection of the influential input parameters, namely:

Criterion #1: the absolute value of variation in rod surface temperature T_{clad} is $\mathbf{\Delta T_{ref} = 50K}$

Criterion #2: the variation in rewet time t_{rew} is $\mathbf{\Delta t_{rew} = 10\%}$

Criterion #3 (confirmation criterion): the variation in elevation of the quench front versus time $\mathbf{\Delta QF_{elev} = 10\%}$

Initially, the criterion #1 was understood as a difference in maximum temperature reached at the elevation selected (local PCT). Later, it was modified to "time trend" difference, i.e., maximum difference of cladding temperature in film boiling HT mode.

The following responses were used:

1. **PCT and cladding temperature time trend (max difference of Tclad before 200s) at elevation 1625 mm**
2. **Rewet time for elevation 1625 mm**
3. **Quench front position at 300 s for confirmation**

Selection of parameters

Initial list of parameters

Initial of list of potentially influential input parameters was based on the Sample List provided in Appendix A of Specifications for the Phase II with some modifications accounting for features of the code used and experience of performing reflood calculations.

Tab B.12.3 Initial list of input parameters

Input Basic Parameter /boundary conditions	
1.	Pressure
2.	Flooding velocity
3.	Fluid temperature
4.	Initial wall temperature
5.	Power density – bundle power
6.	Power density – Fz dependent on temperature
7.	Cladding heat capacity
8.	MgO heat capacity
9.	Hydraulic diameter
10.	Form loss coefficients
Input Global Parameter	
1.	Interface friction coefficient (correlation in code)
2.	Interface friction via input deck
3.	Wall heat transfer coefficient (all modes)
Input Coefficient Parameter	
1.	Droplet Weber (critical) number
2.	Droplet entrainment
3.	Effect of spacer grids on CHF and transition boiling heat transfer coefficient
4.	Interfacial area

Note: Weber critical number was understood as a local parameter in film boiling heat transfer correlation only. Weber numbers used in other correlations in the code were not affected.

Final list of Influential Parameters

Final list of influential parameters is presented in the Table below. Multipliers are presented in the table for the most of the parameters, while for We critical number and thermal coefficient of electrical resistance reference values and MIN/MAX values are presented.

Tab B.12.4 Final list of influential input parameters

Parameter	Subroutine	Fortran variable / Key word	Multiplier REF / REF value	Multiplier MIN	Multiplier MAX	T_{clad} variation [°C]	Position [mm]	t_{rew} variation [s]	Position [mm]
Power density – bundle power	input deck	scaling factor for table	1.0	0.95	1.05	-24.5/+31.5	1625	-18.5/+19.2	1625
Power density – electrical resistance dependent on temperature (k_ρ)	input deck	cntrlvars	k_ρ=1.7E-4	k_ρ=0	k_ρ=6.E-4	-31.1/+29.1	1625	-3.4/-3.6	1625
Interface friction coefficient	fidisj, fidis2	fic	1.0	0.8	1.2	-52.3/+55.3	1625	-31.3/+34.6	1625
Wall heat transfer coefficient (all modes)	input deck	fouling factor	1.0	0.9	1.1	+41.6/-37.9	1625	+23.1/-19.2	1625
Droplet Weber (critical) number	pstdnb	numerical coefficient=7.5 in block calculating qrwd	REF=7.5	MIN=3.0	MAX=15.	-43.4/+22.6	1625	-5.5/+9.8	1625
Interfacial area	fidisv, fidis2	surfa	1.0	0.8	1.2	-43.6/+51.9	1625	-31.8/+36.3	1625
	phantv, phantj	svslg, sannu, slslg							

Wall-to-fluid heat transfer model

Wall-to-fluid heat transfer model corresponds to that of released RELAP5/mod3.2 code version rather than to RELAP5/mod3.3. No reflood option is available. Absence of reflood model should be compensated by detailed basic nodalization (opinion of code developer).

Conclusions

Wall heat transfer coefficient has appeared the strongest influential parameter, taking into account relatively narrow range of variation. During phase III it will be checked whether its variation covers other parameters, such as interfacial area and drag, in order to reduce the total number of variable parameters to apply CIRCE method.

It will be kept in mind that in a real plant application, boundary condition parameters such as pressure, coolant flow and temperature are obviously influential, as well as local power uncertainty. But uncertainties of these parameters are external for the system code, and for experiment being analysed, should be known from the experimental data. Therefore, during PREMIUM Phase III this type of uncertainties will not be considered.

Thus, the list of influential parameters identified in Phase II includes:

1. Bundle power
2. Local power
3. Interfacial friction
4. Interfacial area
5. Wall heat transfer coefficient
6. Droplet Weber (critical) number – will be changed to film boiling HTC.

This list is subject to critical review in the beginning of Phase III taking into account the findings of other RELAP users.

B.13 UPC&CSN (Spain) results

Model description

Tab B.13.1 UPC code and software platform

Institution name	Code version	Software platform
UPC	RELAP5 mod 3.3 patch 4	Cygwin (Unix emulator) under Windows

Nodalization and basic geometrical properties

Taking in consideration the aim of PREMIUM benchmark and Phase II specifications, the nodalization adopted covers only the lower plenum, test section and upper plenum of FEBA experimental facility.

In the following page, a sketch of the nodalization is given, including, for each hydrodynamic component, its numbering, the type of component and its associated boundary conditions. Heat structures and grids are also sketched.

Main geometrical parameters:

- **General parameters for all hydrodynamic components**
  - Wall roughness: 1.27e-7

- **Test section (pipe 102)**
  - Subdivided in 25 sub-volumes according to:
    - Power distribution
    - Grid height
    - Uniformity between sub volumes
    - Length range recommended by RELAP5 manual for reflood model (0.15m-0.61m)
  - Heights/lengths
    - Total 4.091 m
    - Heated 3.900 m (volumes 2 to 24)
  - Flow area 3.8932e-3 m
  - Hydraulic diameter 13.47m m

- **Spacer grids:** the central grid is modelled differently than the rest of the grids, due to its significantly greater length (which is 38 mm for normal grids and 180 mm for the central grid)
  - Normal grids (placed at heights 390m, 935m, 1480m, 2570m 3115m and 3660m):
    - Reynolds number independent energy loss coefficients (k loss): 1.2
    - No flow area change
    - No hydraulic diameter change
  - Central grid (placed at height 2115m):
    - Reynolds number independent energy loss coefficients (k loss): 1.2
    - Flow area: 3.1150e-3 m (80% of normal test section area grid 3.8932e-3 m)
    - Hydraulic diameter: 3.33 mm (taking in account the drastic increment of wet perimeter and the 20% reduction of flow area)

- **Outlet (single junction 103)**
  - Reynolds number independent reverse flow energy loss coefficients (k loss): 1.e6

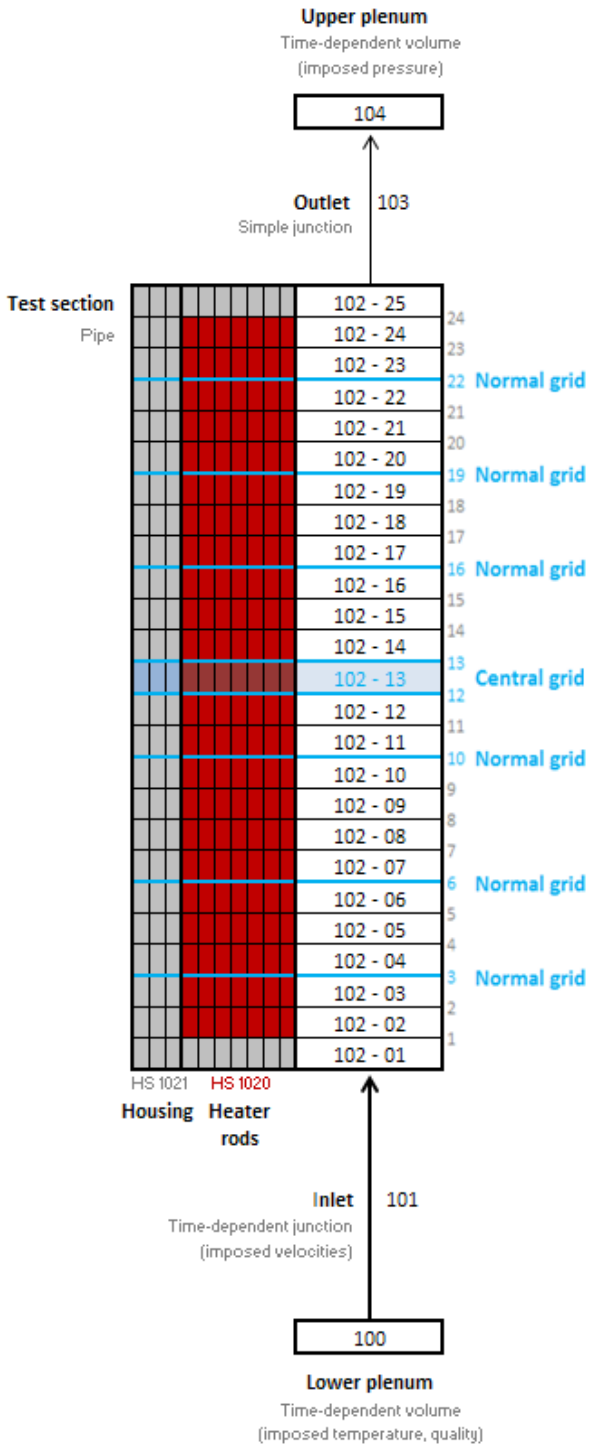

Fig B.13.1 Sketch of FEBA nodalization for RELAP5 by UPC

- **Heater rods (heat structure 1020)**
  - Radial mesh: 8 radial nodes
  - Total heat transfer area: 3454 m^2
  - Maximum linear heat rate: 2.43 kW/m
  - Heat transfer hydraulic diam.: 13.47 mm and 10.78 mm for central grid
  - Fouling factor: 0.75

- **Housing (heat structure 1021)**
  - Radial mesh: 3 radial nodes
  - Total heat transfer area: 1285 m^2
  - Heat transfer hydraulic diam.: 39.75 mm and 28.98 mm for central grid
  - Fouling factor: 1.0

Boundary and initial conditions
The boundary conditions applied to the model are the usual ones, recommended in RELAP manual:

Tab B.13.2 Boundary conditions for FEBA input data deck for RELAP5 by UPC

Magnitude	Affected elements	Value range	Comments
Feed-water temperature	Time-dependent volume 100	309-336 K	
Inlet quality	Time-dependent volume 100	0	Only liquid at inlet
Flooding velocity	Time-dependent junction 101	3.77-3.82 cm/s	Initial oscillations ignored
System pressure	Time-dependent volume 104	4.03-4.19 bar	Initial oscillations ignored
Bundle power	Heat structure 1020	121-199 kW	
Heat losses	Heat structure 1021	0 kW	Insulation considered perfect

The initial conditions applied to the model are:

- **Pipe 102**: 100% vapour (q=1) and experiment nominal pressure 4.1 bar
- **Initial velocities**: 0 for all hydrodynamic components

Adopted models (flags)
The following specific flags of RELAP5 mod 3.3 have been activated for hydrodynamic components:

- **Test section (pipe 102)**: rod bundle interphase friction model has been activated in the hydraulic nodes of the test section by setting flag b=1.
- **Test section (pipe 102)**: full abrupt area change model has been activated in the hydraulic junction surrounding the central grid (sub-volume 13) by setting flag a=1.
- **Heater rods (heat structure 1020)**: reflood model with 4 fine mesh divisions is set. “Vertical bundle without cross flow” heat transfer mode (110) has been set at the boundary of the heat structure representing the heater rods.
- **Housing (heat structure 1021)**: reflood model with 4 fine mesh divisions is set. “Default” heat transfer mode (101) has been set at the boundary of the heat transfer structure representing the housing.

Radiation has not been taken into account in the calculations.

Assumptions and steady-state achievement
The conditioning phase has not been simulated and no steady-state calculation is performed, as the initial calculation of RELAP seems to meet the initial boundary conditions and any variable show unrealistic transients at the beginning of the calculation.

The additional assumptions made at the model development and application are:

- RELAP time step control option chosen is 3;
- Initial temperature is considered constant in all the nodes of the heat structure representing the housing and in the radial direction in the heat structure representing the rods. See separate Microsoft Excel file for initial temperature of rods and housing;
- 12-word format for additional boundary conditions is used in the heat structure representing the rods, while 9-word format is used in the heat structure representing the housing;
- The experimental data like cladding temperatures or pressure losses have been compared with the calculated data by interpolating values given by the closer sub-volumes.

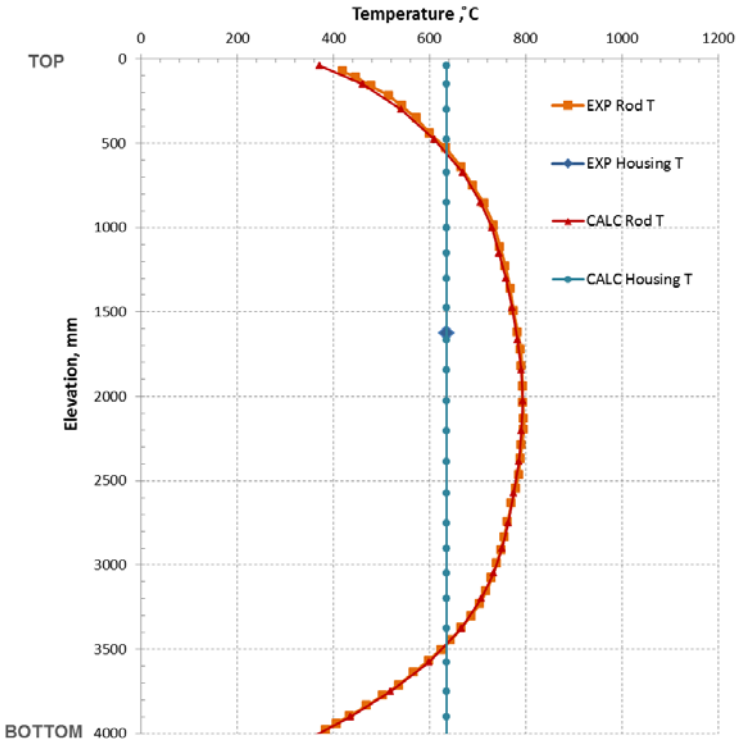

Fig B.13.2 Steady-state temperature profile

Base case results

Figures of all (exp-calc) responses

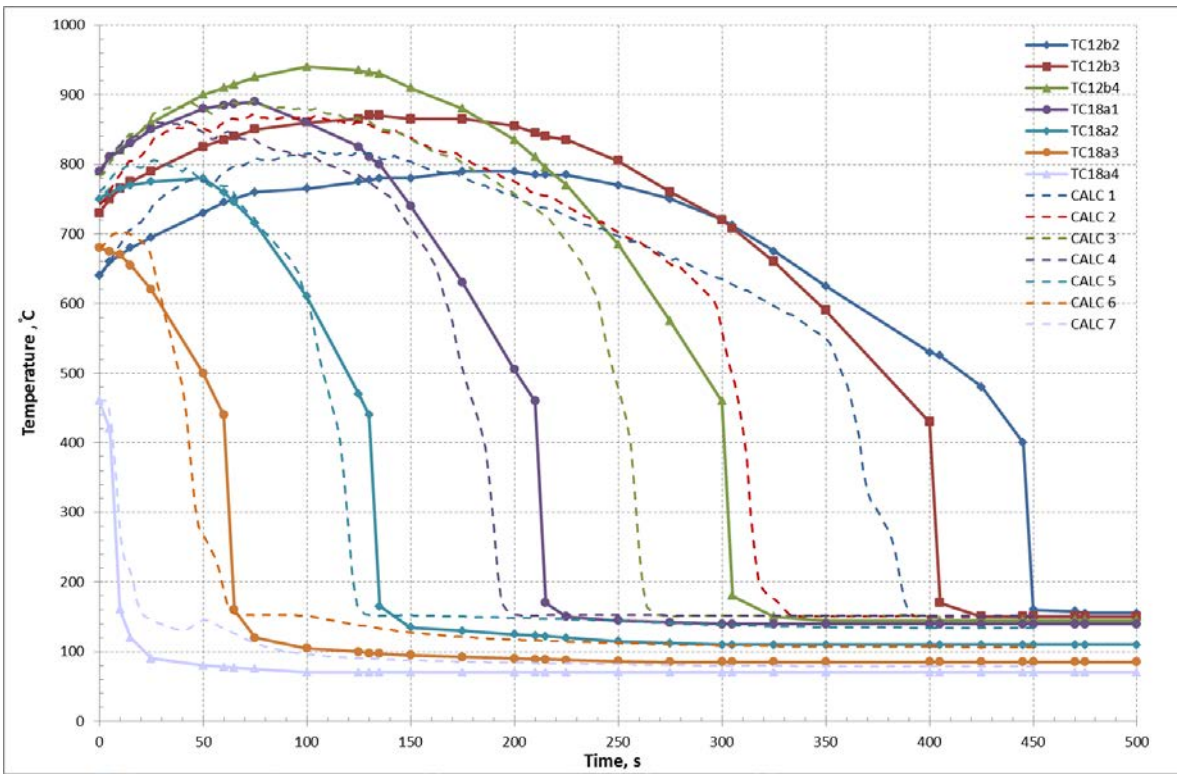

Fig B.13.3 Base case cladding temperatures

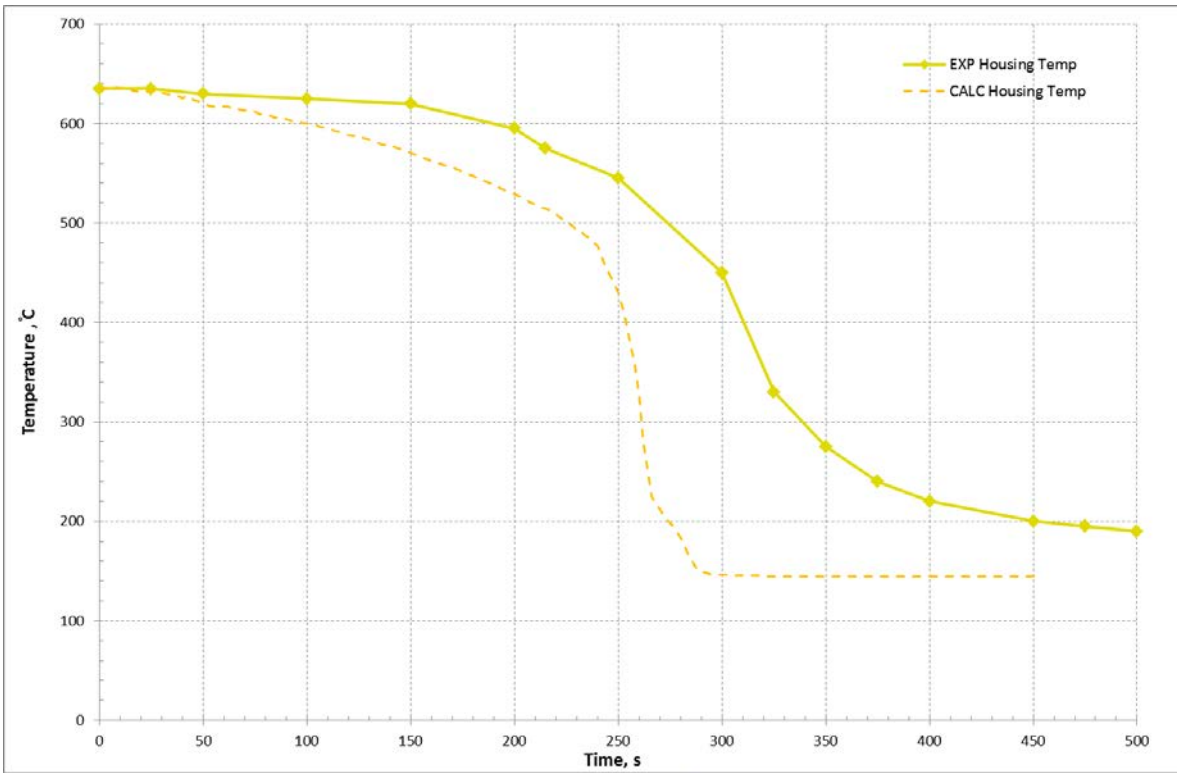

Fig B.13.4 Base case housing temperature

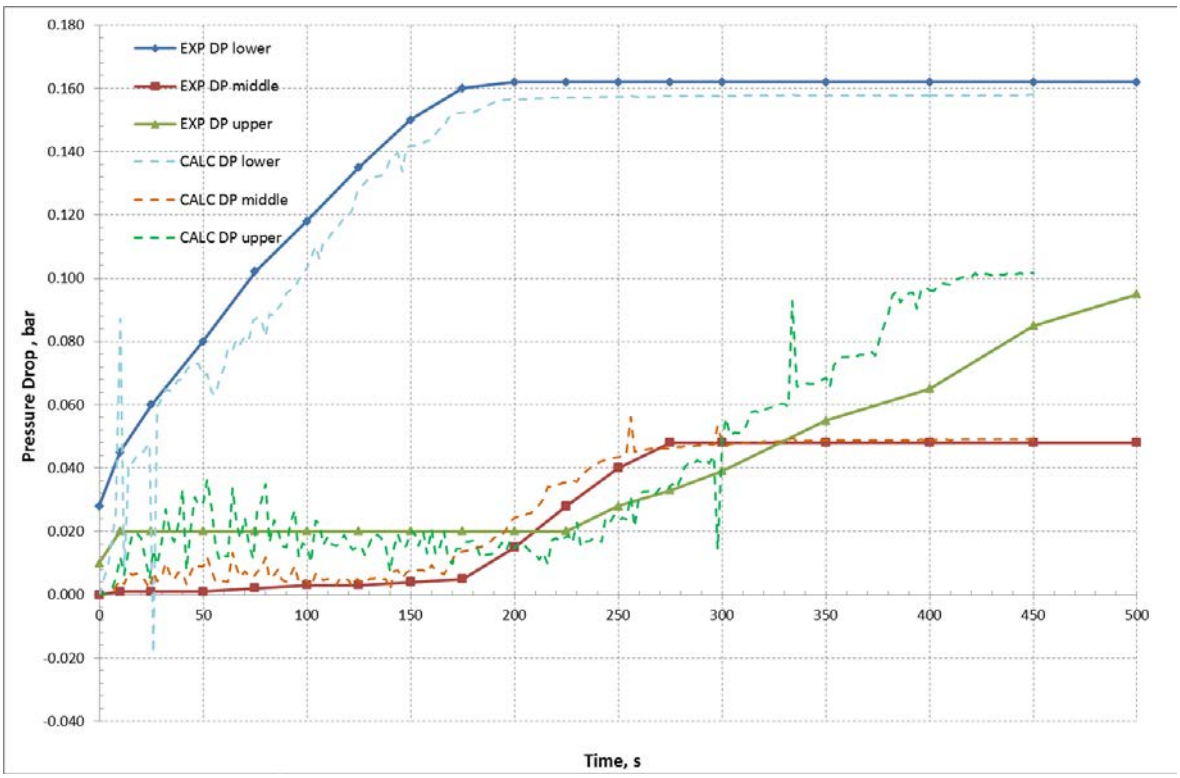

Fig B.13.5 Base case pressure drops

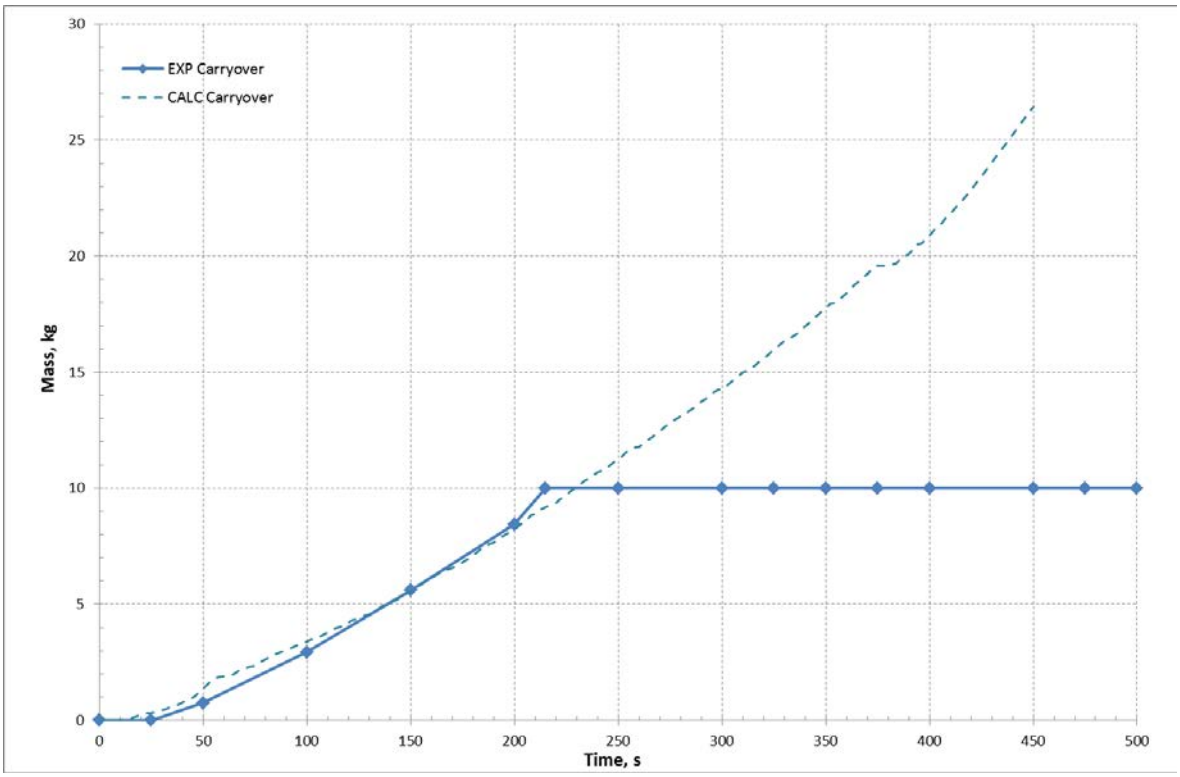

Fig B.13.6 Base case liquid carryover

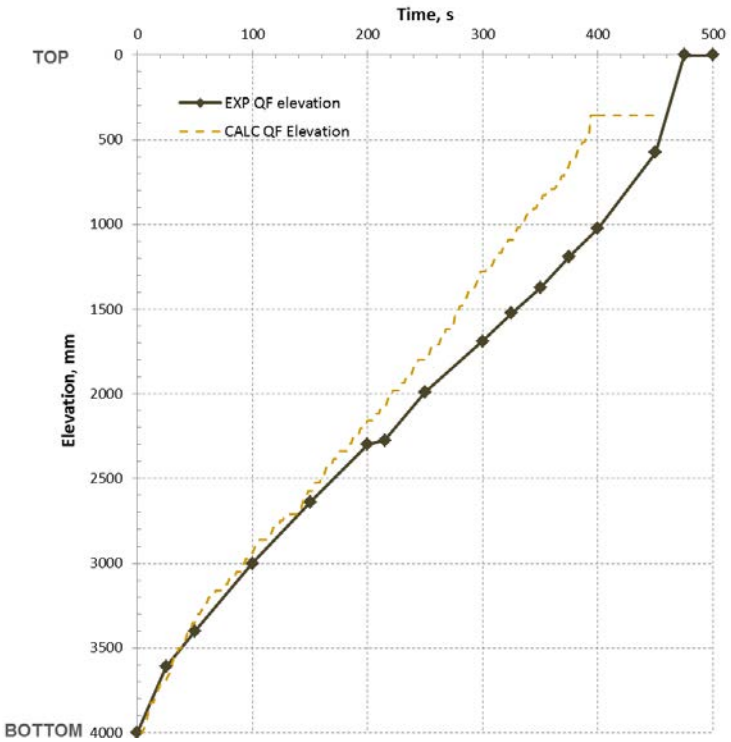

Fig B.13.7 Base case quench front propagation

PCT and bundle quench time

Tab B.13.3 Base case PCT and bundle quench

Institution name	PCT (˚C)	Position (mm)	Bundle quench (s)
UPC	890.82	1665	392

Criteria for selection of influential input parameters

The criteria of selection are based on the suggested criteria given in the Specifications for the Phase II.

As sketched in the next Figure which represents the cladding temperature time trend at height 1680 mm (at which the PCT takes place), an influential IP has to be such that its extreme value in the range of variation causes the following change in the either of two main reflood responses (at least one out of two criteria should be fulfilled):

- **Criterion #1**: The absolute value of variation in rod surface temperature T_{clad} is ΔT_{ref} = 50K.
- **Criterion #2**: The variation in rewet time t_{rew} is Δt_{rew} = 10% (which corresponds to 26s for height 1680 mm).

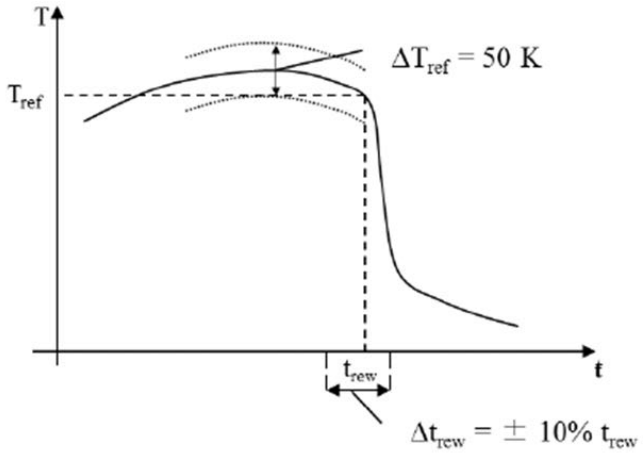

Fig B.13.8 Criteria for selection of influential parameter

Additionally, once the potential influential IP have been selected, the following criteria must be applied in order to ensure the "realism" of these Input Parameters:

- **Criterion #3**: Limited qualitative impact on the responses' time trends. Notably, the variation of an IP should not cause the drastic changes in rod surface temperature time trends (sudden deviations, oscillations) which may be caused by phenomenology different from that of reflood or by physical or numerical instabilities.
- **Criterion #4**: The range of variation (to make the parameter "influential") shall be consistent with the level of knowledge on the correspondent IP, e.g. the change in heater element density cannot be larger than the real known physical limits.
- **Criterion #5** (if applicable): In case a preliminary uncertainty evaluation is available, the range of variation of the single IP should not be responsible of the overall uncertainty of the responses.

Selection of parameters

Initial list of parameters

The initial list of input parameters considered as potentially influential for reflood-related phenomena is based on the Sample List provided in Appendix A of Specifications for the Phase II and classified according to the Definitions provided in Specifications for Phase II.

Tab B.13.4 Initial list of input parameters

Input Basic Parameter	
1	Pressure
2	Mass flux
3	Fluid temperature
4	Initial wall temperature
5	Initial housing temperature
6	Power density
7	Ni Cr 80 20 (cladding) thermal conductivity
8	Ni Cr 80 20 (cladding) heat capacity
9	MgO thermal conductivity
10	MgO heat capacity
11	Stainless steel thermal conductivity
12	Stainless steel heat capacity
13	Hydraulic diameter
14	Form loss coefficients
Input Global Parameter	
1	Film boiling heat transfer coefficient: wall-to-liquid
2	Film boiling heat transfer coefficient: wall-to-gas
3	Interfacial friction coefficient: dispersed vapour
4	Interfacial friction coefficient: bubbles and droplets
5	Interfacial friction coefficient: global
6	Interphase heat transfer coefficient: wet wall
7	Interphase heat transfer coefficient: dry wall
8	Interphase heat transfer coefficient: global
Input Coefficient Parameter	
1	Droplet Weber (critical) number
2	Quench front threshold distance for HTC transitions: Weismann (bottom)
3	Quench front threshold distance for HTC transitions: Weismann (top)
4	Quench front threshold distance for HTC transitions: Bromley
5	Minimum droplet diameter: volumes
6	Minimum droplet diameter: junctions

Final list of Influential Parameters

Tab B.13.5 Final list of influential input parameters

Parameter	Subroutine	Fortran variable / Key word	Multiplier REF / REF value	Multiplier MIN	Multiplier MAX	T_{clad} variation [°C]	Position [mm]	t_{rew} variation [s]	Position [mm]
Initial wall temperature	input deck	-	620-1070K	0.95	1.05	-27 / +30	1680	-2 / +6	1680
Power density	input deck	-	200 kW	0.9	1.1	-22 / +29	1680	-22 / +20	1680
Film boiling heat transfer coefficient: wall-to-liquid	PSTDNB	hfb	1.0	0.4	2	+50 / -23	1680	+60 / -34	1680
Film boiling heat transfer coefficient: wall-to-gas	PSTDNB	hv	1.0	0.4	2	+25 / -33	1680	-48 / -8	1680
Interfacial friction coefficient: dispersed vapour	FIDISJ	fic	1.0	0.5	1.5	+9 / -18	1680	-15 / +20	1680
Interfacial friction coefficient: bubbles and droplets	FIDIS2	fic	1.0	0.5	1.5	-7 / +13	1680	-45 / +45	1680
Interfacial friction coefficient: global	PHANTJ	fij	1.0	0.5	1.5	0 / +12	1680	-49 / +40	1680
Interphase heat transfer coefficient: dry wall	DISPDRYHIF	hifc, higc, hgfc1	1.0	0.1	10	+57 / -15	1680	+9 / -77	1680
Interphase heat transfer coefficient: global	PHANTV	hif, hig, hgf	1.0	0.1	10	+62 / -12	1680	+38 / -86	1680
Minimum droplet diameter: volumes	FIDISV	dcon(2)	1.5 mm	0.33	2	-22 / +36	1680	-59 / +22	1680
Minimum droplet diameter: junctions	FIDIS2	dcon(2)	1.5 mm	0.33	2	+76 / -8	1680	+22 / -45	1680

Wall-to-fluid heat transfer model

The specific reflood model adopted by RELAP5 is explained in Section 4.4 of RELAP4 manual Volume 4. Besides adding an axial heat conduction model in the heat structures in which the reflood model is on, the correlations of transition boiling and film boiling, as well as interphase drag and other details are modified. The meshing of the reflood heat structure is refined in the surroundings of the quench front, in which a boiling curve is traced, defining the use of the different correlations. Also, correlations change when the quench is near to the top of the reflood heat structure.

Conclusions

Among the parameters that fulfil the criteria, the list of input parameters that will be used in the Phase-III is:

- Film boiling heat transfer coefficient: wall-to-liquid
- Film boiling heat transfer coefficient: wall-to-gas
- Inter facial friction coefficient: dispersed vapour
- Interfacial friction coefficient: bubbles and droplets
- Interphase heat transfer coefficient: dry wall
- Interphase heat transfer coefficient: global
- Minimum droplet diameter: volumes
- Minimum droplet diameter: junctions

This list includes all the influential parameters, except these two influential parameters dismissed to be used in Phase III:

- The global Interfacial friction coefficient, which is apparently less significant than the two separate coefficients (dispersed vapour and bubbles/droplets), which have opposed effects on T_{clad}.
- The Input Basic Parameters (IBP, marked as *input deck*), have been dismissed due to their incompatibility with CIRCÉ.

The input parameters selected for Phase III will be used following the instructions given in CIRCE guidelines. In order to verify their adequacy for CIRCE statistics method, some checks will have to thoroughly performed, concerning:

- Independence between parameters (e.g. minimum droplet diameter will be in principle incompatible with interfacial friction coefficient)
- Linearity of parameters with responses (linearity hypothesis has to be accomplished)
- Distribution of the derivative vectors (normality hypothesis has to be accomplished)
- Significance to CIRCE (capacity of group of parameters to explain the difference of calculated and experimental responses)
- Etc.